UCRL 10097

University of California

Ernest O. Lawrence Radiation Laboratory

TWO-WEEK LOAN COPY

This is a Library Circulating Copy which may be borrowed for two weeks. For a personal retention copy, call Tech. Info. Division, Ext. 5545

A HYDRODYNAMIC MECHANISM FOR THE COALESCENCE OF LIQUID DROPS

Berkeley, California

DISCLAIMER

This document was prepared as an account of work sponsored by the United States Government. While this document is believed to contain correct information, neither the United States Government nor any agency thereof, nor the Regents of the University of California, nor any of their employees, makes any warranty, express or implied, or assumes any legal responsibility for the accuracy, completeness, or usefulness of any information, apparatus, product, or process disclosed, or represents that its use would not infringe privately owned rights. Reference herein to any specific commercial product, process, or service by its trade name, trademark, manufacturer, or otherwise, does not necessarily constitute or imply its endorsement, recommendation, or favoring by the United States Government or any agency thereof, or the Regents of the University of California. The views and opinions of authors expressed herein do not necessarily state or reflect those of the United States Government or any agency thereof or the Regents of the University of California.

Research and Development

UCRL-10097

UC-4 Chemistry
TID-4500 (17th Ed.)

UNIVERSITY OF CALIFORNIA

Lawrence Radiation Laboratory
Berkeley, California

Contract No. 7405-eng-48

A HYDRODYNAMIC MECHANISM FOR THE COALESCENCE OF LIQUID DROPS

Sidney B. Lang

(Ph.D. Thesis)

May, 1962

Printed in USA. Price $3.50. Available from the
Office of Technical Services
U. S. Department of Commerce
Washington 25, D.C.

A HYDRODYNAMIC MECHANISM FOR THE COALESCENCE OF LIQUID DROPS

Contents

Abstract vii

I. Introduction 1

A. Motivation for Problem 1

B. Literature Review 1

C. Scope of Work 2

II. Theoretical Studies 4

A. Factors Suggesting This Approach 4

B. Theoretical Model 6

C. Thinning-Film Model 10

1. Assumptions 10

2. Quasi-Equilibrium Force Balance 10

3. Thinning Model 13

a. Fluid Velocity 13

b. Energy Dissipation 16

c. Drop-Approach Solution 18

d. Comparison with Flattened-Sphere Model 21

e. Pressure Drop in Film 21

4. Electrical Effects and Disjoining Pressure 23

a. Electroviscosity 23

b. Disjoining Pressure 26

c. Electric Double-Layer Repulsion 27

D. Film Instability 27

1. Rayleigh Cylinder 27

2. Flat Film—Taylor Instability 31

a. Inviscid Solution 31

b. Effect of Viscosity 44

3. Spherical-Shell Film—Rayleigh Instability 49

4. Flat or Metastable Film—Large Disturbances 57

E. Effect and Analysis of Disturbances 61
1. Disturbances Caused by Sonic or Subsonic Noise 61
2. Disturbance Produced by a Falling Drop 65
3. Analysis of Random External Disturbances 66
F. Summary of Model 68
III. Experimental Equipment, Techniques of Operation, Calibrations, and Property Measurement 74
A. Coalescence Equipment and Methods of Operation 74
1. Equipment Description 74
a. Bath System 74
b. Coalescence Cell and Glass Assembly 77
c. Dropping Tips 79
2. Operation 85
a. Cleaning Procedure 85
b. Assembly 86
c. Experimental Run 91
d. Analysis of Run 96
B. Sonic Equipment 99
1. Equipment Description 99
2. Calibration 103
C. Materials 116
D. Physical Properties 118
1. Density 118
2. Interfacial Tension 118
3. Viscosity 121
IV. Experimental Results 122
A. Preliminary Studies 122
1. Surface Renewal 122
2. Distance between Dropping Tip and Interface 122
3. External Vibration 125
4. Method of Purification 128
5. Drop Aging 130

B. Effects of Drop Size and System Physical Properties 132
C. Effect of Induced Disturbances 138
1. Telephone Speaker. 138
2. Swimming-Pool Speaker. 141
3. Subsonic Disturbances. 144
D. Effects of Contamination and Surfactants 150
1. Accidental Contamination 152
2. Effect of Surfactants 154
E. Natural Sonic Disturbances 158
1. Measurement of rms Frequency Spectrum. 158
2. Computed Sonic Disturbances. 163
V. Discussion and Analysis of Results 167
A. Discussion of the Experimental Results 167
1. Effect of Drop Size and Liquid System. 167
2. Effect of Induced Disturbances 174
3. Contamination and Surface-Active Agents. 175
B. Future Work. 177
C. Applications 178
D. Summary. 179
Acknowledgments. 183
Appendices 184
A. Statistical Analyses 184
1. Experimental Run-Consistency Test. 184
2. Statistical Analysis of the Effect of Material Purification Method 184
3. Statistical Analysis of the Effect of Drop Aging 186
4. Statistical Analysis of Sonic Frequency Disturbance Runs .191
B. Coalescence Run Experimental Data. 193
Nomenclature 249
References 255

A HYDRODYNAMIC MECHANISM FOR THE COALESCENCE OF LIQUID DROPS

Sidney B. Lang
(Ph.D. Thesis)
Lawrence Radiation Laboratory
University of California
Berkeley, California

May, 1962

ABSTRACT

The coalescence of liquid drops at planar interfaces was studied theoretically and experimentally. The mechanism of coalescence was found to occur in two parts. In the first part, the drop (phase 1) approaches the interface through the continuous medium (phase 2) and deforms the interface by creating a spherical depression in it. The thin spherical shell of phase 2 material between the drop and the interface is slowly squeezed out under the combined action of surface and gravity forces. The phase 2 film becomes thinner at a rate inversely proportional to the cube of its thickness. When the film becomes sufficiently thin, the second part of the mechanism occurs. Because a denser liquid always overlies a less dense liquid at one of the interfaces of the film, the interface is inherently unstable with respect to long-wavelength disturbances (Taylor instability). If such a disturbance is introduced into the proper interface, the disturbance will grow exponentially in time until the film disintegrates, causing coalescence of the drop. A sufficiently intense disturbance of any wavelength can also rupture the metastable film, causing coalescence. The ease of rupture of the phase 2 film increases with decreasing thickness of the film. The disturbances can originate from any source yielding a fluctuating pressure at the interface, i.e., mechanical vibration, thermal convection currents, Marangoni instability, or other. Because these disturbances arrive randomly in time, coalescence times are also random. Drop rest-times were predicted to decrease with decreasing drop radius, decreasing phase 2 viscosity and decreasing frequency of disturbance.

The effect of density difference and interfacial tension depends upon whether film thinning or film rupture is the rate-determining step in coalescence.

Coalescence measurements were made in an all-glass thermostatted cell. The two-component systems water-benzene, water-anisole, ethylene glycol-benzene, tributyl phosphate-water, and water-Aroclor 1248 were studied. Both artificial sonic and artificial subsonic disturbances were found to decrease the drop rest-times, as predicted by the theory. Measurement of the natural sonic pattern present in the coalescence cell by means of a special microphone showed the presence of intense but short-time disturbances. Studies with surfactants showed that concentrations of less than 0.02 m$\underline{M}$ of surface-active agent in the water-benzene system could increase coalescence times by a factor of 2. Experimental changes in drop size and system properties agreed with the theory, qualitatively. Because of the microscopic nature of the theory and the macroscopic nature of the experimental results, exact experimental verification of the theory is not possible.

I. INTRODUCTION

A. Motivation for Problem

The industrial physical scientist or engineer is frequently faced with the problem of either separating a liquid dispersion into its components or making such a dispersion stable for a long period of time. A major factor in the study of these problems is the rate of coalescence of drops of the dispersed phase. Although much information has been obtained on coalescence by studies of the rate of separation of a dispersion, a more complete understanding of coalescence requires a detailed analysis of a simple system. Several workers have studied the coalescence of a drop at a flat interface, but no complete theory has been proposed. It was the goal of this work to provide such a theory and to test it experimentally.

B. Literature Review

When a drop (phase 1) of a more dense liquid falls through a less dense fluid (phase 2) to the interface between the phase 1 and phase 2 liquids, the drop often remains at the interface a period of time before it coalesces with the bulk phase-1 material. This time period has been called the coalescence time, drop rest-time, or drop life-time. One of the earliest discussions of coalescence was by Reynolds who observed drops of water floating on the surface of ponds.[1] In this case, the phase 2 fluid was air. One of the earliest thorough investigations was by Mahajan who allowed drops of methanol, ethanol, ether, turpentine, and kerosene to fall through air onto the surface of the same fluids.[2] He observed stepwise coalescence in several cases, and noted that coalescence times increased with movement or oscillation of the interface, with viscosity, with purity of the fluids, and with saturation of the air above the fluid.

Cockbain and McRoberts noted that the rest-times of drops were not constant, but that if a sufficient number of drops was examined, a reproducible distribution curve could be obtained.[3] By plotting the

logarithm of the fraction of drops which had not coalesced in time t vs t, these authors concluded that coalescence consisted of two distinct processes. The first consisted of drainage of the phase 2 film, and the second of a localized displacement of the stabilizer molecules at the interface, causing rupture of the film. This mechanism cannot account for the stability of drops in a pure two-component system, however. Gillespie and Rideal replaced the second mechanism with a theory involving a probability of rupture.[4] The results of later investigators did not agree with the mathematical formulation of their theory.[5,6] Gillespie and Rideal also noted an increase in stability with drop radius.

Picknett,[5] and Elton and Picknett,[7] studied the effect of the addition of salts to the aqueous phase in the water-anisole system and noted a marked decrease in drop rest-times. Watanabe and Kusui proposed that coalescence occurred because of a defect in the emulsifier layer around the drop at the point where the drop contacts the interface.[8] Another investigation in emulsified systems was by Nielsen, Wall and Adams, who noted that any factor that disturbs the interface on a molecular scale decreases the stability of drops.[6] A series of papers from McGill University postulated a mechanism for partial coalescence, and investigated the effect of temperature change and electric fields on coalescence.[9-13]

Derjaguin and Prokhorov,[14] and Prokhorov,[15,16] have investigated the coalescence of two drops of liquid brought into contact in air. Several meteorological papers have considered coalescence between water droplets in a cloud.[17,18]

C. Scope of Work

It was immediately recognized from the great variety, and occasional lack of consistency, in the theories described in the literature that a basic understanding of the coalescence process could be obtained only by study of a relatively simple system. Accordingly, the scope of this investigation is governed by the following considerations:

(a) Coalescence would be at flat interfaces only;

(b) Only the first stage of coalescence would be examined;

(c) The liquid systems considered would not contain a third component, a restriction that was later relaxed to allow the study of the effect of minute traces of a contaminating material;

(d) An explanation of the random nature of coalescence times was of major importance; and

(e) The effect of drop size and system properties on drop rest-times should be ascertained.

A theoretical description of the coalescence process for a single drop is presented in Section II. This theory accounts for the random nature of coalescence times and the effect of drop size and system properties. Section III contains a description of the equipment used in the experimental study, and the method of operation of this equipment. Certain calibrations were necessary for the sonic disturbance generating and detecting equipment. The techniques of calibration and their results are also included in Section III. The experimental results obtained in the study, and a limited discussion, are found in Section IV. A comparison of the experimental results with the theory, some suggestions for future work, applications, and a short summary, are given in Section V. Appendix A contains typical examples of the statistical calculations used in the study. All the experimental coalescence data measured are presented in special tabular form in Appendix B.

A form for the presentation of coalescence data has been adopted from the literature.[5,9] A plot of the fraction of drops coalesced within a certain time t, vs time t, corresponds to a statistical distribution curve. Accordingly, such a graph will be called a coalescence distribution curve. It should be emphasized that the coalescence measurements used in making such a plot are taken one at a time.

A convention has been adopted for identification of the drop and continuous phases. The drop phase is always called phase 1, whether it be more or less dense than the continuous phase. The continuous phase is always called phase 2 in the discussion. In a liquid-system name, the first fluid is phase 1; the second fluid, phase 2. For example, in the water-benzene system, water is phase 1 (the drop phase) and benzene is phase 2 (the continuous phase).

II. THEORETICAL STUDIES

In this section, the theoretical coalescence model on which the experiments were based is developed. The first two sections describe the factors suggesting this type of approach and give an overall picture of the model. The last four sections describe the model in detail.

A. Factors Suggesting This Approach

Many workers have noted the random nature of coalescence times[3-7,9,11] but few have even attempted to suggest an explanation, and none have given adequate explanations. The approach used here was suggested by several significant observations in coalescence experiments, and by a number of studies of the hydrodynamic stability of cylinders and flat surfaces.[19-24]

Several models have been proposed for the shape of a drop after it has been released from the dropping tip and approaches the interface. One of the first of these models, suggested by Gillespie and Rideal,[4] is depicted schematically in Fig. 1(a). Derjaguin and Kussakov had observed interferometrically a similar depression when a glass plate was pressed against a bubble of air submerged in a vessel of water.[25] Derjaguin and Prokhorov,[14] and Prokhorov,[16] had also observed depression in each of two drops of hexane which were pressed together in an atmosphere of air. Two models were suggested by Picknett,[5] and by Elton and Picknett.[7] They found that when the drop was distant from the flat interface, it approached the interface at the same rate that a solid sphere would approach an infinite wall through a viscous medium. This rate of approach was inversely proportional to the separation distance between the sphere and the wall. When the sphere was sufficiently close to the wall, its rate of approach became equal to that of a circular disk approaching an infinite wall through a viscous medium. This rate of approach was inversely proportional to the cube of the distance of separation between the disc and the wall. The sphere and the disc models are shown in Fig. 1(b,c) respectively. Charles,[9] and Charles and Mason,[11] applied the sphere-approach model to the coalescence times of high interfacial-tension systems, such as mercury and glycerol solutions. They felt that this was a system in

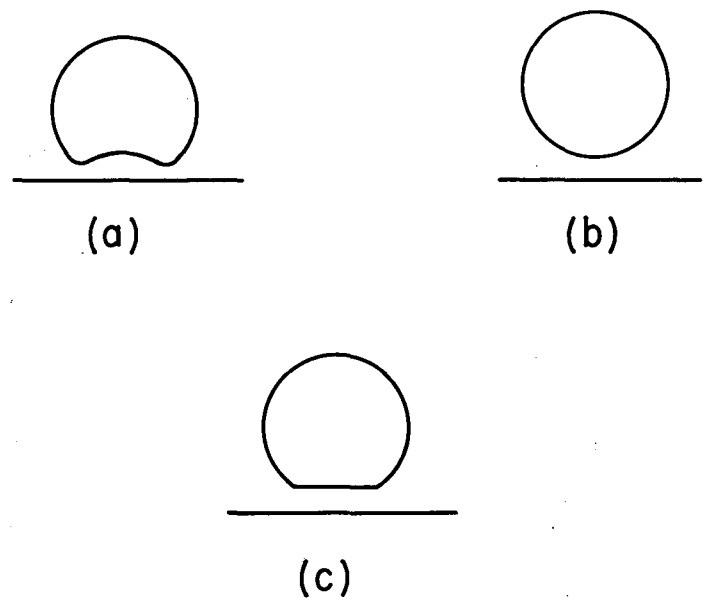

MU-26976

Fig. 1. Drop-approach models: (a) Gillespie and Rideal model, reference 4; (b) Spherical model, reference 5; (c) Disc or flattened sphere model, reference 5.

which the drops would remain highly spherical because of high interfacial tension. (This conclusion is incorrect because of the very great density difference that more than offsets the interfacial-tension effect.) They applied the disc-approach model to systems of lower interfacial tension, such as water-hydrocarbon systems.

Because the special design of the coalescence cell used in this work eliminated the interfacial meniscus (see Section III) which usually makes observations in the plane of the interface impossible, the rate-of-approach problem could be resolved. It was observed that if the phase 2 liquid were of low viscosity, the drop would reach a motionless, quasi-equilibrium position (with respect to the interface), within 0.1 sec after leaving the dropping tip. With the highest-viscosity phase-2 liquid used (203 cp), the time period from the moment of drop release until the quasi-equilibrium position was reached was about 0.3 sec, only a small fraction of the total coalescence time. A photograph of the drop in the quasi-equilibrium position is shown in Fig. 2. Note that the drop remains almost spherical and that the interface is locally indented to accommodate the drop. A model that fits these experimental observations is described in the next two sections.

An entirely different approach was used to explain the random nature of coalescence times in this work. Lord Rayleigh,[19,20] and G. I. Taylor,[21] have investigated two types of hydrodynamic instability which now bear their names. These instabilities are initiated by small disturbances and, under certain conditions, they can grow very rapidly and eventually cause disintegration of fluid formations. Hydrodynamic instability is proposed as the final step in a coalescence process.

B. Theoretical Model

The theoretical model will now be described. Although the theory is developed for the case in which phase 1 is denser than phase 2, the model is equally applicable to the converse situation.

A drop of phase-1 liquid falls from the dropping tip and descends to the nearly motionless quasi-equilibrium position at the interface shown in Fig. 3. This idealization is physically analagous to the situation

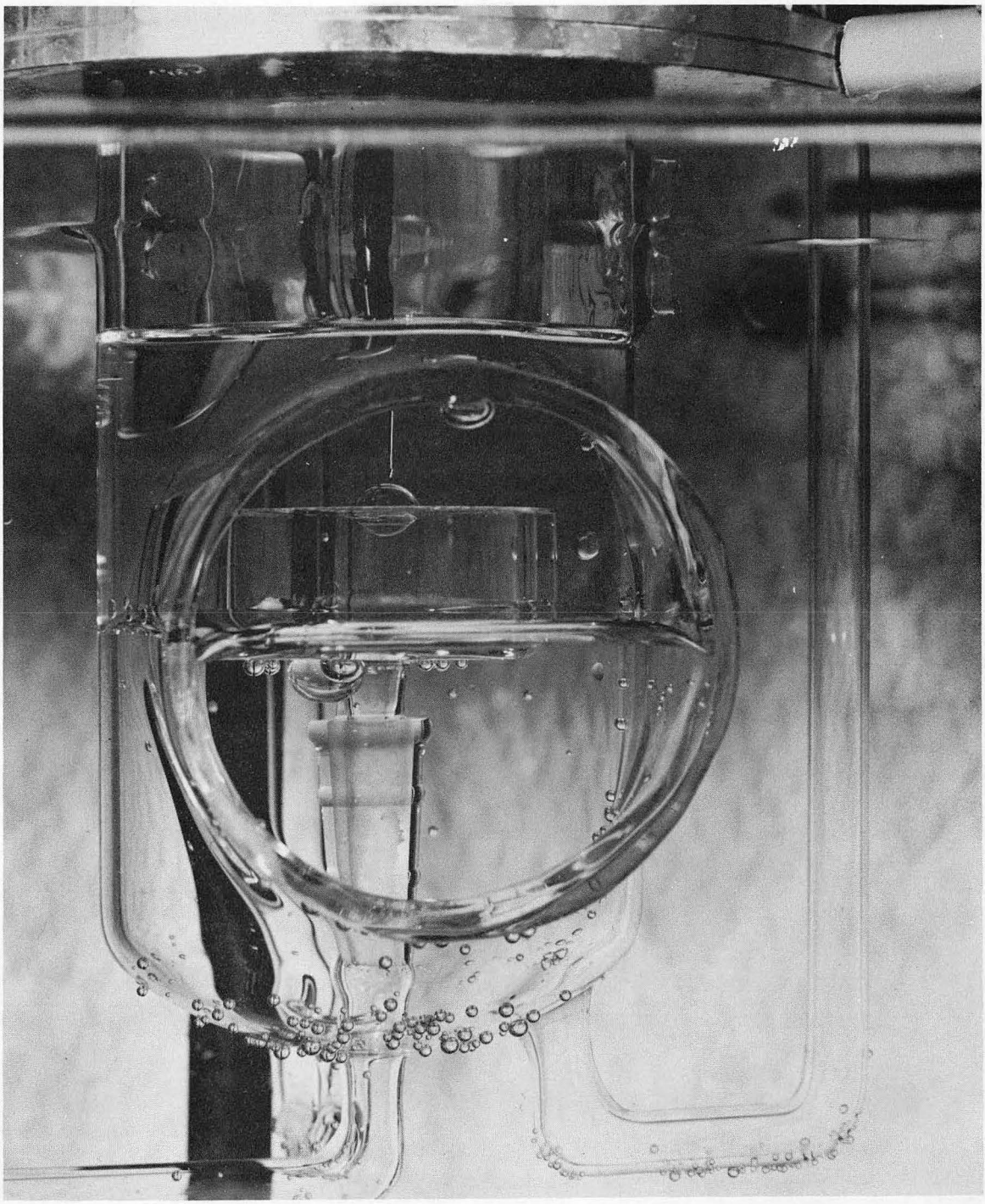

ZN-3101

Fig. 2. Photograph of drop (indicated by arrow) in quasi-equilibrium position at interface.

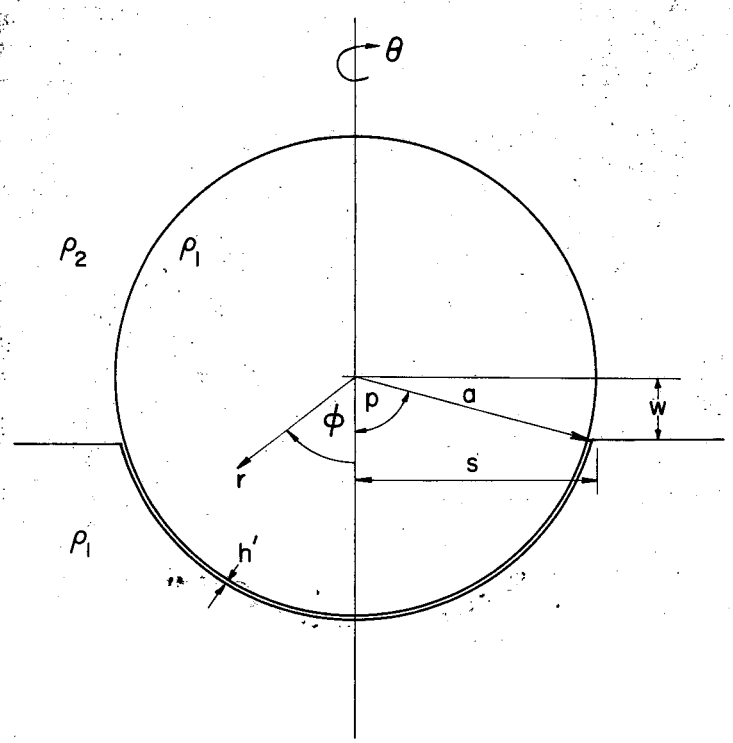

MU-26935

Fig. 3. Film-thinning model.

photographed in Fig. 2. The drop is separated from the phase 1 material below the interface by a thin film of phase 2. The amount of depression of the interface by the drop can be computed by assuming that the drop is a solid sphere and the interface behaves as a taut but deformable membrane. The thin film of phase 2 is gradually squeezed out under the action of gravity and surface forces; however, it is shown that this process is an extremely slow one. If the film becomes sufficiently thin before the instability discussed next sets in, the rate of thinning is further retarded by the electroviscous effect and disjoining forces.

We suppose that a mechanical disturbance creates a system of surface waves in one or both of the interfaces between the phases. Because of the Rayleigh-Taylor instability, under the proper conditions, these waves will grow exponentially in time until the spherical shell of phase 2 is ruptured. Phase 1 material will then flow through the "hole", causing coalescence. It is very important to note that the shell must be inherently metastable (discussed in a later section) or unstable for coalescence to occur in a short period of time because of the extremely slow rate of thinning of the film under the force of gravity. This point is illustrated by a numerical example in a later section.

What is the source of the mechanical disturbances that create the wave systems? These disturbances are caused by the sounds and vibrations present in any building housing scientific laboratories containing pumps, compressors, blowers, or similar apparatus. These disturbances, modified by their travel through the solid walls and floors of the building, undergo interference, scattering, and absorption, and arrive at the coalescence cell as discrete, randomly spaced bursts of sound. The random time of their arrival is one of the major factors that determines coalescence times. The other more subtle factors arise from the nature of the instability process. A theory describing the manner in which these disturbances create waves, and a method for their experimental analysis, is given in a later section.

The three topics just described and the assumptions involved in their discussion form the remainder of this section.

C. Thinning-film Model

1. Assumptions

The thinning-film model is based upon the following major assumptions:

(a) The drop behaves like a solid sphere, having the same volume as the liquid drop.

(b) The drop falls off the dropping tip and instantaneously reaches a quasi-equilibrium position in the interface determined only by surface and gravity forces.

(c) A film of phase 2 liquid is trapped beneath the drop, uniform in thickness, but very thin in comparison to the radius of the drop.

(d) The fluid flow in the film is laminar, and the flow pattern is symmetrical about a vertical axis. Velocities in the radial direction are negligible in comparison to tangential velocities.

(e) The film of phase 2 decreases in thickness with time under the action of the surface and gravity forces. The potential energy released in this manner is converted into kinetic energy of motion of the phase 2 liquid. This kinetic energy in turn is dissipated in the form of heat by viscous forces.

The assumptions are all reasonable physically, with the possible exception of uniform film thickness, which is more carefully examined below. The model is developed in the first two subsections. The effects of additional forces are discussed in the third subsection.

2. Quasi-Equilibrium Force Balance

The quasi-equilibrium position reached by the drop according to assumptions (a) and (b) is shown in Fig. 3. The drop sinks into the interface until the center of the drop is a distance w above the level of the interface. Thus p, the angle between the vertical axis and a line drawn from the center of the drop to the point at which the drop surface "touches" the interface, is related to w by $w = a \cos p$, where a is the drop radius. (If p is greater than $\pi/2$ then w is less than zero and the drop center is below the level of the interface.) In this

idealized model, the surface forces act on the drop periphery at an angle p with the horizontal. Thus, the surface forces produce the upward force,

$$F_U = (2\pi s)\ \sigma \sin p = 2\pi\sigma a \sin^2 p. \tag{1}$$

The mass of phase 1 liquid above the interface level is acted upon by gravity to produce a downward force. The volume of the drop between the level of the interface and a horizontal plane dividing the sphere into hemispheres is given by[27]

$$\frac{1}{6}\pi w\ (3s^2 + 3a^2 + w^2).$$

Adding the hemispheric volume above the horizontal dividing plane, we get the total volume of the drop above the interface,

$$\frac{2}{3}\pi a^3 + \frac{1}{3}\pi a^3 \cos p\ \ (\sin^2 p + 2).$$

(Note that if the center of the drop is below the interface, the sign of the second term in this expression will be negative and it will be subtracted from the hemispheric volume.) The gravity forces, therefore, yield a downward-force component

$$F_D = (\rho_1 - \rho_2) g \left[\frac{2}{3}\pi a^3 (1 + \frac{1}{2}\cos p \sin^2 p + \cos p) \right]. \tag{2}$$

We have here neglected the buoyant force resulting from the presence of the film of phase 2 because of assumption (c). The force balance is derived by equating Eq. (1) to Eq. (2). After some simplification and rearrangement we get

$$\frac{3\sigma}{\Delta\rho g a^2} = Q(p),$$

where

$$Q(p) = \frac{1}{\sin^2 p}\left(1 + \frac{1}{2}\cos p \sin^2 p + \cos p\right). \tag{3}$$

The function of Q(p) is given graphically in Fig. 4.

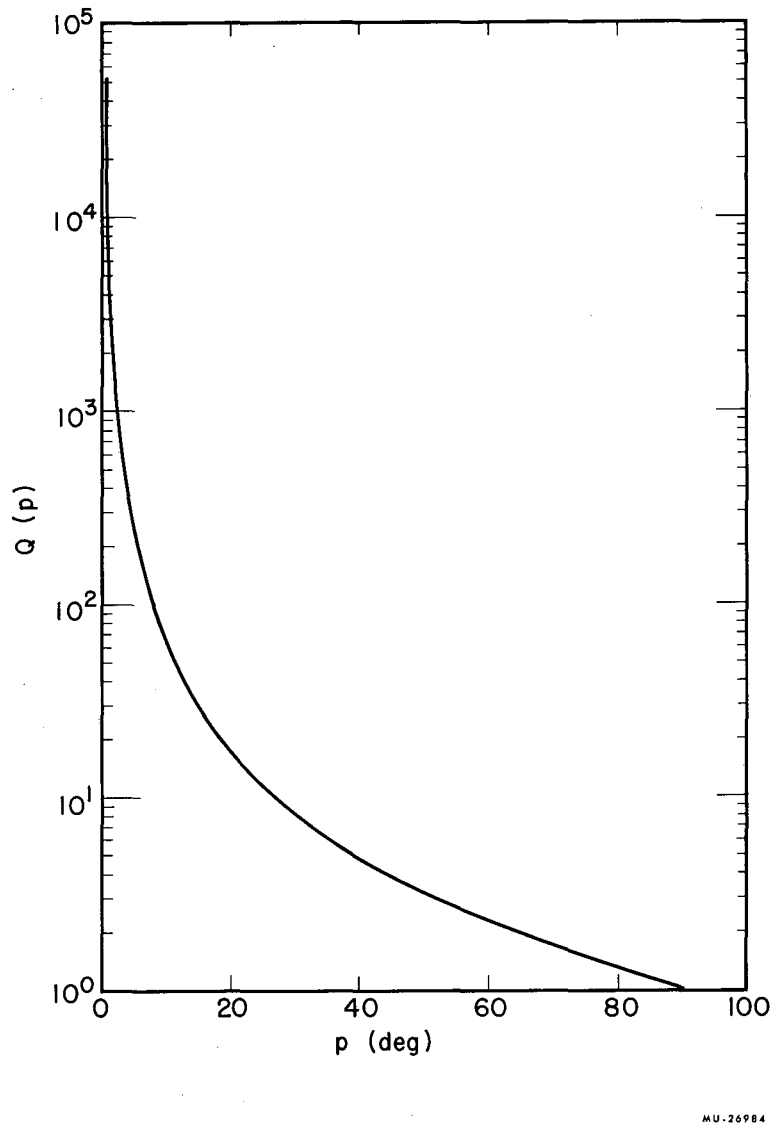

Fig. 4. Plot of Q(p) as a function of p.

3. Thinning Model

According to assumption (b), the drop reaches the quasi-equilibrium position defined by Eq. (3) instantaneously. Then the thin film of phase 2 liquid begins to decrease in thickness because of the combined action of the surface and gravity forces. During this time, the angle p remains constant. Successive thicknesses of the film h' are shown, greatly exaggerated, in Fig. 5.

a. Fluid Velocity. Let us first calculate the fluid velocity in phase 2. By assumptions (c) and (d), we realize that the flow pattern in an arbitrary small area is the same as the laminar flow between two infinite parallel plates, i.e. the flow has a parabolic velocity distribution. Therefore, the tangential fluid velocity, $u_\phi(r,\phi)$, obeys the relation

$$u_\phi(r,\phi) = (r-a)(a+h'-r)\,\psi(\phi) \quad . \tag{4}$$

Here r and ϕ represent the radius and polar angle coordinates, respectively, of the spherical coordinate system, and h' is the thickness of the spherical shell. $\psi(\phi)$ is an angular function to be determined presently. We note that at either r = a or r = a + h', the velocity is zero. In addition, the boundary condition that the velocity must be zero on the vertical axis requires that $\psi(0) = 0$. At an arbitrary angle ϕ, the area of a differential element of the cross-section of the shell equals $2\pi r \sin\phi\, dr$ (the same as an element of the area of a right circular cone). The volumetric rate of flow of phase 2 out through this differential area is obtained by multiplying the area by the flow velocity, and the total rate of flow can be found by integrating across the channel:

$$N_\phi = \int_a^{a+h'} 2\pi r \sin\phi (r-a)(a+h'-r)\,\psi(\phi)\, dr$$

$$= \pi a^4 \sin\phi \left(\frac{H^4}{6} + \frac{H^3}{3}\right)\psi(\phi), \tag{5}$$

where

$$H \equiv \frac{h'}{a} \; .$$

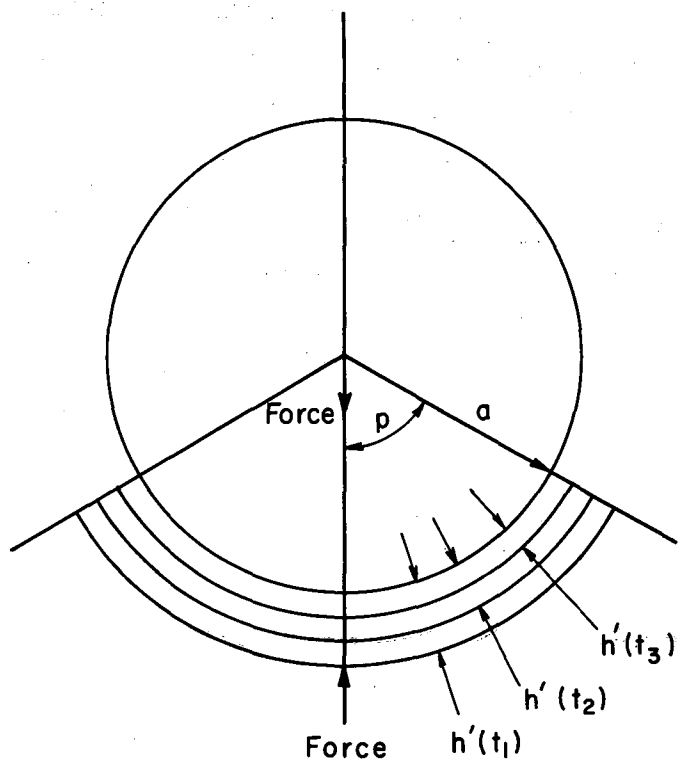

MU-26978

Fig. 5. Exaggerated view of thinning-film model. Film thicknesses at three values of t are shown.

If we define $\mathcal{H}(H) \equiv a^4\left(\frac{H^4}{6} + \frac{H^3}{3}\right)$,

the flow rate through the channel at an angle $\phi + \Delta\phi$ is given by

$$N_{\phi+\Delta\phi} = \pi\mathcal{H}(H)\Delta\phi\ [\psi(\phi)\cos\phi + \frac{d\psi(\phi)}{d\phi}\sin\phi]. \tag{6}$$

In deriving Eq. (6), we have assumed $\Delta\phi$ small so that $\sin\Delta\phi \approx \Delta\phi$, $\cos\Delta\phi \approx 1$, and $\psi(\phi+\Delta\phi) \approx \psi(\phi) + \frac{d\psi(\phi)}{d\phi}\Delta\phi$. Now, we note that the volume contained in a spherical sector bounded by two right circular cones of vertex angles ϕ and $\phi+\Delta\phi$, respectively, is given by[17]

$$\frac{2}{3}\pi r^3[\cos\phi - \cos(\phi+\Delta\phi)].$$

Thus the total volume contained in the spherical shell channel between ϕ and $\phi+\Delta\phi$ is given by

$$\frac{2}{3}\pi[(a+h)^3 - a^3][\cos\phi - \cos(\phi+\Delta\phi)]. \tag{7}$$

The volumetric flow rate of fluid out of the channel must, by a material balance, equal the time rate of change of the channel volume. Equating the time derivative of Eq. (7) to the difference between Eqs. (6) and (5) and simplifying, the differential equation defining $\psi(\phi)$ is found by

$$\frac{d\psi}{d\phi} + \psi\cot\phi = -2a^3\ \frac{(1+H)^2}{\mathcal{H}(H)}\ \frac{dH}{dt}. \tag{8}$$

The solution to the homogeneous equation can readily be found by quadratures, as

$$\psi_H = k\csc\phi, \tag{9}$$

where k is an arbitrary constant of integration.
The particular solution is found by the Lagrange method of variation of parameters by assuming

$$\psi_p = k(\phi)\csc\phi. \tag{10}$$

The complete solution is then found as

$$\psi = k \csc \phi + 2 \cot \phi \frac{a^3}{\mathcal{H}(H)} \quad (1+H)^2 \frac{dH}{dt} . \tag{11}$$

Using the boundary condition $\psi(0) = 0$ to find k, and substituting the result into Eq. (4), we finally obtain the velocity expression

$$u_\phi = \frac{12a(R-1)(1+H-R)(1+H)^2}{(H^4 + 2H^3)} \quad (\cot \phi - \csc \phi) \frac{dH}{dt} \tag{12}$$

where $R \equiv \frac{r}{a}$.

b. Energy Dissipation. At this point we make use of assumption (e) by equating the rate of work done in decreasing the film thickness to the rate of energy dissipation in the volume of the film. The rate of energy dissipation is equal to the integral of the viscous dissipation function, Φ, over the film volume. Because of the vertical symmetry, the only nonvanishing terms in Φ are[28]

$$\Phi = \mu_2 \left\{ \left[2\left(\frac{1}{r \sin \theta} \frac{\partial u_\phi}{\partial \phi} \right)^2 \right] + \left[\frac{\sin \theta}{r} \frac{\partial}{\partial \theta} \left(\frac{u_\phi}{\sin \theta} \right) \right]^2 + \left[r \frac{\partial}{\partial r} \left(\frac{u_\phi}{r} \right) \right]^2 \right\} . \tag{13}$$

Here μ_2 is the absolute viscosity of the phase 2 liquid, and θ is the azimuthal angle of the spherical coordinate system.

Let us investigate the magnitudes of the partial derivatives appearing in Eq. (13). It can be easily shown that u_ϕ contains variable terms of order H^2, $\frac{\partial u_\phi}{\partial r}$ variable terms of order H, and $\frac{\partial u_\phi}{\partial \phi}$ variable terms of order H^2. Thus the energy dissipation integral reduces to

$$\iiint_V \Phi \, dv = \iiint_V \mu_2 \left(\frac{\partial u_\phi}{\partial r} \right)^2 dv =$$

$$\times \int_1^{1+H} \int_0^{p} (\cot \phi - \csc \phi)^2 \sin \phi \, R^2 (2+H-2R)^2 d\phi \, dR,$$

where

$$\chi = 2\pi\, a^3 \mu_2 \left[\frac{12(1+H)^2}{H^4+2H^3} \quad \frac{dH}{dt} \right]^2 . \tag{14}$$

The result of the integration, upon dropping all H terms of higher powers than -3 (H is much less than 1, by assumption (c), is

$$24\pi \quad \frac{a^3 \mu_2}{H^3} \left(\frac{dH}{dt}\right)^2 \quad P(p), \tag{15}$$

where

$$P(p) = \cos p - 1 - (4 \ln \cos p/2).$$

The rate of energy dissipation is equal to the rate of work done on the film by force F, or $-F\, a \frac{dH}{dt}$. Equating the rate of energy dissipation to the rate of work done, we find

$$dt = - \frac{24\, \pi a^2 \mu_2 P(p)}{F} \quad \frac{dH}{H^3} . \tag{16}$$

If F is constant, Eq. (16) can be integrated to yield the result

$$t_2 - t_1 = \frac{12\pi\, a^2 \mu_2}{F} (\cos p - 1 - 4 \ln \cos p/2) \left(\frac{1}{H_2^{\,2}} - \frac{1}{H_1^{\,2}} \right) . \tag{17}$$

A special case of Eq. (17) is of interest. In the limit as a becomes very large and p becomes very small, the thinning spherical shell approximates the case of a disc of radius c approaching an infinite plane through a viscous medium. Taking the limit of Eq. (17),

$$\lim_{\substack{a \to \infty \\ p \to 0}} \frac{(t_2 - t_1)F}{12\pi\mu_2 \left(\frac{1}{h'^{\,2}_2} - \frac{1}{h'^{\,2}_1} \right)} = \lim_{\substack{a \to \infty \\ p \to 0}} a^4 (\cos p - 1 - 4 \ln \cos p/2)$$

$$\lim_{\substack{a \to \infty \\ p \to 0}} a^4 \left[(1 - p^2/2 + p^4/24) - 1 - 4\,(-p^2/8 - p^4/192) \right] = \lim_{\substack{a \to \infty \\ p \to 0}} \frac{a^4 p^4}{16} .$$

But in the limit, c = a p, and we find

$$t_2 - t_1 = \frac{3\pi\mu_2 c^4}{4F}\left(\frac{1}{h'^2_2} - \frac{1}{h'^2_1}\right). \tag{18}$$

This is the result originally found by Reynolds.[29]

c. Drop-Approach Solution. The force F is a combination of F_U and F_D (from Eqs. (1) and (2), respectively, or twice F_U. Substituting $2\,F_U = F$ into Eq. (17), we get the final result,

$$t_2 - t_1 = \frac{3a^3\mu_2}{\sigma}\,J(p)\left(\frac{1}{h'^2_2} - \frac{1}{h'^2_1}\right), \tag{19}$$

where

$$J(p) = \frac{\cos p - 1 - (4\,\ell n \cos p/2)}{\sin^2 p}.$$

A plot of J(p) as a function of p is given in Fig. 6. If $h_1' \gg h_2'$ and if a time scale is chosen such that $t_1 = 0$, then Eq. (19) becomes the simpler form

$$t_2 = \frac{3a^3\mu_2}{\sigma}\,J(p)\left(\frac{1}{h'^2_2}\right). \tag{20}$$

Now by use of either Eq. (19), or Eq. (20) and Eq. (3), we can determine the film thickness at any time from a knowledge of the drop radius and the physical properties of the system. Plots of film thickness as a function of time for the systems water-benzene and water-anisole for several drop sizes are given in Fig. 7. Ewers and Sutherland[30] have stated that the thickness of a soap film would have to be less than 50 Å for it to be ruptured through random molecular motion. We note from Fig. 7 that, with the possible exception of the very smallest drops, the times needed for these films to decrease in thickness to 50 Å are

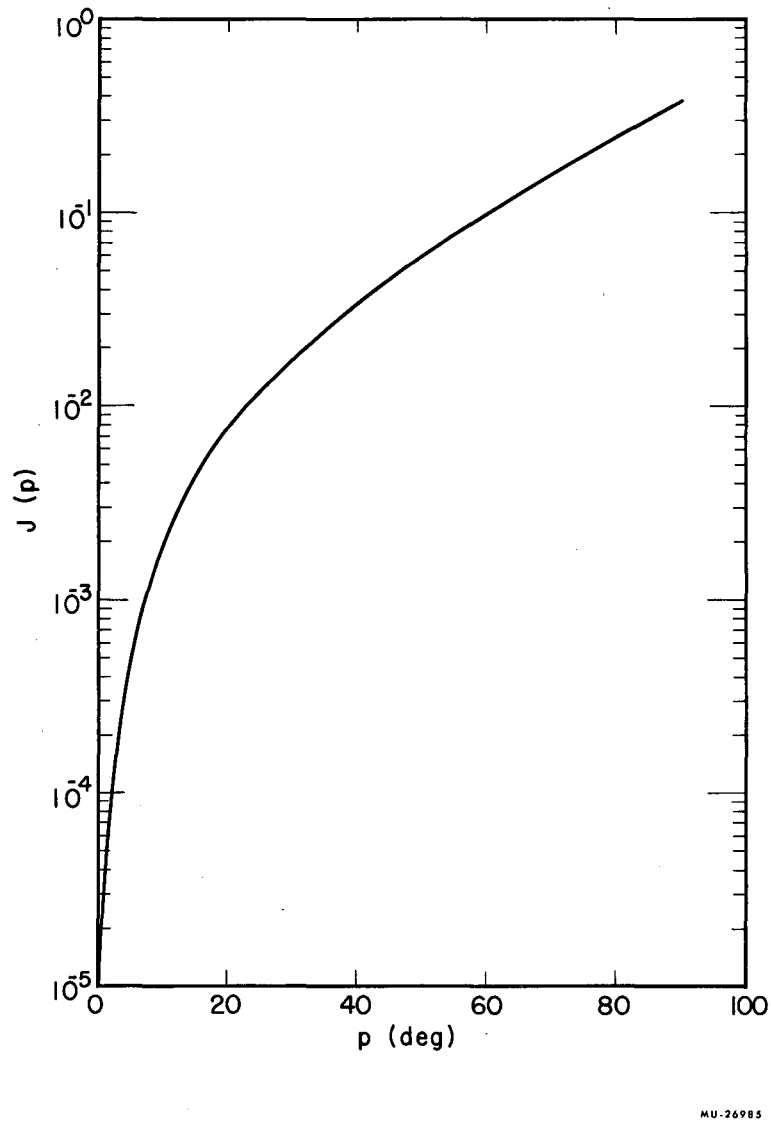

Fig. 6. Plot of J(p) as a function of p.

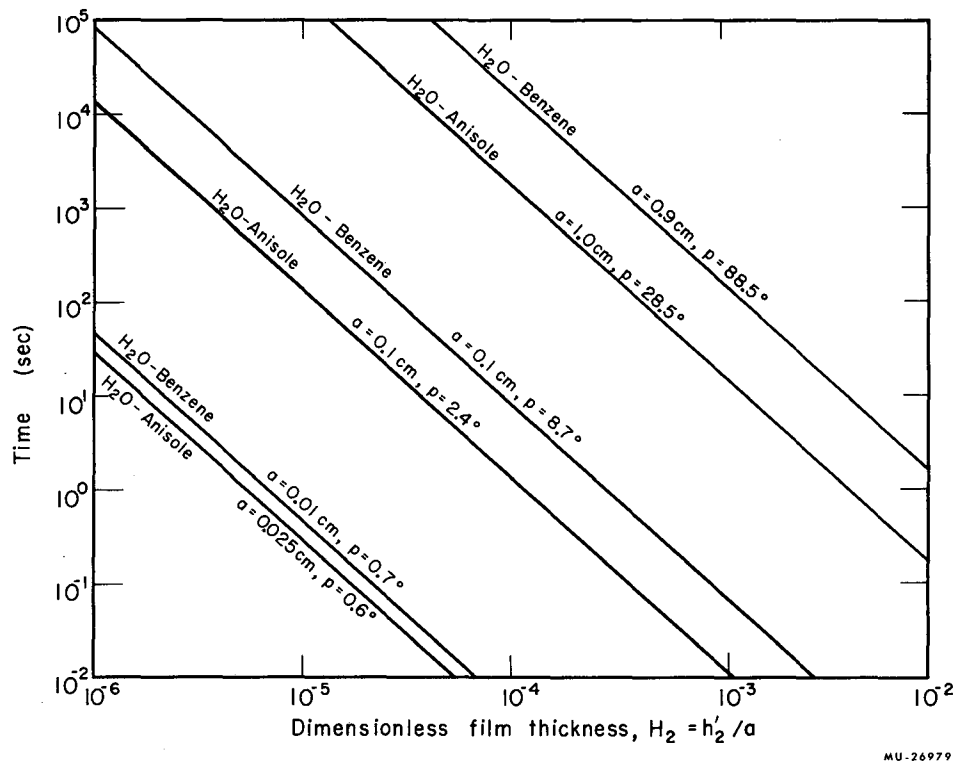

Fig. 7. Dimensionless film thickness H_2 as a function of time t_2 for the water-benzene and water-anisole systems.

several orders of magnitude greater than the experimental rest-times of 1 to 100 sec in Table XVI. We can therefore conclude that an additional mechanism other than the squeezing out of a thin film by surface and gravity forces is needed to explain drop coalescence. This additional mechanism is proposed in the next section.

d. Comparison with Flattened-Sphere Model. Several workers[9,11] have combined Eq. (18) with an expression due to Derjaguin and Kussakov,[25] to derive an expression giving the rate of approach of a flattened sphere to an infinite plane through a viscous medium. It is of interest to compare the film thicknesses calculated by means of Eq. (18) with the more realistic model of this work. Because, in both cases, the film thickness decreases with the reciprocal of the square root of the elapsed time, the ratio of the film thicknesses computed from the two models will be a constant for a given system. As one might expect, the ratio of the times for the film to decrease in thickness from H_1 to H_2 calculated from the two models, is a function of the angle p only. The ratio is

$$T = \frac{t_2 - t_1 \text{ (spherical-shell model)}}{t_2 - t_1 \text{ (flattened-sphere model)}} = 4\, J(p)\, Q(p). \tag{21}$$

A plot of this ratio as a function of p is given in Fig. 8. Note that when p is small, the spherical-shell model gives a faster rate of thinning, but when p is large, the flattened-sphere model gives the faster rate.

e. Pressure Drop in Film. Chappelear stated that the pressure drop in the flowing film might be so great as to distort an easily deformable drop and thus invalidate the assumption of uniform film thickness.[31] This possibility was investigated by solving the Navier-Stokes equations for the pressure drop. Dropping second order, time dependent, and gravitational terms, the tangential direction Navier-Stokes equation in spherical coordinates becomes[32]

$$\frac{1}{r}\frac{\partial P}{\partial \phi} = \mu_2\left[\frac{\partial^2 u_\phi}{\partial r^2} + \frac{2}{r}\frac{\partial u_\phi}{\partial r} + \frac{1}{r^2}\frac{\partial^2 u_\phi}{\partial \phi^2} + \frac{\cot\phi}{r^2}\frac{\partial u_\phi}{\partial \phi} - \frac{u_\phi}{r^2 \sin^2\phi}\right]. \tag{22}$$

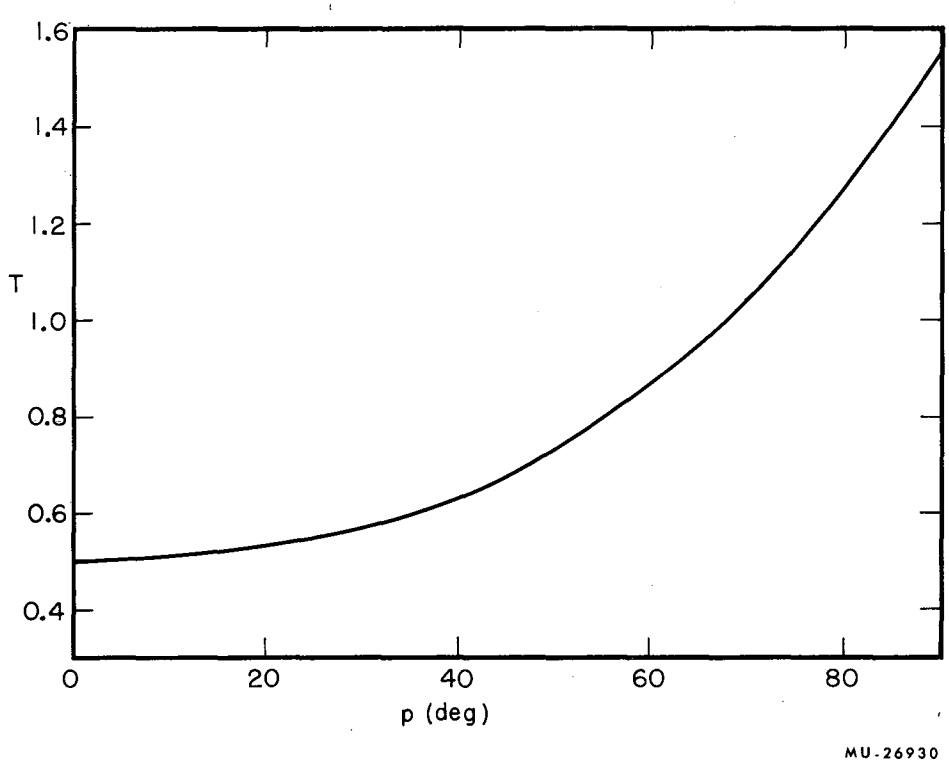

Fig. 8. Plot of T vs p.

Taking the various partial derivatives of Eq. (22), we find that

$$\frac{\partial P}{\partial \phi} = \frac{12\mu_2}{R(H^4+2H^3)} \frac{dH}{dt} (\cot\phi - \csc\phi)(-6R^2+4R+2HR). \tag{23}$$

If we note that $H \ll R$ (or equivalently, assume no pressure gradient in the r direction), Eq. (23) upon integration from $\phi = 0$ to $\phi = p$ becomes

$$P-P_o = \frac{-48\mu_2}{H^4+2H^3} \frac{dH}{dt} \ln \cos p/2 .$$

Substituting the value of dH/dt from Eq. (16), we get as the final result for the pressure drop across the film

$$\Delta P = \frac{4\sigma}{a} \frac{\ln \cos p/2}{J(p)} , \tag{24}$$

where p is found by Eq. (3).

Some values of this pressure drop for the water-benzene and water-anisole systems are given in Table I. Because these pressure drops are insignificant in comparison to the 1-atm pressure prevailing in the cell, the supposition of Chappelear appears to be incorrect.

4. Electrical Effects and Disjoining Pressure

Several additional factors might modify the results in Eq. (19) for very small values of h'. Because the theoretical and experimental studies were not designed to examine these factors, they will be discussed in a brief and qualitative manner.

a. Electroviscosity. Whenever an electrical double layer at an interface in an ionic liquid is sheared, a potential difference, known as a streaming potential, is set up in the plane of the shear. This potential will tend to retard the flow due to the effect of the potential on the ions of the double layer. Because this retardation produces an effect identical to that of viscosity, the retardation is known as the electroviscous effect. It has been studied extensively by Elton.[33,34]

Table I. Calculated pressure drop across film.

System	Drop radius (cm)	Pressure drop (dynes/cm^2)
Water-benzene	0.5	481
Water-benzene	0.05	4810
Water-anisole	1.0	214
Water-anisole	0.05	4000

Elton has calculated the change in the rate of approach of two parallel discs due to the electroviscous effect. He assumed that the Reynolds equation (18) was applicable, with the bulk viscosity replaced by a viscosity including the electroviscous effect. A numerical example of his calculations is given in Table II. The bulk viscosity was assumed

Table II. Calculated effect of electroviscosity on approach rate of two discs.[a]

Distance of separation (cm)	Time in ionic liquid (sec)	Time in non-ionic liquid (sec)
10^{-4}	2.5×10^{3}	2.4×10^{3}
5×10^{-5}	1.1×10^{4}	9.6×10^{3}
2×10^{-5}	1.4×10^{5}	6.0×10^{4}
10^{-5}	1.4×10^{6}	2.4×10^{5}
5×10^{-6}	2.0×10^{7}	9.6×10^{5}

[a] From reference 33.

to be 1 cp, the force between the disks was 1000 dynes, and the disk radius was 1 cm. He assumed that the zeta-potential in the ionic fluid was 100 mV, the dielectric constant was 80, and the electrical conductivity of the fluid was 10^{-6} ohm^{-1} cm^{-1} (these values correspond to the properties of water). It should be noted that the electroviscous effect is not of great importance until the distance of separation is less than 10^{-4} cm.

Calculated film thicknesses at coalescence (see Sec. V-A) are not much smaller than 10^{-4} cm for larger drops. In the case of Picknett's experimentation with the water-anisole system, the drop sizes were very small, and calculated viscosities based on Reynolds' thinning model showed

the predicted effect of electroviscosity.[4] Further, Picknett also observed a decrease in drop rest-times with increasing concentration of electrolyte in the aqueous phase. According to Elton's result, the effective viscosity of an electrolyte solution decreases with increasing concentration of electrolyte. Picknett's coalescence data again seems to confirm the presence of an electroviscous effect.

b. Disjoining Pressure. When a fluid is squeezed out between two bodies, a resisting force can be measured which is not due to the viscosity of the fluid. This force is a measure of the long-range attraction of the molecules of the two bodies on the molecules of the fluid. It is manifested only when the fluid layer is very thin. Derjaguin and Kussakov have termed it the disjoining pressure and have measured its magnitude in a number of systems as a function of the film thickness.[25,26] These workers forced bubbles of air or hydrogen against the lower surfaces of glass or mica sheets submerged in various liquids. A typical value of the disjoining pressure was 500 dynes/cm^2 for a film thickness of 10^{-5} cm. Theoretical calculations of Frenkel indicate that the disjoining pressure should vary as the reciprocal of the cube of the film thickness,[35] but his calculated values of the disjoining pressures were low by an order of magnitude. Elton has suggested that the disjoining pressures measured were really due to the fact that the film had not yet reached an equilibrium state.[34] Comment on this statement is beyond the scope of this work.

The disjoining pressure would alter the film model by adding an additional term to F in Eq. (16). If the term were dependent on film thickness, the integral over H would then include this additional force term. Disjoining pressure has little effect on drop rest-times if the drops are not exceedingly small.

c. Electric Double-Layer Repulsion. If the diffuse electric double layers adjacent to two interfaces overlap, the interfaces can be expected to repel one another. The magnitude of this repulsion increases with increasing potential drop across each double layer, and will increase with decreasing film thickness. Derjaguin and Kussakov state that for aqueous films, the effective double-layer thickness is 10^{-4} to 10^{-5} cm for pure water and less for electrolyte solutions.[26] This effect, therefore, is probably not of great importance in coalescence measurements in pure systems, but is extremely important when surface-active agents or electrolytes are present. The electric-double-layer effect will be discussed further in Sec. V.

D. Film Instability

The mechanism that causes the rupture of the phase 2 film and thus coalescence, is discussed in this section. Because of the great difficulty of this problem, instability is discussed in terms of highly idealized models and simple geometries. The direct application of the theory to the quantitative prediction of drop rest-times is, therefore, somewhat difficult.

1. Rayleigh Cylinder

One of the first stability analyses was performed by Lord Rayleigh on a cylinder of ideal fluid free from gravitational effects.[19,20] This problem serves as an excellent introduction to stability analysis. To illustrate a particular point, a somewhat different approach than Rayleigh's was developed in this work.

We know from everyday observation that thin cylinders or threads of liquids are inherently unstable and will break up into a geometric configuration having less surface area, namely, a series of small spheres. Rayleigh considered such a cylinder, originally of radius a_o and infinite in length, to be perturbed by an arbitrary infinitesimal disturbance. He wished to determine whether this disturbance would grow in time until the cylinder disintegrated, or whether it would decay and disappear. The disturbance (mathematically) can be expanded in a Fourier series, and, if only linear operations are performed, only a single term of the series

need be studied. The radius of the cylinder, after perturbation, can be described by

$$r = a + \alpha \sin kx, \tag{25}$$

where α is the amplitude of the component of the disturbance having a wave number, $k = 2\pi/\lambda$. The mean radius a is not necessarily equal to a_o. By physical reasoning we can see that the volume of the cylinder per wavelength must be the same both before and after perturbation is applied. For the disturbance to grow in time, the surface area of the cylinder must decrease.

We can calculate the surface area of the cylinder by means of Pappus' theorem, which states that the surface area generated by a plane curve revolved about an axis is equal to the length of that curve times the distance traveled by its centroid.[36] The length of a sine wave can be found by integrating a differential arc length element. The length of $\alpha \sin kx$ equals

$$\frac{1}{k} \int_0^{2\pi} \sqrt{1 + \alpha^2 k^2 \cos^2 X} \quad dX$$

$$= \frac{\sqrt{1 + \alpha^2 k^2}}{k} \int_0^{2\pi} \sqrt{1 - \frac{\alpha^2 k^2}{1+\alpha^2 k^2} \sin^2 X} \quad dX$$

$$= \frac{\sqrt{1 + \alpha^2 k^2}}{k} \quad E\left(2\pi, \sqrt{\frac{\alpha^2 k^2}{1+\alpha^2 k^2}}\right), \tag{26}$$

where the substitution, $X = kx$, has been made.

$$E\left(2\pi, \sqrt{\frac{\alpha^2 k^2}{1+\alpha^2 k^2}}\right)$$

is the normal elliptic integral of the second kind, and can be simplified to

$$4E\left(\sqrt{\frac{\alpha^2 k^2}{1+\alpha^2 k^2}}\right),$$

the complete elliptic integral of the second kind.[37] The elliptic integral

can be expanded in a power series, and because of the small value of the argument (α was assumed infinitesimal), the series can be terminated after the second term to yield

$$4E\left(\sqrt{\frac{\alpha^2k^2}{1+\alpha^2k^2}}\right) \approx 2\pi\left(1 - \frac{1}{4}\,\frac{\alpha^2k^2}{1+\alpha^2k^2}\right).$$

The length of the sine curve is thus

$$\frac{\sqrt{1+\alpha^2k^2}}{k}\quad 2\pi\left(1 - \frac{1}{4}\,\frac{\alpha^2k^2}{1+\alpha^2k^2}\right) \approx \frac{2\pi}{k}\left(1 + \frac{1}{4}\,\alpha^2k^2\right),$$

where several simplifications have been made. Obviously, the sine wave is longer than the length of the side of the original cylinder. The centroid of the sine wave travels $2\pi a$ in generating the surface, giving a total surface area per wavelength of

$$S = \frac{4\pi^2 a}{k}\left(1 + \frac{1}{4}\,\alpha^2k^2\right). \tag{27}$$

The volume of the cylinder can be found by a simple integration:

$$V = \frac{1}{k}\int_0^{2\pi} \pi\, r^2 dX = \frac{2\pi^2a^2}{k} + \frac{\alpha^2\pi^2}{k}. \tag{28}$$

But this volume must equal the volume of the unperturbed cylinder, $2\pi^2a_o^{\,2}/k$. Equating the two volumes, we find

$$a \approx a_o\left(1 - \frac{1}{4}\,\frac{\alpha^2}{a_o^{\,2}}\right). \tag{29}$$

Thus the mean radius of the perturbed cylinder is less than the radius of the original cylinder. Substituting Eq. (29) into Eq. (27), we find the new surface area is

$$S = 4\pi^2\,\frac{a_o}{k}\left(1 - \frac{1}{4}\,\frac{\alpha^2}{a_o^{\,2}} + \frac{1}{4}\,\alpha^2k^2\right). \tag{30}$$

Subtracting out the original surface area, the change in area due to perturbation is

$$\Delta S = \frac{\pi^2 a_o \alpha^2}{k} \left(k^2 - \frac{1}{a_o^2}\right) . \tag{31}$$

If we have $ka_o < 1$, the surface area decreases upon perturbation and the criteria of stability of the Rayleigh cylinder has been found. The resolution of the paradox concerning the length of a generating line in the surface is that, to compensate for the greater volume of fluid that is included in the peaks of the sine wave than is excluded from the valleys, the mean radius of the perturbed cylinder must decrease. It will be demonstrated later in this section that a similar situation does not occur in the case of a sphere.

Rayleigh showed that if $ka_o < 1$, the Fourier components of the disturbance grow exponentially in time. Depending upon the original amplitude of the components and their time constants, one or more will grow to a size comparable to the radius of the cylinder and cause it to disintegrate. Rayleigh computed the values of the time constants using ideal fluid theory, but the study has been extended to cases with a real inner fluid,[38,39] and with both real inner and outer fluids.[40,41] In these cases, the viscosity caused the magnitudes of the time (or growth) constants to decrease, but it did not affect the stability criteria. This fact is characteristic of stability studies.

Rayleigh also showed that a wavelength 4.508 times the initial cylinder diameter grows in amplitude more rapidly than any other. As an example, he showed that a disturbance corresponding to a 4.508 cm wave length on a 1-cm jet would grow as $\exp[t/0.115]$. Boys confirmed the theory experimentally in a qualitative manner,[42] and Castleman has applied the theory to atomization studies.[43]

The driving force for this, the Rayleigh instability, is the decrease in potential energy of the system due to a decrease in surface area. The next subsection considers an instability due to another type of driving force.

2. Flat Film-Taylor Instability

Suppose that a glass of water is resting on a table. Experience tells us that any small irregularities in the surface will tend to be damped out. However, if we turn that glass of water upside down, the iregularities will become very jagged and spikes of water and air will form. This example is an illustration of the Taylor instability. If an interface is accelerated normal to itself in a direction from the denser to the less dense medium, the interface is stable and irregularities will die out. (By convention, the acceleration to which a system is subjected is oppositely directed to the force acting on it.) However, if an interface is accelerated in a direction from the less dense to the denser medium, irregularities of the surface will tend to grow. In this study, the only acceleration of interest is due to gravity. Therefore, the driving force for the Taylor instability is the reduction of the gravitational potential energy of a system.

The Taylor instability was proposed by Taylor[21] for an ideal fluid and was checked experimentally by Lewis.[44] Bellman and Pennington extended the theory to include the effects of surface tension and viscosity.[22] Bankoff has proposed a model of high-flux heat transfer based on the effect,[24] and Aranow and Witten have explained the origin of Schaefer's expansion patterns by means of the theory.[45]

a. Inviscid Solution. The Taylor instability will now be used to explain why the thin film of phase 2 liquid described in Sec. C above disintegrates in much less time than that calculated from the drop-approach model alone. The analysis is based on the following major assumptions:

(a) The fluids behave in a nonviscous manner and their state of motion can be described by a velocity potential. The inviscid restriction is relaxed in the next subsection. The fluids are incompressible.

(b) For simplicity, a two-dimensional problem will be solved, i.e., the fluid velocities do not vary in the y direction. This assumption is not a very restrictive one and relaxation of it produces results similar to those found below.

(c) Only infinitesimal disturbances will be considered. This restriction is caused by the mathematical difficulties of treating a more general, nonlinear case.

(d) All velocities are very small.

Suppose a layer of fluid density, ρ_2, and thickness, 2h, to lie between two semi-infinite (in the z direction) layers of fluid, the upper fluid with a density ρ_1; the lower one a density ρ_3. At a time t = 0 the interfaces are perturbed in an arbitrary manner. The form of the interfaces can be expressed at any instant later, not violating assumption (c), by the following expressions, which are the decomposition of the disturbance into a Fourier series

$$\eta_h = \sum_{n=1}^{\infty} \alpha_{h,n} \exp[q_n t] \cos k_n x + h,$$

and

$$\eta_{-h} = \sum_{n=1}^{\infty} \alpha_{-h,n} \exp[q_n t] \cos k_n x - h . \tag{32}$$

Here, the amplitude corresponding to a wave number k_n is α_n. The growth constant q is the quantity of interest. If q is real and positive, the disturbance will grow in time; if it is real and negative, the disturbance will be damped out; and if it is imaginary, the disturbance will remain the same in magnitude, but the surface will oscillate in a periodic manner. If q is imaginary, $q = C_p k$, where C_p is the phase velocity of the waves. Because only linear operations will be performed, we can solve this problem in terms of a single Fourier component and then generalize the result. Therefore, let the surfaces be represented instead by

$$\eta_h = \alpha \exp[qt] \cos kx + h,$$

and

$$\eta_{-h} = -\beta \exp[qt] \cos kx - h . \tag{33}$$

The geometry is depicted schematically in Fig. 9. At this point, the goal of this computation can be seen. If one or both of the waves grow exponentially in time, they will quickly achieve such an amplitude that the film will be ruptured. It is not necessary for the film to become thinner only under the action of ordinary surface and gravity forces, because a new driving force for film rupture has been considered.

The motion of each layer of fluid must obey the equation of continuity, which, by assumption (a) is expressed by Laplace's equation

$$\nabla^2 \Phi = \frac{\partial^2 \Phi}{\partial x^2} + \frac{\partial^2 \Phi}{\partial z^2} = 0,$$

where Φ is the velocity potential.

By use of the method of separation of variables, a solution of the form

$$\Phi = \cos kx \, (A \exp[kz] + B \exp[-kz])$$

is found. Because the velocity potential of the two semi-infinite masses of fluid must vanish at infinity, the three velocity potentials in the system can be written

$$\begin{aligned} \Phi_1 &= A \cos kx \exp[-kz]; \\ \Phi_2 &= (B \exp[-kz] + C \exp[kz]) \cos kx; \\ \Phi_3 &= D \cos kx \exp[kz]. \end{aligned} \tag{34}$$

The constants A, B, C, and D, can be found from the kinematic boundary condition, noting assumption (c):[46]

$$\left(\frac{\partial \eta}{\partial t}\right) = -\left(\frac{\partial \Phi}{\partial z}\right)_{\text{interface}} \tag{35}$$

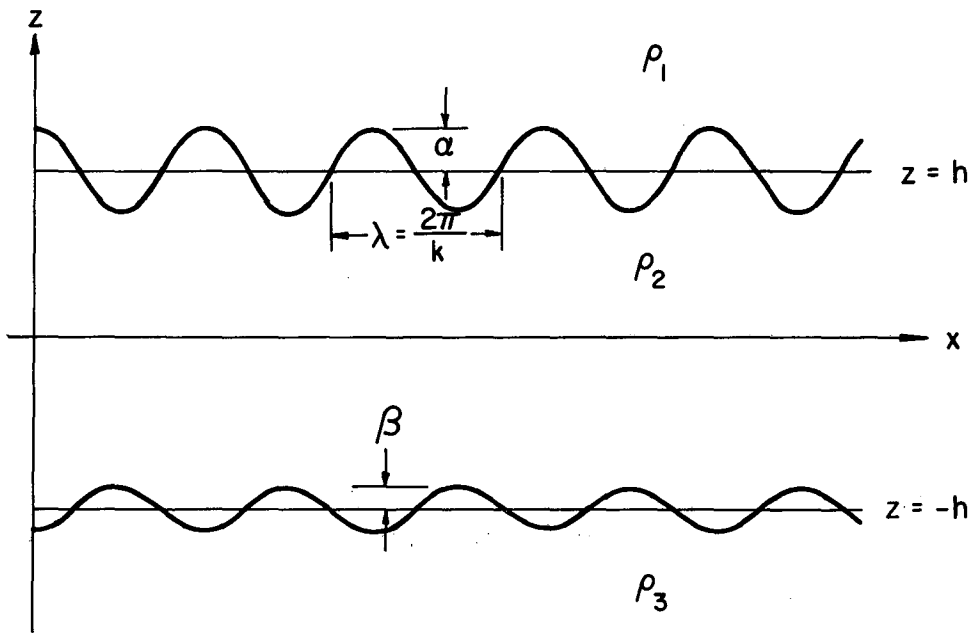

MU-26934

Fig. 9. Sketch of geometry of flat-film model with Taylor instability. Waves shown correspond to Eq. (33) at $t = 0$.

If the necessary differentiations are performed on Eqs. (33) and (34), the following algebraic equations result:

$$\alpha q \exp[qt] \cos kx = Ak \exp[-hk] \cos kx$$

$$= (Bk \exp[-hk] - Ck \exp[hk]) \cos kx,$$

and

$$-\beta q \exp[qt] \cos kx = (Bk \exp[hk] - Ck \exp[-hk]) \cos kx$$

$$= -Dk \exp[-hk] \cos kx .$$

These equations can easily be solved by determinants to yield the constants,

$$A = \frac{\alpha q}{k} \exp[qt + hk] ,$$

$$B = -\frac{\beta q \exp[qt]}{2k \sinh 2hk} (\gamma \exp[-hk] + \exp[hk]),$$

$$C = -\frac{\beta q \exp[qt]}{2k \sinh 2hk} (\exp[-hk] + \gamma \exp[hk]), \tag{36}$$

and

$$D = \frac{\beta q}{k} \exp[qt + hk],$$

where amplitude ratio, $\gamma \equiv \alpha/\beta$ has been defined.

The velocity potentials in the three phases may be related to one another with the equations of motion. By use of assumption (a), the equations can be integrated to give[47]

$$\frac{P}{\rho} = \frac{\partial \Phi}{\partial t} - \Omega - u^2 , \tag{37}$$

where a constant has been absorbed into the derivative term.

Further, by use of assumption (d), the term involving the square of the velocity u^2 can be dropped, and the equations become

$$\frac{P}{\rho} = \frac{\partial\Phi}{\partial t} - gz, \tag{38}$$

where the potential term Ω has been replaced with gz because only gravitational forces need be considered.

Let us first look at the case of no interfacial tension. Then the dynamic boundary condition requires that there be no discontinuity in pressure across the interfaces. If Eq. (38) is written for each phase, and the pressures are equated at the interfaces, we derive the two equations

$$\rho_1 \left(\frac{\partial\Phi_1}{\partial t}\right)_{z=h} - g\rho_1\eta_h = \rho_2 \left(\frac{\partial\Phi_2}{\partial t}\right)_{z=h} - g\rho_2\eta_h , \tag{39}$$

and

$$\rho_2 \left(\frac{\partial\Phi_2}{\partial t}\right)_{z=-h} - g\rho_2\eta_{-h} = \rho_3 \left(\frac{\partial\Phi_3}{\partial t}\right)_{z=-h} - g\rho_3\eta_{-h} . \tag{40}$$

If the changes of variables, $\xi \equiv z-h$ and $\zeta \equiv z+h$ are introduced into Eqs. (39) and (40) respectively, the equations become

$$\rho_1 \left[\frac{\partial\Phi_1(\xi+h)}{\partial t}\right]_{\xi=0} - g\rho_1(\alpha \exp[qt] \cos kx)$$

$$= \rho_2 \left[\frac{\partial\Phi_2(\xi+h)}{\partial t}\right]_{\xi=0} - g\rho_2(\alpha \exp[qt] \cos kx),$$

and

$$\rho_2 \left[\frac{\partial\Phi_2(\zeta-h)}{\partial t}\right]_{\zeta=0} - g\rho_2(-\beta \exp[qt] \cos kx)$$

$$= \rho_3 \left[\frac{\partial\Phi_3(\zeta-h)}{\partial t}\right]_{\zeta=0} - g\rho_3(-\beta \exp[qt] \cos kx) .$$

Evaluating these expressions at t = 0, we find

$$\frac{\rho_1\gamma q^2}{k} - g\rho_1\gamma = \frac{-\rho_2 q^2}{k \sinh 2hk} (\gamma \cosh 2hk + 1) - g\rho_2\gamma, \tag{41}$$

and

$$\frac{-\rho_2 q^2}{k \sinh 2hk} (\gamma + \cosh 2hk) + g\rho_2 = \frac{\rho_3 q^2}{k} + g\rho_3 . \tag{42}$$

Equations (41) and (42) can each be solved for γ,

$$\gamma = \frac{-\dfrac{\rho_2 q^2}{k \sinh 2hk}}{\dfrac{\rho_1 q^2}{k} + g(\rho_2-\rho_1) + \dfrac{\rho_2 q^2}{k} \coth 2hk} , \tag{43}$$

and

$$\gamma = \frac{\dfrac{\rho_3 q^2}{k} + g(\rho_3-\rho_2) + \dfrac{\rho_2 q^2}{k} \coth 2hk}{-\dfrac{\rho_2 q^2}{k \sinh 2hk}} . \tag{44}$$

Now, if γ is eliminated from Eqs. (43) and (44) we obtain after some simplification the following quartic equation for q

$$q^4[\rho_1\rho_3 + \rho_2^2 + (\rho_1\rho_2 + \rho_2\rho_3) \coth 2hk]$$

$$+ q^2[\rho_2 kg(\rho_3-\rho_1) + \rho_2 kg(\rho_3-\rho_1) \coth 2hk]$$

$$+ k^2g^2(\rho_2-\rho_1)(\rho_3-\rho_2) = 0 . \tag{45}$$

If, now, we assume for simplicity that $\rho_1=\rho_3$ (which is the physical situation in coalescence), we can solve Eq. (45) for q^2

$$q^2 = \pm \frac{kg(\rho_2-\rho_1)}{(\rho_1^2 + \rho_2^2 + 2\rho_1\rho_2 \coth 2hk)^{1/2}} \quad . \tag{46}$$

From this striking result, we see that there are not just two, but four, growth constants. The two imaginary values of q correspond to waves traveling in the positive and negative x directions, the negative real value corresponds to damping, and the positive real value represents instability. The sign of the density difference term does not affect the presence or absence of a real positive q. To resolve this paradoxical situation, let us look at the case when h is very large; then Eqs. (43), (44), and (46) reduce to

$$\gamma = -\frac{\rho_1}{\rho_2} \sinh 2hk - \frac{kg(\rho_1-\rho_2)}{\rho_2 q^2} \sinh 2hk - \cosh 2hk, \tag{47}$$

and

$$q^2 = \pm \frac{(\rho_1-\rho_2)kg}{\rho_1+\rho_2} \quad . \tag{48}$$

Suppose ρ_1 is greater than ρ_2; from physical intuition we would expect the upper interface to be unstable, and the lower one stable. Substitute the positive value of q^2 from Eq. (48) into Eq. (47). We then find that

$$\gamma = -\left(2\frac{\rho_1}{\rho_2} + 1\right) \sinh 2hk - \cosh 2hk,$$

which has a very large absolute value (the negative sign merely indicates that our sign convention in Eq. (33) was incorrect). Thus, the unstable wave is of much greater initial amplitude at the upper interface than at the lower as expected. If we substitute the negative value of q^2 into Eq. (47), we find

$$\gamma = \sinh 2hk - \cosh 2hk,$$

which approaches zero as h becomes large. This indicates that the stable wave exists predominantly at the lower interface, again confirming our intuition. Suppose now that h is very small. Then γ in Eq. (43) approaches -1, and we see that both the stable and the unstable waves must have equal initial amplitude.

Before continuing, we can summarize two important conclusions. First, in a system containing two free interfaces, two wave systems exist corresponding to a single wave number. If the interfaces are far apart, the wave systems act independently of one another, each in a separate interface. If the two interfaces are close together, however, both wave systems exist in each interface, the relative initial amplitudes of the waves in the upper and lower interfaces depending upon γ. Second, if a denser phase overlies a less dense phase in the layered system, the system will always be inherently unstable. The growth constant of the instability increases without limit as the wave number increases.

Let us now see how these results are modified by the inclusion of interfacial tension. The Young-Laplace equation,[48] shows that the difference in pressure on the two sides of an interface is not zero, but is equal to the interfacial tension times the sum of the reciprocals of the radii of curvature of the interface. By assumption (c), these pressure differences are[47]

$$(P_1-P_2)_h = \sigma\left(\frac{\partial^2\eta_h}{\partial x^2}\right) = -\sigma(\alpha k^2 \exp[qt] \cos kx), \tag{49}$$

and

$$(P_2-P_3)_{-h} = \sigma\left(\frac{\partial^2\eta_{-h}}{\partial x^2}\right) = \sigma(\beta k^2 \exp[qt] \cos kx). \tag{50}$$

The effect of Eqs. (49) and (50) is to add the term σk^2 to the denominator of Eq. (43) and the numerator of Eq. (44). The quartic equation in q now becomes

$$q^4[\rho_1\rho_3 + \rho_2^2 + (\rho_1\rho_2 + \rho_2\rho_3) \coth 2hk]$$

$$+ q^2[\rho_2 kg(\rho_3-\rho_1)(1+\coth 2hk) + \sigma k^3(\rho_1+\rho_3)$$

$$+ 2\sigma k^3\rho_2 \coth 2hk]$$

$$+[k^2g^2(\rho_2-\rho_1)(\rho_3-\rho_2) + \sigma k^4 g(\rho_3-\rho_1) + \sigma^2 k^6] = 0. \tag{51}$$

If again we let $\rho_1=\rho_3$, Eq. (51) can be solved for q^2 by the quadratic formula to yield

$$q^2 = \frac{-(\sigma k^3\rho_1 + \sigma k^3\rho_2 \coth 2hk) \pm \sqrt{R_1}}{\rho_1^2 + \rho_2^2 + 2\rho_1\rho_2 \coth 2hk}$$

where

$$R_1 = k^6[\sigma^2\rho_2^2 (\coth^2 2hk-1)]$$

$$+ k^2[g^2(\rho_1-\rho_2)^2(\rho_1^2+\rho_2^2 + 2\rho_1\rho_2 \coth 2hk)\ ]. \tag{52}$$

Two criteria now determine the region of stability of the film. Negative values of q^2 (stability regions) will always result both if the radicand in Eq. (52) is always $\geqslant 0$, and if the numerator of Eq. (52) is always negative. Because the term $(\coth^2 2hk -1)$ is always $\geqslant 0$, the radicand is always $\geqslant 0$. The second condition is fulfilled if

$$k \geqslant \left[\frac{g}{\sigma} (\rho_1-\rho_2)\right]^{1/2}, \text{ for } \rho_1 > \rho_2 . \tag{53}$$

We have derived an upper limit on the value of wave numbers that will permit instability to develop. The limit is based only on physical properties, not geometrical ones. The result is the same as that found by

Bellman and Pennington for a single interface.[22] If, now we eliminate q^2 between Eqs. (43) and (44) (including the σk^2 terms), we are able to derive the following expression for γ,

$$\gamma = \frac{-2g(\rho_1-\rho_2)(\rho_1 \sinh 2hk + \rho_2 \cosh 2hk) \pm \sqrt{R_2}}{2\theta\rho_2}$$

where

$$R_2 = [2g(\rho_1-\rho_2)(\rho_1 \sinh 2hk + \rho_2 \cosh 2hk)]^2 + 4\theta\psi\rho_2^{\,2};$$

$$\theta = g(\rho_1-\rho_2) - \sigma k^2 ,$$

$$\psi = -g(\rho_1-\rho_2) - \sigma k^2 . \tag{54}$$

By allowing h to become very large, we can see which choice of the sign of the radical corresponds to the wave normally predominant at the upper interface and which corresponds to that predominant at the lower. It is easily shown that a choice of + for the sign will give very small values of γ, and a choice of - will give large values, which corresponds to the wave of instability. These results are in agreement with those of Keller and Kolodner,[23] if we further assume that $\rho_1 = 0$.

We have reached an additional interesting conclusion, in showing that the presence of a nonzero interfacial tension has placed an upper limit upon the value of the wave number k that will cause an instability to propagate. It is obvious that the real positive value of q must reach a maximum between k = 0 and $k = \left[\frac{g}{\sigma}(\rho_1-\rho_2)\right]^{1/2}$. This is shown in Fig. 10, where values of q vs k for different film thicknesses are presented. Physical properties corresponding to the water-benzene system were used in making the plot. Corresponding values of γ are shown in Fig. 11. We note that if 2h is large, the values of q corresponding to a given k are large, but the values of γ corresponding to the unstable wave are small.

Let us now apply this discussion to the coalescence of a liquid drop. From the stability criterion, Eq. (53), we note that the smallest wavelength that can cause instability is still much larger than the

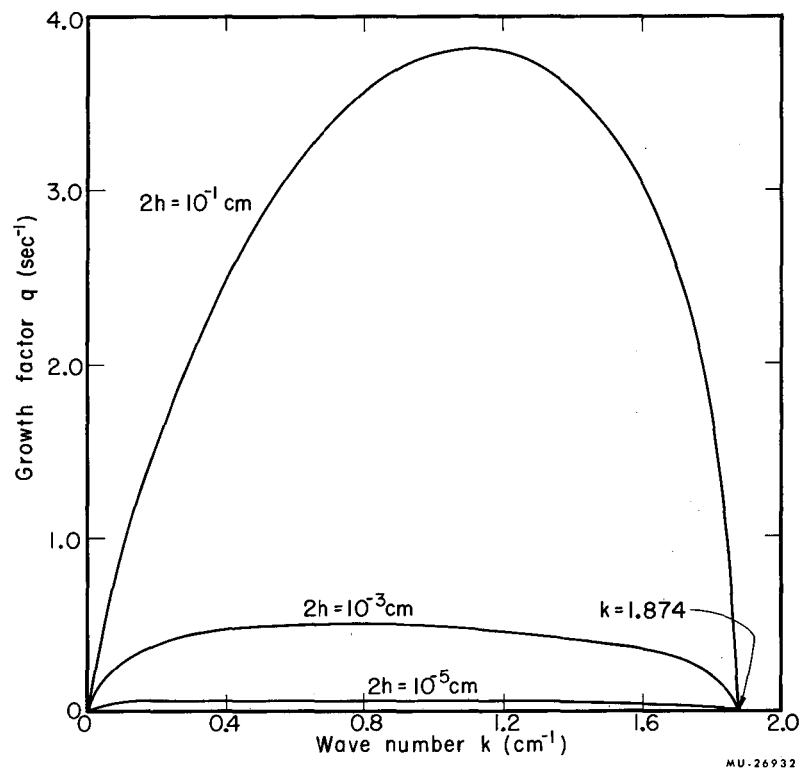

Fig. 10. Growth factor as a function of wave number for several film thicknesses. Physical properties used correspond to the water-benzene system.

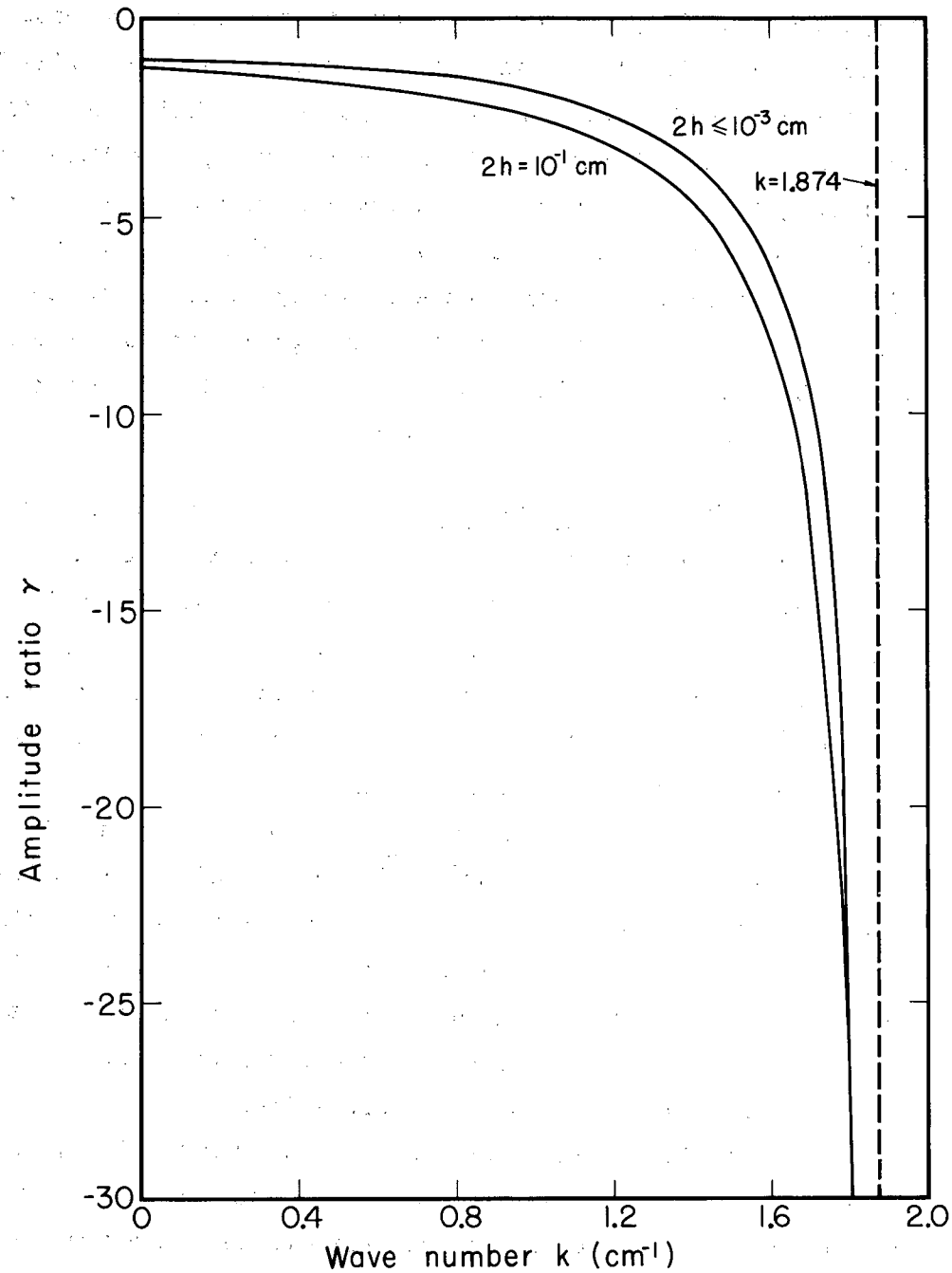

Fig. 11. Amplitude ratio corresponding to the unstable disturbance as a function of wave number and film thickness. Physical properties used correspond to the water-benzene system.

diameter of most liquid drops. Therefore, for an instability to develop, the longer wavelengths must originate in the interface between the phases rather than on the lower surface of a drop. This wave will be stable on the lower interface because here ρ_2 is above. This wave will be propagated through the phase 2 film to the upper (or drop) interface. The efficiency of propagation γ increases as 2hk becomes smaller, i.e., for a given value of film thickness, the efficiency is highest for large wavelengths (small k); for a given wavelength, the efficiency increases as the film becomes thinner. The rate at which instability grows depends upon both h and k, as can be seen in Fig. 10. This discussion will be incorporated with the drop-approach model in a later section.

b. Effect of Viscosity. The exact solution for the effect of viscosity on the stability of a free surface entails the solution of the Navier-Stokes equations. Bellman and Pennington solved the problem for a single free surface and found that it was only possible to find an upper bound for the values of q^2 without resorting to lengthy numerical techniques.[22] They found that viscosity had no effect on the stability criterion but that it did decrease the values of q^2.

A method has been developed by Stokes for computing the rate of viscous damping of surface waves.[47] The method involves the very strong assumptions that the flow be irrotational, and that velocities be very small at points distant from the interface. If, however, the viscosities of the two phases are small and of the same order of magnitude, this method produces results very similar to those obtained by means of the Navier-Stokes equations, even though the assumptions are partially violated. Several situations will be examined to illustrate this point. Because an unstable wave grows in amplitude as a positive exponential term and viscous damping acts as a negative exponential, the value of the growth constant with viscous damping is given by

$$q_v = q + \tau , \tag{55}$$

where τ is the viscous damping constant.

The method consists of equating the average rate of dissipation of energy due to viscosity to the rate of change of the energy contained in the progressive surface waves. The amplitude of the waves then decreases proportionally to the term, $\exp[\tau t]$. If we assume that the motion is irrotational, the average rate of dissipation of energy is[47]

$$\overline{\dot{E}_D} = \left[- \mu \iint_{\Sigma} \frac{\partial u^2}{\partial n} \, ds \right]_{av} \tag{56}$$

where $u = -\nabla\Phi$ and $\frac{\partial}{\partial n}$ represents differentiation with respect to the outward normal. The integration is performed over the bounding surfaces of the fluid mass and the bar indicates a time average. The total energy (both potential and kinetic) contained in the progressive waves is given by[47]

$$\overline{E_W} = \left[\rho \iint_{\Sigma} \Phi \frac{\partial \Phi}{\partial n} \, ds \right]_{av} . \tag{57}$$

If we equate the average rate of dissipation of energy to the rate of change of the wave energy,

$$\overline{\dot{E}_D} = \frac{d\overline{E}_W}{dt} ,$$

we find that

$$\tau = \frac{\left| \overline{\dot{E}_D} \right|}{2 \, \overline{E}_W} . \tag{58}$$

Let us first calculate τ for the case of two superposed fluids. By study of Eq. (34), we see that the velocity potentials will be of the form

$$\Phi_1 = C_1 \exp[-kz] \cos(kx-qt),$$

and

$$\Phi_2 = C_2 \exp[kz] \cos(kx-qt),$$

where C is a constant, and 1 and 2 represent the upper and lower phases, respectively. These potentials stand for progressive waves. The velocity in each phase is found by computing the negative gradient of the velocity potential. If the amplitude of the waves is infinitesimal, the normal derivatives can be found by differentiating in the z direction. The results of the integrations over surface areas one wave length λ in the x direction and unity in the y direction are

$$\overline{\dot{E}_{D_1}} = -2k^3\mu_1 C_1^2\lambda,$$

$$\overline{\dot{E}_{D_2}} = -2k^3\mu_2 C_2^2\lambda,$$

$$\overline{E}_{W_1} = \frac{1}{2}\rho_1 k C_1^2\lambda;$$

and

$$\overline{E}_{W_2} = \frac{1}{2}\rho_2 k C_2^2\lambda .$$

From Eq. (58) we find the viscous damping factor as

$$\tau = -2k^2 \frac{\mu_1+\mu_2}{\rho_1+\rho_2} \tag{59}$$

This is the same result as obtained by Bankoff.[49] Koussakov computed the viscous damping coefficient by means of the Navier-Stokes equations and found (for low viscosities),[50]

$$\tau = -2k^2 \frac{\xi\rho_1\mu_1 + \rho_2\mu_2}{(\xi\rho_1+\rho_2)(\rho_1+\rho_2)} , \tag{60}$$

where

$$\xi = \left(\frac{\rho_1\mu_2}{\rho_2\mu_1}\right)^{1/2} .$$

If the viscosities of the two phases are small, Koussakov's result is very similar to that of Eq. (59). If the results of Eq. (59) are used to compute q_v by means of Eq. (55), we find

$$q_v = \left[kg \frac{(\rho_1-\rho_2)}{(\rho_1+\rho_2)} \right]^{1/2} -2k^2 \frac{\mu_1+\mu_2}{\rho_1+\rho_2} , \tag{61}$$

where the value of q for two superposed layers was taken from Taylor.[21] Bellman and Pennington estimated an upper bound for q_v of

$$q_v < \left[kg \frac{(\rho_1-\rho_2)}{(\rho_1+\rho_2)} + k^4\left(\frac{\mu_1+\mu_2}{\rho_1+\rho_2}\right)^2 \right]^{1/2} - k^2 \frac{\mu_1+\mu_2}{\rho_1+\rho_2} .$$

The approximate method gives a result slightly less than the upper bound estimate. On the basis of these two comparisons, the approximate method seems to yield good results, provided the viscosities are low.

Let us now apply this technique to the thin-film case discussed in the previous section. For simplicity, velocity potentials of progressive waves are used instead of the stationary-wave velocity potentials of Eqs. (34) and (36). If the surface integrals of Eqs. (56) and (57) are evaluated and the results simplified, we find

$$\overline{\dot{E}}_{D,1} = -2\mu_1 k \beta^2\gamma^2 q^2 \lambda ,$$

$$\overline{\dot{E}}_{D,2,U} = - \frac{\mu_2 k \beta^2 q^2 \lambda}{\sinh^2 2hk} (\gamma^2 \sinh 4hk + 2\gamma \sinh 2hk),$$

$$\overline{\dot{E}}_{D,2,L} = - \frac{\mu_2 k \beta^2 q^2 \lambda}{\sinh^2 2hk} (2\gamma \sinh 2hk + \sinh 4hk),$$

$$\overline{\dot{E}}_{D,3} = - 2\mu_3 k \beta^2 q^2 \lambda,$$

$$\bar{E}_{W,1} = \frac{\rho_1 \beta^2 \gamma^2 q^2 \lambda}{2k},$$

$$\bar{E}_{W,2,U} = \frac{\rho_2 \beta^2 q^2 \lambda}{4k \sinh^2 2hk} (\gamma^2 \sinh 4hk + 2\gamma \sinh 2hk),$$

$$\bar{E}_{W,2,L} = \frac{\rho_2 \beta^2 q^2 \lambda}{4k \sinh^2 2hk} (2\gamma \sinh 2hk + \sinh 4hk),$$

and

$$\bar{E}_{W,3} = \frac{\rho_3 \beta^2 q^2 \lambda}{2k}, \tag{62}$$

where 1, 2, and 3 indicate the three liquid layers, and the subscripts U and L denote whether the surface integration was over the upper or lower interface, respectively.

Because the waves in one interface determine the amplitudes of the waves in the other interface through the ratio γ, we can assume that τ is given by Eq. (58), where $\bar{\dot{E}}_D$ and $\bar{E}_W$ are the totals of the contributions of both interfaces. Then, the damping factor is

$$\tau = \frac{-2k^2 \left\{ (\gamma^2+1)\mu_1 + \frac{\mu_2}{2 \sinh^2 2hk} \left[(\gamma^2+1)(\sinh 4hk + 4\gamma \sinh 2hk\right] \right\}}{\rho_1(\gamma^2+1) + \frac{\rho_2}{2 \sinh^2 2hk} \left[(\gamma^2+1) \sinh 4hk + 4\gamma \sinh 2hk)\right]} \tag{63}$$

where $\rho_1=\rho_3$ and $\mu_1=\mu_3$.

The limiting cases for small and large values of 2hk are of interest. When 2hk is very small, τ becomes

$$\lim_{2hk \to 0} = -2k^2 \frac{(\gamma^2+1)\mu_1 + \frac{\mu_2}{\sinh 2hk}(\gamma+1)^2}{(\gamma^2+1)\rho_1 + \frac{\rho_2}{\sinh 2hk}(\gamma+1)^2} . \tag{64}$$

where 2hk is large, τ becomes

$$\lim_{2hk \to \text{large}} \tau = -2k^2 \frac{\mu_1+\mu_2}{\rho_1+\rho_2} . \tag{65}$$

As a check on the assumption that we should add the contributions of the two interfaces, we can easily show that an energy rate balance around each interface individually, if 2hk is large, produces the same result as Eq. (65).

A graph of values of τ for various film thicknesses is given in Fig. 12. For low viscosity fluids, the correction to the growth factor is quite small.

3. Spherical-Shell Film-Rayleigh Instability

We have seen that a cylinder is inherently unstable because its curved surfaces decrease in surface area when they are perturbed. Is the same situation also true in the case of a spherical-shell film? This question will be investigated by the same technique used to study the stability of the flat film with one exception. The effect of gravity will be ignored because of the extreme difficulty of describing its effect on a curved surface.

The following assumptions are made in the treatment of the spherical shell model:

(a) The model is geometrically a spherical shell very thin in comparison to its radius.

(b) The liquids dealt with are inviscid and their velocities can be described by a velocity potential. The validity of this assumption is ascertained by studying the effect of viscosity on a flat film.

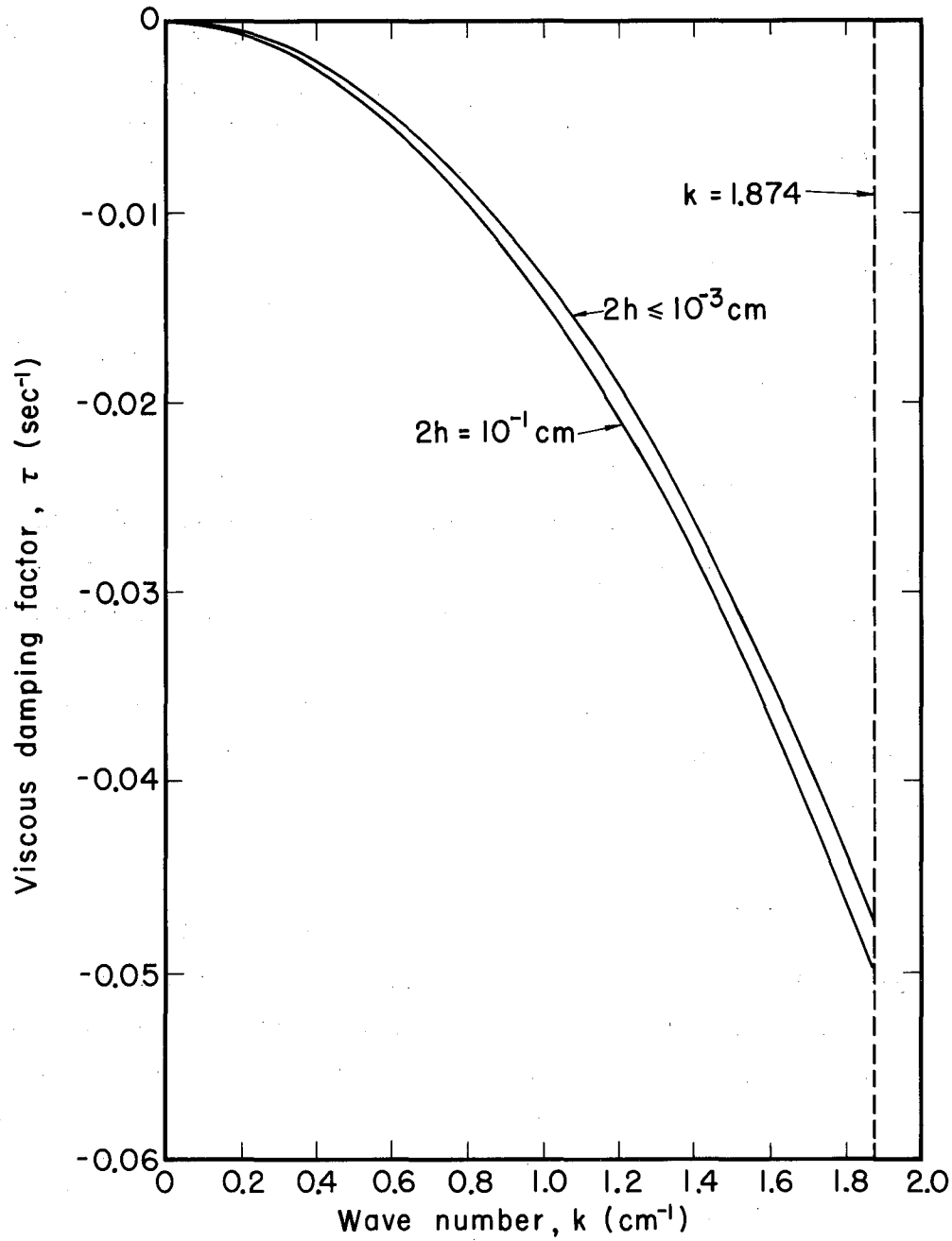

MUB-1112

Fig. 12. Viscous-damping factor as a function of wave number for various film thicknesses. Physical properties correspond to water-benzene system.

(c) The effect of gravity on the model is negligible.

(d) The velocity patterns are symmetrical about a vertical axis.

(e) Disturbances produce initially infinitesimal perturbations of the spherical surfaces.

A sketch of the model is given in Fig. 13. Because of assumption (b), the fluid flow in each of the three regions obeys Laplace's equation which, in spherical coordinates, is

$$\nabla^2\Phi = \frac{1}{r^2} \frac{\partial}{\partial r}\left(r^2 \frac{\partial\Phi}{\partial r}\right) + \frac{1}{r^2 \sin\phi} \frac{\partial}{\partial\phi}\left(\sin\phi \frac{\partial\Phi}{\partial\phi}\right) = 0. \tag{65}$$

To solve Eq. (65) by the method of separation of variables, we substitute $\Phi(r,\phi) = R(r)\, X(\phi)$, and find

$$r^2 \frac{d^2R}{dr^2} + 2r \frac{dR}{dr} - n(n+1)\, R=0, \tag{66}$$

and

$$\frac{1}{\sin\phi} \frac{d}{d\phi}\left(\sin\phi \frac{dX}{d\phi}\right) + n(n+1)\, X=0, \tag{67}$$

where $n(n+1)$ is the separation constant.
The first of these is Cauchy's equation, and by making the transformation $r = e^w$ we find

$$R(r) = C_1 r^n + C_2 r^{-n-1}. \tag{68}$$

Equation (67) has bounded solutions over the entire sphere only if n is an integer.[51] Making the substitution $\mu = \cos\phi$, we find the only finite solution to Eq. (67) to be

$$X(\mu) = C_3 P_n(\mu), \tag{69}$$

where $P_n(\mu)$ is the Legendre polynomial. Thus a solution to Laplace's equation is

$$\Phi_n = A_n r^n P_n(\mu) + B_n r^{-n-1} P_n(\mu). \tag{70}$$

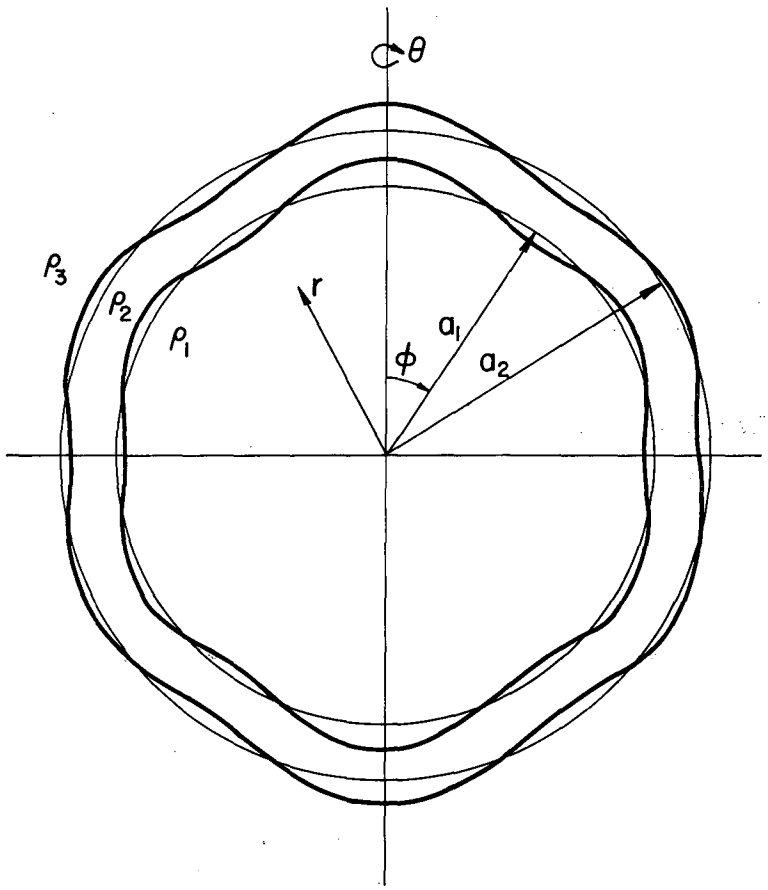

MU-26977

Fig. 13. Spherical-shell model—Rayleigh instability. Surfaces are perturbed by a Legendre polynomial of order 6.

In fluid region 1, Φ_1 must be bounded at 0, and in region 3, Φ_3 must be bounded at infinity. Therefore, the velocity potential in each of the three regions must be an infinite series, a representative term of which is

$$\Phi_{n,1} = A_n \, r^n \, P_n(\mu),$$

$$\Phi_{n,2} = (B_n \, r^n + C_n r^{-n-1}) \, P_n(\mu),$$

and

$$\Phi_{n,3} = D_n \, r^{-n-1} \, P_n(\mu). \tag{71}$$

Because of the orthogonality of the Legendre polynomials, we can express the shapes of the interfaces as infinite series of Legendre polynomials where the constants are determined by means of the appropriate orthogonality principles.[52] These series are

$$\eta_I = a_1 + \sum_n \alpha_{n,I} \exp[q_n t] \, P_n(\mu),$$

and

$$\eta_{II} = a_2 + \sum_n \beta_{n,II} \exp[q_n t] \, P_n(\mu) . \tag{72}$$

The subscripts I and II refer to the inner and outer interfaces respectively. In all the work that follows, we equate only eigenfunctions corresponding to the same eigenvalue. For this reason, it will be expedient to express only a single term of the various infinite series. This is analagous to the use of a single term to represent the Fourier series in the flat-film problem.

Invoking assumption (e) we can determine the constant terms in the velocity potentials from the kinematic boundary condition[47]

$$\frac{\partial \eta}{\partial t} = -\left(\frac{\partial \Phi}{\partial r}\right)_{\text{interface}}.$$

The velocity potentials can then be found as

$$\Phi_1 = -\frac{\alpha q \exp[qt]}{n\, a_1^{n-1}} r^n P_n(\mu) , \tag{73}$$

$$\Phi_2 = -\frac{\beta q \exp[qt] P_n(\mu)}{(a_2^{2n+1} - a_1^{2n+1})} \left[\frac{r^n}{n} (-\gamma a_1^{n+2} + a_2^{n+2}) + \frac{r^{-n-1}}{n+1} (a_1^{2n+1} a_2^{n+2} - \gamma a_1^{n+2} a_2^{2n+1}) \right] , \tag{74}$$

and

$$\Phi_3 = \frac{\beta q \exp[qt]}{(n+1) a_2^{-n-2}} r^{-n-1} P_n(\mu) , \tag{75}$$

where the amplitude ratio $\gamma \equiv \frac{\alpha}{\beta}$.

The dynamic boundary conditions are based upon the use of the Young-Laplace equation[42] (invoking assumption c):

$$P_{I,1} - P_{I,2} = \sigma \left(\frac{1}{R_1} + \frac{1}{R_2} \right)_I ,$$

$$P_{II,2} - P_{II,3} = \sigma \left(\frac{1}{R_1} + \frac{1}{R_2} \right)_{II} . \tag{76}$$

The sum of the reciprocals of the radii of curvature can be found from a general expression given by Landau and Lifshitz as[53]

$$\frac{1}{R_1} + \frac{1}{R_2} = \frac{2}{a} + \left\{ \begin{matrix} \alpha \\ \beta \end{matrix} \right\} \frac{P_n(\mu)}{a^2} (n-1)(n+2), \tag{77}$$

where we have again noted assumption (d). If the drop is not too small, the first term in Eq. (77) can be neglected in comparison with the

second term. Because of assumption (c), the equations of motion give the pressure at any point as

$$\frac{P}{\rho} = \frac{\partial \Phi}{\partial t} . \tag{78}$$

We use Eqs. (76), (77), and (78) to obtain the two expressions

$$\rho_1 \left.\frac{\partial \Phi_1}{\partial t}\right|_{r=a_1} - \rho_2 \left.\frac{\partial \Phi_2}{\partial t}\right|_{r=a_1} = \sigma \frac{\alpha P_n(\mu)}{a_1^{\,2}} (n-1)(n+2), \tag{79}$$

and

$$\rho_2 \left.\frac{\partial \Phi_2}{\partial t}\right|_{r=a_2} - \rho_3 \left.\frac{\partial \Phi_3}{\partial t}\right|_{r=a_2} = \sigma \frac{\beta P_n(\mu)}{a_2^{\,2}} (n-1)(n+2) . \tag{80}$$

If Eqs. (73), (74), and (75) are substituted into Eqs. (79) and (80), and the resulting equations are solved for γ, we find

$$\gamma = \frac{-\dfrac{\rho_2 q^2 (2n+1)}{a_2^{\,2n+1} - a_1^{\,2n+1}} \left(\dfrac{a_1^{\,n}\, a_2^{\,n+2}}{n(n+1)} \right)}{-\dfrac{\rho_1 q^2 a_1}{n} - \dfrac{\rho_2 q^2}{a_2^{\,2n+1} - a_1^{\,2n+1}} \left(\dfrac{1}{n} a_1^{\,2n+2} + \dfrac{a_1 a_2^{\,2n+1}}{n+1} \right) - \dfrac{\sigma (n-1)(n+2)}{a_1^{\,2}}} , \tag{81}$$

and

$$\gamma = \frac{\dfrac{\rho_3 q^2 a_2}{n+1} + \dfrac{\rho_2 q^2}{a_2^{\,2n+1} - a_1^{\,2n+1}} \left(\dfrac{a_2^{\,2n+2}}{n} + \dfrac{a_1^{\,2n+1}\, a_2}{n+1} \right) + \dfrac{\sigma (n-1)(n+2)}{a_2^{\,2}}}{\dfrac{\rho_2 q^2 (2n+1)}{a_2^{\,2n+1} - a_1^{\,2n+1}} \left(\dfrac{a_1^{\,n+2}\, a_2^{\,n}}{n(n+1)} \right)} . \tag{82}$$

If we equate Eqs. (81) and (82) and expand a_2 as a binomial series in powers of (h'/a_1), we finally arrive at

$$q^4 a_1^2 \left[\rho_1^2(n^2+n)\left(\frac{h'}{a_1}\right)^2 + \rho_1\rho_2(2n+1)\left(\frac{h'}{a_1}\right)\right]$$

$$+ \frac{q^2\sigma}{a_1} n(n+1)(n-1)(n+2)\left[\rho_1(2n+1)\left(\frac{h'}{a_1}\right)^2 + 2\rho_2\left(\frac{h'}{a_1}\right)\right]$$

$$+ \left[\frac{\sigma n(n+1)(n-1)(n+2)}{a_1^2}\left(\frac{h'}{a_1}\right)\right]^2 = 0. \tag{83}$$

Also, note that we have set $\rho_1=\rho_3$. Cube and higher powers of (h'/a_1) have been dropped because of assumption (a). Equation (83) can be solved for q^2 by means of the quadratic formula

$$q^2 = \frac{-M \pm (M^2 - 4LN)^{1/2}}{2L}, \tag{84}$$

where L, M, and N are defined by

$$L \equiv a_1^2\left[\rho_1^2(n^2+n)\left(\frac{h'}{a_1}\right)^2 + \rho_1\rho_2(2n+1)\left(\frac{h'}{a_1}\right)\right],$$

$$M \equiv \frac{\sigma}{a_1} n(n+1)(n-1)(n+2)\left[\rho_1(2n+1)\left(\frac{h'}{a_1}\right)^2 + 2\rho_2\left(\frac{h'}{a_1}\right)\right],$$

and

$$N \equiv \left[\frac{\sigma n(n+1)(n-1)(n+2)}{a_1^2}\left(\frac{h'}{a_1}\right)\right]^2.$$

Now we can investigate the stability of the thin spherical shell. The shell will be inherently stable if the growth factor q is imaginary, or if q^2 is always negative. The term q^2 will be negative only if both

of the following conditions are met

$$M^2 - 4LN \geqslant 0$$

$$(M^2 - 4LN)^{1/2} \leqslant |M| \tag{85}$$

Computing the value of the radicand in Eq. (84), we find

$$\rho_1^{\,2}\left(\frac{h'}{a_1}\right)^4 + 4\rho_2^{\,2}\left(\frac{h'}{a_1}\right)^2 ,$$

which is always $\geqslant 0$. The second condition will be met, since the product LN is $\geqslant 0$, because both L and N are always positive or zero. We thus arrive at the interesting conclusion that the spherical shell model is always inherently stable under the effects of surface forces alone. A Rayleigh instability cannot exist in a spherical shell. This fact may perhaps explain the remarkable resistance to mechanical damage of soap films and bubbles.[48,54]

4. Flat or Metastable Film—Large Disturbances

The discussion thus far has been confined to the effects of infinitesimal disturbances. If the film is inherently unstable, these grow with time until the film is ruptured. Can a disturbance be of such intensity that it might cause a rupture even if the film is inherently stable? The film can be ruptured provided that it is in a lower state of potential energy after rupture than before. Let us consider an infinite film of thickness 2h, and suppose that a disturbance of wavelength λ is imposed upon it. This flat film initially had a surface area (per unit width) of 2λ per wavelength and a volume of $2h\lambda$ per wave length. If the volume corresponding to each wavelength were reformed into a cylinder after the film was ruptured, each cylinder would have the volume $2h\lambda = \pi r^2$ and the surface area $2\pi r = 2(2h\pi\lambda)^{1/2}$. Now if the surface area of the cylinder is less than that of the flat film, we see that a sufficiently intense disturbance can cause the film

to break up (reduce its potential energy). This surface area criterion is fulfilled if $\lambda > 2\pi h$. Obviously, this stability criterion is less restrictive than the one based on a Taylor instability (Eq. 53). For reference, we will call this the metastable flat film.

It is of great interest to determine the energy of a wave system with sufficient amplitude to rupture a thick film. Only one exact solution to the equations of ideal fluid motion for arbitrarily large waves is known—Gerstner's trochoidal wave.[46] The surface of the fluid can be described by the parametric equations

$$x = \frac{\theta}{k} + \frac{1}{k} \exp[bk] \sin \theta,$$

and

$$z = b - \frac{1}{k} \exp[bk] \cos \theta, \tag{86}$$

where $\theta = kA + qt$.

Here A and b are parameters that give the horizontal and vertical coordinates, respectively, of a fluid particle when the wavelength is zero. Parameter b also describes the amplitude of the waves $b = -\infty$ corresponding to an infinitesimal wave and $b = 0$ corresponding to the largest possible wave, a cycloid. (In order to describe the shape of the free surface boundary of a liquid film as the waves grow in amplitude, it is necessary to shift the origin of the coordinate system to keep the volume of fluid per wavelength a constant.) Figure 14 illustrates trochoidal waves of successively larger amplitude. It can be shown that a trochoidal wave of wavelength $\lambda = 2\pi/k$ will cause the rupture of a film λ/π or less in thickness—this is the same criterion as the surface area criterion discussed above.

The energy of a trochoidal wave can be found easily. We will examine the case of a liquid of density ρ bounded by a vapor of negligible density. The total energy is made up of three contributions, the kinetic energy, the potential energy due to gravity and the potential energy due to surface forces. Thus we have

$$E = E_k + E_g + E_\sigma \quad . \tag{87}$$

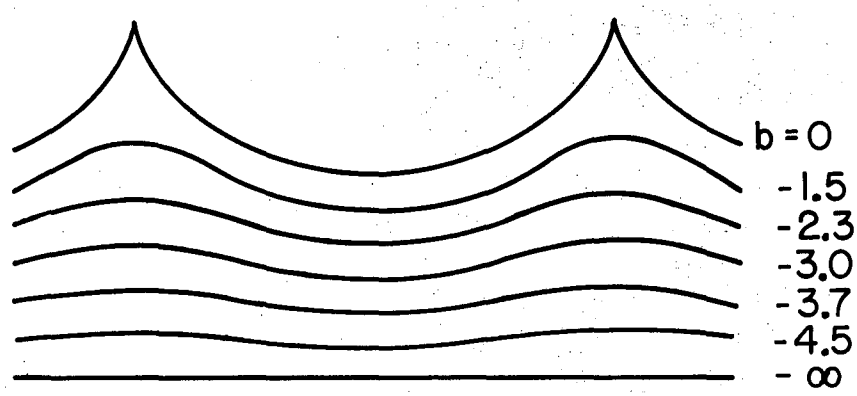

MU-26936

Fig. 14. Trochoidal waves. The amplitudes correspond to a wave number $k = \pi / 6$ and the parameter b indicated on the drawing. The limiting cases of a straight line and cycloid are shown.

The energies are given per wavelength and per unit width of surface. The kinetic energy is given by

$$E_k = \frac{\pi c^2 \rho \Gamma^2}{8} \left(1 - \frac{\pi^2 \Gamma^2}{2\lambda^2}\right), \tag{88}$$

where c is the velocity of propagation of the wave, and Γ is the height of the wave crest above the trough. The potential energy due to gravity is given by

$$E_g = \frac{g \rho \lambda \Gamma^2}{16} \left(1 - \frac{\pi^2 \Gamma^2}{2\lambda^2}\right). \tag{89}$$

The potential energy due to surface forces is given by the surface tension times the increase in surface area due to the wave,

$$E_\sigma = \sigma \left[\int_0^{\frac{2\pi}{k}} \sqrt{1 + \left(\frac{dz}{dx}\right)^2} \, dx - \frac{2\pi}{k} \right]$$

$$= \sigma \left[\frac{2}{k} \int_0^{\pi} \sqrt{K_1 + K_2 \cos\theta} \, d\theta - \frac{2\pi}{k} \right],$$

where $K_1 = 1 + \exp[2bk]$ and $K_2 = 2 \exp[bk]$.

The integral can be evaluated as shown in Byrd and Friedman[37] to give the final result

$$E_\sigma = \sigma \left[\frac{4}{k} \left(1 + \exp[bk]\right) E\left(\frac{2\exp[bk/2]}{1 + \exp[bk]}\right) - \frac{2\pi}{k} \right], \tag{90}$$

where

$$E\left(\frac{2\exp[bk/2]}{1 + \exp[bk]}\right)$$

is the complete elliptic integral of the second kind. The surface area is shown as a function of exp[bk] in Fig. 15. Wave propagation velocity c can be computed from the requirement that the kinetic energy of a progressive wave must equal the sum of the surface and gravitational potential energies. The total energy is analogous to the energy of activation used by chemical kineticists—it represents the energy barrier that a system must cross in order to pass from one state to another. Figure 16 is a graph of the total kinetic and potential energy per unit area of a trochoidal wave with $\Gamma = 2h$ in the water-air system. It is also a graph of the energy barrier that must be exceeded in order to rupture a water film of thickness 2h (not including the energy required to overcome double layer or disjoining forces). Although the calculations described in this section pertain to single-phase systems, they could be extended to cover the more general case of a film placed between two semi-infinite layers of another fluid.

E. Effect and Analysis of Disturbances

The disturbances discussed in the previous section can arise in a number of ways, i.e., through fluctuating fluid pressures caused by sonic or subsonic noise, through fluid motion caused by thermal or velocity gradients, through interfacial turbulence caused by chemical potential gradients, or even by fluid motion caused by molecular-scale disturbances. In general, the most important disturbance is that caused by sonic or subsonic noise. The manner in which such disturbances may arise is discussed in the first subsection below. The magnitude of the disturbance produced by a falling drop is discussed in subsection 2. A method for analyzing the random pressure fluctuations induced by natural external disturbances is given in subsection 3.

1. Disturbances Caused by Sonic or Subsonic Noise.

The following description gives a possible way in which a disturbance might arise through a sonic noise. Suppose a plane wave of sound impinges upon the interface between two liquid media.[53] A portion of the sound beam will be reflected back into the first medium, and another portion

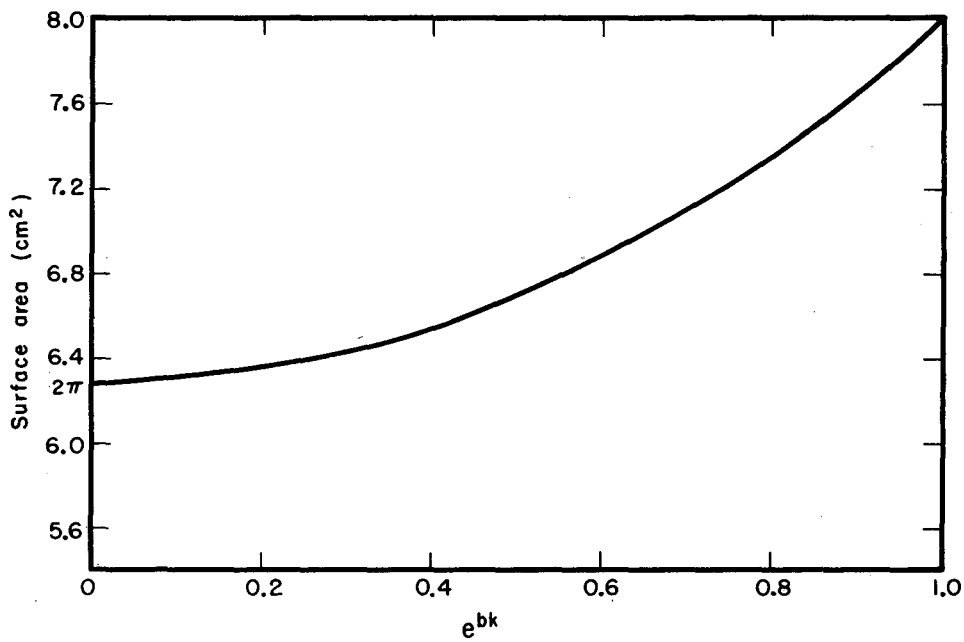

Fig. 15. Surface area of a trochoidal wave as a function of exp [bk]. Surface areas correspond to areas unity in extent in the x and y directions.

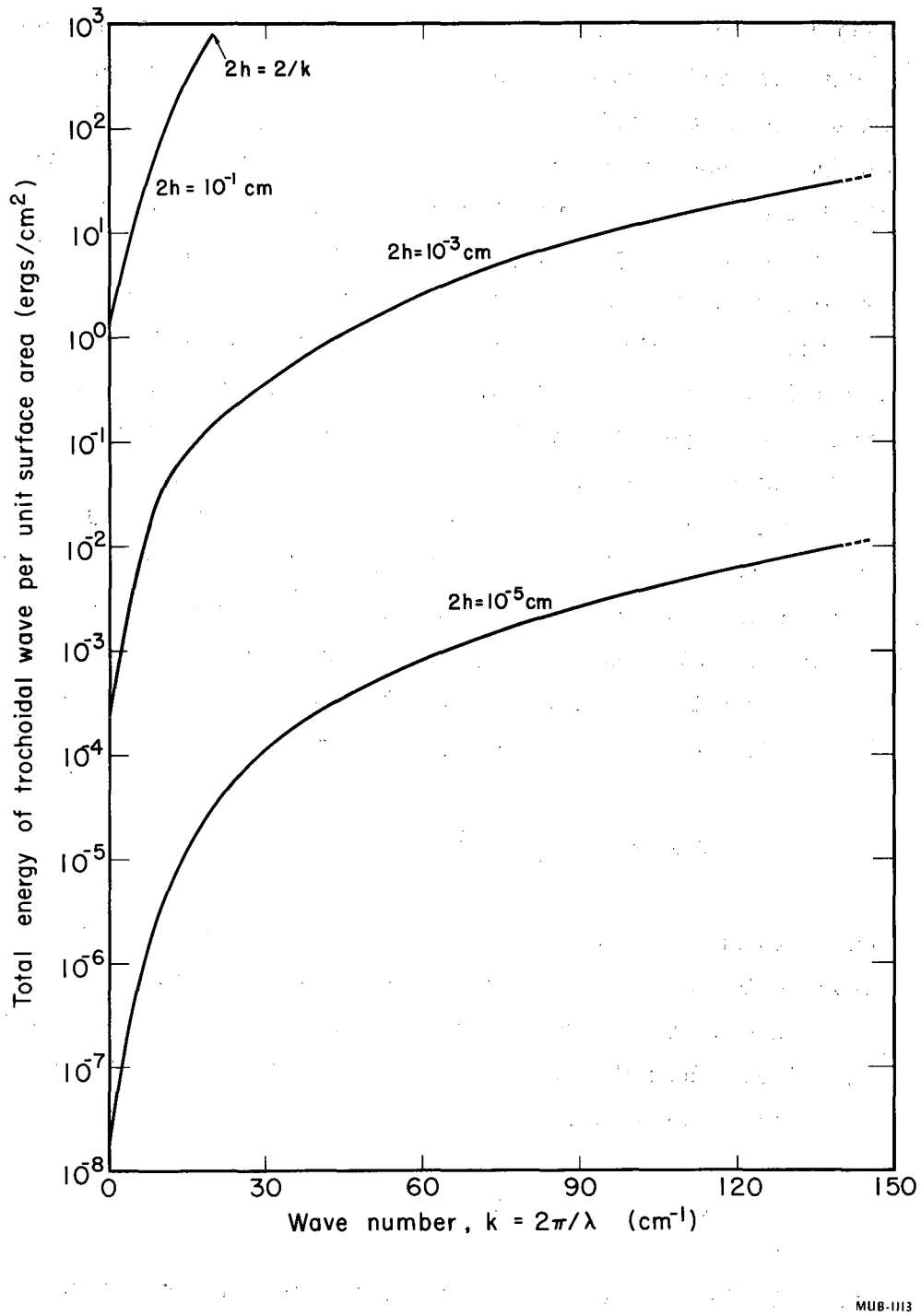

Fig. 16. Total kinetic and potential energy of a trochoidal wave with $\Gamma = 2$ h. Energies correspond to an area unity in extent in the x and y directions. Physical properties used are for the air-water system.

will be refracted because of the change in acoustic impedance between the media and will pass on into the second medium. A pressure will be exerted on the interface between the media because of the difference in momenta of the sound beams on opposite sides of the interface. If the interface is the boundary between two liquids, surface waves can be imposed upon the interface and the pressure will do work on the fluid particles composing these waves. The waves will then propagate along the interface away from the point of incidence of the sound beam. The rate at which energy is carried away by the waves is determined by the group velocity of the waves.[47] By such an argument, we could write an energy balance around the point of incidence of the sound beam which would enable us to compute the wave amplitudes. A knowledge of the intensity of the sound, its angle of incidence, its frequency, and the physical properties of the two liquids is needed. Sufficient information for our purposes can be obtained without a detailed solution of the problem, however.

First, let us calculate the energy carried out of the system by the surface waves. The energy of a progressive wave is given by

$$\frac{1}{2} g \, (\rho_1 + \rho_2) \cdot \alpha^2 \, , \tag{91}$$

per unit area of surface. The energy is carried out of the system at the group velocity, which is equal to a constant times the phase velocity. The constant lies between 1/2 and 3/2, depending upon the wavelengths. Therefore, the rate at which energy is carried out of the system by surface waves is proportional to

$$C_p \, g(\rho_1 + \rho_2) \cdot \alpha^2 ,$$

where C_p is the phase velocity of the waves. The phase velocity is given by the expression

$$C_p^{\,2} = \nu^2 \lambda^2 = \nu^2 \left(\frac{2\pi}{k}\right)^2 = \frac{|\rho_1 - \rho_2|}{\rho_1 + \rho_2} \frac{g}{k} + \frac{\sigma}{\rho_1 + \rho_2} k \, . \tag{92}$$

Here ν is the frequency of the disturbance in cps.

Now the energy available for producing the surface waves will be proportional to the energy of the sound wave which, in turn, is proportional to the square of the sound pressure.[53] Let us now express the proportionality between the energy available for production of surface waves and the rate of transmission of energy along the surface. After some rearrangement we find

$$\alpha^2 \approx \frac{P_{rms}^{\ 2}}{C_p \ g \ (\rho_1 + \rho_2)} \ , \tag{93}$$

where P_{rms} is the root-mean-square sound pressure in dynes/cm^2. We can now state several qualitative conclusions. The amplitude of the waves produced is proportional to the sound pressure. If the frequency of the sound is low and the density differences between phases is small, the waves will be of large amplitude (gravity waves). If the surface tension is low and the sound frequency is in the low sonic range, the amplitude of the waves will also be large (capillary waves). These conclusions are in agreement with the results obtained for the trochoidal waves or metastable films as we would expect.

2. Disturbance Produced by Falling Drop

Let us now calculate the amplitudes of the waves that are produced by a drop falling to the interface and creating it own disturbance. The energy released when the drop falls is just the potential gravitational energy, approximately

$$\frac{4}{3} \pi \ a^3 \ \Delta\rho \ g \ L, \tag{94}$$

where L is the distance between the center of gravity of the drop before and after it falls. Because of the small velocities, the energy dissipated by viscous forces has been ignored. The energy of a system of progressive

waves is

$$\frac{1}{2} g(\rho_1 + \rho_2) \alpha^2 A, \tag{95}$$

where A is the area covered by the wave system. If Eq. (94) is equated to Eq. (95), the amplitude of the waves can be found as

$$\alpha^2 = \frac{8}{3} \pi a^3 \frac{(\rho_2 - \rho_1)}{(\rho_1 + \rho_2)} \frac{L}{A} . \tag{96}$$

As an example, for the water-benzene system, if a = 0.3 cm, L = 1 cm, and A = 10 cm^2, the amplitude is 0.0388 cm. This result will be used to explain the erratic data often found when large drops were used.

3. Analysis of Random External Disturbances

It was found that the externally-generated random disturbances observed in the coalescence cell could be measured by means of a sensitive microphone and a wave analyzer. The equipment, operating techniques, and results are discussed in Sec. III and Sec. IV. However, the theoretical method of analysis is more appropriately discussed first.

The assumption was made that the random disturbances observed in the coalescence cell were generated by the operation of equipment, footsteps, etc., and were modified by interference, scattering, and absorption, to reach the coalescence cell in the form of very short periodic sounds. An excellent way of analyzing such sounds is to impose low- and high-band-pass filters so that an arbitrarily narrow range of frequencies can be observed. The use of a microphone and a tunable device such as a wave analyzer enables one to measure the frequency spectrum of a noise that is periodic in time.

It would be desirable to use a wave analyzer that would measure the amplitude of an infinitesimally narrow frequency band. However, a wave analyzer in fact admits a rather wide band of frequencies. Corresponding to a true frequency spectrum, $g(\omega)$, a wave analyzer actually yields

$$\hat{g}(\omega_o) = \int_{-\infty}^{\infty} K(\epsilon, \omega-\omega_o)\, g(\omega)\, d\omega, \tag{97}$$

for a given wave number setting ω_o. Here the kernel of the integral equation is a function such that

$$\int_{-\infty}^{\infty} K(\epsilon, \omega-\omega_o)\, d\omega = 1, \tag{98}$$

for all ω_o.

This kernal represents the band width accepted by the wave analyzer, and ϵ is a measure of the narrowness of this band. Ideally, in the limit, ϵ should approach zero so that the kernal approaches the Dirac delta function.[55] Then Eq. (97) becomes

$$\hat{g}(\omega_o) = \int_{-\infty}^{\infty} \delta(\omega-\omega_o)\, g(\omega)\, d\omega = g(\omega_o), \tag{99}$$

and the wave analyzer yields the true frequency spectrum. The kernal could be found by fitting an algebraic function to the experimental response curve supplied by the wave analyzer manufacturer.

The solution of Eq. (97) would be very different or impossible, however. Therefore, the assumption will be made that the kernal equals a Dirac delta function, and the result of Eq. (99) will be used.

The frequency spectrum of a time function can be found by taking the Fourier transform of the time function. According to our assumption, the disturbances are of the form

$$f(t) = \begin{cases} P \cos \omega_o t, & -a \leq t \leq a \\ 0, & |t| > a \end{cases} \tag{100}$$

The Fourier transform of f(t) is given by

$$g(\omega) = \frac{1}{\sqrt{2\pi}} \int_{-\infty}^{\infty} f(t) \exp[i\omega t]dt, \tag{101}$$

Inserting Eq. (100) into Eq. (101) and integrating, we find

$$g(\omega) = \frac{P}{\sqrt{2\pi}} \quad \frac{\sin\,(\omega-\omega_o)\,a}{\omega - \omega_o} \quad . \tag{102}$$

Suppose, instead, that the time function is displaced from the origin of time as follows

$$f(t) = \begin{cases} P \cos \omega_o(t-t_o), & t_o-a \leqslant t \leqslant t_o + a \\ 0, \quad t < t_o - a, & t > t_o + a \end{cases} \quad . \tag{103}$$

By making a simple algebraic transformation, we can find the Fourier transform of Eq. (103) as

$$g(\omega) = \frac{P \exp[i\,\omega_o t_o]}{\sqrt{2\pi}} \quad \frac{\sin\,(\omega-\omega_o)\,a}{\omega - \omega_o} \quad . \tag{104}$$

A displacement in time of f(t) has only introduced a phase-angle change in its frequency spectrum. Because the wave analyzer does not yield phase information, we shall never be able to determine the exact time at which a disturbance occurs. However, if the disturbance is repeated frequently enough in time so that the inertia of the wave analyzer meter is overcome, we will be able to measure the amplitude, time duration, and frequency of the disturbance. Because coalescence data are fairly reproducible, the disturbances must occur with sufficient frequency to give a response on the wave analyzer. Equation (102) is applied to appropriate experimental data in Sec. IV.

F. Summary of Model

The model developed in this chapter will now be briefly summarized. A liquid drop falls off the dropping tip and almost instantaneously reaches a quasi-equilibrium position at the interface. Its position can be determined by means of a force balance on the drop. The force of gravity and

the surface forces attempting to restore the planar shape of the interface, gradually squeeze the film of phase 2 out from beneath the drop against the viscous forces. If the film becomes much thinner than 10^{-4} cm, electroviscous, disjoining-pressure, and double-layer repulsion forces also help to retard the thinning of the film. It can be seen that the drop may not coalesce in tens of thousands of seconds, if film thinning is the only important effect. However, the upper surface of the phase 2 film is inherently unstable with respect to long-wavelength disturbances. It can also be ruptured by almost any sufficiently intense disturbance, especially as it attenuates. As the film becomes thinner, the efficiency with which long-wavelength disturbances can be propagated into the upper film surface becomes greater. These low-frequency disturbances may be beats generated by interference between higher frequency sources, for example. A wave perturbed by low-frequency disturbances will grow exponentially in time at the upper interface until its amplitude is sufficient to rupture the film and cause coalescence. An intense disturbance might rupture the metastable film even though its wavelength is too short to promote an unstable situation.

The shape of the drop rest-time distribution curve can now be explained qualitatively. Until the phase 2 film is sufficiently thin, no disturbance will be intense enough either to rupture the film directly or be propagated through to the upper surface of the film (if the disturbance has a sufficiently long wavelength to cause instability). Disturbances arrive in the system randomly. When the film is thicker, the disturbances cause waves that grow much more rapidly, thus causing the median drop rest-time to be lower than the average of the lowest and highest rest-times.

Table III contains a summary of the way in which the various parameters developed in the coalescence model vary with physical properties. The variation of film thickness h' with physical properties was determined from Eq. (20) and from the graph of J(p) vs Q(p) given in Fig. 17. It will be noted from the graph, that to a good approximation, J(p) is

TABLE III. Effect of system properties on model parameters.

Parameter	Property	As property decreases, parameter — —
q^2	$\Delta\rho$	Decreases
(real q)	σ	Increases
	2h	Decreases
$\lvert\gamma\rvert$	k	Decreases
	2h	Decreases (weakly)
	σ	Decreases
$\lvert\tau\rvert$	μ_1, μ_2	Decreases
	ρ_1, ρ_2	Increases
	k	Decreases
	2h	Decreases (weakly)
α^2	P_{rms}	Decreases
	$\Delta\rho$	Increases
	σ	Increases
	k	Increases
h'	a	Decreases
(t held constant)	$\Delta\rho$	Decreases
	σ	Increases
	μ_2	Decreases

TABLE III (continued)

Parameter	Property	As property decreases, parameter --
k (gravity waves)	ν	Decreases
	$\rho_1 + \rho_2$	Decreases
	$\Delta\rho$	Increases
k (Capillary waves)	ν	Decreases
	$\rho_1 + \rho_2$	Decreases
	σ	Increases

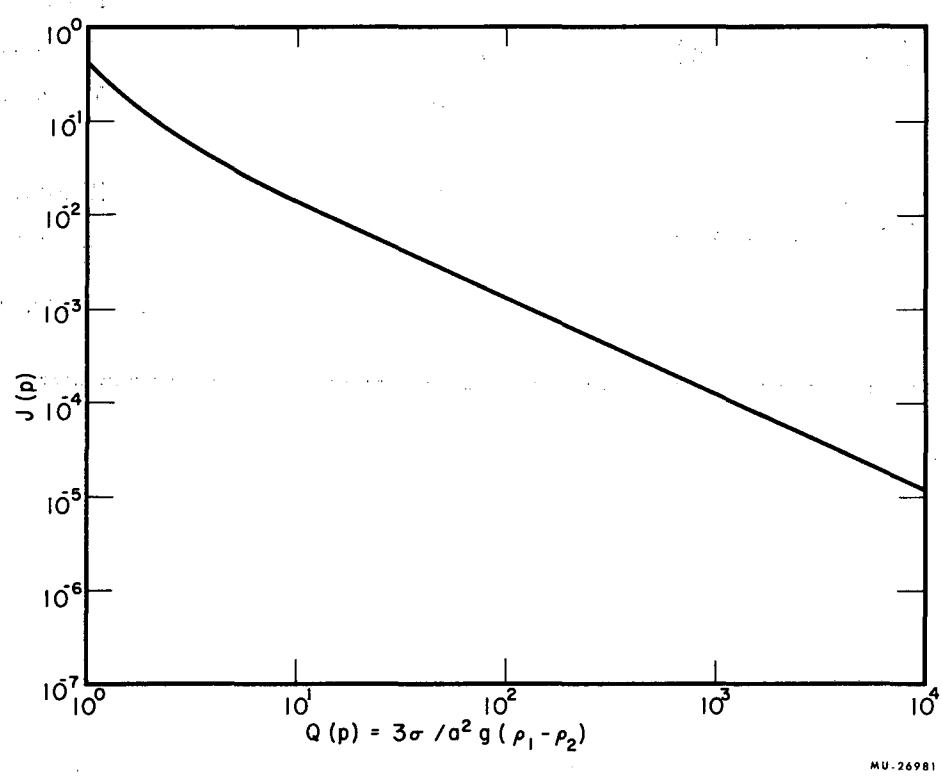

Fig. 17. Graph of J(p) vs Q(p).

inversely proportional to $Q(p)$. The behavior of q^2, γ, τ, and α^2 were determined from Eqs. (52), (54), (63), and (93), respectively.

We see that to promote rapid coalescence by means of the Taylor instability, we require a rapidly decreasing h', a large q^2, small absolute values of γ and τ, a large α^2, and a value of k that satisfies the expression

$$k \leqslant \left[\frac{g(\rho_1 - \rho_2)}{\sigma}\right]^{1/2}, \qquad \rho_1 > \rho_2 . \tag{105}$$

A small value of μ_2 and a large value of P_{rms} will assist in satisfying the h' and α^2 requirements. But we note that, with regard to $\Delta\rho$ and σ, the requirements of the thinning model and the Taylor instability model are different. A small $\Delta\rho$ and a large σ are required in the thinning model, and the opposite is true in the Taylor instability problem. This paradox gives a theoretical explanation for the experimental difficulties in predicting coalescence times.

In the case of the metastable flat film, a rapidly decreasing value of h' and a large value of α^2 are required for rapid coalescence. Again, a small value of μ_2 and a large value of P_{rms} will assist in the satisfaction of the h' and α^2 requirements. But where the thinning model requires a large value of σ, the rapid rupture of the metastable flat film is promoted by a small value of σ. A low value of $\Delta\rho$ will promote rapid coalescence, both by decreasing the value of h' for a given t and by increasing the value of α^2.

As discussed in Sec. V, the often conflicting effect of various physical properties on the two steps in the coalescence process makes the prediction of drop rest-times a most difficult problem.

III. EXPERIMENTAL EQUIPMENT, TECHNIQUES OF OPERATION, CALIBRATIONS, AND PROPERTY MEASUREMENT

The types of experimental equipment and techniques used in this study are divided into four categories. The equipment and techniques used in the coalescence studies, sonic studies and in the materials preparation are described in the first three sections. The equipment and techniques used in measuring physical properties are described in the final section.

A. Coalescence Equipment and Methods of Operation

1. Equipment Description

a. Bath System. A three-tank circulating water system was used to provide a constant-temperature bath for the coalescence equipment and the physical property measuring equipment, and storage for the various liquids used. A photograph of the experimental area, and a schematic diagram of the water-bath system are shown in Figs. 18 and 19, respectively. The temperature of the water was controlled at 25°C. in a 30-gal Plexiglas tank by a Hallikainen Thermotrol Unit (Hallikainen Instruments, Berkeley, California) that actuated two 500-watt immersion heaters. The Thermotrol Unit maintained a constant temperature by a proportional control with reset mode of control. Chilled water at 40°F was circulated through a copper coil immersed in the bath to remove excess heat. Fresh filtered water was added through a solenoid valve during the night to make up for evaporation losses. Water was pumped from this tank by an Eastern Model D-11 Pump (Eastern Industries, New Haven, Connecticut) into a 21 × 21 × 8-in. Plexiglas tank located on a table several feet away. This tank was equipped with clamps to hold flasks of liquid materials and a polyethylene rack to hold pycnometer bottles. Water was returned to the 30-gal tank by gravity flow.

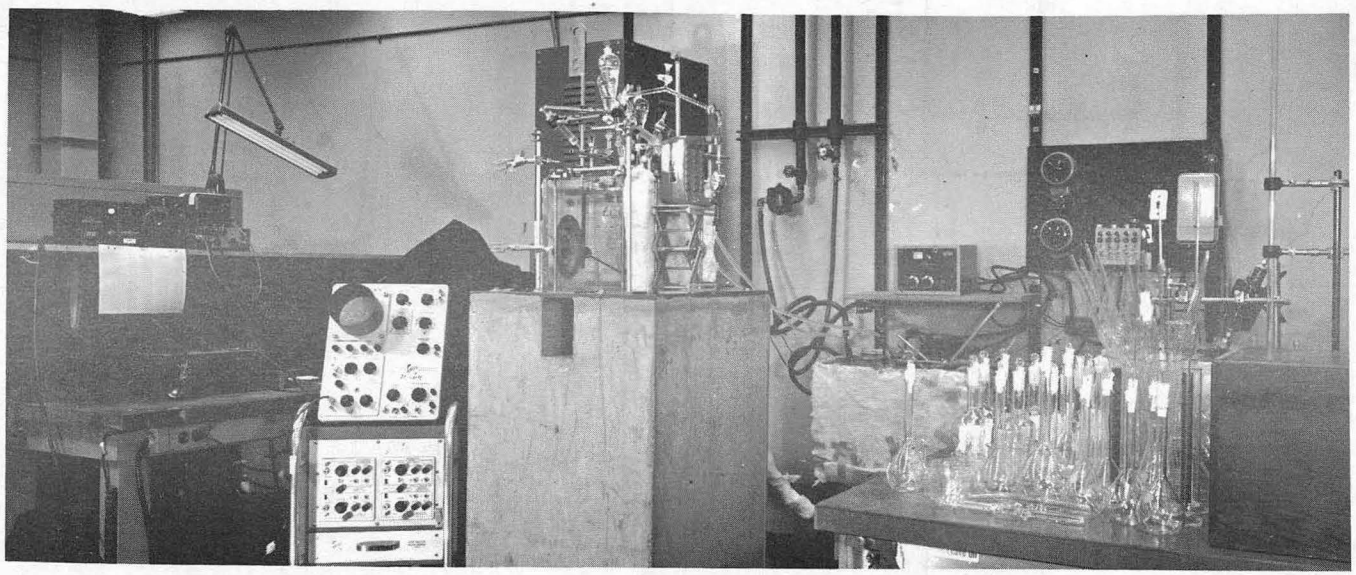

ZN-3102

Fig. 18. Main experimental area. From left to right are shown the sonic disturbance-generating equipment, an oscilloscope, experimental tank and concrete pillar, 30-gallon tank and temperature controller, and a table with glassware and a constant-temperature bath (partially visible).

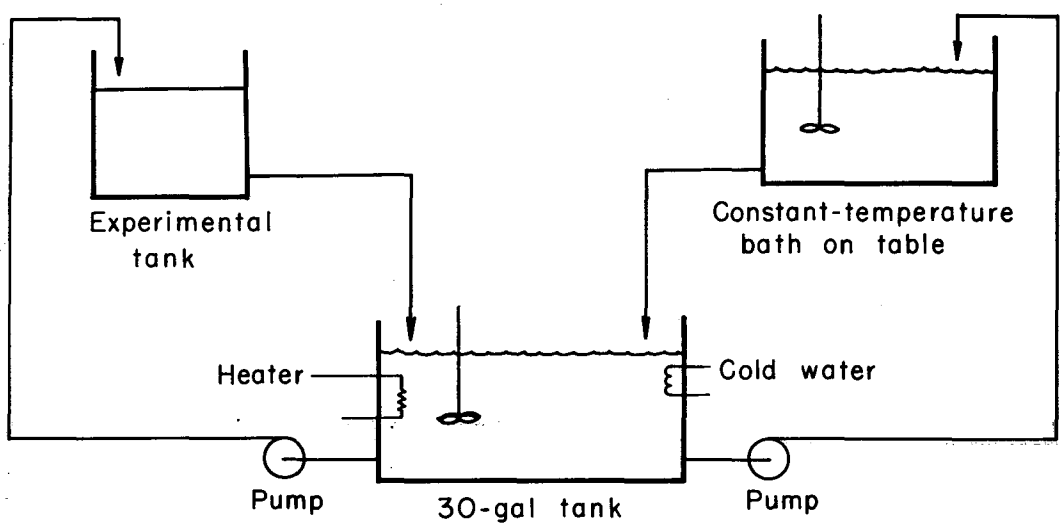

Fig. 19. Schematic diagram of the constant-temperature bath system.

The experimental 12 × 12 × 12-in. Plexiglas tank was bolted to a 1/2-in. steel plate which in turn was bolted and grouted to a reinforced concrete pillar 4 ft. high which weighed 2600 lbs. This pillar was itself grouted to the concrete floor of the laboratory which rested on solid earth. The pillar was designed to eliminate accidental movement of the coalescence equipment during operation and to damp out the effects of vibration in the building. A removable aluminum rod framework was bolted to the tank to hold the coalescence cell. Another Eastern D-11 Pump was used to circulate water to this tank and drainage was by gravity.

Beckmann differential thermometers, which had been calibrated against a platinum resistance thermometer, were placed in all three tanks. Gillespie and Rideal suggested that the random coalescence times they observed might be due to temperature gradients in their cell.[4] To check on such a possibility, temperatures were measured at 12 uniformly spaced points in the experimental tank. All temperatures were found to lie in the range 24.994 to 25.012°C. It seemed unlikely that temperature differences of this magnitude could affect coalescence times. To further improve the temperature control, all the tanks and most of the interconnecting rubber hose lines were insulated with glass wool.

b. Coalescence Cell and Glass Assembly. The coalescence cell was designed with several special provisions. A means for flushing out the interface to remove contaminants and then making the interface planar was provided. The meniscus at the interface could be eliminated so that observations could be made in the plane of the interface. The cell was designed so that drops of the denser phase could be allowed to fall to the interface, or drops of the lighter phase could be allowed to rise to the interface from below. A photograph of the cell appears in Fig. 20.

The cell was constructed from a 2-in. pyrex glass tee. A plane glass observation window was sealed into the sidearm of the tee. The bottom of the tee was sealed and three sidearms were attached, one of which was connected to a female ground glass joint inside the cell.

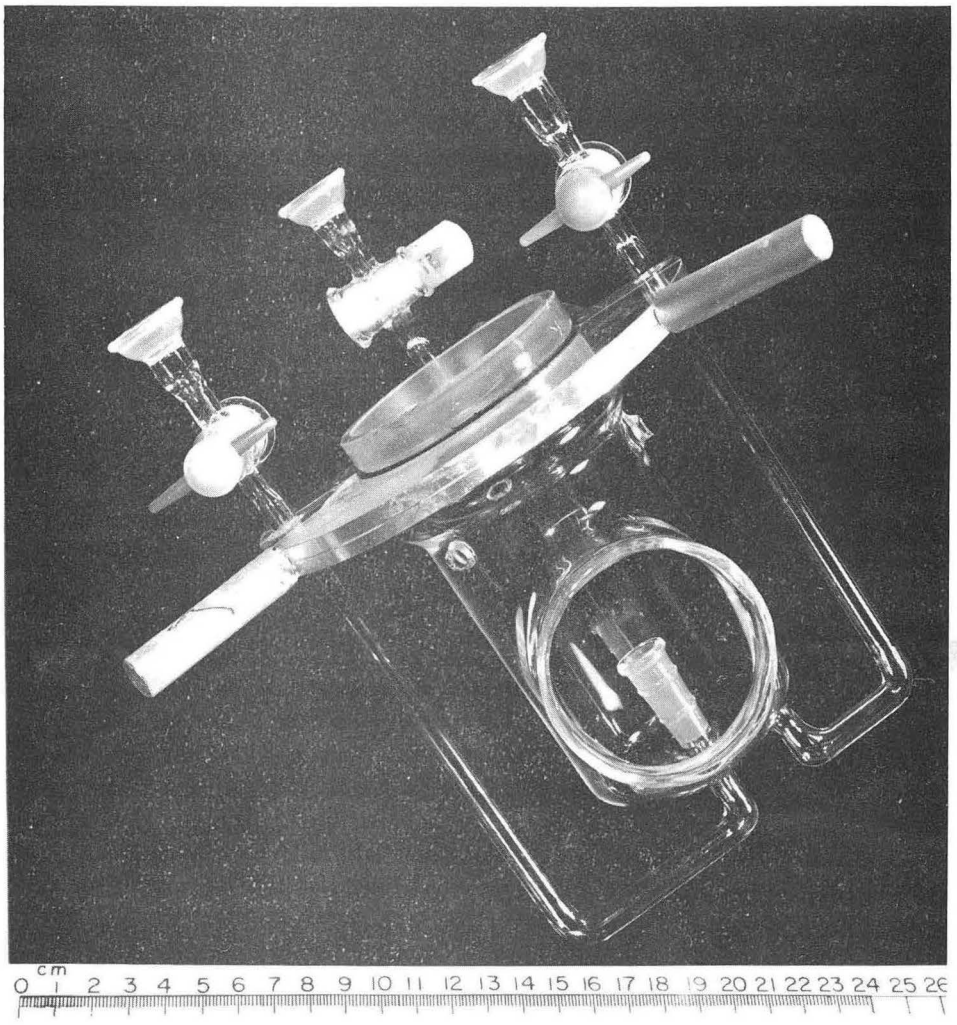

ZN-3103

Fig. 20. Coalescence cell.

When phase 1 was the denser fluid, a glass cup was inserted in this joint, and the interface at which coalescence took place was adjusted to be in the plane of the lip of the cup. If phase 1 wetted the glass better than phase 2, and if the level of the interface outside the cup was below the lip of the cup, no meniscus was present in the cup. The interface in the cup could be made nearly planar. When phase 2 was the denser phase (drops released upward), the cup was replaced with a glass adapter that held a dropping tip. (A cup, a glass adapter, several metal dropping tips, and a metal dropping tip adapter are shown in Fig. 21). In this case, the meniscus could not be eliminated and the interface was slightly curved. The function of the other sidearms is explained in the next section. An aluminum bracket attached the cell to the rod framework that supported the cell in the thermostat.

The cell top, shown in Fig. 22, fit the cell by means of a ground glass joint. Dropping tips were attached onto a glass tube which passed through the cell top. An enlarged portion of this tube (about 3 ml in volume) provided enough residence time for the drop-forming liquid to come to thermal equilibrium with the rest of the liquid. Also attached to the cell top was an air filter to prevent dust from being drawn into the cell when the liquid levels were changed. The filter consisted of a Millipore No. HAWG02500 0.45-μ-pore cellulose filter disk (Millipore Filter Corp., Bedford, Massachusetts) held in a glass joint by a Teflon O ring.

Teflon stopcocks minimized contamination of the liquids, and clamped spherical ground-glass joints were used for all connections. Because no grease was used on the ground glass joints, all connections were placed above the water line in the thermostat. A Syringe Microburet Model No. SB2 (Micro-Metric Instrument Co., Cleveland, Ohio) used to form drops was attached to a small laboratory jack mounted next to the experimental tank.

c. Dropping Tips. The dropping tips were made according to the specifications of Harkins[56] so that the volume of the drops could be determined accurately. The specifications required the dropping tip to be cut off at right angles to its length in such a manner that the

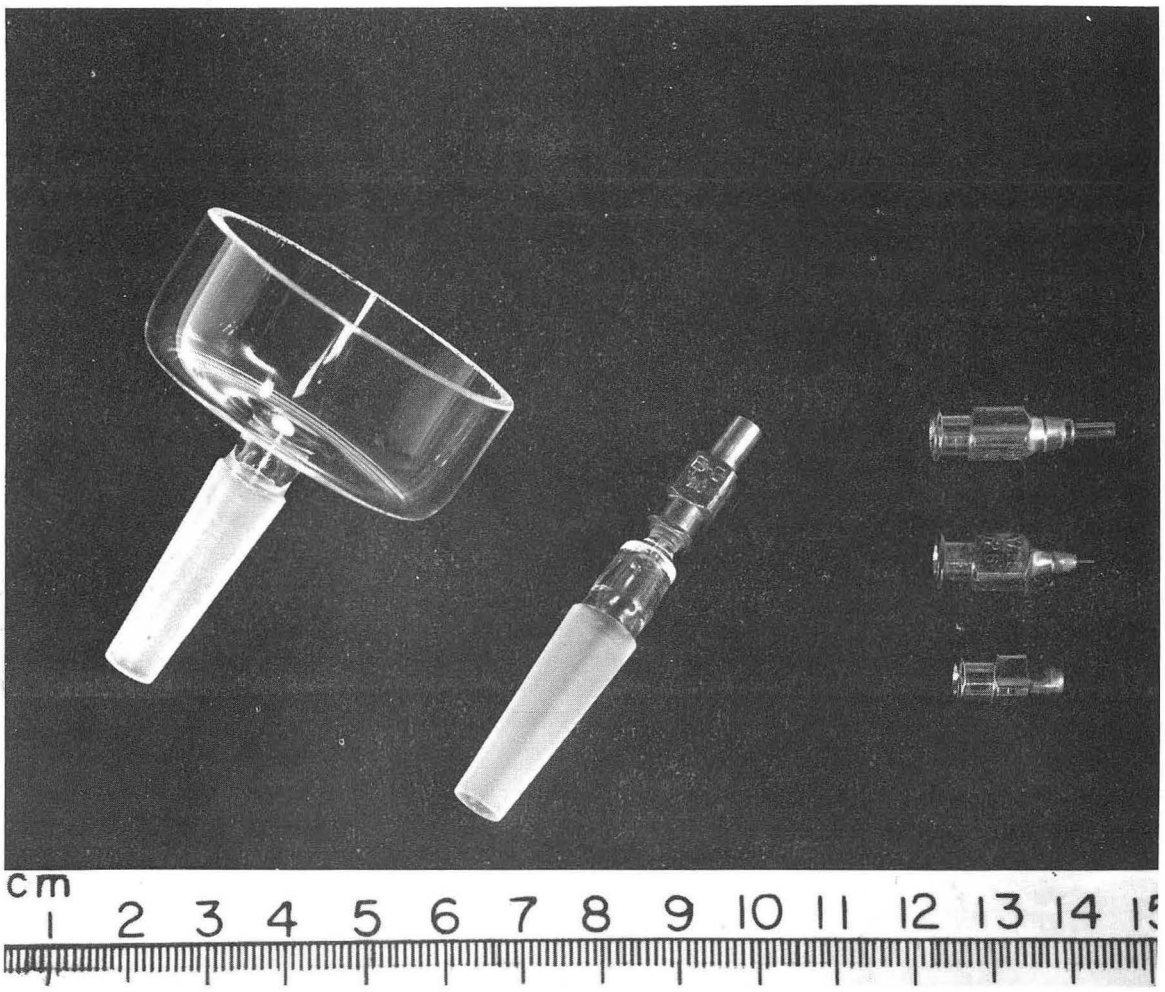

ZN-3104

Fig. 21. A coalescence cup, a glass dropping-tip adapter with a dropping tip, two dropping tips, and a metal dropping-tip adapter.

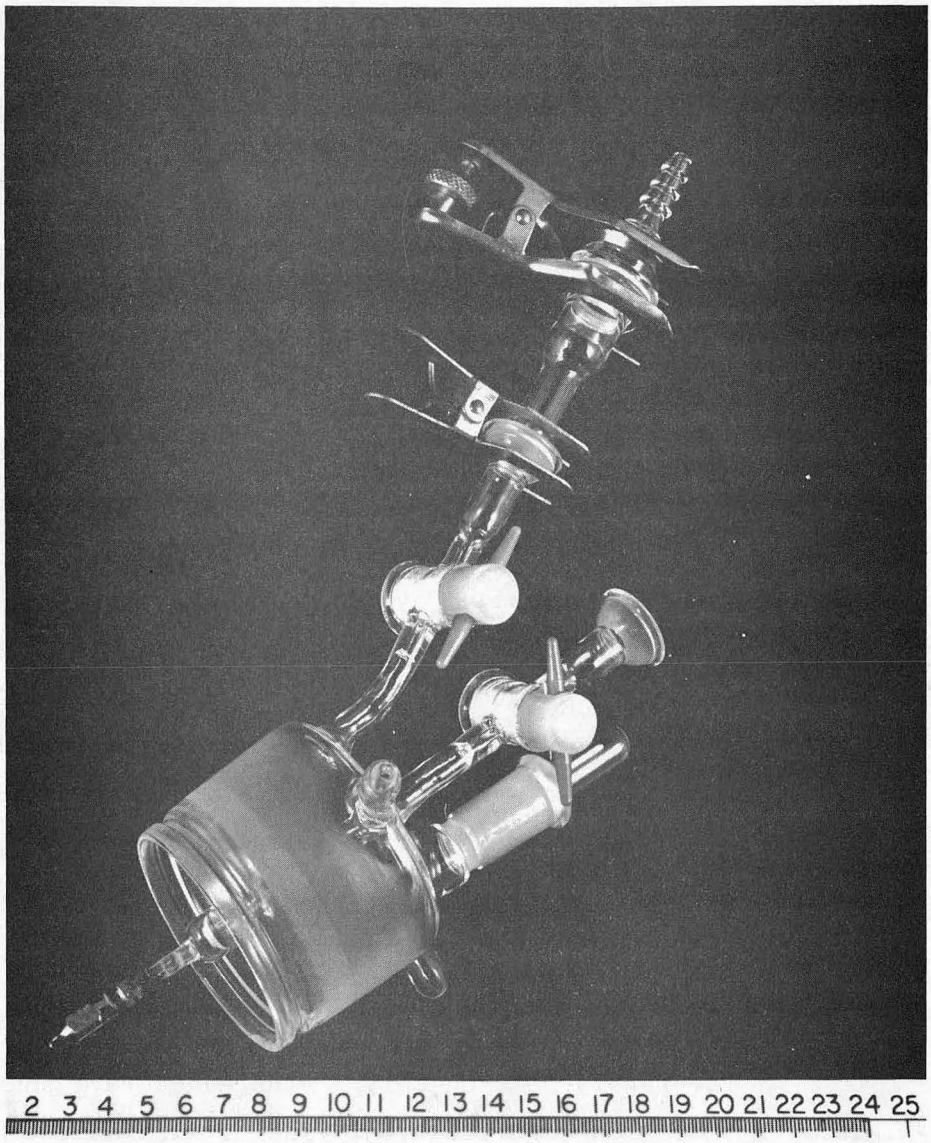

ZN-3105

Fig. 22. Coalescence cell top, with air filtering mechanism and attached dropping tip.

edges are sharp and free from defects under 10X magnification. The following technique was used to make the tips:

Five of the seven dropping tips were hypodermic needles that had been cut off about a centimeter above their bases with a hacksaw. The other tips were made by soldering a short piece of stainless steel tubing on to the Luer base of a hypodermic needle. Then, five-5/16 in. holes were drilled into a 3-in. brass block. A 1/16 in. deep circular area was milled into a smaller brass block. The circular area was lightly greased, and the block containing the holes was placed on top of the circular area. The dropping tips were placed on the ends of hypodermic syringes which were then inserted into the holes of the brass block. Molten Wood's metal (which melts below the boiling point of water) was poured into the holes of the brass block and was drawn up into the syringes so that the dropping tips were completely filled with and surrounded by Wood's metal. After the Wood's metal solidified, the smaller block was removed, leaving a thin circular disk of Wood's metal attached to the larger block. This disk contained the ends of the dropping tips. The Wood's metal and the rough ends of the dropping tips were ground away using successively finer grades of emery cloth on a rotary power grinder. The final polishing was by hand, using crocus cloth. Fig. 23 shows the brass block containing four dropping tips after the final polishing. The dropping tips were removed from the block by melting the remaining Wood's metal with boiling water.

The tips were used only if the edges were sharp and free from defects under 40X magnification. The outside diameters of the tips were measured with a 200X microscope and a travelling table, the position of which could be determined to within 1μ. Table IV gives the average radius of each of the seven tips used. The radii were determined by averaging six uniformly spaced diameter measurements on each tip. In no case did a measured diameter of a tip differ by more than 1% from the average of the six measurements. Tips 2 and 3 were damaged during the course of the experiment and were replaced with Tips 4 and 5, respectively.

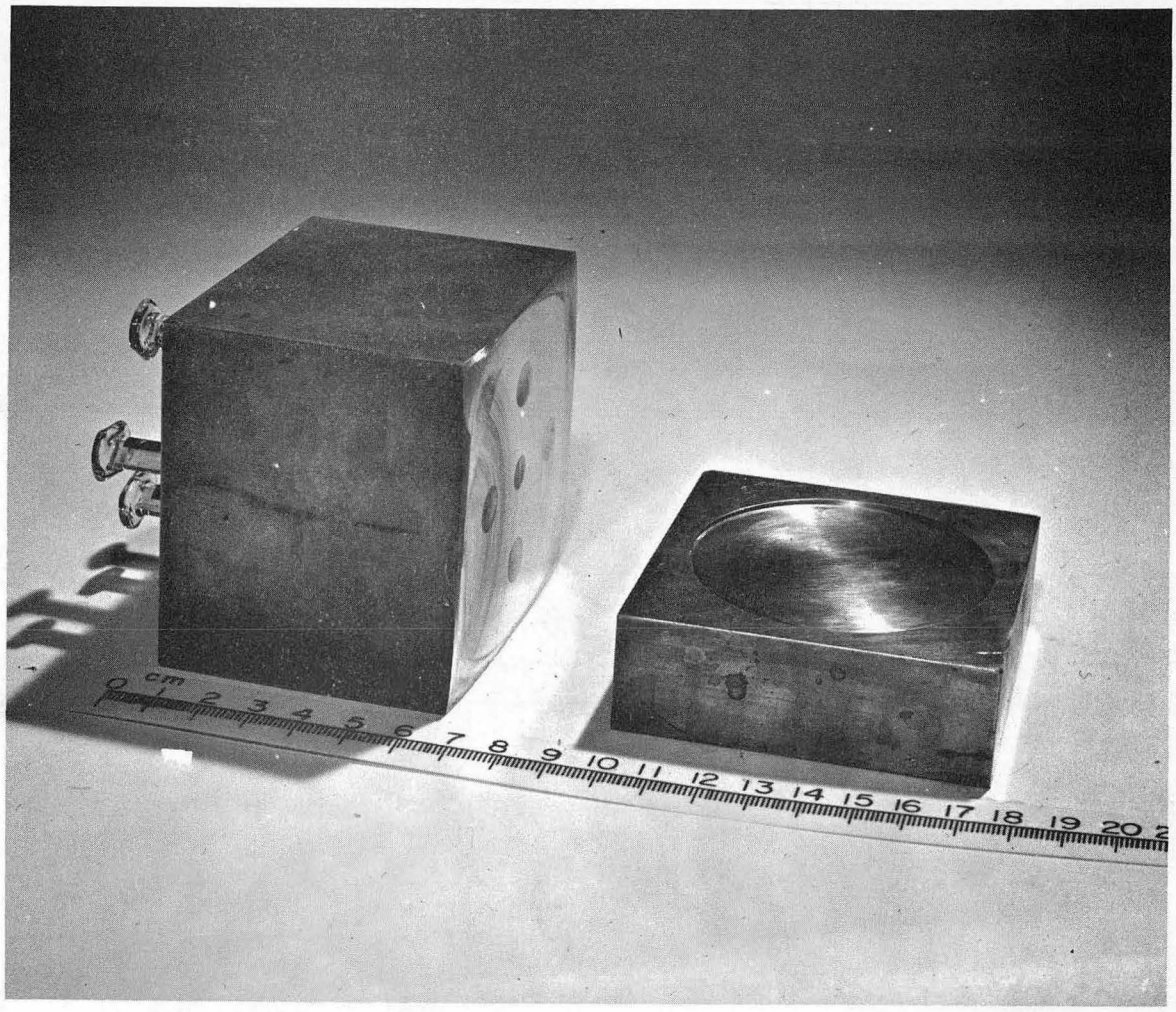

ZN-3106

Fig. 23. Brass blocks used in polishing dropping tips. Note the hypodermic syringes in the block on the left, and the circular groove in the block on the right.

TABLE IV. Dropping tips.

Dropping tip No.	Dropping tip made from	Outside radius (cm)
1	Stainless steel tubing	0.2406
2	Hypodermic needle 13G	0.1202
3	Hypodermic needle 19G	0.0530
4	Hypodermic needle 13G	0.1208
5	Hypodermic needle 19G	0.0535
6	Hypodermic needle 26G	0.0236
7	Stainless steel tubing	0.1362

2. Operation

Each coalescence run can be divided into four main operations: a cleaning procedure, an equipment assembly stage, the experimental run itself, and an analysis of the data (usually a statistical analysis).

a. Cleaning Procedure. To minimize the effect of either soluble or insoluble contaminants on the experimental results, an elaborate primary cleaning procedure and a simpler secondary cleaning procedure were adopted. The primary procedure was carried out between major sets of experimental runs, i.e., whenever the liquid materials were changed or whenever a different effect was being studied. The secondary cleaning procedure was used after each day's operations. The primary procedure was never used less frequently than every four days.

For the primary cleaning procedure, each piece of glass or Teflon used in the coalescence equipment was carefully rinsed with acetone at least three times or until all water-soluble material had been removed. The acetone was removed by rinsing under hot running water. Each item was then immersed in chromic acid cleaning solution, which was then heated to about 200°C with infrared lamps for 6 to 24 hours. Next, it was removed from the hot acid and rinsed either under running distilled water, or with at least 20 rinses of distilled water. Then each item was rinsed at least three times with filtered, deionized, distilled water (the method of preparation of this water is described below in Sec. C), and was wrapped in aluminum foil. The wrapped glassware was dried in an oven at 130°C and was stored in a dust-tight wooden box until used. Flasks, beakers, pipettes, and other materials used in the work were also cleaned in this manner.

The secondary cleaning procedure consisted of the following. The equipment was completely dissassembled and each part carefully rinsed three times with one of the liquids used in that particular study, before reassembly. The chief purpose of the secondary cleaning procedure was the removal of dust and other insoluble contaminants. No part of the equipment which would come into contact with the liquids was ever touched with bare hands after it was cleaned.

b. Assembly. The coalescence equipment could be assembled so that either the phase 1 liquid was the denser phase (drops were allowed to descend to the interface) or the phase 2 liquid was the denser one (drops were allowed to rise upward to the interface). The assemblage of the equipment and the method of operation of the two modes were similar.

In both cases, the cell was attached to the rod framework by the cell bracket. Because of the fragile nature of the cell, a special mechanism to hold the rod framework rigidly outside the experimental tank while the cell was being attached was devised. This mechanism is illustrated in Fig. 24. When phase 1 was the denser liquid, a coalescence cup was inserted in the female s.t. joint inside the cell and the appropriate dropping tip was attached to the cell top. The distance between the end of the dropping tip and the interface in the cup was adjusted to a minimum either by wrapping a short piece of thin Teflon tape (Scotch Brand Plastic Film No. 547, 1/2 in. wide, made by Minnesota Mining and Manufacturing Co., St. Paul, Minnesota) around the male joint of the coalescence cup before inserting it into the cell so as to raise the cup lip, or by inserting a dropping tip adapter between the dropping tip and the cell top. One of these adapters, machined from a hypodermic needle Luer joint, is shown in Fig. 21. The distance from the end of the dropping tip to the interface was generally adjusted to about two drop diameters, so that the drop was never forced to the interface, but was allowed to fall freely. The complete assembly for the mode in which phase 1 was the denser liquid is shown in Figs. 25, 26, and 27. The part numbers in the following description refer to Fig. 27. Phase 1 liquid was admitted to the cell from funnel F1 until it reached a level about 1 cm below the lip of the coalescence cup. Phase 2 liquid was admitted to the cell from funnel F2 until it reached a level about 1 cm above the end of the dropping tip. Funnel F3 was used to fill the hypodermic syringe attached to the microburet and the interconnecting tubing up to the dropping tip with phase 1 liquid. By careful manipulation of the syringe plunger and stopcocks S1, S2, S3, and S4, it was possible

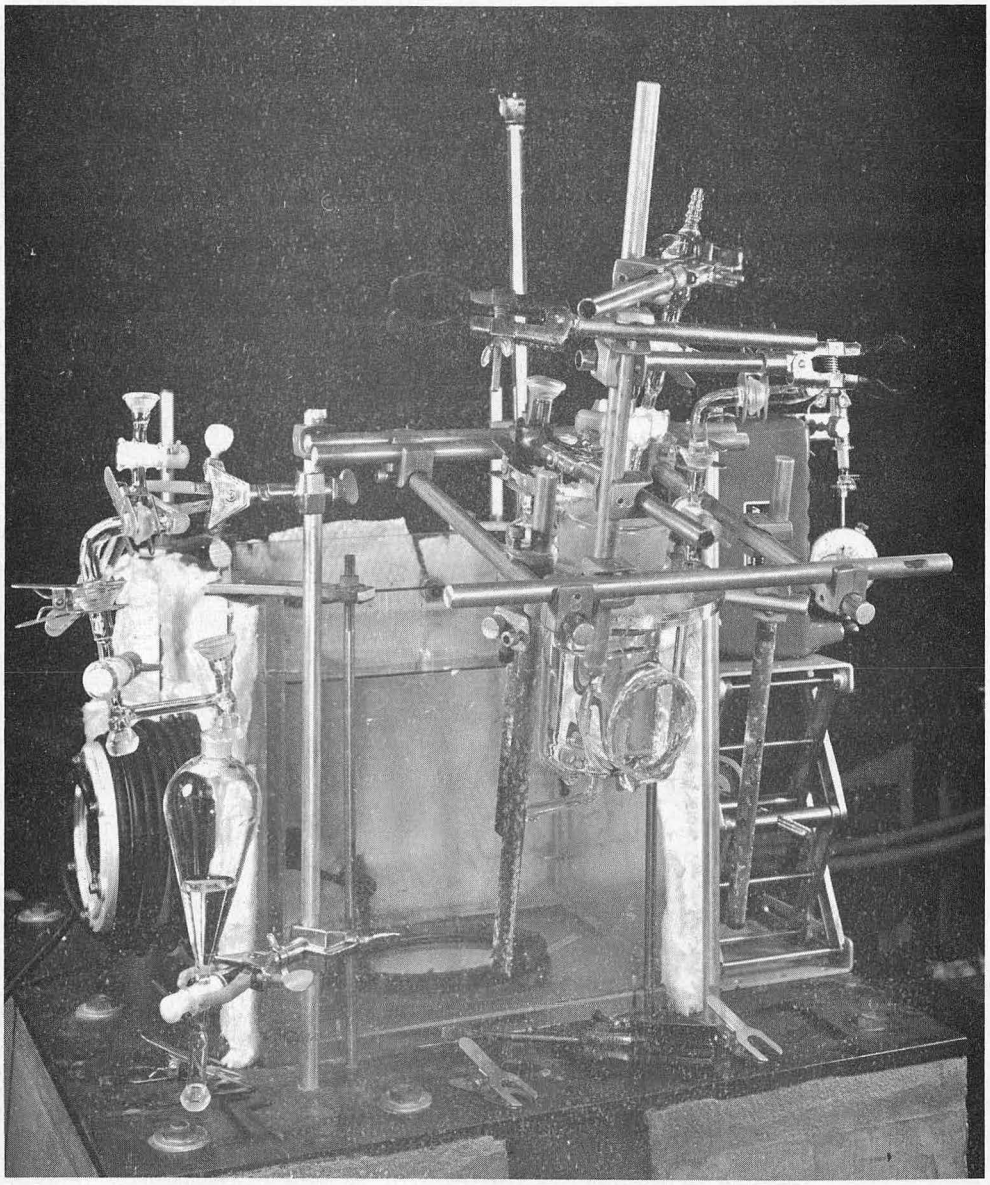

ZN-3107

Fig. 24. Framework for holding coalescence cell during assembly.

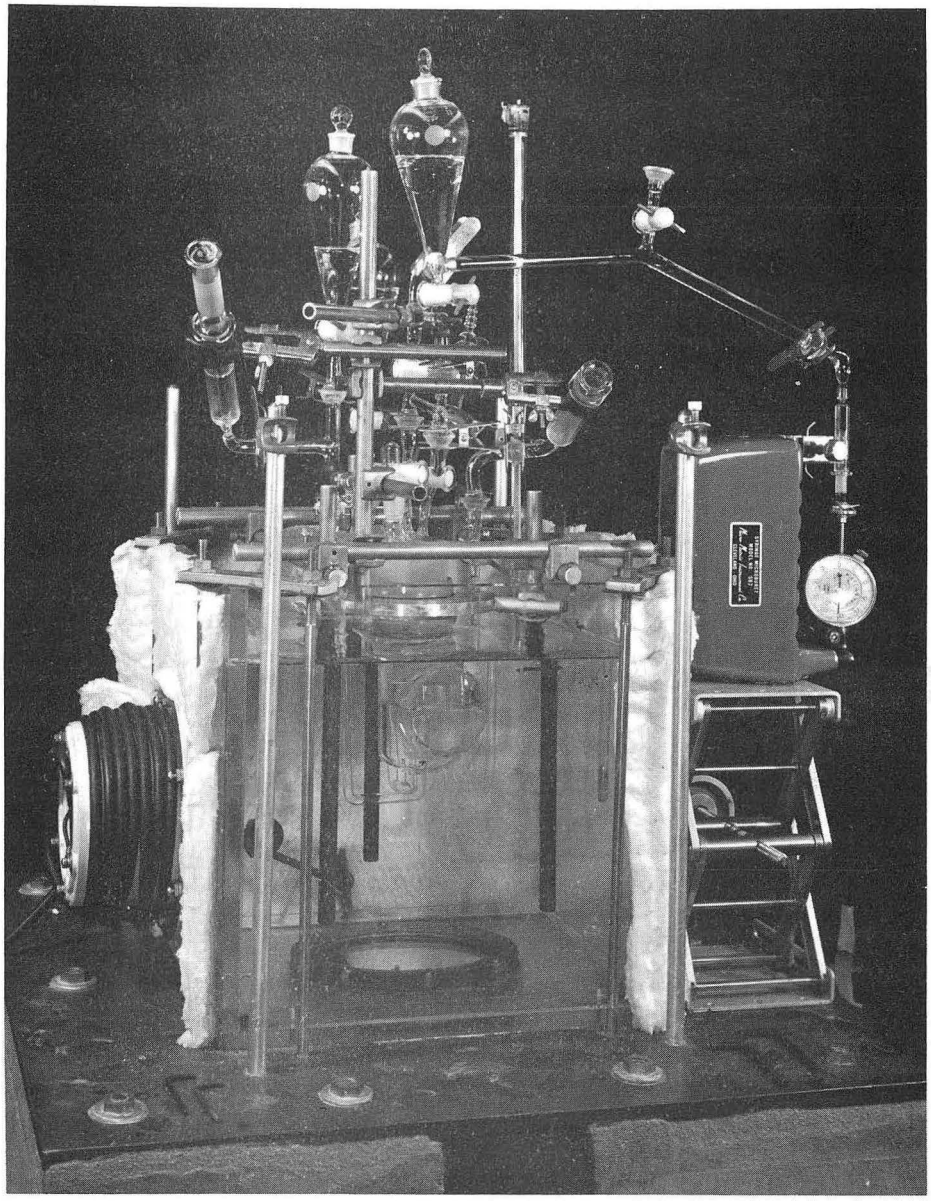

ZN-3108

Fig. 25. Coalescence equipment for phase 1 denser than phase 2. The swimming-pool speaker can be seen on the left side of the experimental tank, and the microburet on a laboratory jack on the right side. The coalescence cup is in the cell.

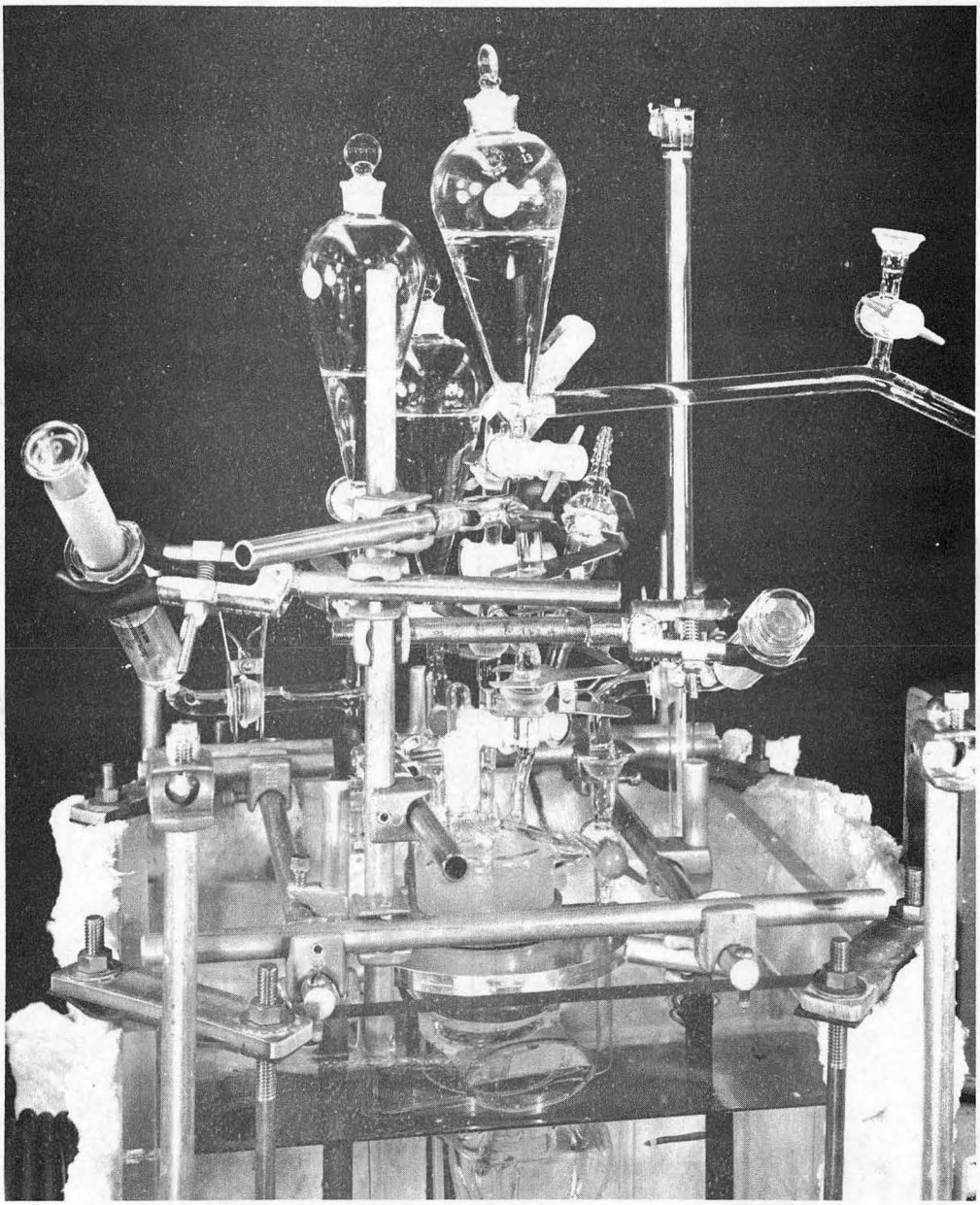

ZN-3109

Fig. 26. Close-up view of coalescence equipment for operation when phase 1 is denser than phase 2.

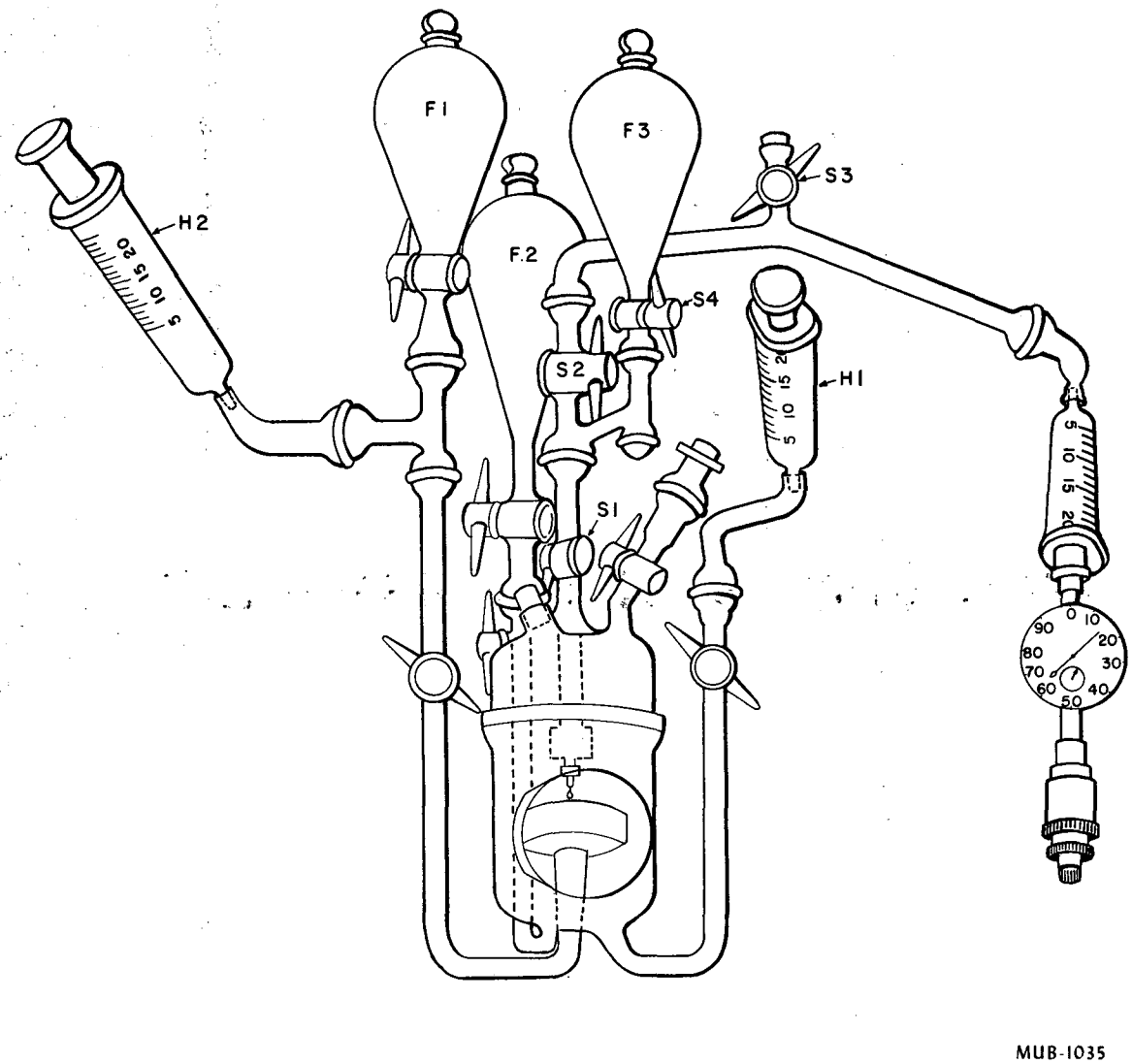

Fig. 27. Schematic diagram of coalescence equipment for operation when phase 1 is denser than phase 2. The legend is explained in the text.

to eliminate all the air bubbles in the tubing. The interface in the coalescence cup was flushed free from contaminants by causing the cup to overflow with the liquid from funnel F1. Excess fluid could be removed from the cell with hypodermic syringe H1, and the interface in the cup could be made planar by adjusting the position of the plunger in syringe H2. Even very slight concavity or convexity in the interface in the cup could be detected by observing the mirrorlike reflections on the interface. The syringe in the microburet could be refilled from funnel F3 during a run by manipulation of stopcocks S2 and S3.

The complete assembly for the mode in which phase 2 was the denser liquid is shown in Figs. 28, 29, and 30. The part numbers refer to Fig. 30. In this mode, the coalescence cup was replaced with a glass adapter with the appropriate dropping tip. Phase 2 liquid was admitted to the cell from funnel F1 until the liquid level was the minimum distance above the end of the dropping tip. Phase 1 liquid was admitted to the cell by means of a pipette inserted through the opening in the cell top. The hypodermic syringe held by the microburet and the interconnecting tubing up to the dropping tip were filled with phase 1 liquid through funnel F2. The interface was freed from contaminants by means of a pipette inserted through the opening in the cell top. Nothing was provided for making the interface planar. Excess liquid could be removed from the cell by means of syringe H1. The syringe in the microburet was filled from funnel F2 when necessary.

c. Experimental Run. Before an experimental run was begun, it was necessary to allow the cell and its liquid contents to come to thermal equilibrium with the thermostat. Because the liquids were stored in a constant-temperature bath at 25°C, and because the room temperature never departed by more than 3 or 4 degrees from this point, it was decided that one hour was adequate for thermal equilibration. After one hour, the interface was renewed once. After an additional 15 minutes, the experiments were begun.

Fifty coalescence measurements were found sufficient to enable the coalescence distribution curve to be drawn accurately.[3,10,11] The circulation of constant-temperature water in the experimental tank caused

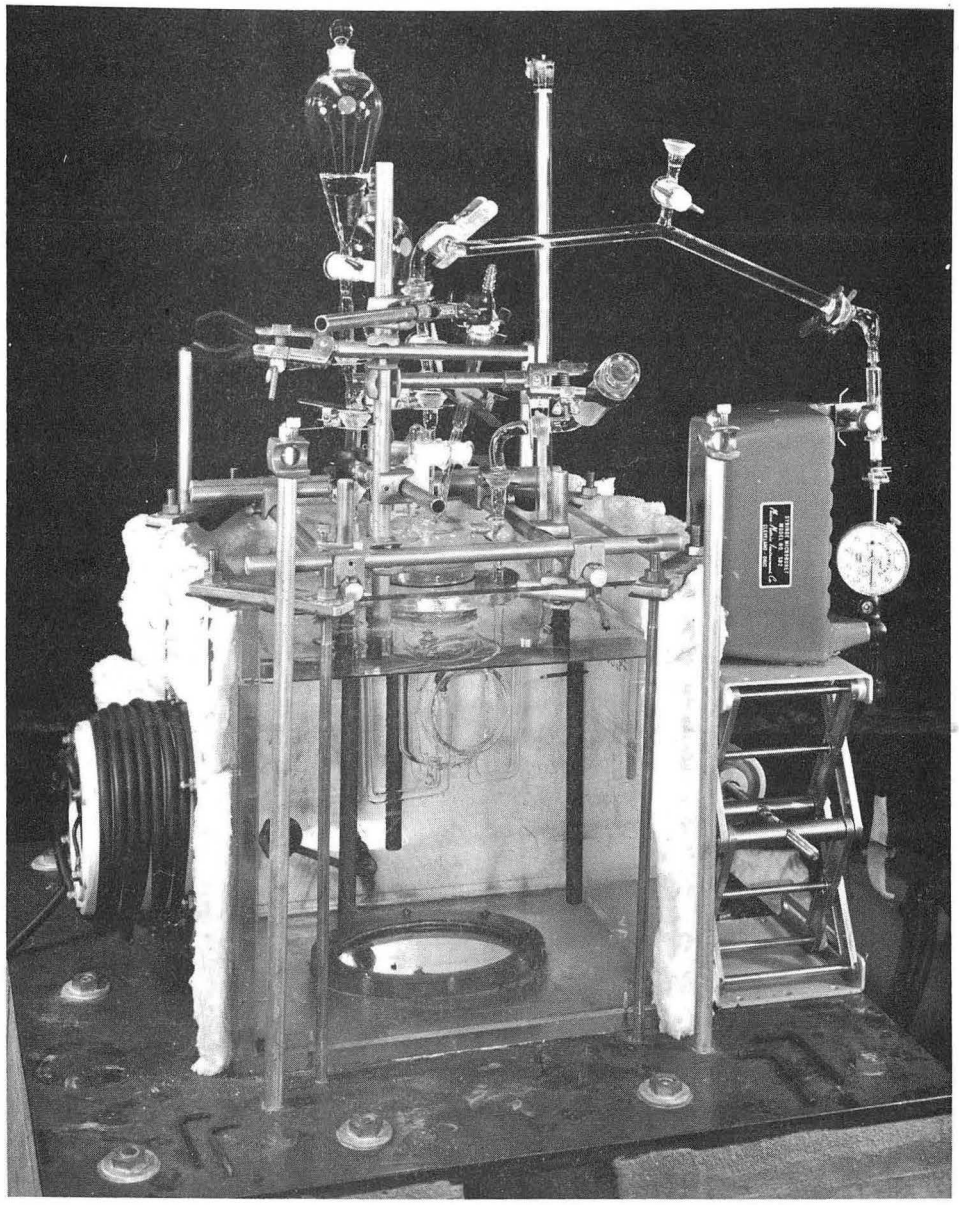

ZN-3110

Fig. 28. Coalescence equipment for operation when phase 2 is denser than phase 1. Note the glass adapter and dropping tip in the coalescence cell.

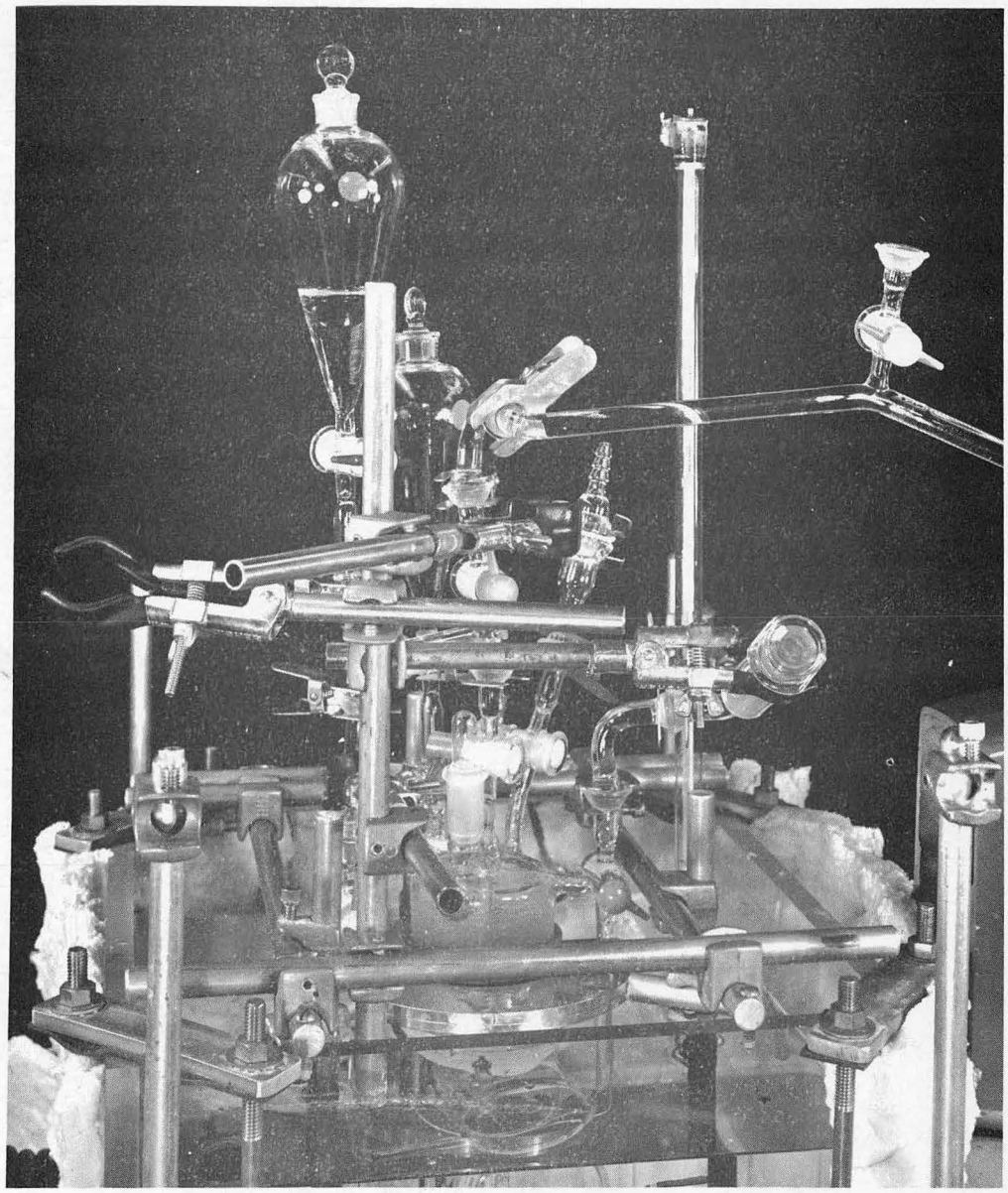

ZN-3111

Fig. 29. Close-up view of coalescence equipment for operation when phase 2 is denser than phase 1.

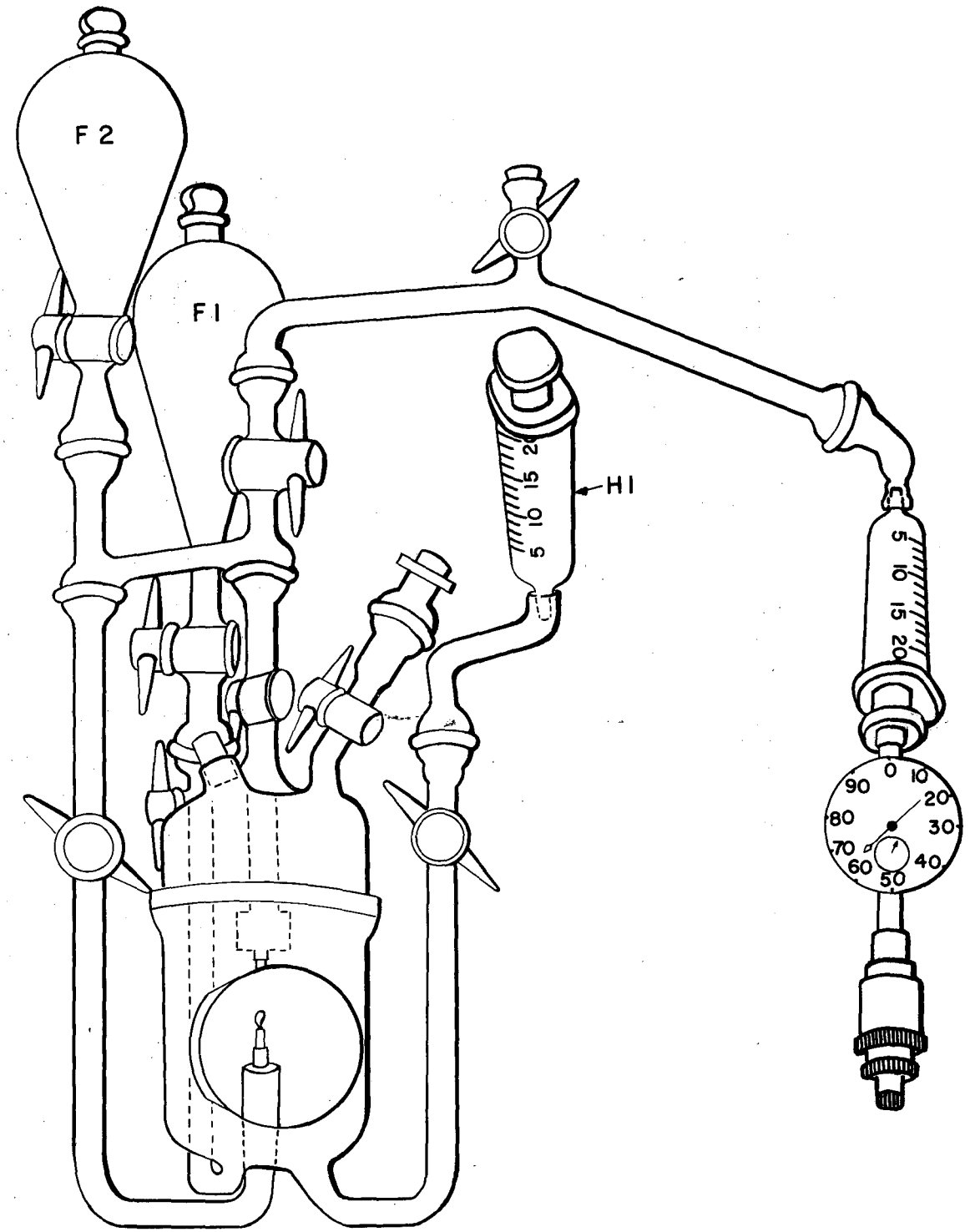

MUB-1034

Fig. 30. Schematic drawing of coalescence equipment for operation when phase 2 is denser than phase 1. The legend is explained in the text.

excessive vibration in the coalescence cell, and so the pump supplying water to this tank was shut off while coalescence measurements were being made. In most of the experiments, a run of fifty measurements was subdivided into four groups of 12 or 13 coalescence measurements each. The temperature of the experimental-tank water would fluctuate over the range 25 ± 0.1°C during the half-hour time required for the 12 or 13 measurements. The size of the hypodermic syringe in the microburet was selected so that this number of drops could be produced without refilling the syringe.

The procedure used during a run in which phase 1 was the denser one was as follows: When 15 minutes had elapsed since the interface renewal, the water pump was shut off and measurements were commenced. The first coalescence time in any group was discarded. Each drop was rapidly formed almost to full size with the microburet. The drop was allowed to hang from the dropping tip for one minute in order to come to thermal and chemical equilibrium with the surrounding fluid; then the drop was very slowly forced off the dropping tip by an additional movement of the microburet. The technique of drop formation was the same as the one recommended in the drop-volume method of measuring surface or interfacial tension.[48] In runs 1-27, the drops were aged for 15 seconds rather than for 1 minute. Also, in runs with extremely small drops, the microburet control was not sufficiently delicate to allow the drops to be aged for a full minute. The coalescence time was measured with a stopwatch from the time at which the drop reached the interface until the first-stage coalescence process occurred. The stopwatch had been calibrated previously against an electric timer. With the exception of the systems using very viscous liquids, the time that elapsed between the drop's falling off the tip and its reaching the interface was less than 0.1 sec. The reaction time of the experimenter in actuating the stopwatch was also less than 0.1 sec, and the two reaction times involved in a singel measurement were considered to be self-cancelling. After every 4 or 5 drops, the interface was made very slightly concave so that the drops would remain approximately

in the center of the cup prior to coalescence. After either 12 or 13 coalescence times were measured, the water pump was turned on, the interface was renewed and made nearly planar, the syringe was refilled, and the cycle begun again. The procedure when phase 2 was denser than phase 1 was nearly the same. In some runs, the method of grouping was changed so that a different type of analysis could be made.

As many as three complete runs were made in a day. Either 30 minute's time was allowed between runs, if the cell was opened to change dropping tips, or 15 minutes, if the cell was not opened. In the high-frequency sonic-disturbance runs, the 12 groups of 3 runs in a day were permuted by means of a table of random permutations[57] to minimize any error caused by cumulative contamination.

d. Analysis of Run. Several items were computed for each run, to characterize the shape of the coalescence time distribution curve. These items included the average time $\bar{t}$, median time t_m, the 10-and 90-percentile points $t_{.10}$ and $t_{.90}$, and the variance σ^2. The 10-and 90-percentile points were more representative of a run than the lowest and highest coalescence times, which were often inexplicably erratic.

Subdivision of a run into four groups provided a useful statistical test for the consistency of the data in a run. Each of the four groups was considered to be a separate treatment with 12 or 13 replications. An analysis of variance was made on each run to determine if the difference between groups or treatments (i.e., the group average) was statistically significant.[57] Snedecor's F-distribution[58] was used to check for statistical significance of the differences between groups. Although a large number of runs showed significance even at the 1% level, it was not felt that this was sufficient a priori reason for discarding the data. However, it was noted that each run discarded because of accidental contamination of the test fluids showed very strong significance at the 1% level. A numerical example of an analysis of variance on a run is given in Appendix A-1. The variance of the data in a run was calculated from this analysis of variance, and, as a result, it has

a number of degrees of freedom corresponding to a subdivision into four groups rather than a variance calculated on the basis of a single group.

The drop volume was calculated from the interfacial tension, the density difference between the two phases, and the dropping tip radius by the drop-volume (or drop-weight) procedure.[48] The relation between the drop volume and the other variables is given by

$$v = \frac{2\pi r \sigma f\,(r/v^{1/3})}{\Delta \rho g} , \qquad (106)$$

where v is the drop volume in cm^3, r is the dropping tip radius in cm, $f(r/v^{1/3})$ is a tabulated function, and the other variables have their usual significance. Experimental values of $f(r/v^{1/3})$ for $r/v^{1/3}$ between 0.30 and 1.60 are given by Harkins.[56] However, for small values of the dropping-tip radius, recourse must be made to the theoretical values of Lohnstein[59,60] which were checked experimentally at later date by Dunken.[61] Lohnstein's tables give $f(r/a)$ where a, the capillary constant, equals $\left(\frac{2\sigma}{\Delta\rho g}\right)^{1/2}$. Because of the relative inaccessibility of this tabulation, the values are repeated in Table V. Ordinarily, the use of the calibrated microburet would provide an additional check on the drop volume. However, it was found that leakage in the joints between the syringe and the dropping tips was so great that the volumes measured on the microburet were seriously in error.

All of the experimental data, including the points of subdivision into groups, the various statistical parameters described above, and comments, are given for each run in Appendix B.

TABLE V. Drop-volume method correction factor.[a]

r/a	f(r/a)	r/a	f(r/a)
0.00	1.0000	0.1	0.805[b]
0.01	0.9520	0.2	0.741
0.02	0.9258	0.3	0.701
0.03	0.9047	0.4	0.679
0.04	0.8863	0.5	0.657
0.05	0.8698	0.6	0.643
0.06	0.8547	0.7	0.637
0.07	0.8407	0.8	0.634
0.08	0.8275	0.9	0.627
0.09	0.8151	1.0	0.608
0.10	0.8033[b]		

[a] From reference 61.

[b] The two different values of f(0.10) are due to a difference in calculation methods in the two regions, 0 to 0.10, and 0.1 to 1.0. The accuracy of the drop-volume method for this range of r/a is such that either value of f(0.10) can be used.

B. Sonic Equipment

A variety of types of electronic equipment were used in the sonic studies. The equipment and techniques, and results of the loudspeaker and microphone calibrations, are described below.

1. Equipment Description

It was desired to produce and detect sonic frequency disturbances within the coalescence cell which was submerged in the thermostat. Several types of loudspeakers and microphones were constructed or purchased before statisfactory results were obtained. The first unit to be tested could be used either as a loudspeaker or as a microphone. It consisted of the sensing unit of a sound-power telephone (Wheeler RV-102, SPT-102 Cartridge for Sound-power telephone, Wheeler Electronic Corp., Waterbury, Connecticut) mounted by means of an O-ring gasket in a brass case. The electrical leads were brought out of the case through a shielded coaxial cable contained within a long copper tube. This unit was called the telephone speaker or microphone and is illustrated in Fig. 31. Because of bad resonances and water leaks when the unit was used as a speaker, and large size and poor sensitivity when the unit was used as a microphone, the unit was discarded after a few experimental runs.

A swimming-pool speaker (Universal Model MM-2FUW Flush Mounting Underwater Loudspeaker made by Universal Loudspeakers Inc., White Plains, New York) was then purchased and mounted on the side of the experimental tank. It proved to be very satisfactory over a wide range of frequencies.

A small microphone was made by sealing a barium titanate piezoelectric disk into a vial filled with transformer oil in a manner similar to suggested procedure[62] for constructing a hydrophone. This device was more sensitive than the telephone microphone, but unfortunately, it also proved to be sensitive to the radio-frequency electromagnetic radiation produced by the Thermotrol unit. The microphone finally adopted was made by drilling several small holes

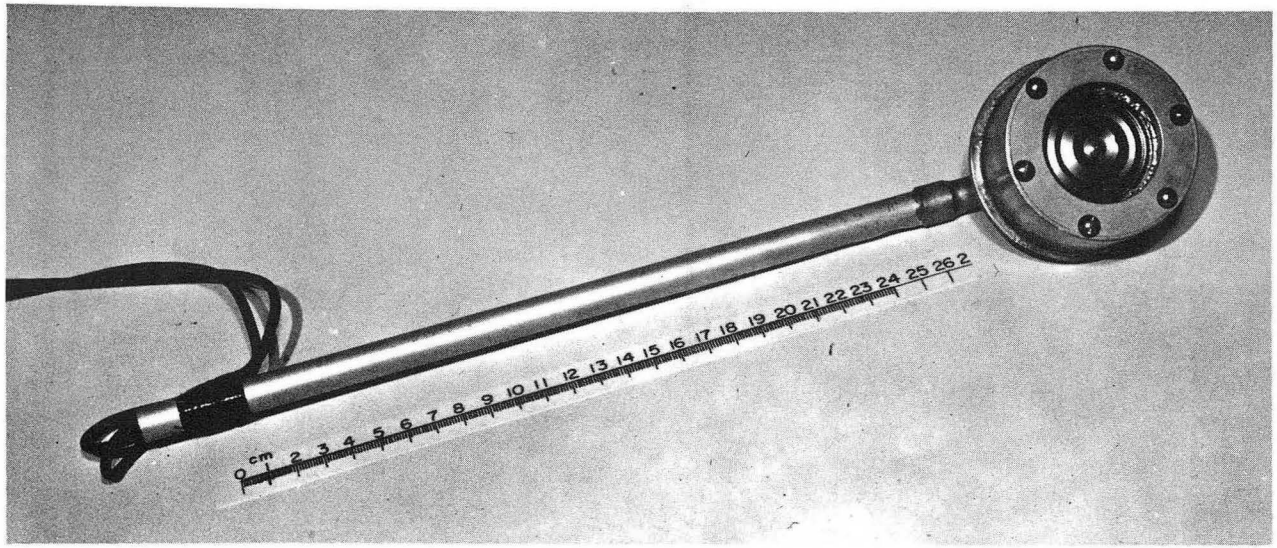

ZN-3112

Fig. 31. Photograph of telephone speaker or microphone.

through the center of the back of the sensing disk of a Turner Model 9X Microphone (Turner Microphone Company, Cedar Rapids, Iowa) and soldering the back of the disk to a small brass case. Attached to the case was a long copper tube for mechanical support and a coaxial cable connected to the disk leads. Transformer oil was poured into the coaxial cable sheath until it reached a level at which the hydrostatic pressure inside the disk was the same as the pressure in the cell or in the experimental tank. This technique eliminated the hydrostatic pressure effect on the bimorph Rochelle-salt sensing element of the disk. This microphone was so sensitive that, with the oscilloscope described below used as detector, it responded to the disturbance produced by a small Allen wrench falling on the floor 15 feet away from the concrete pillar. Fig. 32 is a photograph of this crystal microphone.

Sounds of various frequencies were produced by connecting a General Radio Type 1210-B R-C Oscillator (General Radio Company, Cambridge, Massachusetts) to a McIntosh Model MC-30-watt Audio Amplifier (McIntosh Laboratory, Inc., Binghamton, New York) which was in turn connected to the loudspeaker. The beat frequency experiments were performed using 2 R-C Oscillators in parallel. In some experiments, white noise was generated by replacing the R-C Unit Oscillator with a General Radio Type 1390-A Random Noise Generator (General Radio Company, Cambridge, Massachusetts). The voltages imposed on the loudspeaker as well as those produced by the microphone were measured with a Tektronix Type 541A oscilloscope (Tektronix, Inc., Portland, Oregon) with a Plug-In Unit Type D having a voltage sensitivity of 1 mV/cm. Random noise measurements were made by connecting the crystal microphone to either the oscilloscope or to a Hewlett-Packard Model 302A wave analyzer (Hewlett-Packard, Palo Alto, California). (In some of the early work, the older Model 300A Harmonic Wave Analyzer was used). Impedance measurements were made on the swimming pool and telephone speakers with a General Radio Type 650-A impedance bridge with the oscilloscope and a Trimm, Inc. B-42 Headset (Trimm Inc., Libertyville, Illinois) as null detectors. When the impedance bridge was used as a modified Wheatstone Bridge (see next section), a General Radio Type

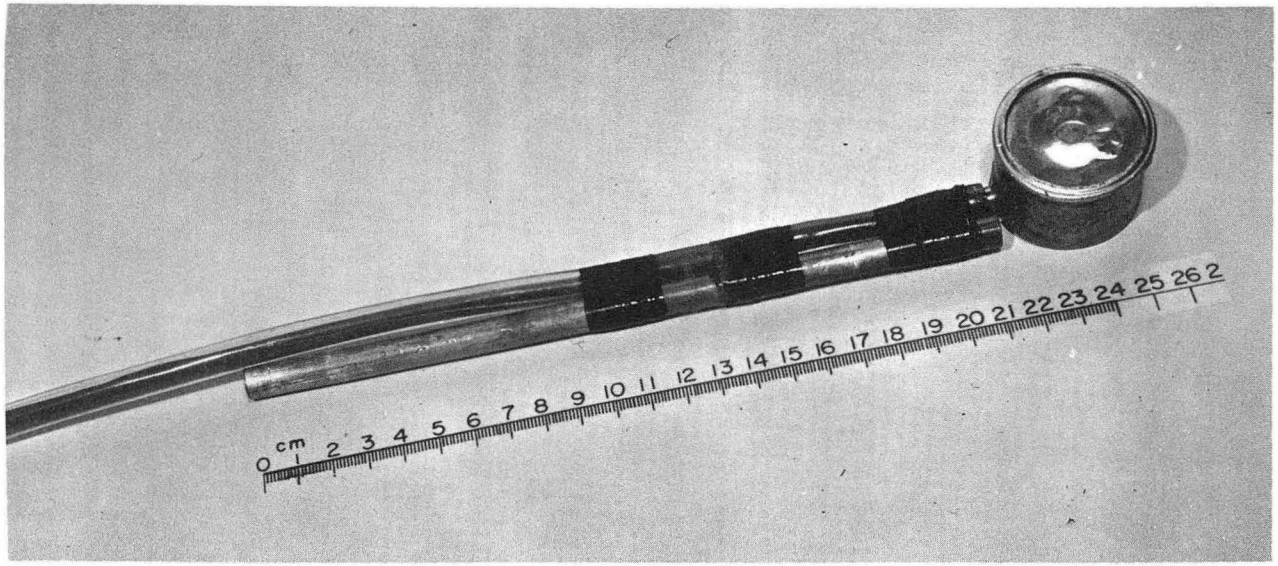

ZN-3113

Fig. 32. Photograph of crystal microphone.

219-M decade condenser was shunted across arm A of the bridge. An overall view of the electronics equipment is given in Fig. 33.

2. Calibration

So that sound pressures in the coalescence cell could be related to power dissipation in the loudspeaker, it was necessary to measure the impedances of the telephone and swimming pool speakers, perform an absolute calibration on the crystal microphone, and measure the microphone response to various speaker power inputs. These calibrations were performed over a frequency range extending from either 50 or 65 cps up to 10,000 cps.

A speaker was considered to behave electrically as an inductance in series with a resistance. Two methods can be used to measure the impedance with an impedance bridge. The first method, called the Method of A-C Resistance with Reactance, determines the resistance very accurately, and the inductance less accurately, by means of the modified Wheatstone Bridge circuit shown in Fig. 34(a). The second method, called the Inductance Method, measures the inductance very accurately and the resistance less accurately by means of the Maxwell Bridge shown in Fig. 34(b). In both methods, the speakers were immersed in water, the R-C unit oscillator was used for the power source, and an oscilloscope and a headset were used as null detectors. The following arbitrary convention was set up to determine which method should be used in different frequency ranges.

If $R \geqslant 2\ X_L$, the Method of A-C Resistance with Reactance was used;

if $X_L \geqslant 2R$, the Inductance Method was used;

if $X_L/2 < R < 2\ X_L$, the arithmetic average of the results of the two methods was used.

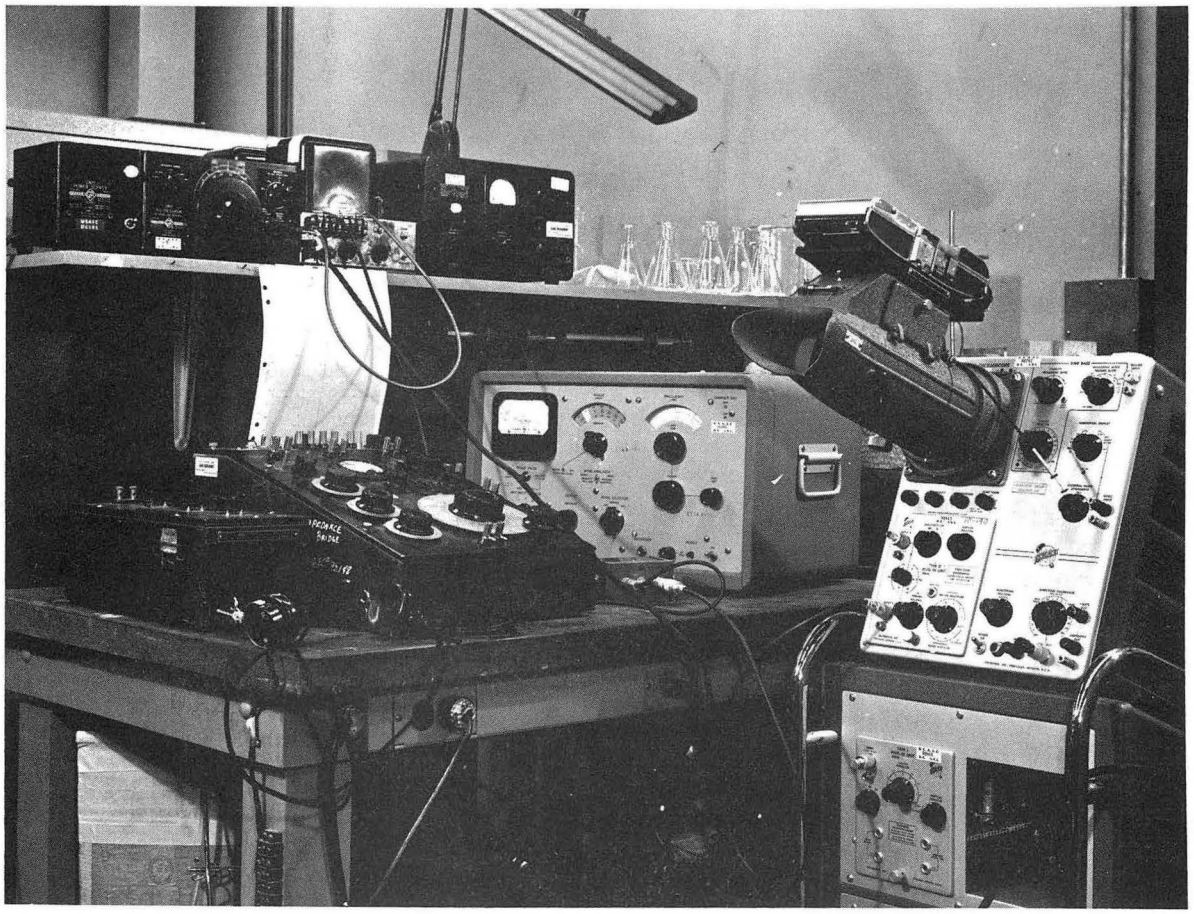

ZN-3114

Fig. 33. Photograph of the electronics equipment used in the study. From left to right on the shelf are shown the R-C oscillator, amplifier, and random-noise generator. On the table, from left to right, are the decade condenser box, headset, impedance bridge, and harmonic wave analyzer. The oscilloscope with a camera for photographing the oscilloscope trace is shown at the right side of the photograph.

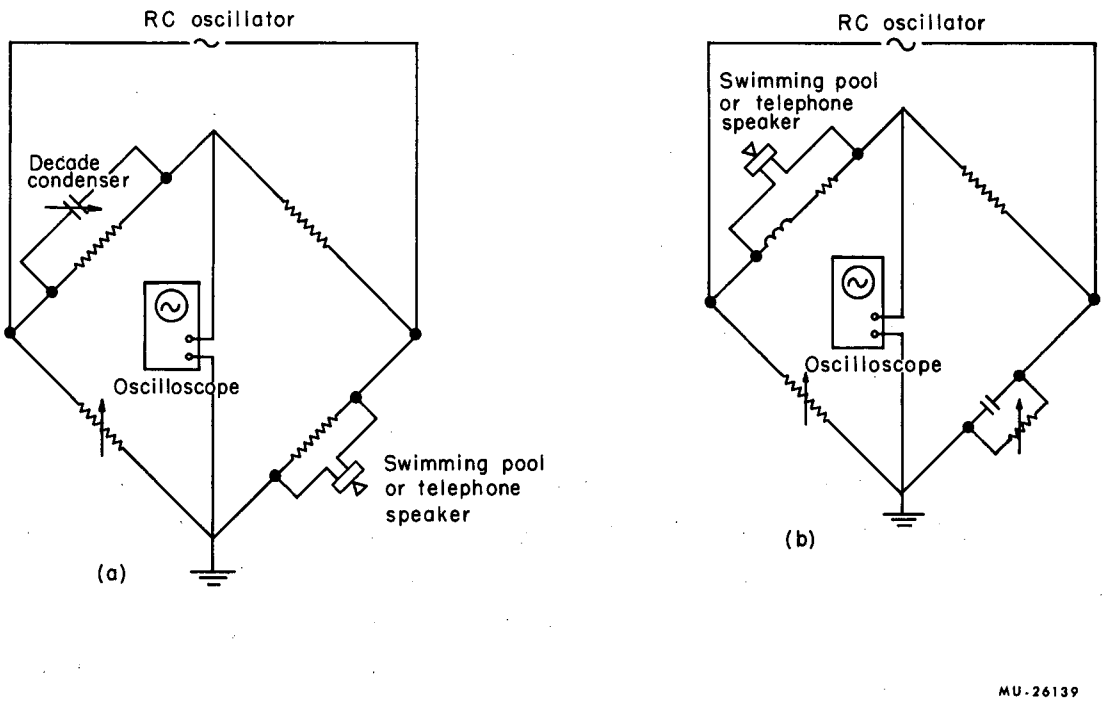

Fig. 34. Schematic diagrams of the impedance bridge circuits. All electrical parts not identified by name on the drawing are parts of the internal mechanism of the General Radio 650-A impedance bridge: (a) modified Wheatstone Bridge circuit; (b) Maxwell Bridge circuit.

The following formulas were used to relate resistance R, inductance L, inductive reactance X_L, impedance, Z, current I, voltage E, and power P:

$$Z = [R^2 + (2\pi\nu L)^2]^{1/2} ,$$

$$X_L = 2\pi\nu L,$$

$$I = \frac{E}{Z} , \tag{107}$$

and

$$P = I^2 R.$$

Here ν represents the frequency in cps.

The resistance, inductive reactance, and impedance of the telephone and swimming-pool speakers are given in Figs. 35 and 36, respectively. An absolute microphone calibration technique is given by Beranek.[63] This technique yields the voltage produced by the sound pressure field that would exist at the microphone location, if the microphone were not there. The technique requires the test microphone, a sound source, and a unit that can act as either a microphone or as a speaker (a reversible transducer). The theory is based on the electrical reciprocity principle and does not require any absolute standards. In principle, the calibration should be performed in an anechoic (echo-free) chamber, but this is impractical for a liquid system. One can check to see if his test chamber is large enough (an infinite chamber would be physically analogous to an anechoic chamber) by seeing if the pressure calibration remains the same when the spacing between microphone and speaker is changed.

The calibration technique is illustrated schematically in Fig. 37. In the first step (Fig. 37a), the test microphone and the reversible transducer are alternately exposed to the same sound source at the same distance d (cm), to yield the microphone voltages, e'_{oc}

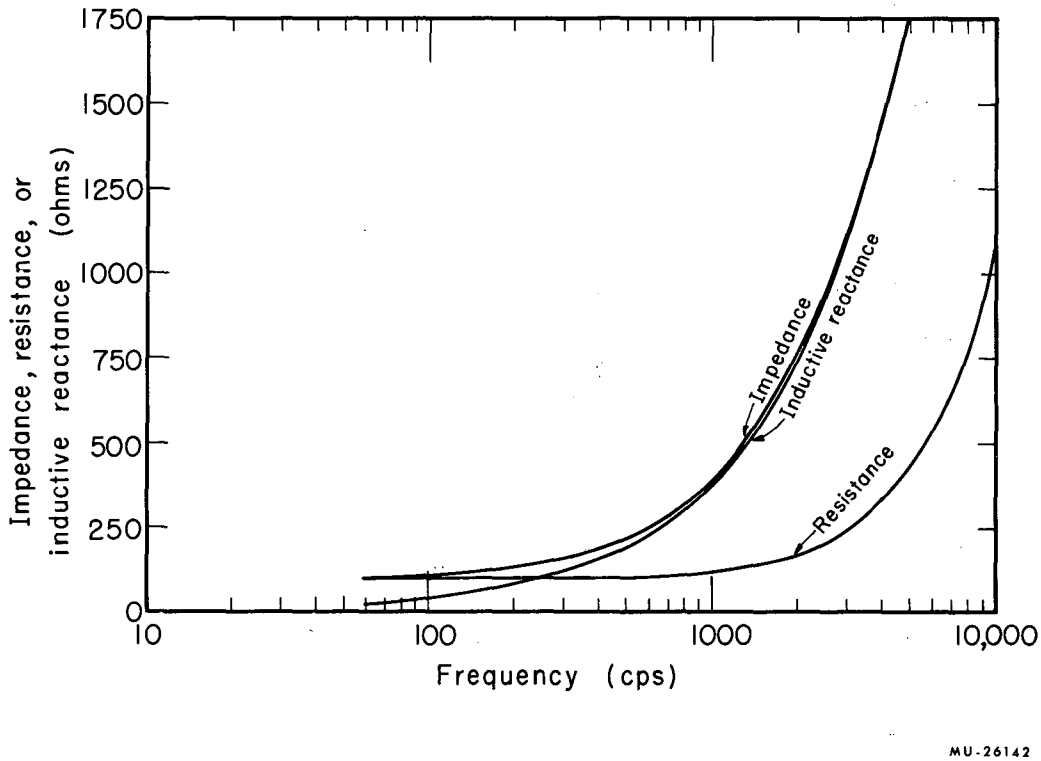

Fig. 35. Impedance, resistance, and inductive reactance of the telephone speaker.

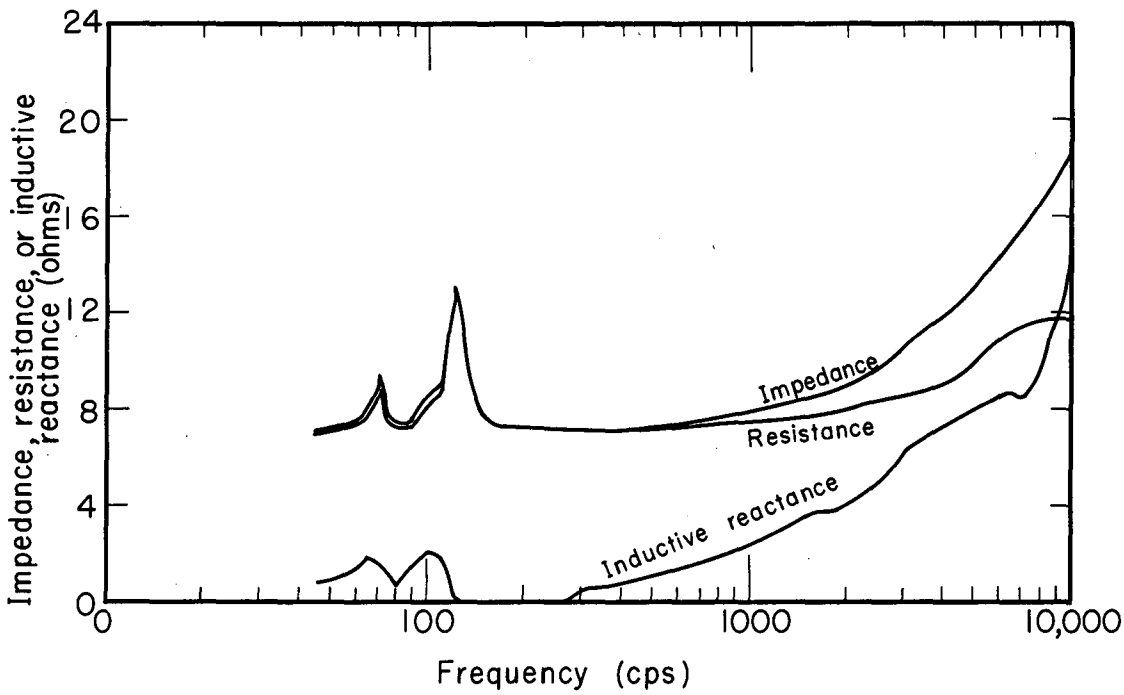

MU-26141

Fig. 36. Impedance, resistance, and inductive reactance of the swimming-pool speaker.

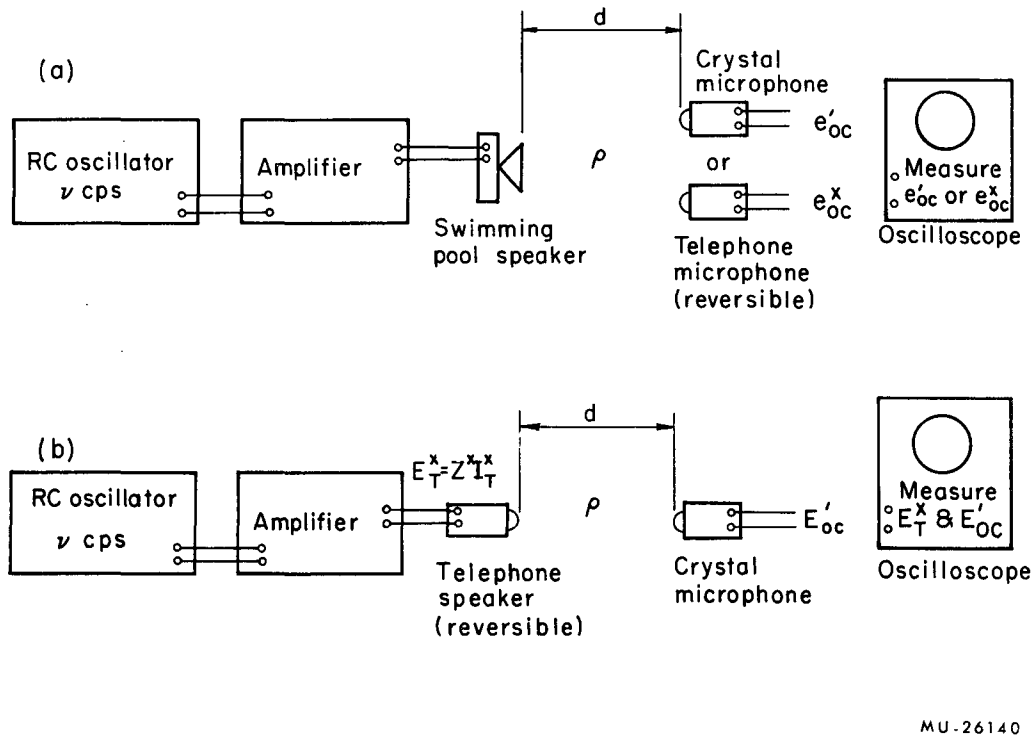

Fig. 37. Microphone reciprocity calibration technique: (a) Responses of crystal microphone and telephone microphone to swimming-pool speaker are measured; (b) Response of crystal microphone to telephone speaker is measured.

and e^x_{oc} , respectively. In the second step (Fig. 37b), the test microphone is exposed to the reversible transducer now acting as a speaker at distance, d (cm). The voltage response of the test microphone, E'_{oc} , is found corresponding to the current, I^x_T , driving the reversible transducer. The only additional information needed is the acoustic impedance of the medium ρ c, where ρ is the density of the liquid and c is the velocity of sound in the medium, and λ, the wavelength of the sound in the medium. Then, M^x_o , the voltage sensitivity (volts/dyne cm^{-2}) for the reversible transducer is given by

$$M^x_o = \left| \left[\left(\frac{E'_{oc}}{I^x_T} \right) \left(\frac{e^x_{oc}}{e'_{oc}} \right) \frac{2d\lambda}{\rho c} \times 10^{-7} \right]^{1/2} \right| . \qquad (108)$$

The corresponding voltage sensitivity for the test microphone M'_o is given by

$$\frac{M^x_o}{M'_o} = \frac{e^x_{oc}}{e'_{oc}} . \qquad (109)$$

In terms of the frequency, ν , voltage E^x_T driving the reversible transducer, and impedance Z^x of the reversible transducer, Eqs. (108) and (109) can be changed to

$$M'_o = \left| \left[\left(\frac{E'_{oc}}{E^x_T} \right) \left(\frac{e'_{oc}}{e^x_{oc}} \right) \frac{2d\ Z^x}{\rho\ \nu} \times 10^{-7} \right]^{1/2} \right| . \qquad (110)$$

In this calibration, the swimming-pool speaker served as the sound source, the telephone speaker-microphone as the reversible transducer, and the crystal microphone as the test microphone. The error due to the presence of a finite chamber rather than an anechoic one was apparently small, as shown by the close agreement between values of M_o' and M_o^x at various values of d. The calibration results for the crystal and telephone microphones are given in Figs. 38 and 39, respectively.

In order that the sound pressure within the coalescence cell could be determined without the inconvenience of inserting the crystal microphone each time a measurement was desired, a graph relating the voltage and frequency imposed on the swimming pool speaker to the rms sound pressure in the coalescence cell was prepared. To make the measurements, the crystal microphone was inserted into the open coalescence cell, which was filled with water. The crystal microphone was rotated through four uniformly spaced positions to give the rms sound pressure corresponding to each frequency-voltage combination imposed on the swimming-pool speaker. The four values obtained were averaged to give the final result. At a number of frequencies and voltages, the signal produced by the microphone was either of a much higher frequency than that imposed on the speaker or was made up predominantly of noise. These points corresponded to echoes or resonances in the experimental tank, and were not included in the graphical presentation of the data in Fig. 40. The sound pressures corresponding to the voltages and frequencies imposed on the telephone speaker in certain of the experimental runs are given in Table VI.

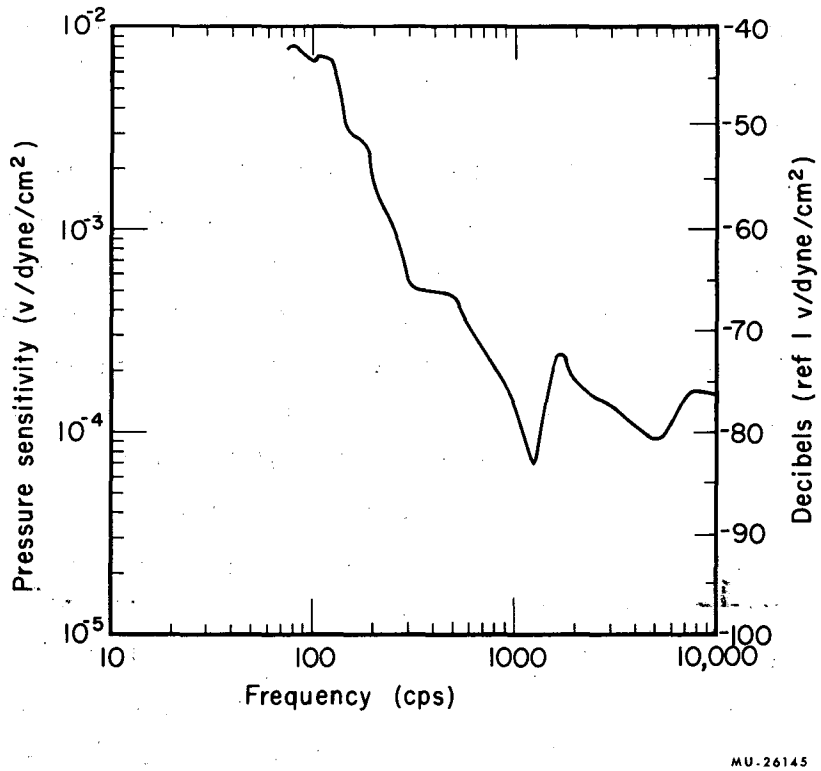

Fig. 38. Pressure sensitivity of crystal microphone as a function of frequency.

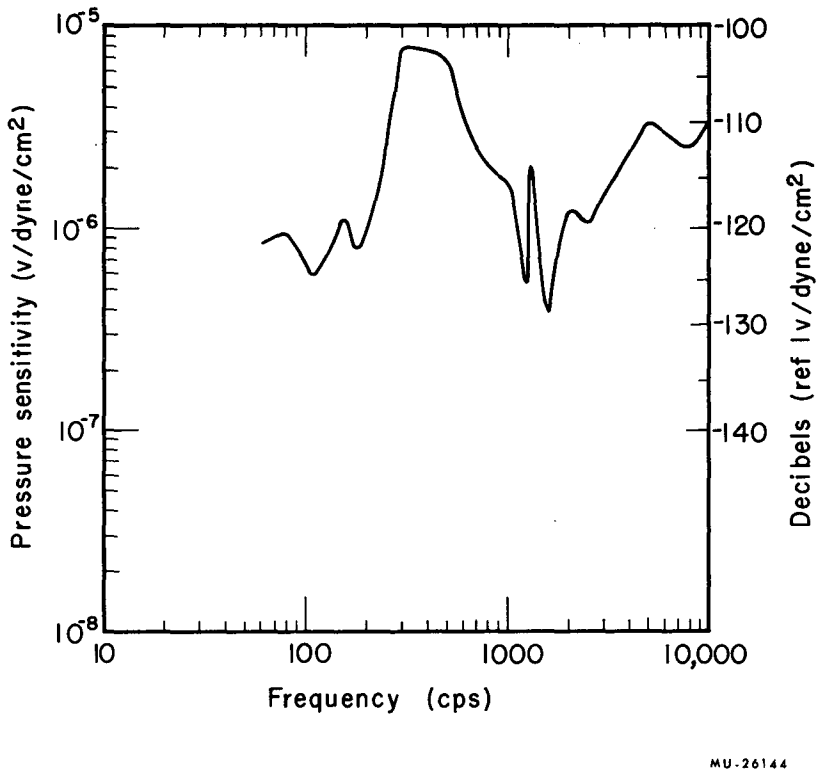

Fig. 39. Pressure sensitivity of telephone microphone as a function of frequency.

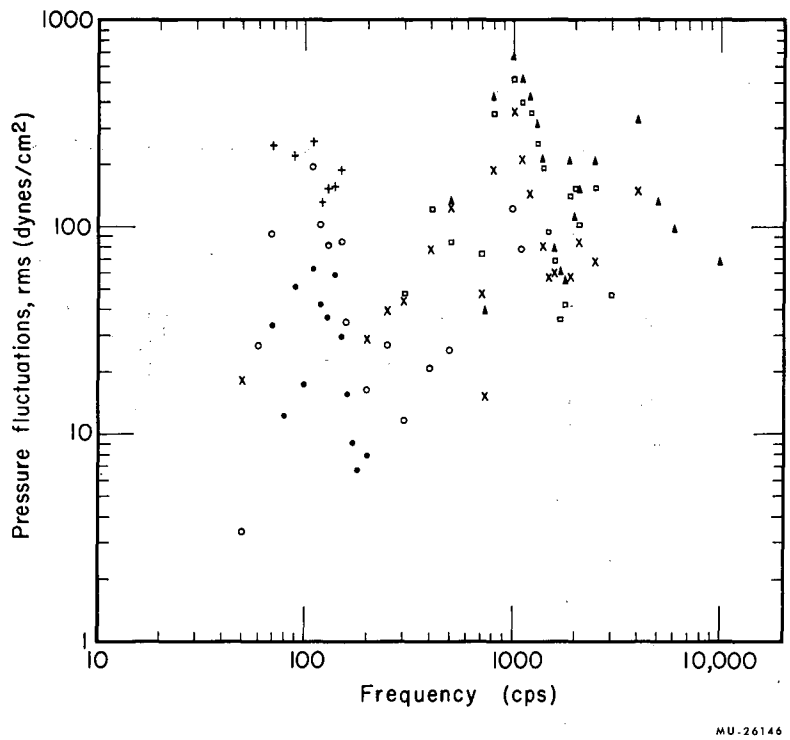

Fig. 40. Pressure fluctuations produced in coalescence cell by operation of swimming-pool speaker at various voltage-frequency combinations.

Swimming-pool speaker voltage (rms volts)	Symbol
0.7	●
1.8	○
3.5	+
5.3	x
8.8	□
14.1	▲

TABLE VI. Sound pressures produced by the telephone speaker.

Speaker voltage	Frequency (cps)	Rms sound pressure (dynes/cm^2)
8.1	100	4.6
10.2	250	152.0
12.7	500	398.0
18.7	500	408.0
19.8	2500	23.9

C. Materials

To minimize the effects of contamination, special techniques were devised to remove small quantities of both soluble and suspended impurities from the liquids used in this study.

The water used as an experimental fluid as well as the water used as a final rinse was prepared by passing distilled water from the laboratory system through two columns containing ion-exchange resins (Dowex, ion exchange resins, Rio-Rad Laboratories, Richmond, California). The ion-exchange treatment lowered the electrical conductivity of the water from 1×10^{-6} mhos to 5×10^{-8} mhos. The water was passed through a 0.45-μ Millipore filter to remove any suspended matter and was stored until use in 1-gal Pyrex bottles. The filtration and storage reintroduced carbon dioxide from the atmosphere and sodium, borate, and silicate ions from the glass. Water could be removed from the bottle through a special polyethylene dispenser, so that it did not pick up dust from the air (Pioneer Reagent Dispenser, made by Pioneer Plastics, Dayton, Ohio).

Benzene (except for some of the benzene used in the method-of-purification tests) was purified by fractional crystallization by a procedure similar to one suggested by Schwab and Wichers.[64] A 7-lb. bottle of reagent-grade benzene (Baker and Adamson Reagents, Allied Chemicals, General Chemicals Division, New York) was placed in a 1-gallon aluminum can. The can was stored at -2°C for about 24 hours, or until half of the benzene was frozen. The can was then shaken violently to wash the surface of the benzene crystals. The liquid benzene was discarded, the crystals were melted, and the process was repeated twice more. The final portion, about 1/8 of the original volume, was filtered through a 0.45-μ Millipore filter before use. The efficiency of this treatment is compared with that of fractional distillation in the mass spectrographic data (Sec. IV-A).

N-tributyl phosphate (J. T. Baker Chemical Company, Phillipsburg, New Jersey) was purified by a single vacuum distillation over

sodium bicarbonate using an 18-in. column packed with glass Raschig rings. The sodium bicarbonate reacted with any acidic products that might have been formed in the distillation. The first and last quarters of the distillate were discarded. Anisole (Eastern Chemical Corporation, New York) was purified by distillation in a 30-in. column filled with "Heli-pak" (No. 3013, Podbielniak, Inc., Chicago, Illinois), only the middle fraction being retained.

Ethylene glycol (Eastman Organic Chemicals, Distillation Products Industries, Rochester, New York) and Aroclor 1248 (a tetrachlorinated diphenyl from Monsanto Chemical Company, St. Louis, Missouri) were not further purified. Three surface active agents, which were not further purified, were also used: Span 80, sorbitan mono-oleate; Tween 81, sorbitan mono-oleate plus 5 molecules of ethylene oxide (both from Atlas Powder Co., Wilmington, Delaware); and sodium oleate (J. T. Baker Chemical Company, Phillipsburg, New Jersey). (Sorbitan is an inner ether produced from sorbitol, a sugar alcohol made by reduction of glucose).

It was necessary that the phase 1 and 2 materials be mutually saturated at 25°C. The saturation was accomplished by placing several hundred ml of each of the two phases in a 500-ml flask which was clamped in the constant-temperature bath located on the table. The two phases were stirred vigorously for a minimum of 24 hours by Teflon-coated magnetic stirring bars actuated by magnets attached to laboratory stirrers located under the tank. This tank and the stirring apparatus is shown in Fig. 41. The flasks of materials were stored in the constant-temperature bath until they were used. A somewhat different procedure, described in Sec. IV, was used for liquid phases containing a surface-active agent.

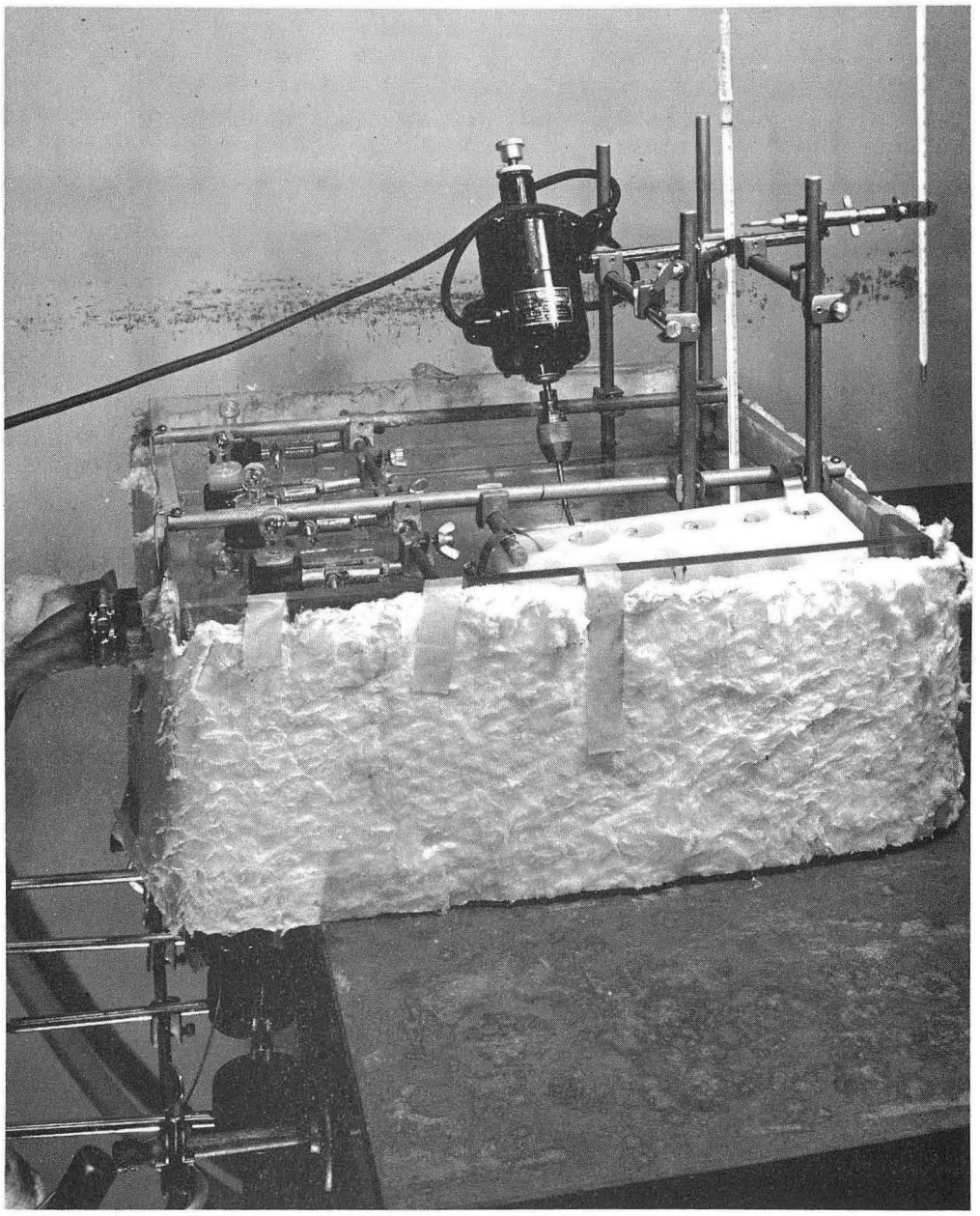

ZN-3115

Fig. 41. Photograph of constant-temperature bath located on table. The magnetic stirring units beneath the tank, the 500-ml flasks in the bath, and the polyethylene pycnometer-bottle holder are also shown.

D. Physical Properties

1. Density

The densities of the various liquid materials used were determined from the weights of the contents of 10-ml pycnometer bottles, whose volume had been previously found by a calibration with water. The bottles were filled with the proper liquids, placed in the constant-temperature bath at 25°C for 30 minutes, and quickly weighed. Because of high evaporation losses in the type of pycnometer bottle used, the scatter in replicate weighings was rather high. Each value given was the average of four to six weighings. The standard deviation as a percentage of the mean value of density ranged from 0.03 to 0.06%. The standard deviation as a percentage of the mean density differences, $\Delta \rho$, however, varied from 0.08% in the case of Aroclor 1248 and water to 6.0% in the case of anisole and water. The densities determined, and the calculated density differences of the various systems, are summarized in Table VII. The presence of a surface-active agent in the water-benzene system was assumed to have no effect on the density difference. The densities of the pure materials used in this study were taken from the literature.

2. Interfacial Tension

All interfacial and surface tension measurements were made with a ring tensiometer (Cenco-Du Nouy Interfacial Tensiometer No. 70545, Central Scientific Company, Chicago, Illinois) and a 6-cm platinum ring. Before any measurements were made, the plane of the ring was made horizontal as determined by observations with a cathetometer (Gaertner Scientific Corporation, Chicago, Illinois). The liquids studied were stored in a constant-temperature bath at 25°C until used; then they were poured into a Petri dish for the measurements.

It was noted that when surface and interfacial tensions of known systems were measured, the tensiometer correction factors of

TABLE VII. Measured physical properties at 25°C (liquid phases mutually saturated).

Phase 1	Phase 2	ρ_1 (g/cm^3)	ρ_2 (g/cm^3)	$\rho_1 - \rho_2$ (g/cm^3)	μ_2 (cp)	σ (dynes/cm)
Water	Benzene	0.9976	0.8733	0.1243	0.590	34.71[a]
Tributyl phosphate	Water	0.9763	0.9964	-0.0201	0.973	9.9
Water	Aroclor 1248	0.9966	1.4471	-0.4505	203	40.9
Water	Anisole	0.9975	0.9886	0.0089	0.957	25.5[b]
Ethylene glycol	Benzene	1.1029	0.8762	0.2267	0.612	7.4

[a] From reference 68.

[b] Refer to discussion in text (Sec. D-2).

Harkins and Jordan[70] yielded low results in every case. This difficulty was probably due to the fact that the ring used was not completely circular. Harkins et al[70] showed that the interfacial tension σ can be found from the tensiometer reading M by

$$\sigma = \frac{Mg}{4\pi R} F , \qquad (111)$$

where R is the radius of the ring.
The experimental correction factors F found by Harkins and Jordan were found to be proportional to $M/\Delta\rho$ by Zuidema and Waters.[71]

It was decided to compute a correction curve for the particular ring used. Tensiometer readings were taken on the systems water, benzene, and n-heptane against air, and the benzene and n-heptane against water. Correction factors for these systems were then computed using literature values of σ, and the following correction factor equation was derived, using least squares:

$$F = 0.001148 \, (M/\Delta\rho) + 0.8625 . \qquad (112)$$

The interfacial tensions determined from Eq. (111) are given in Table VII.

Because of the extremely low density difference in the water-anisole system, the tensiometer correction factor could not be determined from Eq. (112). Therefore, the value of 25.82 at 20°C[72] was corrected to 25°C by an approximate technique. Antonow's rule states that the interfacial tension between two liquids equals the difference between the surface tensions of the two liquids measured individually against air (each liquid being saturated with the other), minus a work of adhesion correction.[68] It was assumed in this study that the work of adhesion was relatively independent of temperature and that the surface tensions of the saturated phases would change by the same amount with temperature as would the surface tensions

of the materials in a pure state. Thus, the surface tension of water decreases by 0.78 dynes/cm when the temperature increases from 20°C to 25°C and the surface tension of anisole changes by 0.48 dynes/cm (calculated from Eotvos Law[48] using the Eotvos constant given by Lange[73]). Thus, using Antonow's rule, the interfacial tension of water-anisole decreases by (0.78 - 0.48)= 0.30 to 25.5 dynes/cm when the temperature increases from 20°C to 25°C.

3. Viscosity

Viscosities were determined by means of Cannon-Fenske viscometers used in a constant-temperature bath according to the procedure ASTM D 445-53T.[74] The viscosity of Aroclor 1248 saturated with water was found in a No. 200 viscometer (Kimble Glass Company, Toledo, Ohio) calibrated with a glycerol solution whose density was 1.1868 g/cm^3. No kinetic energy correction was needed with this large a viscometer. The calculated calibration equation was $\mu/\rho = 0.08078\ t$, where t is the time in seconds during which the test liquid passes from the first viscometer calibration mark to the second, and μ is the absolute viscosity in centipoises.

The other viscosities were measured in a No. 50 viscometer (Kimble Glass Company) which was calibrated with water and benzene. Two fluids were used so that a kinetic energy correction could be calculated. The calibration expression derived was $\mu/\rho = 0.001714\ t - 11.77/t$. In the case of low viscosity fluids, the kinetic energy correction was about 4% of the kinematic viscosity value μ/ρ. The viscosity data measured are given in Table VII.

IV. EXPERIMENTAL RESULTS

A. Preliminary Studies

The effects of surface renewal, distance between the dropping tip and the interface, external vibrations, the method of purification of materials, and drop aging, were studied in a number of preliminary experiments. The experiments described in this section were all made with the water-benzene system, but the conclusions are probably applicable to most other systems.

1. Surface Renewal

Picknett found that, if the interface were not renewed for a long period of time before coalescence measurements were made, the drop rest-times were excessively long.[5] Runs 12, 13, and 14 were made to check this result. Runs 12 and 14 were made in the manner described in Sec. III. Run 13 was made 10 hours after Run 12, and the interface in Run 13 was neither renewed at the beginning nor during the run. Coalescence time-distribution curves for the three runs are given in Fig. 42. Lack of surface renewal in Run 13 had no apparent effect. The disagreement with Picknett's findings probably indicates that some contaminant entered his equipment prior to his test run, whereas contamination was carefully eliminated in this experiment.

2. Distance Between Dropping Tip and Interface

In all the experiments conducted in this study, an attempt was made to minimize the distance a drop would fall between the dropping tip and the interface, through the adjustments described in Sec. III. However, some variation in this distance from run to run was impossible to avoid because it was difficult to adjust the distance precisely. Several sets of runs were made to determine the magnitude of change in this drop-fall distance. In Fig. 43, Runs 6 and 75, in which large drops (r_e = 0.415 cm) fell about 1 mm, are compared with

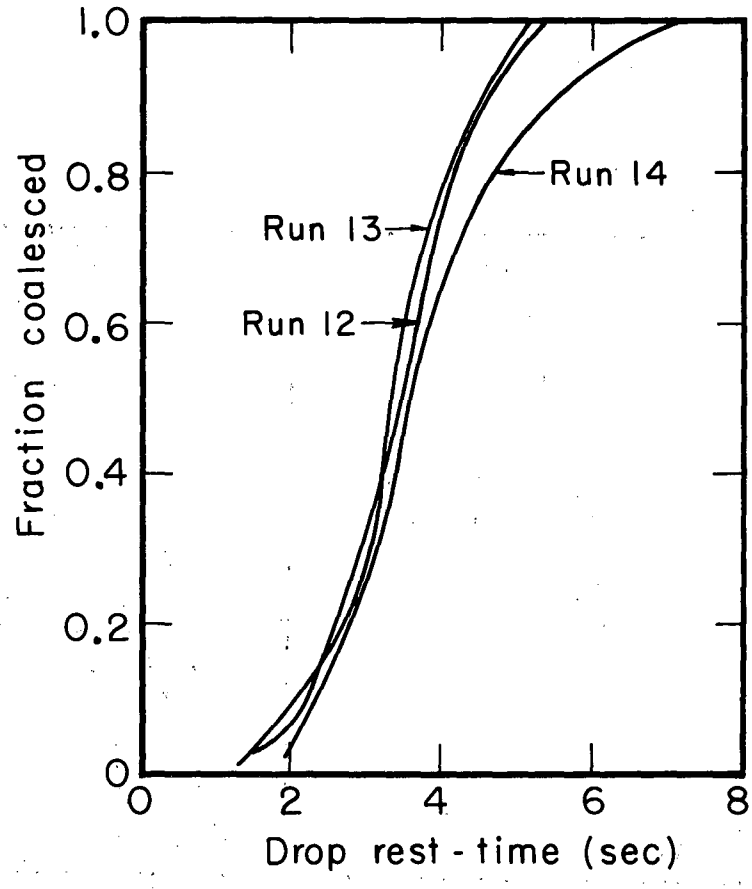

MU-26926

Fig. 42. Coalescence distribution curves showing the effect of surface renewal. Runs 12 and 14 were made in the normal manner; Run 13 was made without surface renewal.

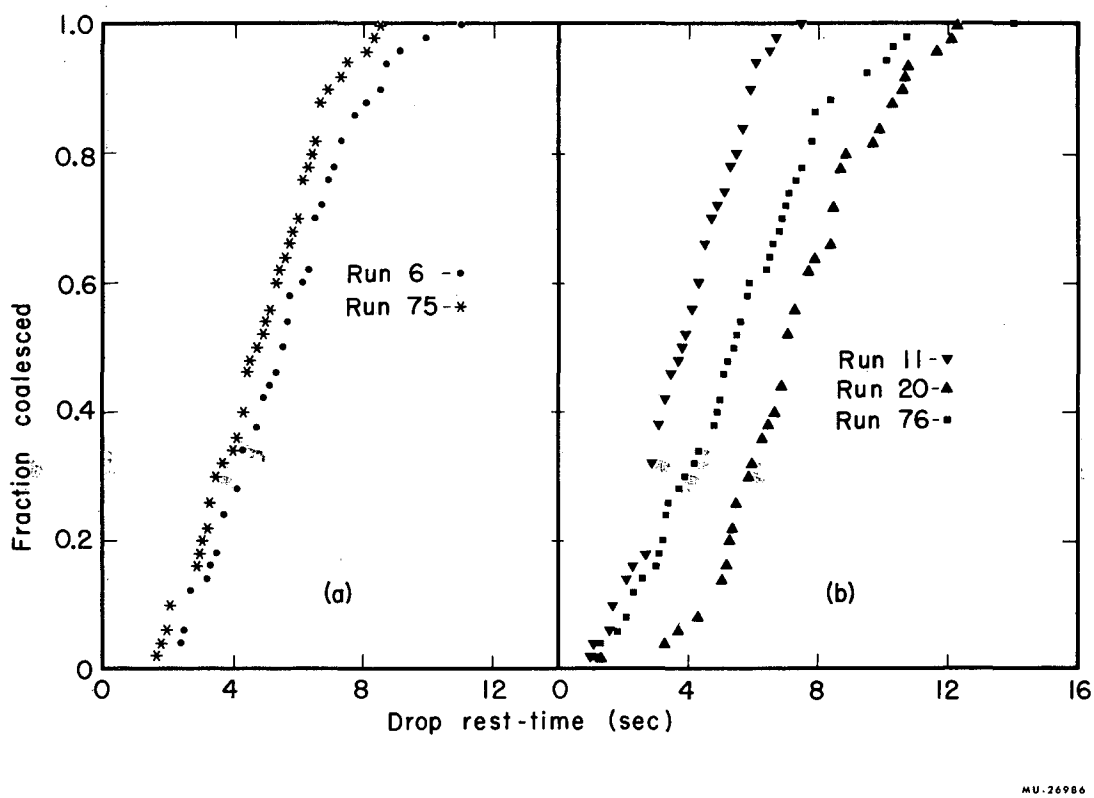

Fig. 43. Coalescence distribution curves showing effect of change of distance between dropping tip and interface. (r_e = 0.415 cm): (a) Runs 6 and 75 made with fall distance ≈ 1 mm; (b) Runs 11, 20, and 76 made with fall distance of 10 to 15 mm.

Runs 11, 20, and 76, in which the drops fell 10 to 15 mm. In Fig. 44, Run 14, in which small drops (r_e = 0.267 cm) fell about 1 mm, is compared with Runs 16 and 17, in which drops of the same size fell about 10 mm to the interface. (The drop-fall distance discussed here is not the distance from the dropping tip to the interface—it is rather the distance between the bottom of the drop, just before it is released from the dropping tip, and the interface.) It can be realized that the effect of greater fall height is much more prominent with the larger drops. This effect is due to the greater kinetic energy carried by the larger drop, due both to its increased mass and its greater velocity of fall. It is also apparent that increased drop-fall height can prolong drop rest-times as well as decrease them. Drop rest-times were increased when the kinetic energy of the falling drop created a system of large waves in the interface which caused the drop to move up and down in a large-amplitude oscillation.

3. External Vibration

An investigation of the effect of mild external disturbances was made. Fig. 45 illustrates the effects of two forms of vibration. Normally, the pump circulating water to the experimental tank was shut off during a run. Here, Run 6, in which the pump was shut off, is compared with Run 7, in which the pump was allowed to operate. Also shown is a comparison between a normal run (Run 14) made during the daytime and Run 12 which was made late at night. It was felt that any effect due to the increased building vibration during the daytime working hours would be noticed in such a comparison but in neither case was a strong effect of vibration shown. This lack of effect was due to the very low intensity of the vibrations in Run 7 and 14 as compared to Runs 6 and 12. Picknett noticed that drop rest-times were increased when a stirring motor in his system was allowed to operate during a measurement.[5] The great importance of external vibration in the problem of coalescence is discussed at length both in Sec. II and again below.

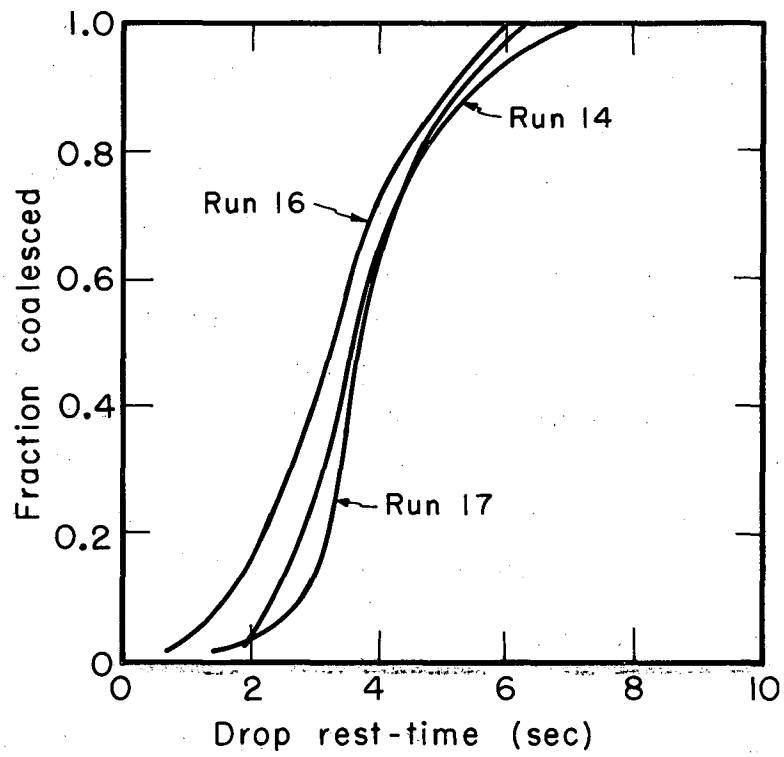

MU-26974

Fig. 44. Coalescence distribution curves showing effect of change of distance between dropping tip and interface: Run 14 made with fall distance $\approx$ 1 mm; Runs 16 and 17 made with fall distance $\approx$ 10 mm (r_e = 0.267 cm).

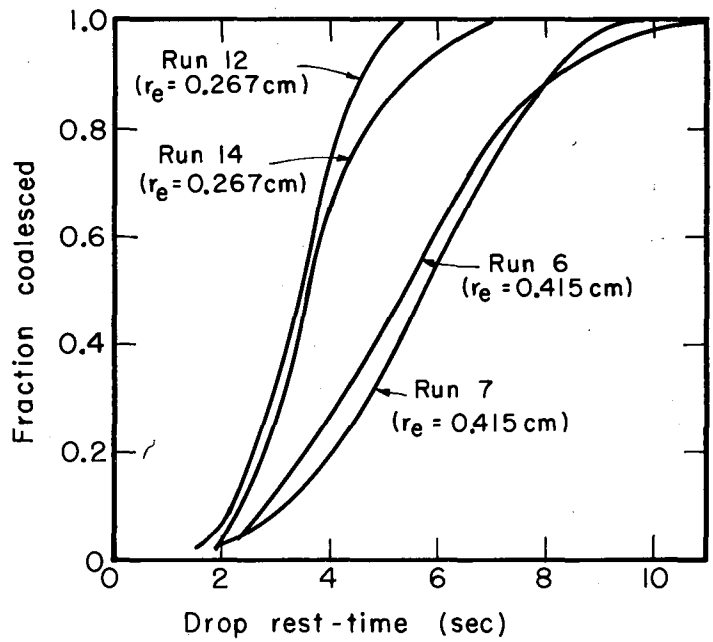

MU-26973

Fig. 45. Coalescence distribution curves showing effect of mild vibration. Run 6 (normal operation) was made with pump circulating water to experimental tank shut off, Run 7 with pump operating, Run 14 in daytime, Run 12 late at night.

4. Method of Purification

In discussing the effect of contamination on drop rest-times, one might ask what effect the degree of purity of the reagents used would have. In Runs 6 through 22, three method of purification of benzene and two of water were examined. Because the effect of certain other variables (some of which have already been discussed here) was studied simultaneously, it was necessary to examine purification methods by a statistical analysis. A statistical design called a Balanced Incomplete Block Design[57] was used; the calculations are presented in Appendix A-2.

One sample of benzene used was purified by a single-stage fractional distillation in a 30-in. column filled with "Heli-pak" followed by drying with anhydrous calcium sulfate and filtration through a 0.45-μ pore filter. A second sample of benzene was purified by fractional crystallization, drying, and filtration. These techniques are described in detail in Sec. III. The third sample of benzene was research grade benzene of 99.93 mol % minimum purity (Phillips Petroleum Company, Bartlesville, Oklahoma), and was not purified further. A mass spectrographic analysis was made of the three samples as well as of the original impure benzene. The results of the analysis are given in Table VIII. It should be noted that fractional crystallization was very effective in removing thiophene and carbon disulfide, but much less so in removing toluene. Because thiophene and carbon disulfide are more likely to have an effect on the surface properties of benzene than toluene, the fractional-crystallization technique was used in the later work.

In the experiments, Runs 6 through 11 were made with fractionally distilled benzene and distilled, deionized, and filtered water. Runs 12 through 16 were made with benzene that had been purified by fractional crystallization, and deionized and filtered water. Runs 17 through 19 were made with benzene that had been fractionally crystallized, and distilled and unfiltered water. Phillips research

TABLE VIII. Mass spectrographic analysis of benzene samples.

Method of purification	Toluene (ppm)[a]	Thiophene (ppm)[a]	Carbon disulfide (ppm)[a]
Baker & Adamson reagent grade[b]	903	142	181
Fractional distillation	13	16	180
Fractional crystallization	58	7	164
Phillips research grade[c]	13	0	190

[a] ppm on a mole basis.

[b] Allied Chemical Company, General Chemical Division, New York.

[c] Phillips Petroleum Company, Bartlesville, Oklahoma.

grade benzene was used with distilled, deionized, and filtered water, in Runs 20 through 22. An analysis of the results of the runs showed the effects of the different methods of purification to be statistically significant at the 2.5% level. The difficulty of reproducing coalescence runs from day to day was so great, however, that it was decided that a consistent technique of materials preparation would produce results as good as those obtained with ultra-pure materials. It should be mentioned, though, that the impurities tolerated should be of low molecular weight, rather than high-molecular-weight compounds which often act as surface-active agents.

5. Drop Aging

Runs 28 and 29 were made to determine the effect of aging the drops for different periods of time before their release from the dropping tip. The results of the two-factor design used in Run 29 were much more satisfactory than those of the completely randomized design[57] used in Run 28. The analysis of Run 29 is given in Appendix A-3; these results are summarized in Table IX. It is noted that the drops that were not aged at all, or which were aged only 15 seconds, coalesced in considerably shorter average times than the drops that were aged 1 or 3 minutes. The latter had average drop rest-times that were nearly identical. On the basis of this run, all drops were aged 1 minute before release, with the exception of a few runs in which the drop size was too small to allow good control of the drop formation process. The effect of changing the time period between the 12 or 13 measurement groups from 15 minutes to 1 hour was also investigated in Run 29. No effect was observable statistically.

TABLE IX. Effect of drop aging.[a]

Aging period	Mean rest-time (sec)
No aging	3.52
15 sec	3.87
1 min	4.46
3 min	4.42

[a]Phase 1 was water, phase 2 was benzene with r_e = 0.267 cm.

B. Effects of Drop Size and System Physical Properties

By interchanging the dropping tips, the effect of drop size on drop rest-times could be determined. As many as four drop sizes were used with a given system, allowing the drop-equivalent radius of the drops to be changed by about a factor of 2. Five different two-component systems were used to ascertain the effect of a change in physical properties. Density differences ranged from 0.0089 through 0.4505 g/cm^3; viscosities ranged from 0.590 through 203 cp; and interfacial tensions ranged from 7.4 through 40.9 dynes/cm. The coalescence distribution curves for the systems water-benzene, n-tributyl phosphate-water, water-anisole, ethylene glycol-benzene, and water-Aroclor 1248 are given in Figs. 46 through 50, respectively. (In the systems named above, the first listed component is the phase 1 material and the second one, the phase 2 material.) The reproducibility of the data was often poor because of the strong influence of minute traces of contaminants. The distribution curves for large drops were also less reproducible because of the large surface disturbances caused by their impact (see preceding section). These surface disturbances, in the form of large-amplitude waves, were very noticeable in low viscosity systems.

In all except three of the systems studied (including the systems containing a surface-active agent discussed below), coalescence occurred in a stepwise manner yielding as many as seven successive daughter drops. In the water- Aroclor 1248 and ethylene glycol-benzene systems, the coalescence was single-stage. This observation confirmed the findings of Charles and Mason, who observed single-stage coalescence whenever the ratio of viscosities of the two phases was less than 0.02 or greater than 11.0.[10] In the water-anisole system, two daughter drops were formed in the first stage of coalescence. This occurrence can be explained by the theory of Charles and Mason, who showed that the daughter drop in a stage of coalescence was formed when the mother drop became distorted in an unstable Rayleigh cylinder. The Rayleigh cylinder was ruptured to yield a

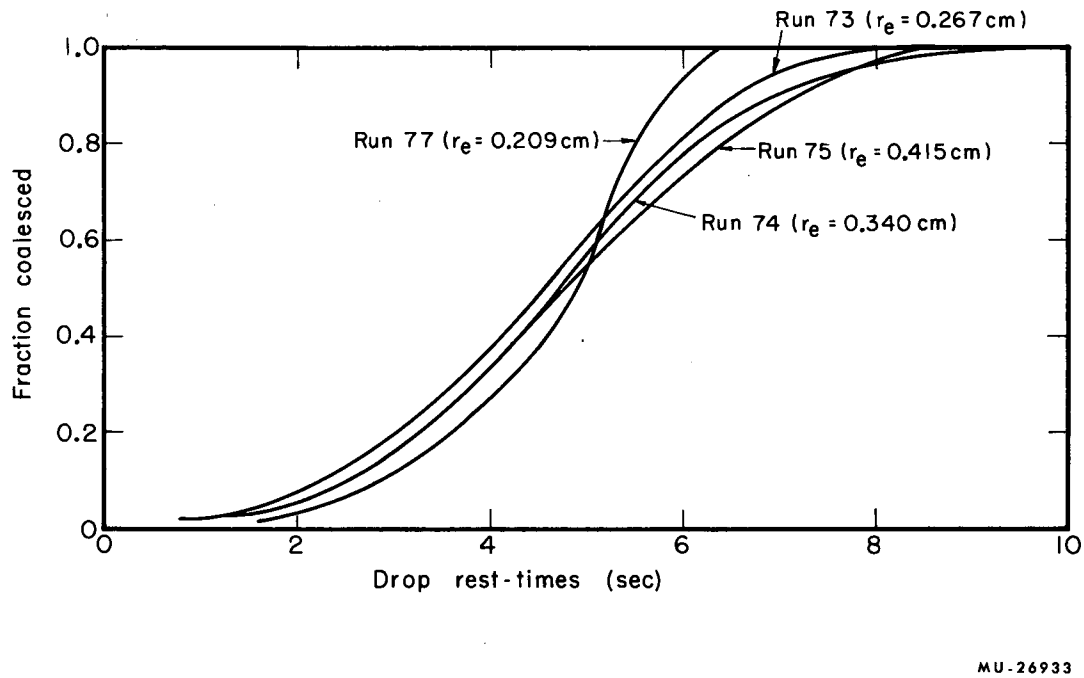

Fig. 46. Water-benzene system coalescence distribution curves.

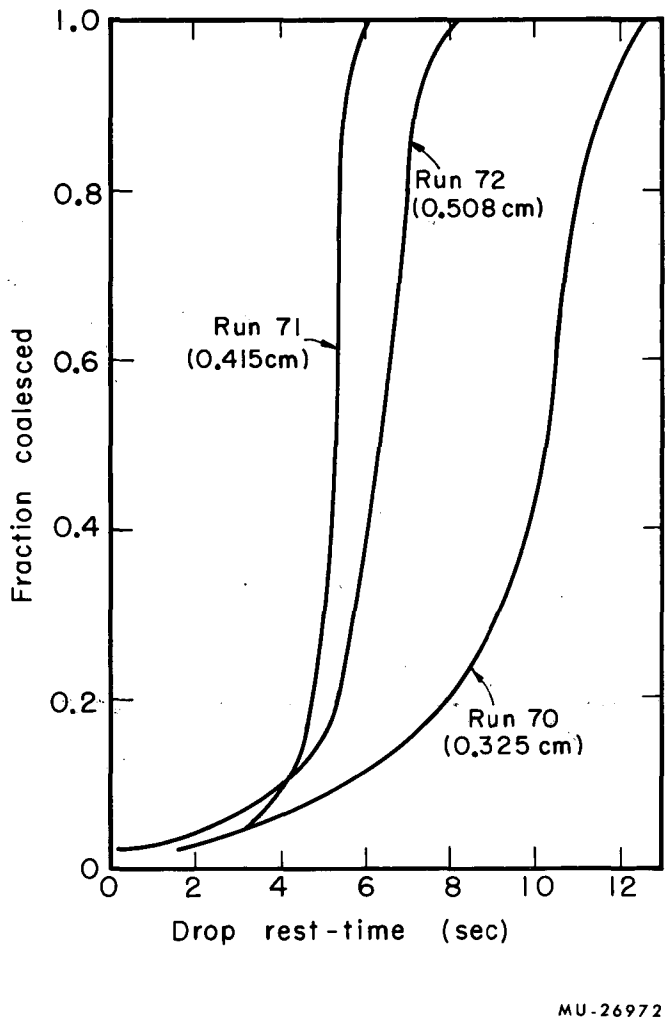

Fig. 47. Tributyl phosphate-water system coalescence distribution curves.

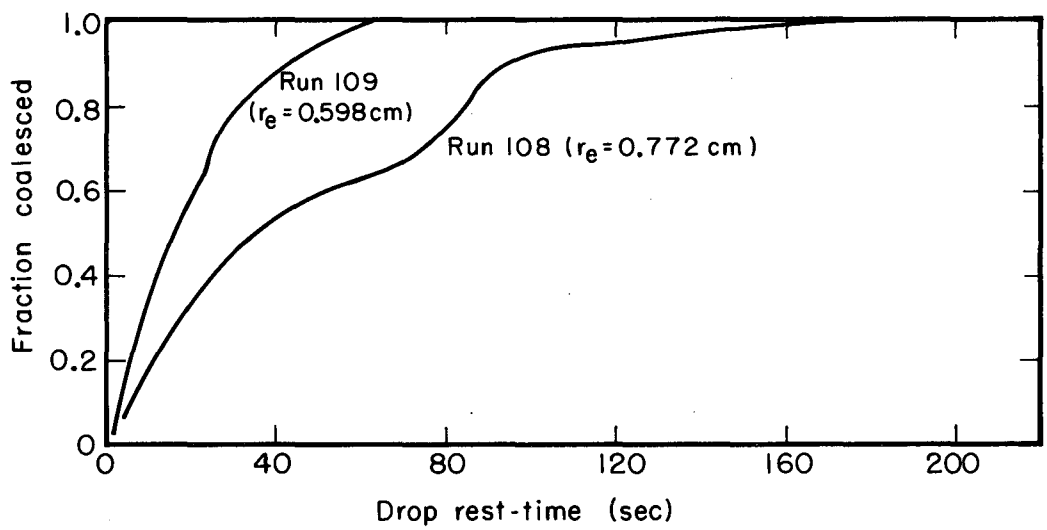

MU-26929

Fig. 48. Water-anisole system coalescence distribution curves.

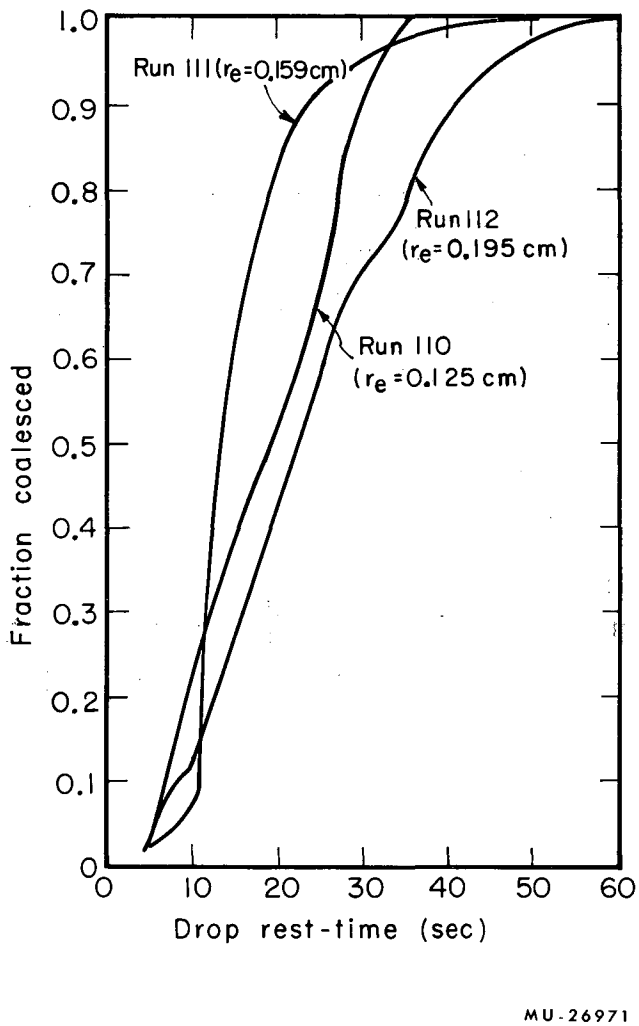

Fig. 49. Ethylene glycol-benzene system coalescence distribution curves.

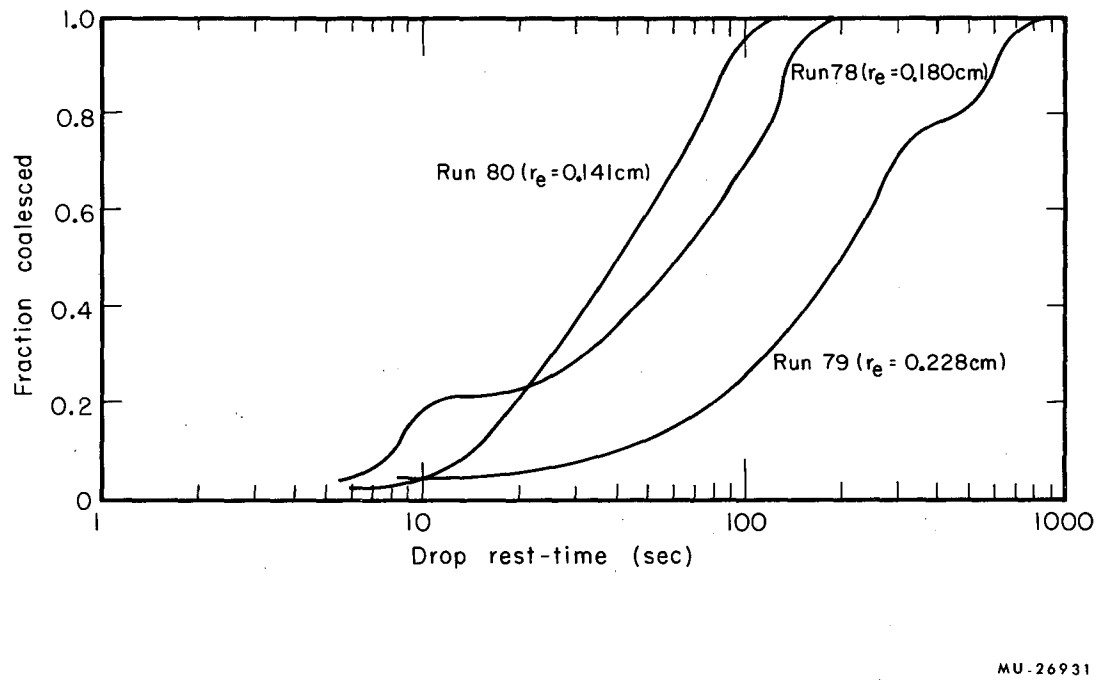

Fig. 50. Water-Aroclor 1248 system coalescence distribution curves.

single daughter drop. In thecase observed in this work the mother drop was so large that it disintegrated into two daughter drops instead of one.

C. Effect of Induced Disturbances

The discussion of hydrodynamic instability in Sec. II suggested the possibility of creating a disturbance in some manner. In general, the effect of an intense sonic disturbance would be to decrease the drop rest-time by initiating the proper type of instability before the naturally present disturbances could initiate an instability. It is also possible for a sonic disturbance to prolong drop rest-times by causing the drop to vibrate up and down independently of the planar interface, effectively increasing the film thickness. Some preliminary experiments were performed using the telephone speaker to produce sonic disturbances; the swimming-pool speaker was used in a more complete study. Interference beats were produced by means of two R-C oscillators to simulate subsonic disturbances. The results obtained in this study are given in the following subsections.

1. Telephone Speaker

The telephone speaker was used as the source of the sonic disturbances in Runs 23 through 27 and 30 through 37. The results obtained were unsatisfactory for two reasons. First, the influence of trace contaminants on coalescence was great enough to partially obscure any effect due to the sonic disturbance. Second, resonances set up in the telephone speaker made it difficult to determine which frequency produced by the speaker was actually altering the coalescence time. The results of Runs 30 through 37 are given in Fig. 51. The sonic disturbances increased the coalescence times slightly in this group, probably by causing the drops to oscillate independently of the planar interface.

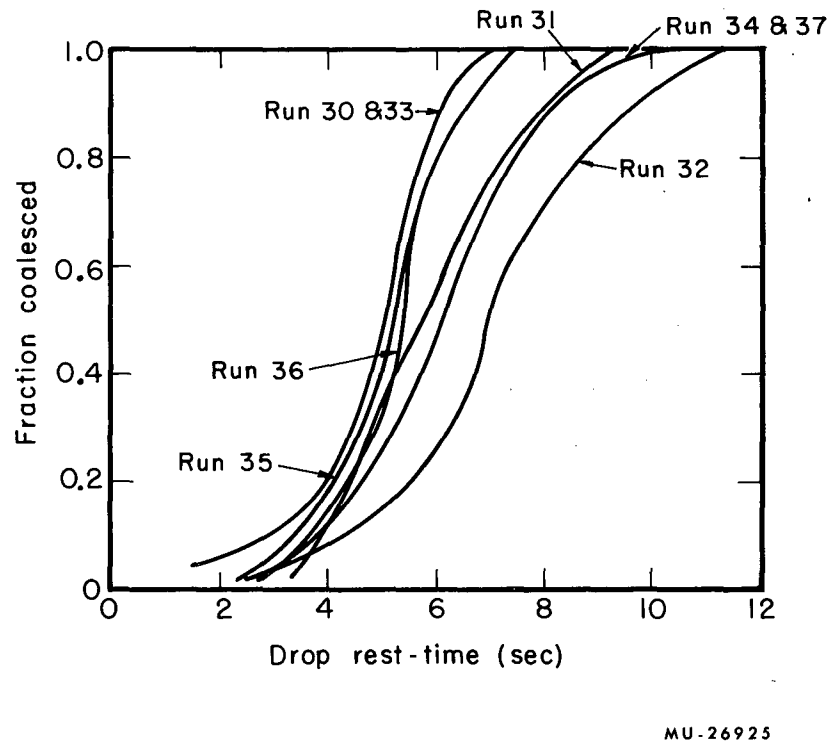

Fig. 51. Effect of sonic disturbances produced by telephone speaker on coalescence distribution curves. Runs are described in Table X.

TABLE X. Sonic disturbances produced by telephone speaker.

Run No.[a]	Disturbance frequency (cps)	Sound pressure (dynes/cm^2)
30,33	None	--
31	500	398
32	250	152
34,37	500	398
35	500	398
36	2500	23.9

[a]Runs 30 and 33, and 34 and 37, respectively, were considered as single runs for Fig. 10.

2. Swimming-pool Speaker

The use of the swimming-pool speaker in the sonic disturbance runs eliminated the second of the two difficulties experienced in the telephone speaker runs. The first difficulty was eliminated by means of a special statistical design--this was the chain design,[57] used to correct for day-to-day changes in the materials used in the coalescence study. It was found that three runs of 50 coalescence measurements each could be made in a single day. One of the three daily runs was made under conditions identical with a run of the previous day, and another of the runs was duplicated the following day. The chain was closed by performing one of the runs on the last day of the series in the same manner as one of the runs on the first day. In the experiments described here, a total of 12 runs were made in four days. Thus, runs using four of the sets of operating conditions were repeated twice, and runs with one of the other four sets of conditions were repeated once. The method of analysis yields a correction factor that is a measure of the day-to-day drift in the properties of the liquid materials. This correction factor was used to shift the time scale of the coalescence distribution curves to eliminate the daily drift. A sample of the calculations employed is given in Appendix A-4.

The effects on coalescence times of seven frequency-voltage combinations applied to the swimming-pool speaker were compared with the results of an experiment in which no disturbances were produced. Two systems were studied—water-benzene and tributyl phosphate-water. The coalescence distribution curves that resulted for the two systems are given in Figs. 52 and 53. Because of the day-to-day drift in system properties, it is difficult to reach definite conclusions from this type of data. When the median values of the curves are shifted on the time scale as determined by the chain-design correction factors, however, the effects of sonic disturbances stand out more clearly. The corrected distribution curves for the

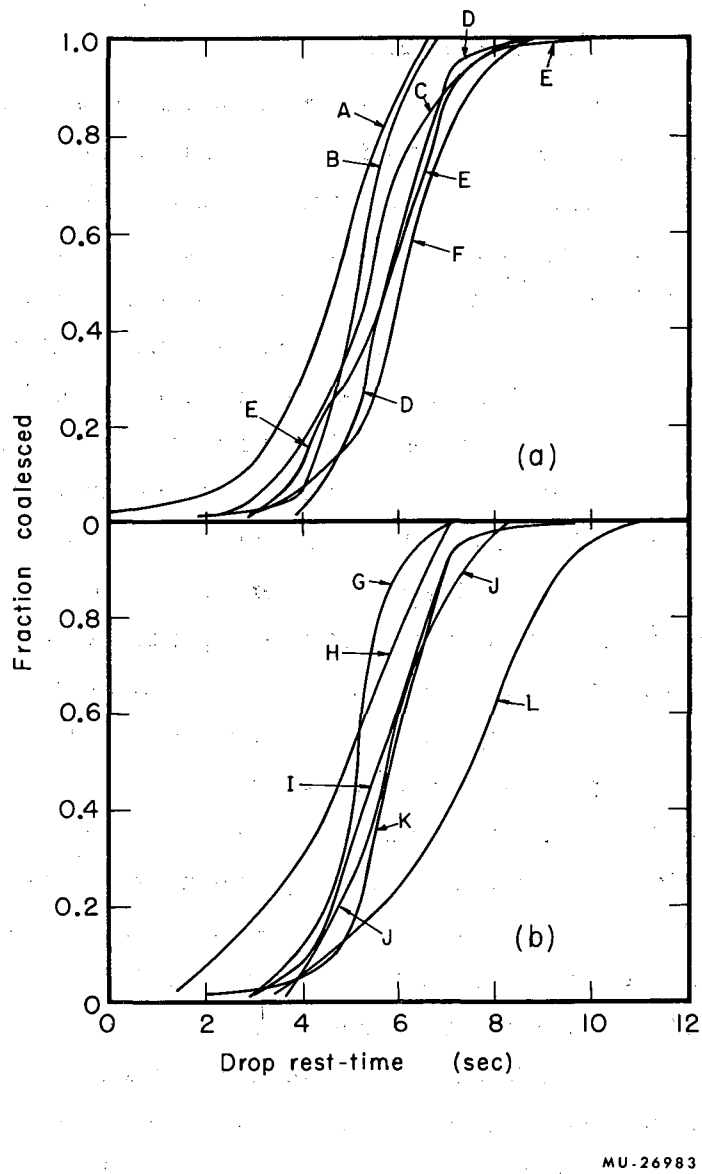

Fig. 52. Effect of sonic disturbances produced by swimming-pool speaker on water-benzene coalescence distribution curves. Curves not adjusted for day-to-day drift. Runs are described in Table XI.

Symbol	Run	Symbol	Run
G	38,41	L	46,49
H	39	B	47
A	40	J	48
E	42,45	I	50,53
F	43	K	51
C	44	D	52

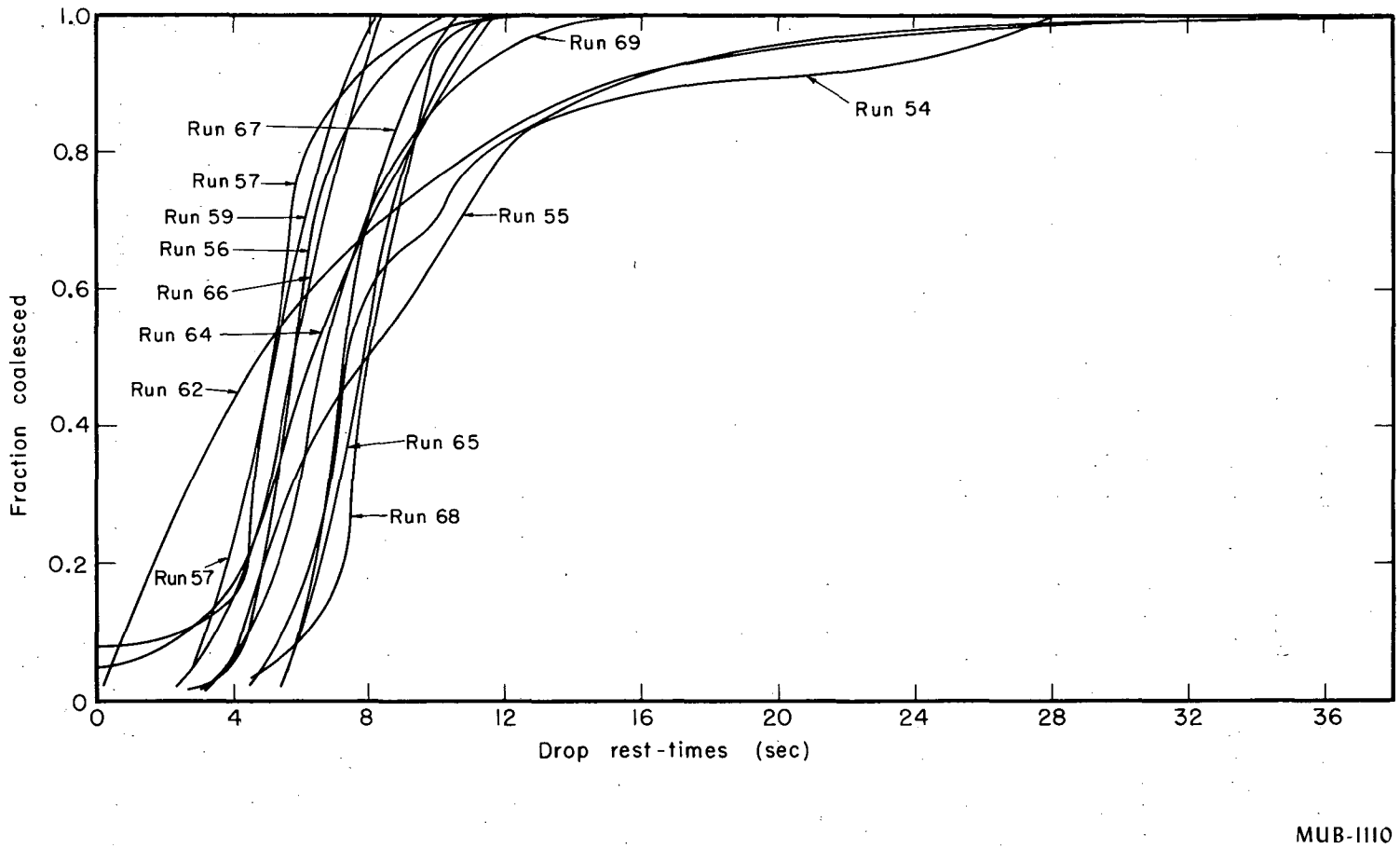

Fig. 53. Effect of sonic disturbances produced by swimming-pool speaker on tributyl phosphate-water coalescence distribution curves. Curves not adjusted for day-to-day drift. Runs are described in Table XI.

water-benzene and tributyl phosphate-water systems are shown in Figs. 54 and 55, respectively.

The results of the statistical calculations are summarized in Table XI. The differences in the median drop rest-times between the runs with sonic disturbances and the runs with no vibration are given. It can be seen that none of the differences in the runs with the water-benzene systems showed statistical significance at the 5% level, but 5 of the 7 types of disturbances showed statistical significance in the tributyl phosphate-water runs. (One type of disturbances used in the tributyl phosphate-water experiments was "white" noise produced by the random-noise generator. Photographs of the oscilloscope traces of this sound pattern are shown in Fig. 56.

The absence of statistical significance for the differences in the water-benzene runs was probably due to the very great day-to-day deviations in the results on that system. We note that, in every significant case, the sonic disturbance decreased the rest-times of the drops. This observation is discussed, in light of the theory, in Sec. V.

3. Subsonic Disturbances

The theory described in Sec. II shows that disturbances of very low frequency should be extremely effective in promoting coalescence. The simplest way of producing low frequency (subsonic) disturbances is by generating interference beats between sonic frequency sounds. Two R-C oscillators were connected in parallel to produce the beats. By setting the oscillator at frequencies near 70 cps; 1, 5, and 10 beats per second could be generated. Photographs of the oscilloscope traces of these beats as well as a pure 70-cps signal are shown in Fig. 57.

The water-benzene system was used in this set of experiments. Three runs of 50 coalescence measurements each were used. In each run, 10 rest-times were determined with no external disturbance, 10 with a pure 70-cps signal, and 10 each with 1, 5 and 10 beats per second of the 70-cps fundamental. In each run, the five conditions of operation were ordered randomly from a table of random permutations.[57]

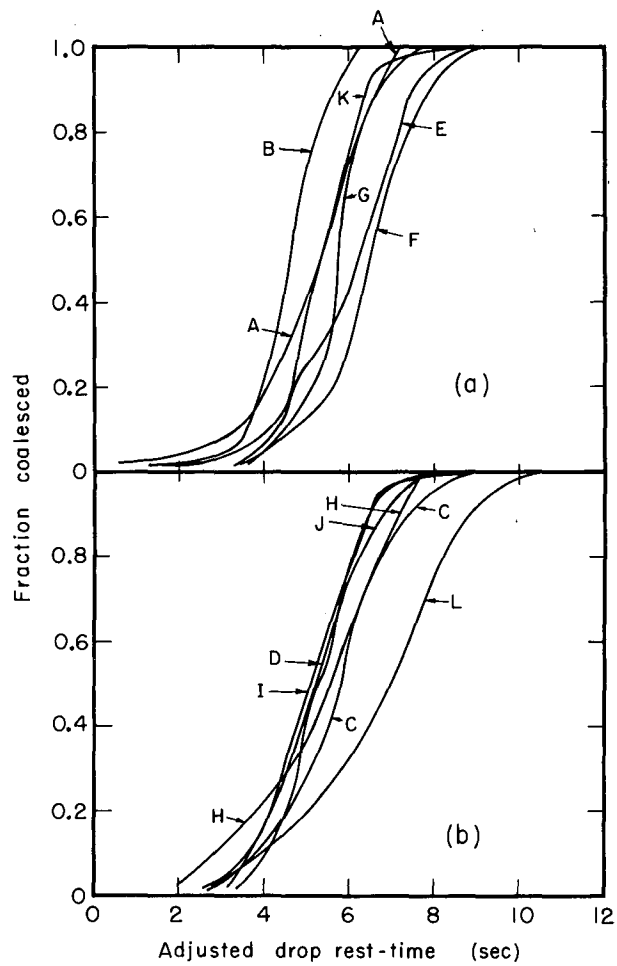

Fig. 54. Effect of sonic disturbances produced by swimming-pool speaker on water-benzene coalescence distribution curves. Curves adjusted for day-to-day drift. Runs are described in Table XI.

Symbol	Run	Symbol	Run
G	38,41	L	46,49
H	39	B	47
A	40	J	48
E	42,45	I	50,53
F	43	K	51
C	44	D	52

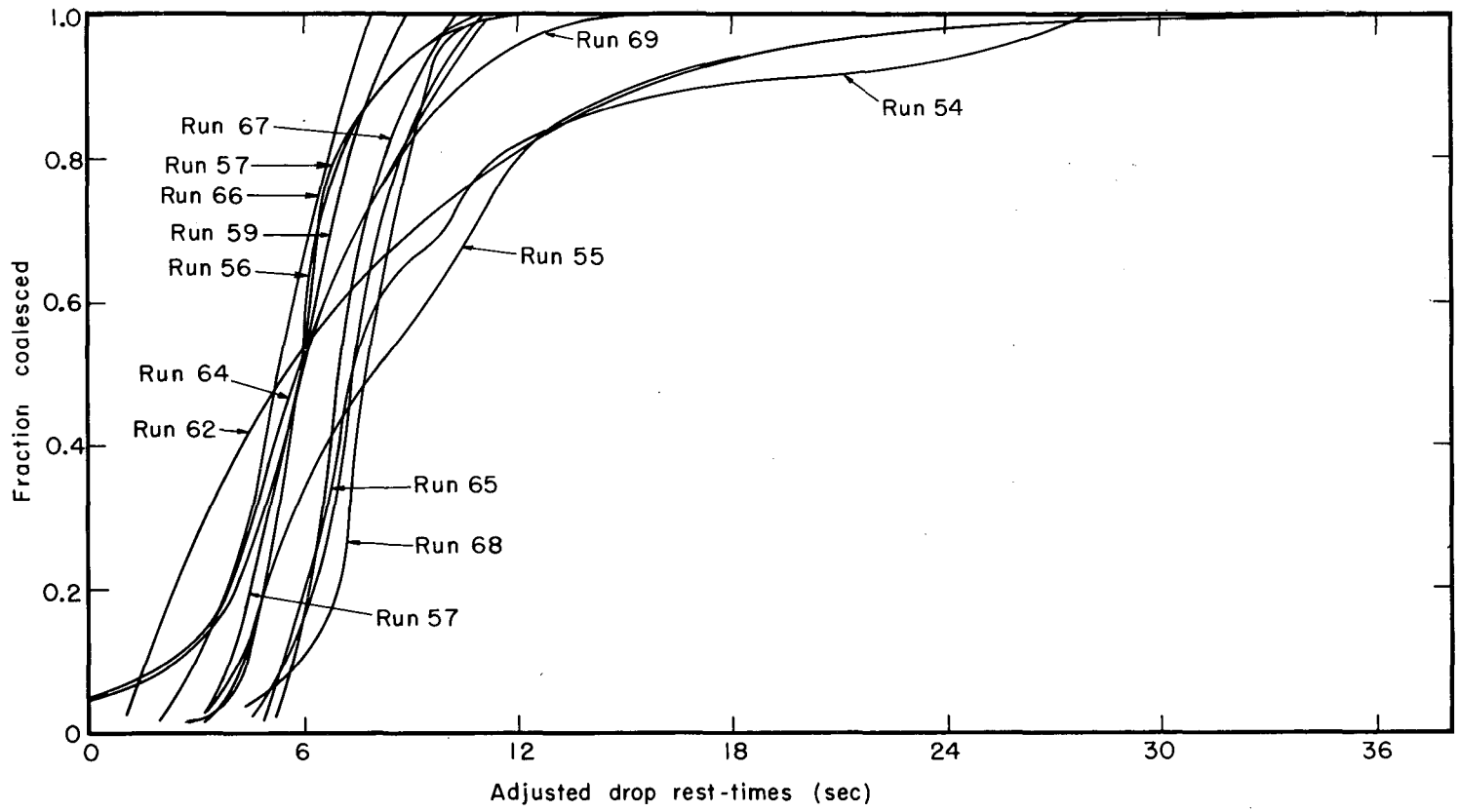

MUB-1109

Fig. 55. Effect of sonic disturbances produced by swimming-pool speaker on tributyl phosphate-water coalescence distribution curves. Curves adjusted for day-to-day drift. Runs are described in Table XI.

TABLE XI. Effect of sonic disturbances on drop rest-times.

System	Run[a]	Disturbance frequency (cps)	Rms sound pressure (dynes/cm^2)	Change in median rest-time due to disturbances (sec)	Level of statistical significance
Water-benzene	38,41,52	None	--	--	--
	51	50	3.4	-0.2	Not sign. at 5%
	43,46,49	50	18.4	+1.3	Not sign. at 5%
	44	250	40.0	+0.3	Not sign. at 5%
	39,42,45	500	25.5	+0.4	Not sign. at 5%
	40	500	125	-0.1	Not sign. at 5%
	47,50,53	738	15.3	-0.6	Not sign. at 5%
	48	2095	85	-0.3	Not sign. at 5%
Tributyl phosphate-water	54,67	None	--	--	--
	69	70	250	-0.8	5%
	55	110	260	+0.7	Not sign. at 5%
	59	200	29	-1.2	5%
	66	300	48	-1.7	1%
	56,57	500	135	-1.4	1%
	65,68	1000	670	+0.4	Not sign. at 5%
	62,64	White noise	--	-1.7	1%

[a]Runs 38 and 41, 46 and 49, 42 and 45, and 50 and 53, respectively, analyzed as single runs. Only the first 25 measurements in Runs 57 and 59 were used in the analysis.

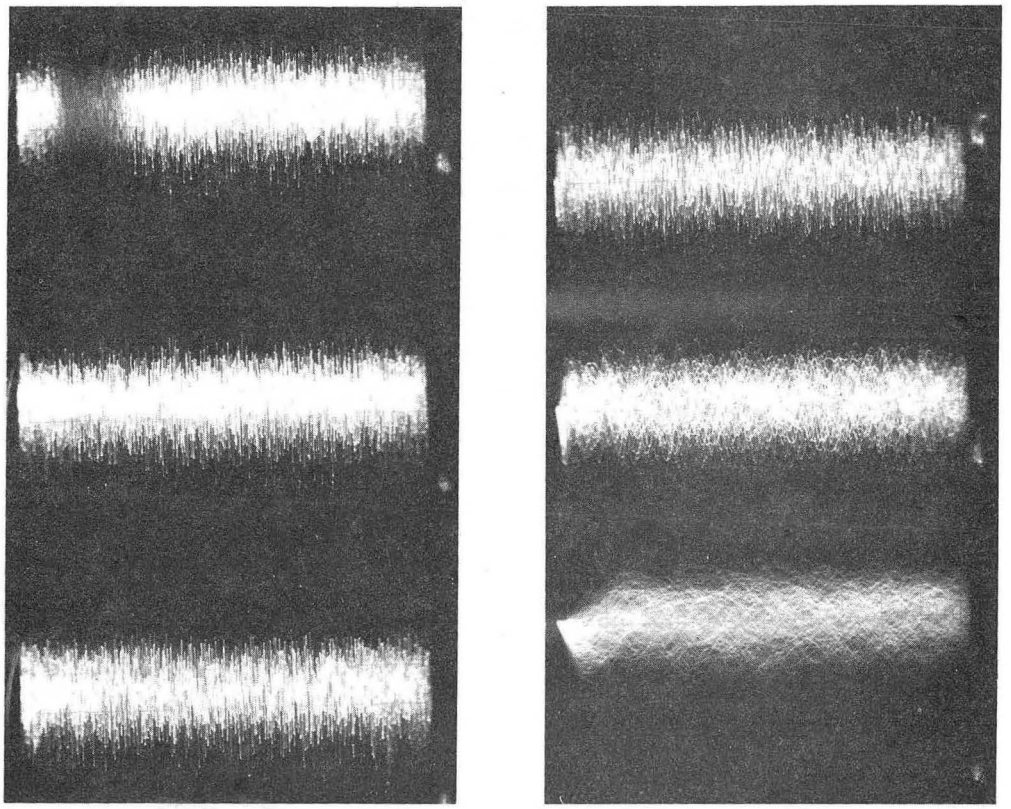

(a) (b)

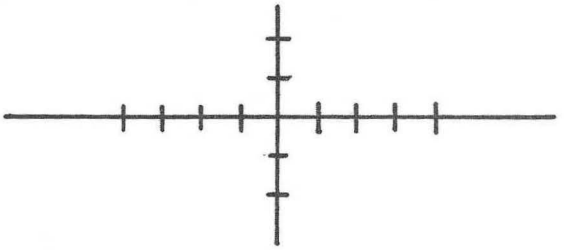

ZN-3118

Fig. 56. Oscilloscope traces of "white" noise. The voltage sensitivity (vertical coordinate) was 20 mV/division. Sweep speeds (horizontal coordinate) were (a) 5, 2, and 1 msec/division; (b) 0.2 msec/division, 50 and 10 μ sec/division.

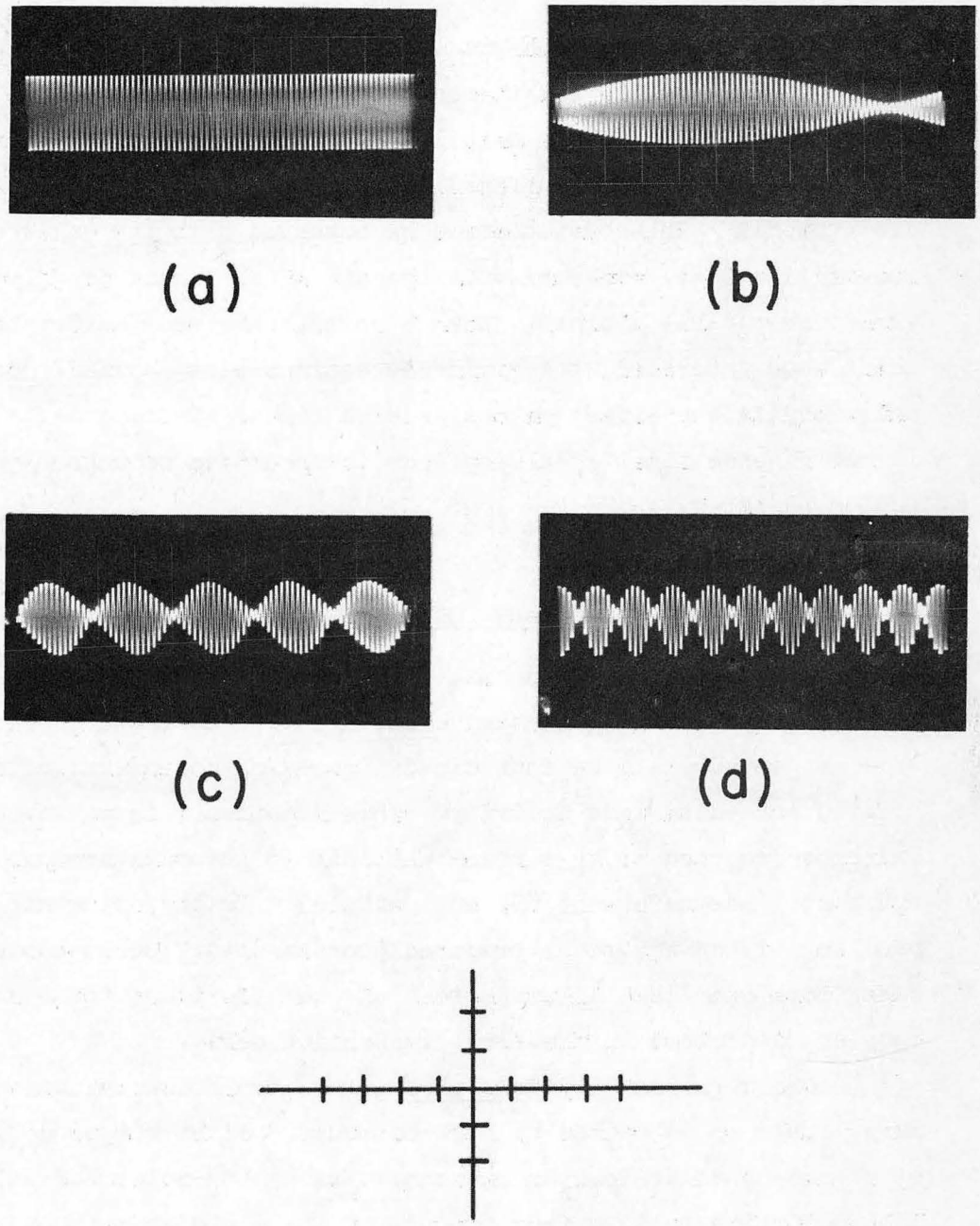

ZN-3116

Fig. 57. Oscilloscope traces of subsonic disturbances. Oscilloscope voltage sensitivity (vertical coordinate) was 5 V/division, and horizontal sweep speed was 0.1 sec/division: (a) Pure 70 cps signal; (b) 70 cps, 1 beat/sec; (c) 70 cps, 5 beats/sec; (d) 70 cps, 10 beats/sec.

The results are summarized in Table XII. We note that the pure 70-cps frequency greatly lengthened the coalescence times. The increase in rest-times was due to the oscillation of the drops at the planar interface caused by a system of small-amplitude waves created by the sonic disturbances. These waves could be observed with the naked eye, and the oscillations, especially in thecase of the small daughter drops, were also plainly visible. When 5 or 10 beats/sec, rather than a pure tone, were generated, the coalescence times were shorter. One beat/sec had a negligible effect on coalescence times. Thus, a definite decrease in coalescence times resulting from the presence of subsonic disturbances is demonstrated.

D. Effects of Contamination and Surfactants

As noted by Nielsen, Wall, and Adams,[6] great difficulty was experienced in reproducing coalescence distribution curves. The greatest source of error appeared to be that minute traces of contaminating materials exhibited marked surface activity. This hypothesis is substantiated by the extremes resorted to by surface chemists to maintain scrupulously clean equipment (see reference 65, for example). In three instances, careless handling of the equipment produced poor results. Because these three cases form excellent illustrations of the effects of trace contamination, they are described in the first subsection below.

One might anticipate *a priori* that trace contamination would be more likely to be caused by high-molecular-weight compounds such as fats, oils, and nonvolatile hydrocarbons, than by low-molecular-weight compounds. This deduction follows from a study of the cleaning methods usually used. The solvents, acid solutions, and other materials used would be far more likely to remove the lower molecular-weight materials than the higher ones. Accordingly, a series of experiments were performed to determine how small a quantity of high-molecular-weight material would be needed to strongly affect coalescence times. The materials used were surface-active agents, but it should be emphasized that this study was not designed to elucidate the effects of surface-active agents in general. However, some preliminary

TABLE XII. Effect of subsonic disturbances on drop rest-times.[a]

Disturbance	t_m (sec)	Change in median rest-time due to disturbance (sec)
None	4.9	--
Pure 70 cps	13.0	--
70 cps, 1 beat/sec	13.8	+0.8
70 cps, 5 beats/sec	9.1	-3.6
70 cps, 10 beats/sec	7.1	-5.4

[a]Water-benzene system, with r_e = 0.267 cm. The sound pressure was 94 dynes/cm^2 rms for pure 70 cps, and 133 dynes/cm^2 rms for beats.

conclusions can be drawn about the effect of the type of surface-active agent. The results of this study are described in the second subsection below.

1. Accidental Contamination

The first five runs performed on the coalescence equipment seemed very peculiar. The materials used in the runs (water-benzene) were not discarded each day, but were allowed to remain in the cell for the duration of the set of experiments. Five coalescence distribution curves were determined over a period of five days under conditions of no external disturbance. The results of three of the runs are presented in Fig. 58. It will be noted that the drop rest-times increased very greatly from run to run. Readings from the micrometer dial of the Micro-buret indicated that the drop size was decreasing from run to run, obviously due to a decrease in the interfacial tension of the phases used. When the cell was disassembled after the fifth run, it was noted that the benzene had a barely visible yellowish tinge. Evaporation to dryness at less than 100°C and ignition at 800°C showed that the contaminant in the benzene was organic, and was present in a concentration of about 0.0126 weight-%. A freezing point analysis performed in equipment similar to that of Mair[66] and Glasgow[67] showed that the concentration of the contaminant was about 0.008 mole-%. The source of the contaminant was found to be the neoprene O ring used to attach the cell top to the coalescence cell. Although great care had been taken to ensure that no liquid material would ever come in contact with the O ring, some benzene vapor had condensed at the top of the cell and dripped down over the O ring, dissolving some material. Consequently, the cell was redesigned to eliminate the O ring.

The two other cases of contamination, because of carelessness, occurred with the tributyl phosphate-water system. In runs 57 to 59, the drop rest-times began to fall abruptly in the range 3.1-3.5 sec, regardless of the type of external disturbance. A slight grayish tinge was noticed in the organic phase. This coloration was traced to the black paint on the brass spring clips that held the spherical joints together. Leakage at these joints dissolved some of the paint, which then

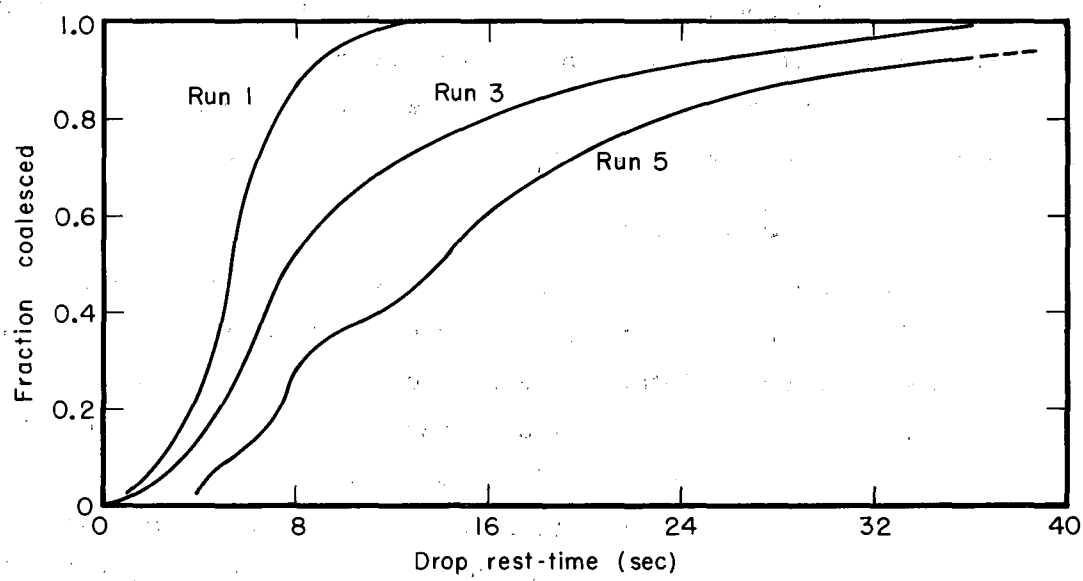

MU-26928

Fig. 58. Effect of accidental contamination on coalescence distribution curves—water-benzene system. Concentration of contaminant increased from Run 1 through Run 5.

diffused into the coalescence cell. The clips were cleaned with an organic solvent and nitric acid until all of the paint was removed. The third case of trace contamination occurred after the cell was cleaned, following the paint incident. It was felt that a number of rinses with acetone followed by 20 rinses with distilled water could be used in lieu of the complete primary cleaning procedure. The very lengthy coalescence times in Run 60 demonstrated the fallacy of any attempt to simplify the cleaning procedure.

The reasons why trace contamination sometimes increases and at other times decreases the rest-times is discussed in Sec. V.

2. Effect of Surfactants

The use of surface-active materials as third components in the water-benzene system created some special problems in producing mutually saturated phases. Because the surface-active agents were somewhat soluble in both phases, it was necessary to mutually saturate measured quantities of the organic and aqueous phases. Also, because these surfactants acted as emulsifying agents, it was often necessary to centrifuge the liquid materials after saturation. The following procedure was therefore adopted. The surfactant was dissolved in either the water or the benzene to form a solution of known concentration. Then 400 ml of the aqueous phase and 80 ml of the organic phase (one of the phases contained the surfactant in solution) were mixed together for exactly 18 hours by means of a magnetic stirrer. The mixing was performed in the 25°C constant-temperature bath. At the end of 18 hours, the organic phase was usually found to be emulsified. The emulsion was broken to yield two clear or very slightly turbid phases by centrifuging at 1000 g's for 10 minutes to 2 hours depending upon the surfactant and its concentration. The only emulsion that could not be broken in this way was one made by mixing an aqueous 0.01 mole-% sodium oleate solution with benzene. In that case, because the aqueous phase was only slightly turbid, the benzene layer was replaced with water-saturated benzene in the coalescence cell and the two phases were allowed to equilibrate for 12 hours before measurements were commenced.

The equilibrium concentrations of the surfactant in the oil and aqueous phases can be calculated from the H.L.B. value, which is a measure of the free energy of transfer of the surfactant molecule from the water to the oil. (The H.L.B. value refers to the hydrophilic-lipophilic balance of the emulsifier molecule. It is discussed at length by Davies and Rideal.[68]) The equilibrium concentrations of the surfactant can be computed from the following equation

$$\text{H.L.B.}-7 = 0.36 \ln\left(\frac{C_w}{C_o}\right) \tag{113}$$

The method of preparation of all the surfactant solutions used, and the calculated equilibrium concentrations of the surfactants, are given in Table XIII.

The interfacial concentrations of the surfactants were computed from Gibbs' equation, which requires a knowledge of the interfacial tension as a function of concentration[68]

$$\Gamma_3^{1,2} = -\frac{C}{RT\Lambda}\frac{d\sigma}{dC} . \tag{114}$$

Here $\Gamma_3^{1,2}$ is the surface excess of the surface-active agent relative to an arbitrary dividing surface where phases 1 and 2 are present in their bulk concentrations. The term Λ is inserted into the equation to take into account the surface excess of both cation and anion in an ionic substance. The interfacial tensions as functions of concentrations are presented graphically in Fig. 59. It was easier to determine $d\sigma/d \ln C$ graphically than $d\sigma/dC$. Therefore, Eq. (114) was rewritten as

$$\Gamma_3^{1,2} = -\frac{1}{RT\Lambda}\frac{d\sigma}{d \ln C} \tag{115}$$

TABLE XIII. Surfactant solutions and interfacial concentrations.

Surfactant	Preparation mole-%	Preparation solvent	H.L.B. value[a]	Equilibrium concentration (milli-moles/l) In water	Equilibrium concentration (milli-moles/l) In benzene	Interfacial tension (dynes/cm)	Λ	$\frac{d\sigma}{d \ln C}$	$\Gamma_3^{1,2}$ (10^{-10} g moles/cm^2)	Area/molecule (Å^2)
None	-	-	-	-	-	34.71	-	-	-	-
Span 80	0.00115	benzene	5.7	0.0031	0.114	26.8	1	-7.22	2.91	58
	0.0115	"	5.7	0.031	1.14	11.6	1	-5.78	2.33	71
	0.102	"	5.7	0.27	10.0	1.3	1	-3.43	1.38	120
Tween 81	0.000109	benzene	11.9	0.00244	-	24.3	1	-2.65	1.07	156
	0.00109	"	11.9	0.0244	-	17.3	1	-3.35	1.35	123
	0.0109	"	11.9	0.244	-	9.3	1	-3.52	1.42	117
Sodium oleate	0.000102	Water	18	0.0566	-	29.7	2	-3.52	0.71	234
	0.00102	"	18	0.556	-	19.6	2	-5.00	1.01	165
	0.0102	"	18	5.56	-	7.0	2	-5.56	1.12	150

[a]Reference 68.

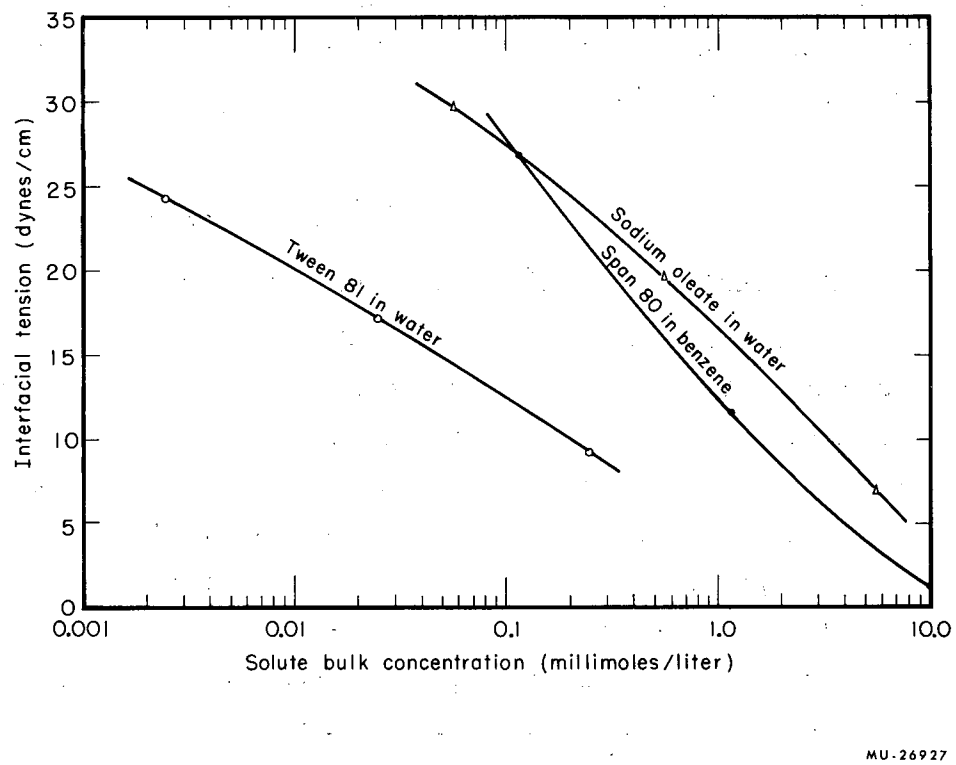

Fig. 59. Interfacial tension as a function of concentration of surfactant.

The interfacial concentrations and the areas per molecule at the interface are also given in Table XIII. Note that the areas per molecule are approximately equal to the cross-sectional area of a long-chain hydrocarbon molecule--therefore, the interface might be considered to be in a saturated state.

Various characteristic parameters of the coalescence distribution curves measured in this study are given in Table XIV. The very strong effect of a minute concentration of surface-active agents on the coalescence times should be noted. Further discussion of these results is deferred to Sec. V.

E. Natural Sonic Disturbances

1. Measurement of rms Frequency Spectrum

It was of interest to determine the characteristics of the natural sonic disturbances in the coalescence cell to see if these disturbances could initiate a hydrodynamic instability leading to ultimate coalescence. The crystal microphone described in Sec. III was used to measure these disturbances by the following procedure. The microphone was placed in the coalescence cell in the position normally occupied by the coalescence cup and was then connected to the wave analyzer. A time-average microphone-voltage output was determined for every frequency setting of the wave analyzer which was a multiple of 10 cps in the range from about 20 to 3000 cps. The pressure fluctuation corresponding to the voltage output was computed from the microphone sensitivity curve, Fig. 38. Because the wave analyzer yields rms voltages, an rms frequency spectrum curve rather than $g(\omega)$ is calculated. The resulting rms frequency spectrum $\frac{g(\omega)}{v\sqrt{2}}$, was plotted as a function of $\nu = \frac{\omega}{2\pi}$ for each of the seven tests as shown in Figs. 60, 61, and 62. In preparing these figures, the assumption that the band width accepted by the wave analyzer is a Dirac delta function has been made (see Sec. II-E). The data points measured have been connected with straight line segments in the figures. If the true peaks did not fall at a

TABLE XIV. Effect of surfactants.

Surfactant	Equilibrium concentration in aqueous phase (milli-moles/l)	Run No.	r_e (cm)	$\bar{t}$ (sec)	t_m (sec)	$t_{0.10}$ (sec)	$t_{0.90}$ (sec)	Variance (sec^2)
Span 80	0.0031	86	0.310	7.55	6.7	2.9	12.7	13.31
		84	0.245	8.08	8.1	3.5	12.1	10.66
		85	0.191	8.10	7.5	2.8	13.9	18.87
	0.031	83	0.230	89.23	93.4	25.3	139.3	1784.72
		82	0.182	27.15	28.6	5.4	47.2	251.86
		81	0.143	21.79	20.0	7.5	38.3	112.39
Tween 81	0.00244	89	0.299	5.38	4.5	1.6	9.3	6.53
		87	0.236	5.60	5.1	2.9	8.6	5.05
		88	0.184	3.94	3.9	1.3	5.7	2.51
	0.0244	90	0.266	11.58	11.3	5.5	17.4	15.59
		92	0.210	9.91	9.5	4.3	15.9	19.37
		91	0.164	6.50	5.7	3.2	11.4	10.93
	0.244	95	0.213	150.60	133.7	10.9	298.1	9509.43
		93	0.168	84.80	70.1	16.5	160.0	3238.07
		94	0.132	62.19	58.5	9.7	111.6	1623.80
Sodium oleate	0.0566	101	0.321	8.71	7.3	2.5	16.0	32.86
		99	0.253	9.93	10.3	5.7	14.8	13.88
		100	0.200	7.82	7.7	3.1	11.7	13.84
	0.566	102	0.277	33.56	25.6	5.9	62.5	351.60
		104	0.218	32.23	35.1	7.3	67.3	457.80
		103	0.171	28.25	23.1	4.9	52.4	400.99
	5.56	106	0.193	9.16	9.0	7.5	10.5	1.87
		105	0.152	12.56	12.1	9.1	14.9	12.22
		107	0.120	6.40	6.3	5.4	7.8	0.99

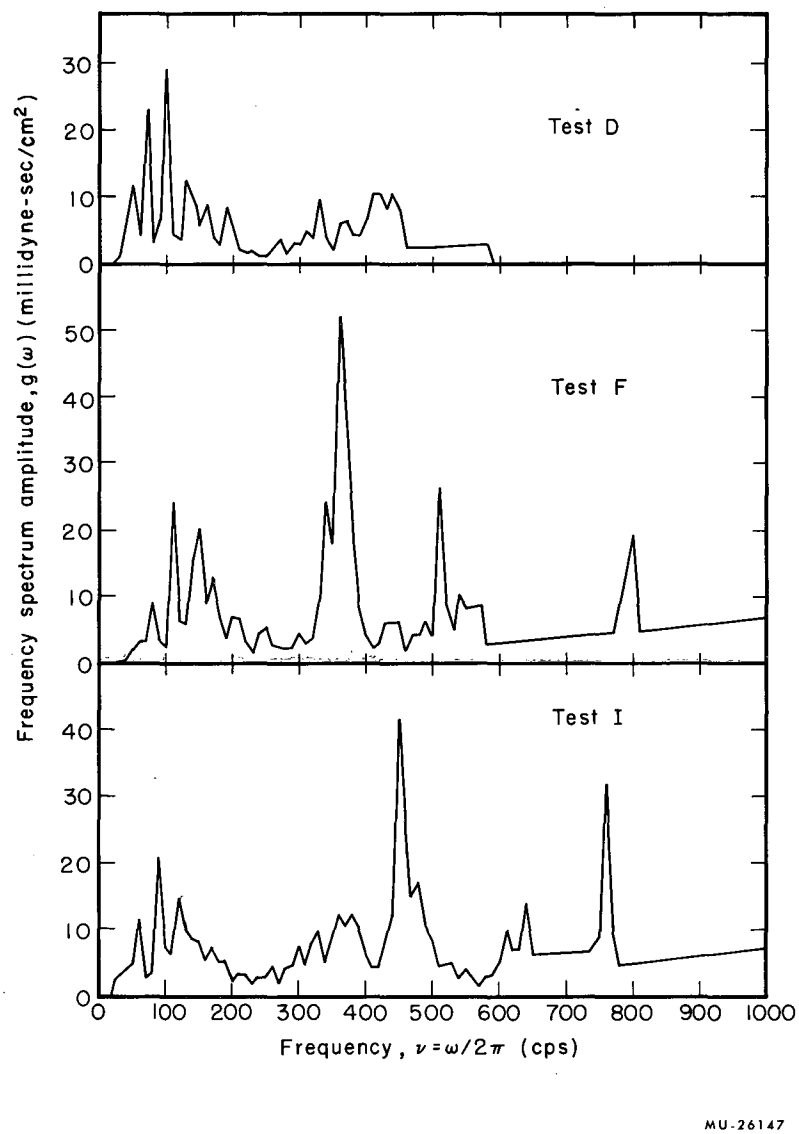

Fig. 60. Rms frequency spectra of naturally-occurring sonic disturbances. All pumps and stirring motors turned off.

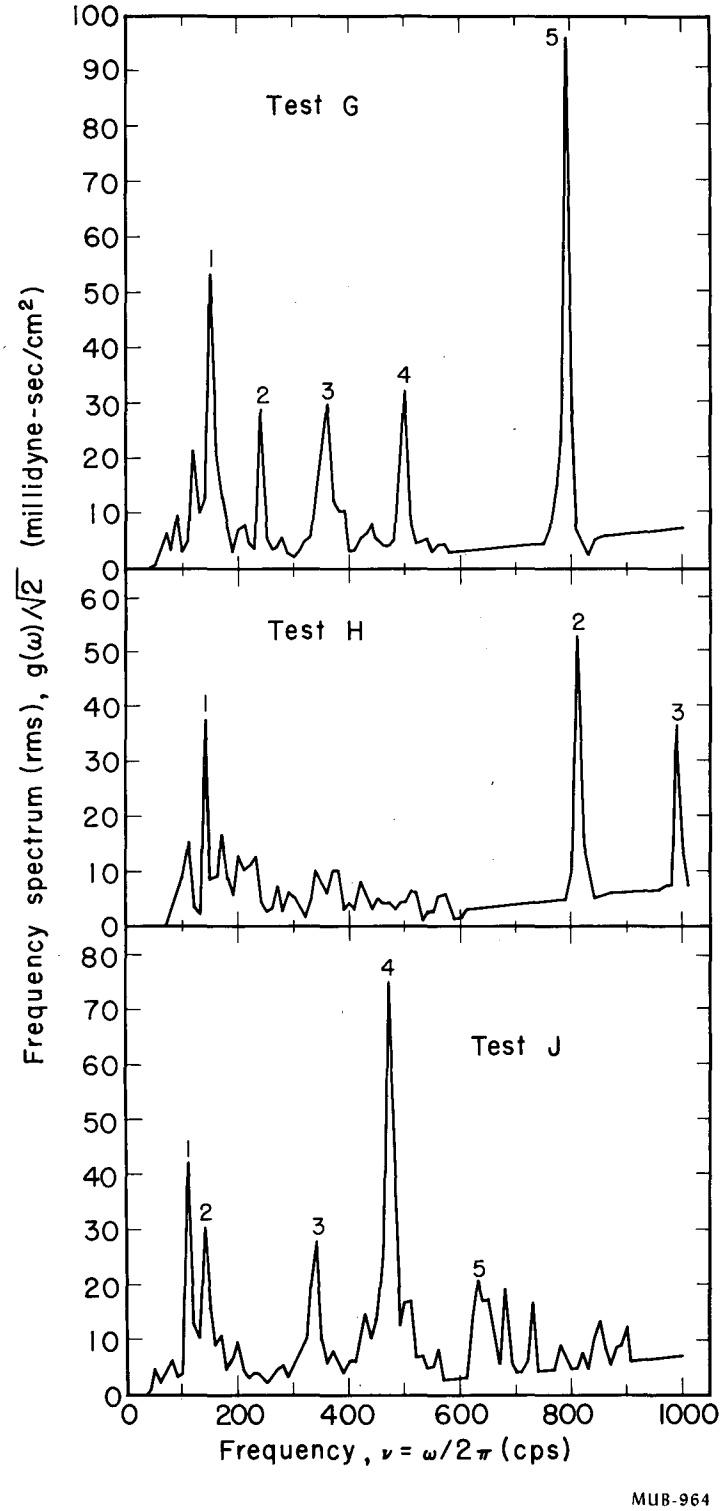

Fig. 61. Rms frequency spectra of naturally occurring sonic disturbances. The pump and stirring motors that were normally allowed to run during coalescence measurements were in operation.

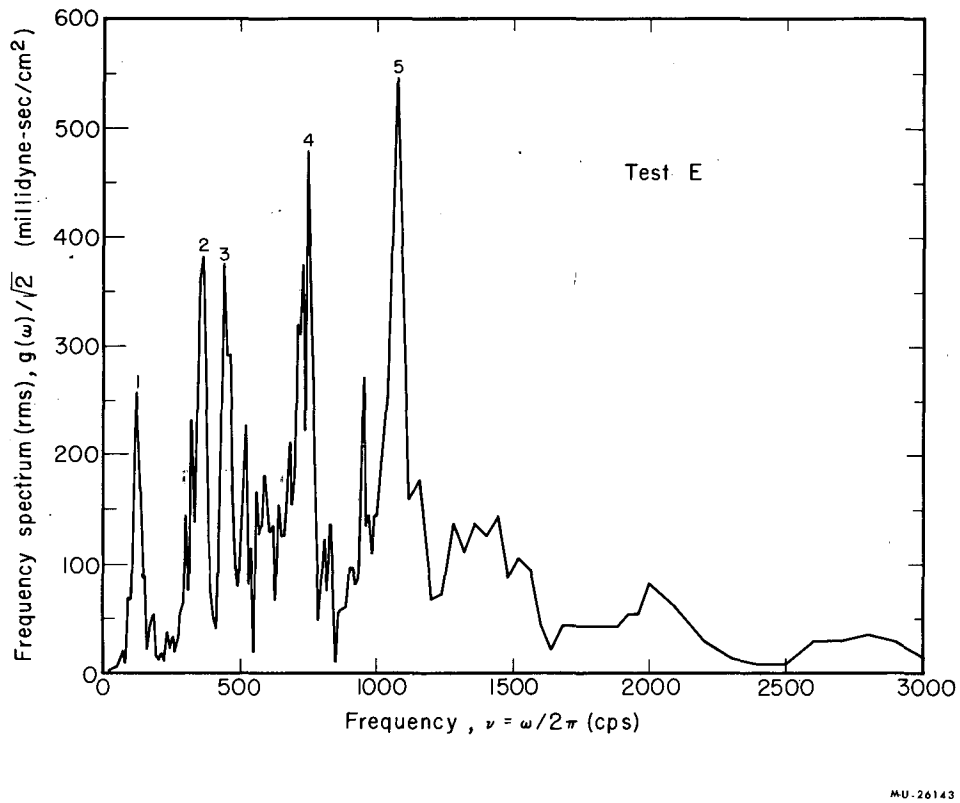

Fig. 62. Rms frequency spectrum of naturally-occurring sonic disturbances. All pumps and stirring motors were in operation.

frequency that was a multiple of 10 cps, the graphical peak would be slightly lower than the true peak. Numerical data were used in the calculations in the second subsection, however. Tests D, F, and I (Fig. 60) were made with all pumps and stirring motors turned off. Although Test D was made on a Saturday, Test F on a weekday, and Test I made during thevery early morning hours on a weekday, certain similarities in the rms frequency spectra are very apparent. Tests G, H, and J (Fig. 61) were made with the pump and stirring motors which were normally allowed to run during coalescence measurements in operation. The three tests were made at different times, and again their reproducibility is apparent. Test E (Fig. 62) was made when the pump supplying constant-temperature water to the experimental tank was in operation. This pump was always turned off during coalescence measurements. A comparison of the three figures shows that the pump and stirring motors used during a coalescence run contributed relatively little additional noise to the coalescence cell, and that to shut off the pump supplying water to the experimental tank was a reasonable precaution. Photographs of the oscilloscope traces produced by the microphone voltages during Tests D, E, and G are shown in Fig. 63.

2. Computed Sonic Disturbances

From the discussion in Sec. II, we see that, if the most prominent disturbances observed were periodic and very short in time duration, they can be described mathematically by Eq. (100). Thus we have

$$f(t) = \left\{ \begin{array}{ll} \sqrt{2}\, P_{rms} \cos \omega_0 t \;, & -a \leq t \leq a \\ 0 \;, & |t| > a \end{array} \right\} . \tag{116}$$

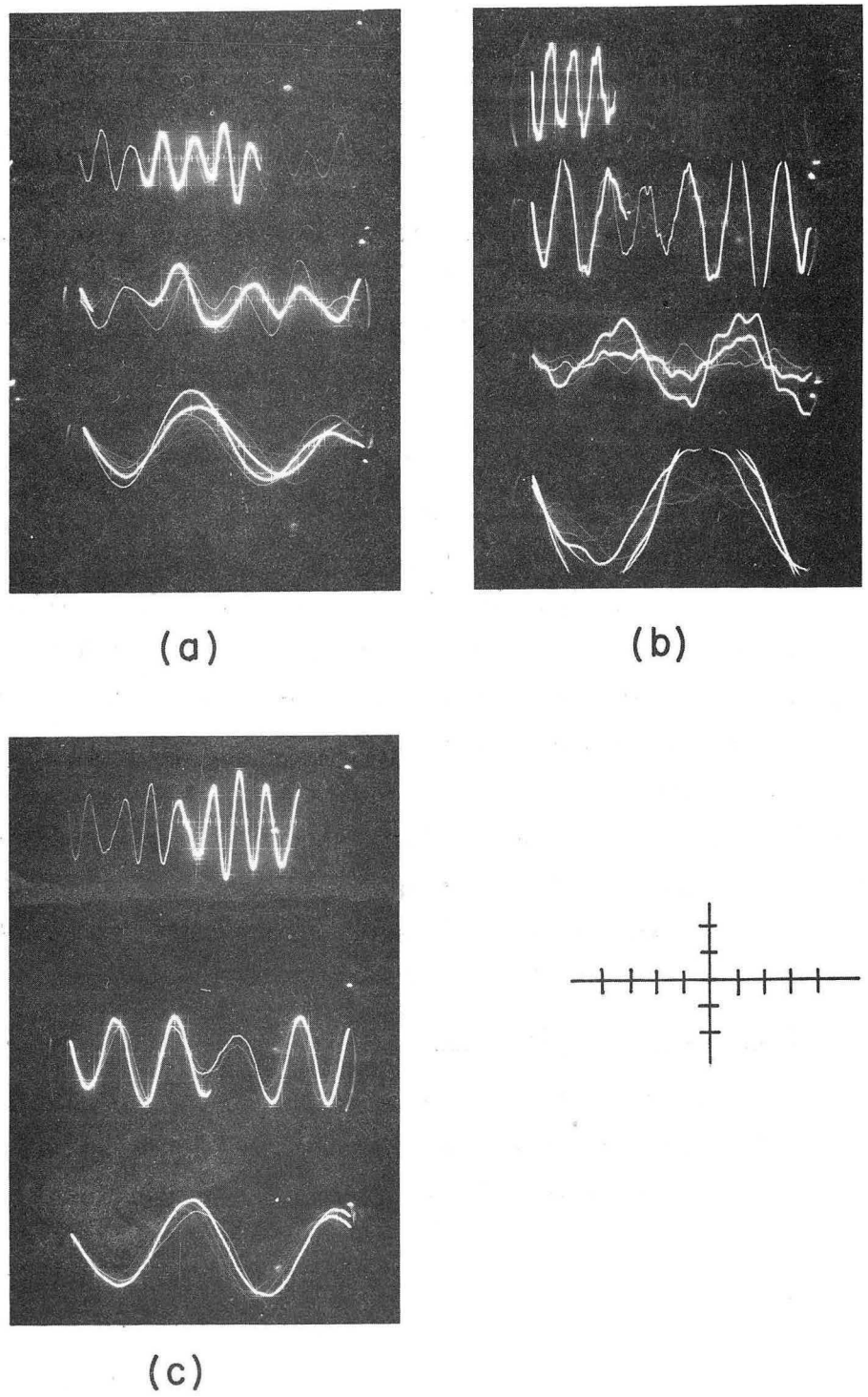

ZN-3117

Fig. 63. Photographs of oscilloscope traces produced by sonic disturbances on crystal microphone: (a) Test D—voltage sensitivity, 5 mV/division: horizontal sweep speeds were 10, 5, and 2 msec/division, respectively; (b) Test E—voltage sensitivity, 20 mV/division: horizontal sweep speeds were 10, 5, 2, and 1 msec/division, respectively; (c) Test G—voltage sensitivity, 5 mV/division: horizontal sweep speeds were 10, 5, and 2 msec/division, respectively.

These disturbances would then have the Fourier transforms—or equivalently, the frequency spectrum amplitude—given by Eq. (102):

$$\frac{g(\omega)}{\sqrt{2}} = \frac{P_{rms}}{\sqrt{2\pi}} \quad \frac{\sin\,(\omega-\omega_0)\,a}{\omega - \omega_0} \tag{117}$$

The three points adjacent to the numbered peaks in Figs. 60,61, and 62 were fitted to Eq. (117) by means of a table of the function, (sin x)/x.[69] The resulting rms pressure amplitude P_{rms}, the frequency ν_0, and the half-time period a, are presented in Table XV. Note that the intensities of these disturbances are much greater than the pressure fluctuations produced by the swimming-pool speaker. This explains the difficulty of influencing coalescence times by induced sonic disturbances.

TABLE XV. Computed sonic disturbances.

Test	Numbered Peak	ν_0 (cps)	a (sec)	P_{rms} (dynes/cm^2)
D	1	100	0.0420	1730
	2	330	0.0338	732
F	1	111	0.0420	1380
	2	362	0.0291	4470
	3	511	0.0395	1660
	4	797	0.0297	1610
I	1	91	0.0392	1300
	2	452	0.0324	3220
G	1	151	0.0338	3930
	2	240	0.0431	1690
	3	358	0.0286	2620
	4	498	0.0326	2430
	5	790	0.0386	5900
H	1	140	0.0426	2200
	2	810	0.0408	3210
	3	991	0.0375	2410
J	1	111	0.0418	2490
	2	141	0.0321	2340
	3	338	0.0289	2420
	4	471	0.0320	5780
	5	632	0.0208	2490
E	1	119	0.0221	29100
	2	356	0.0130	72600
	3	441	0.0215	43700
	4	752	0.0255	47800
	5	1076	0.0087	157000

V. DISCUSSION AND ANALYSIS OF RESULTS

The experimental results described in Sec. IV are discussed in light of the theoretical development in Sec. II, in the first section below. Some future work suggested by this discussion will be described in the second section. Possible applications for the coalescence study will be discussed in the third section. A brief summary concludes this analysis.

A. Discussion of the Experimental Results

A self-consistent theoretical explanation of the coalescence process is developed in Sec. II. However, the explanation deals with the coalescence of a single drop. An experimental investigation, by its very nature, must deal with a large number of coalescence events. In a sense, we have treated coalescence theoretically on a microscopic scale, but experimentally on a macroscopic scale. The connecting link between the microscopic theory and the macroscopic experiments is the disturbance pattern that is responsible for the rupture of the phase-2 film and the coalescence of the drops. Experimentally, we have measured the magnitude of these disturbances, their time duration, and the basic frequency of which they are composed. We could not measure their distribution in time. This basic point virtually precludes the possibility of closely comparing theory with experiment. Certain generalizations, however, are to be made.

1. Effect of Drop Size and Liquid System

One of the basic goals of this study was to determine the effect of the size of the drop and the liquid system on drop-rest times. Table XVI summarizes all the coalescence data available on two-component systems. The theory suggests that a knowledge of the average thickness of the phase-2 film at the time of coalescence is important in the prediction of drop rest-times. Average film thicknesses corresponding to $t_{0.10}$, t_m, and $t_{0.90}$ have been calculated by means of Eq. (20)

Table XVI. Coalescence runs on two-component systems

Data point	Reference	System	Temperature (°C)	ρ_1 (g/cm^3)	ρ_2 (g/cm^3)	μ_2 (cp)	σ (dynes/cm)	r_e (cm)	$t_{0.10}$ (sec)	t_m (sec)	$t_{0.90}$ (sec)	p (deg)	$h'_{0.10}$ (μ)	h'_m (μ)	$h'_{0.90}$ (μ)
1	9	Water-benzene	20	0.9982	0.8790	0.652	35.6	0.384	2.0	4.1	8	33	5.72	4.00	2.86
2	9	"	20	0.9982	0.8790	0.652	35.6	0.416	3.0	5.9	10	38	6.19	4.42	3.39
3	9	"	20	0.9982	0.8790	0.652	35.6	0.544	3.0	11.7	31	50	13.3	6.75	4.15
4	9	"	20	0.9982	0.8790	0.652	35.6	0.604	4.0	18.9	54	56	15.8	7.25	4.29
5	9	CCl_4-water	15	1.6038	0.9991	1.140	41.1	0.336	1.8	3.1	4.8	67	15.4	11.7	9.43
6	9	"	20	1.5942	0.9982	1.005	40.2	0.335	1.5	2.4	3.8	67	15.9	12.6	10.0
7	9	"	25	1.5751	0.9970	0.894	37.5	0.328	1.1	1.5	2.5	66	17.4	14.9	11.5
8	9	"	30	1.5549	0.9956	0.801	35.6	0.323	1.1	1.4	2.1	66	17.0	15.1	12.3
9	9	Water-benzene	15	0.9991	0.8840	0.705	36.2	0.578	8.0	16.1	22.5	52	9.64	6.80	5.76
10	9	"	20	0.9982	0.8790	0.652	35.6	0.566	7.5	14.8	21.0	53	9.51	6.77	5.68
11	9	"	30	0.9956	0.8681	0.564	34.7	0.550	7.5	13.8	18.5	54	8.81	6.51	5.61
12	9	"	40	0.9922	0.8575	0.503	34.6	0.540	7.5	13.2	17.5	54	8.01	6.03	5.24
13	9	Water-n heptane	20	0.9982	0.6838	0.409	50.3	0.464	2.2	3.6	5.6	60	10.2	7.97	6.39
14	9	Water-benzene	20	0.9982	0.8790	0.652	35.6	0.566	---	14.8	---	53	---	6.75	---
15	75	Ethylene glycol-n hexane	20	1.1155	0.6603	0.360	16.1	0.193	1.2	3.0	4.9	52	5.11	3.23	2.53
16	75	"	40	1.0984	0.6412	0.255	15.3	0.193	0.9	1.6	2.7	54	5.35	4.02	3.09
17	75	"	60	1.0814	0.6221	0.216	15.7	0.193	0.6	1.0	1.6	54	5.89	4.56	3.61
18	75	Diethylene glycol-n hexane	20	1.1177	0.6603	0.305	9.9	0.150	1.6	3.8	6.5	52	3.56	2.31	1.77
19	75	"	40	1.1017[a]	0.6412	0.247	9.9	0.150	1.0	1.8	2.9	52	4.06	3.03	2.38
20	75	"	60	1.0867[a]	0.6221	0.215	9.7	0.150	0.9	1.3	1.7	53	4.12	3.43	3.00
21	75	Triethylene glycol-n hexane	20	1.1254	0.6603	0.305	9.8	0.156	1.0	2.3	3.6	55	5.13	3.37	2.70
22	75	"	40	1.1083[a]	0.6412	0.254	9.3	0.156	0.9	1.6	2.7	58	5.41	4.06	3.13
23	75	"	60	1.0923[a]	0.6221	0.217	8.9	0.156	0.8	1.3	2.0	58	5.59	4.38	3.53
24	75	Ethylene glycol-benzene	20	1.1029	0.8762	0.638	7.4	0.170	5.1	11.6	23	48	3.53	2.34	1.66
25	75	"	40	1.0984	0.8575	0.485	7.2[b]	0.170	1.0	1.6	1.9	50	7.59	6.00	5.51
26	75	"	60	1.0814	0.8451	0.388	7.0[b]	0.170	2.6	5.3	8.7	50	4.27	2.91	2.33

(continued)

Table XVI (continued)

Data point	Reference	System	Temperature (°C)	ρ_1 (g/cm^3)	ρ_2 (g/cm^3)	μ_2 (cp)	σ (dynes/cm)	r_e (cm)	$t_{0.10}$ (sec)	t_m (sec)	$t_{0.90}$ (sec)	p (deg)	$h'_{0.10}$ (μ)	h'_m (μ)	$h'_{0.90}$ (μ)
27	75	Diethylene glycol-benzene	20	1.1177	0.8790	0.717	4.0[b]	0.080	11.0	23.0	32	30	0.664	0.454	0.385
28	75	"	40	1.1017[a]	0.8575	0.500	3.8[b]	0.080	5.7	12.0	24	31	0.806	0.555	0.392
29	75	"	60	1.0867[a]	0.8451	0.421	3.6[b]	0.080	4.3	9.6	13	32	0.891	0.597	0.507
30	Run 75[c]	Water-benzene	25	0.9976	0.8733	0.590	34.7	0.415	2.1	4.7	6.9	56	11.9	7.97	6.58
31	Run 74[c]	"	25	0.9976	0.8733	0.590	34.7	0.340	2.6	4.8	7.3	32	3.83	2.82	2.29
32	Run 73[c]	"	25	0.9976	0.8733	0.590	34.7	0.267	2.1	4.7	6.6	24	2.97	1.98	1.67
33	Run 77[c]	"	25	0.9976	0.8733	0.590	34.7	0.209	2.8	4.9	5.8	18	1.05	0.781	0.728
34	Run 72[c]	Tributyl phosphate-water	25	0.9763	0.9964	0.973	9.9	0.508	2.7	6.1	7.3	34	17.9	12.0	10.9
35	Run 71[c]	"	25	0.9763	0.9964	0.973	9.9	0.415	4.1	5.3	5.5	28	8.93	7.85	7.71
36	Run 70[c]	"	25	0.9763	0.9964	0.973	9.9	0.325	4.5	10.1	11.5	22	4.65	3.10	2.91
37	Run 108[c]	Water-anisole	25	0.9975	0.9886	0.957	25.5	0.772	7.1	35.6	90.2	22	8.19	3.66	2.30
38	Run 109[c]	"	25	0.9975	0.9886	0.957	25.5	0.598	4.7	12.3	45.3	16	5.22	3.22	1.68
39	Run 112[c]	Ethylene glycol-benzene	25	1.1029	0.8762	0.612	7.4	0.195	9.0	23.5	40.0	55	3.91	2.42	1.86
40	Run 111[c]	"	25	1.1029	0.8762	0.612	7.4	0.159	10.5	14.0	22.3	44	1.90	1.72	1.36
41	Run 110[c]	"	25	1.1029	0.8762	0.612	7.4	0.125	6.9	20.5	30.8	38	1.45	0.840	0.685
42	Run 79[c]	Water-Aroclor 1248	25	0.9966	1.4471	203.0	40.9	0.228	54.0	206.0	610.0	38	9.49	4.86	2.82
43	Run 78[c]	"	25	0.9966	1.4471	203.0	40.9	0.180	8.3	59.0	137.0	29	12.9	4.85	3.18
44	Run 80[c]	"	25	0.9966	1.4471	203.0	40.9	0.141	14.8	42.0	86.0	22	5.21	3.09	2.16
45	13	Mercury-84% glycerol	20	13.6	1.220	99.6	355.0	0.173	---	9.1	---	52	---	5.55	---
46	13	"	20	13.6	1.220	99.6	355.0	0.244	---	30.3	---	75	---	9.01	---
47	13	"	20	13.6	1.220	99.6	355.0	0.294	---	40.8	---	90	---	14.2	---
48	13	Mercury-96% glycerol	20	13.6	1.252	661.0	370.0	0.248	---	780.0	---	74	---	4.53	---
49	5	Water-anisole	25	0.9975	0.9886	0.957	25.5	0.058	---	7.5	---	1.5	---	0.0112	---
50	5	"	25	0.9975	0.9886	0.957	25.5	0.076	---	10.0	---	2.1	---	0.0204	---
51	5	"	25	0.9975	0.9886	0.957	25.5	0.088	---	12.7	---	2.5	---	0.0268	---
52	5	"	25	0.9975	0.9886	0.957	25.5	0.098	---	15.0	---	2.8	---	0.0324	---

[a] From reference 86.

[b] Estimated. All other physical properties are from references 72 or 76, or Table VII.

[c] The runs are from this work.

for the system in Table XVI. Because the drop diameter does not enter into the film-rupture theory, we would expect the average film thickness at the time of coalescence to be independent of drop size. However, a comparison of values of h'_m corresponding to differently sized drops in a single system indicates some effect of drop size. One theoretical and two experimental explanations can be found for this observation. In comparing values of h'_m we have implicitly assumed that the median coalescence time yields a good estimate of the expectation value of all coalescence times, but our sample is actually much too small for this purpose. The two experimental difficulties have been mentioned in Sec. IV. The surface disturbance created by a large drop falling only a small distance to the interface can greatly reduce drop rest-times. A calculation of the order of magnitude of such a disturbance was given in Sec. II-E. These disturbances are eventually damped out by viscosity, but because they have long wavelengths the damping is a slow process (see Eq. 59). If the coalescence times are long, the effect of these initial disturbances on t_m is lessened considerably. For example, the values of h'_m corresponding to the three drop sizes in the water-Aroclor system are fairly constant because of the long rest times observed in the system. The second experimental difficulty was the effect of trace contraniation. We noted in Sec. IV that the addition of minute quantities of surface-active agents had a very great effect on drop rest times. We might anticipate that systems with high concentrations of surfactants would be much less subject to the effect of trace contamination of an unintentional nature. If the assumption is made that a surfactant produces the effect of a high phase-2 viscosity in the film thinning model, we can calculate the values of $h'_{0.10}/\sqrt{\mu_2}$, $h'_m/\sqrt{\mu_2}$, and $h'_{0.90}/\sqrt{\mu_2}$ from Eq. (20). The results are given in Table XVII. As we would expect, the range of values $h'_{0.10}/\sqrt{\mu_2}$ to $h'_{0.90}/\sqrt{\mu_2}$, over the range of drop sizes in a given system, overlap to a much greater extent than do the ranges, $h'_{0.10}$ to $h'_{0.90}$, in Table XVI (for the systems without surfactant). This is especially noticeable in the more concentrated Span 80 and Tween 81 solutions.

TABLE XVII. Coalescence Runs on Water-Benzene-Surfactant Systems.[a]

Run No.	Surfactant	Concentration in water (milli-moles/l)	r_e (cm)	p (deg)	$h'_{0.10}/\sqrt{\mu_2}$ (cm/cp$^{1/2}$)	$h'_m/\sqrt{\mu_2}$ (cm/cp$^{1/2}$)	$h'_{0.90}/\sqrt{\mu_2}$ (cm/cp$^{1/2}$)
86	Span 80	0.0031	0.310	32	0.00491	0.00324	0.00235
84			0.245	26	0.00237	0.00156	0.00127
85			0.191	20	0.00138	0.000841	0.000617
83		0.031	0.230	38	0.00188	0.000977	0.000800
82			0.182	29	0.00215	0.000933	0.000726
81			0.143	23	0.000980	0.000599	0.000434
89	Tween 81	0.00244	0.299	32	0.00653	0.00390	0.00271
87			0.236	26	0.00263	0.00198	0.00153
88			0.184	20	0.00204	0.00118	0.000973
90		0.0244	0.266	34	0.00373	0.00261	0.00210
92			0.210	27	0.00224	0.00152	0.00116
91			0.164	21	0.00139	0.00103	0.000733
95		0.244	0.213	39	0.00293	0.000835	0.000561
93			0.168	30	0.00133	0.000643	0.000426
94			0.132	23	0.000855	0.000348	0.000252
101	Sodium oleate	0.0566	0.321	31	0.00483	0.00282	0.00191
99			0.253	25	0.00181	0.00134	0.00112
100			0.200	19	0.00132	0.000839	0.000680
102		0.566	0.277	33	0.00348	0.00167	0.00107
104			0.218	27	0.00167	0.000765	0.000549
103			0.171	21	0.00109	0.000505	0.000335
106		5.56	0.193	41	0.00369	0.00336	0.00311
105			0.152	31	0.00174	0.00150	0.00136
107			0.120	25	0.00128	0.00119	0.00107

[a]Physical properties used correspond to pure water-benzene system, with the exception of interfacial tensions which are taken from Table XIII.

Because of the conflicting effect of certain of the physical properties of the systems as described at the end of Sec. II, it is very difficult to predict coalescence times from a knowledge of physical properties without complete information concerning the natural disturbance pattern. An important generalization should be noted immediately. In an environment with few and weak disturbances, rapid coalescence will occur with systems having physical properties such that the film ruptures readily. Conversely, in an environment with many and strong disturbances, rapid coalescence will occur with systems with physical properties that cause the film to thin rapidly. In other words, the one of several successive mechanisms that occurs most slowly will be the "rate-determining step."

The data in Table XVI will now be examined in light of the above generalization and the information in Table III. Let us first examine the water-Aroclor and mercury-glycerol systems. The long median rest times of 42 to 206 sec in the water-Aroclor system are primarily due to the high viscosity of the Aroclor, which causes the film-thinning step to be the rate-determining one. The rest times for the mercury 84%-glycerol system are much shorter in comparison to those for water-Aroclor than can be explained by the decrease in μ_2. The cause for this is revealed by an examination of certain physical properties that have an opposing effect on the parameters determining coalescence times. In the mercury 84%-glycerol system, the extremely high interfacial tension that enters to about the second power in Eq. (20) causes the glycerol film to thin rapidly despite the high density difference and moderately high phase-2 viscosity. The rate of coalescence in the system is also strongly determined by the film-rupture step. In this case, the high value of $\Delta\rho$ overcomes the opposing effect of a high σ, and renders the film subject to a broad range of various wavelength disturbances that promote a Taylor instability. The growth factors of these disturbances are large enough to overcome the viscous damping effect. The extremely high phase-2 viscosity in the mercury-96% glycerol system causes the film-thinning step to be strongly rate-determining, yielding the long median rest-time of 780 sec.

Film rupture was the rate-determining step in the other systems examined. An interesting comparison can be made between the water-anisole and the water-benzene systems. With the exception of $\Delta\rho$, their physical properties do not differ greatly. If film thinning were rate determining, water-anisole would have the shorter rest times because of the very low value of its $\Delta\rho$. However, the rest times for this system are much greater than those for water-benzene, and thus film rupture is the rate-determining step. Both the tributyl phosphate-water and the water-anisole systems have small values of $\Delta\rho$, so that film rupture probably occurs according to the metastable model. Therefore, the system with the smaller interfacial tension should have the shorter rest-times. The data in Table XVI definitely shows that the TBP-water system with a σ of 9.9 has shorter rest times than does the water-anisole system which has a σ of 25.5. The water-benzene system has a sufficiently large $\Delta\rho$ that Taylor instabilities may develop, and despite its σ of 34.7, it has coalescence times of about the same magnitude as the TBP-water system. The carbon tetrachloride-water and water-heptane systems are two more illustrations of dominance of the film-rupture mechanism over the film-thinning one in the determination of rest times. Because of the large $\Delta\rho$ in these two systems, the rest times would be greater than those of thewater-benzene system if film thinning were the rate-determining step. However, both the carbon tetrachloride-water and water-heptane systems exhibit rest-times of only several seconds and thus, film rupture caused by a Taylor instability is the rate-determining step. The film-rupture mechanism was also the rate-determining step in the ethylene glycol-benzene system. The rest-times obtained in this work were about twice as great as those found by Könnecke for similar-size drops with the system.[75] Apparently, the level of natural disturbance was much higher in Könnecke's apparatus than in the equipment described in this report, thus markedly affecting the coalescence times.

Despite insufficient information concerning the disturbance patterns during the coalescence runs, qualitative agreement between

the experiments and the theory is quite good. But we do lack additional information concerning the natural disturbance pattern, and so cannot deduce further concerning the effects of drop size and physical properties on drop rest times. In the suggestions for future work, some possible means of obviating this difficulty are proposed.

2. Effect of Induced Disturbances

The theory developed in Sec. II suggested that we might be able to alter coalescence distribution curves by inducing the proper types of disturbances in the coalescence cell. The results in Sec. IV showed that this endeavor was successful in certain cases.

When sonic frequency disturbances were introduced during measurements on the tributyl phosphate-water system, decreases in drop rest times of 0.8 through 1.7 sec were found (and shown to be statistically significant). Because of the very large day-to-day scatter in the measurements, the low intensities of the disturbances used, and the high interfacial tension, a statistical analysis of the water-benzene system did not show the effect of vibration. The trochoidal wave theory showed that the energy required to rupture a given thickness of film increased greatly with increasing wave number (or increasing frequency). This trend was very apparent with the tributyl phosphate-water results. The sound pressure of the 500 cps disturbance was three times as great as that of the 300 cps disturbance, but the effect on coalescence times was about the same. An even more intense 1000 cps did not show a statistical influence on coalescence times at all.

The experiments using interference beats as subsonic disturbances were difficult to analyze, but did show the expected effect. The selection of 70 cps as the fundamental frequency in these studies was not entirely satisfactory because it caused excessive oscillation of the drop at the interface, prolonging the coalescence time. Higher frequencies could not be used because of difficulty in maintaining the desired beat frequency over a period of time.

The measurements of the natural disturbances present in the system showed clearly why artificially induced disturbances had a weak effect. The maximum power that could be dissipated in the swimming-pool speaker without danger of rupturing its diaphragm could only produce sound pressures of the order of hundreds of dynes/cm^2. The calculations in Table XV show that the natural disturbances, albeit very brief, were of intensities at least one order of magnitude higher than the artifical ones. The natural disturbances strongly masked the effects of the artifical ones.

3. Contamination and Surface-Active Agents

A third component can influence drop rest times either by increasing or decreasing them. The mechanisms of the two effects are quite different. Drop rest times may be decreased when a low-molecular-weight third component is present in non-equilibrium concentrations in the two phases. Charles observed that this effect was due to a small quantity of ethanol in the chloroform-water system.[9] It has been further discussed by Groothuis and Zuiderweg.[77] This decrease in drop rest times results from interfacial turbulence (often called the Marangoni effect). Because of small-scale eddies adjacent to the interface, concentration variations of the third component may exist, giving rise to local variations in the interfacial tension. In an attempt to reduce its potential surface energy by extension or contraction of area, the surface undergoes turbulent motion[68,78,79] which may result in disturbances causing premature coalescence of the drop. The likelihood of such local interfacial tension variations arising in a stagnant system decreases as the concentration of the third component approaches equilibrium. Then decrease in drop rest times would be less likely to occur, and this is also in agreement with experiment.[9]

Drop rest times generally increase when the third component has a high molecular weight. This observation accounts for the necessity of an emulsifying agent to produce a stable emulsion.[48] Many explanations for the stability of emulsions have been given in the literature.[48,68] Only a few of the more pertinent ones will be mentioned here in regard to the

effect of surfactants on drop rest times. The surfactant first decreases the rate of thinning of the phase 2 film mechanically and electrically. Several oriented layers of water of hydration may surround each molecule of surface-active agent, producing a mechanical barrier that must be displaced or removed for coalescence to occur. Surface-active agents enhance the electrical repulsion forces, which decrease the rate of film thinning. Surfactants tend to prevent the growth of instabilities by damping waves at interfaces in a manner similar to that of viscosity. Surfactants also make the film more elastic by enabling the film to "heal" its own weak spots by changes in the dynamic interfacial tension.[30,80]

The data in Table XIV strongly support the arguments that surfactants increase drop rest times. As an example, the median rest time for 0.213-cm drops of 0.244-millimolar Tween 81 in water at a benzene interface was 133.7 sec, as compared to a median rest-time of 4.9 sec for 0.209-cm drops in the water-benzene system. For a given surfactant, the drop rest times increased with concentration of the agent, with one exception. The rest-times of the 5.56-millimolar sodium oleate-benzene system were about one-fourth as long as those of the 0.556-millimolar sodium oleate-benzene system. It was noticeable that the water phase was very turbid, and this observation suggested that the critical micelle concentration (c.m.c.) had been exceeded. Harkins reported a c.m.c. of 7 to 9 millimolar for sodium oleate,[56] a value very similar to the sodium oleate concentration in the experiment discussed. Characteristics of solutions near the c.m.c. are somewhat unusual, so that an effect on coalescence times is not surprising. Insufficient data is available to attempt a theoretical explanation of the influence of micelle concentration on coalescence times.

In industrial emulsion technology, surfactants with lower hydrophilic-lipophilic balance values are used to stabilize water-in-oil emulsions, and those with higher H.L.B. values are used to stabilize oil-in-water emulsions. Similar considerations should apply to drop rest times. The best way to make such a comparison, however, is to measure some rest times with the denser phase as phase 1, and other

rest times with the lighter phase as phase 1. A comparison of relative increases in rest time for the two modes of operation could be correlated with the H.L.B. values. Because such a comparison would have been beyond the scope of this work, this type of data was not taken.

B. Future Work

In the course of the study, a theoretical problem and a number of experiments suggested themselves that will further elucidate the mechanism of coalescence.

An extremely valuable theoretical approach would be a computer simulation of coalescence measurements. As previously mentioned, the connecting link between the microscopic theory and the macroscopic experimental work is a knowledge of the natural disturbance pattern present in the coalescence cell. With the proposed model, and various assumed disturbance distributions (distributed in time both with respect to frequency and intensity), the computer could simulate thousands of coalescence measurements quickly. The effect of the disturbance distribution on the coalescence distribution curves, as well as the effect of changes in drop size and physical properties, could be readily determined. It might even be possible to make allowance in the model for the initial disturbance caused by the falling drop and for trace contamination.

An excellent experimental check on the validity of part of the theoretical model would be a direct measurement of the thickness and shape of the phase 2 film prior to coalescence. One possible approach would be through optical interference patterns. Thicknesses of liquid layers bounded by solids, or gases and gaseous layers bounded by liquids and solids, have been measured in this way.[9,12,25] Extension of the techniques to the measurement of liquid layers bounded by other liquid phases could be feasible. Another means of determining the thickness of the phase 2 film would be a direct measurement of its electrical capacitance. A knowledge of the film geometry and the electrical properties of the phases would allow calculation of the thickness. Care would be needed to avoid introducing an electrostatic attractive force between the drop and the interface.[13]

Measuring the natural noise pattern present in the coalescence cell would also yield some very useful information. Practicable advantage might be taken of the elaborate counting techniques that have been developed in the field of radiochemistry.[81]

C. Applications

Industrial processes that involve coalescence may be classified into two groups: separation processes in which coalescence is desired, such as liquid-liquid settling,[82] and dispersion processes in which coalescence is undesirable, as in mixing or emulsion manufacture. A qualitative discussion of the importance of coalescence studies to a separation process is given below.

Suppose it is desired to separate a dispersed phase-1 from a continuous phase-2 liquid. The dispersed phase is initially distributed throughout the mass of the phase 2 liquid in the form of small drops. These drops will be in motion because of one or more of three causes. An initial velocity field may have been established in the fluid through the previous treatment to which it was subjected. Small drops of fluid may have a velocity because of Brownian motion. All of the drops of phase 1 are affected by acceleration due to gravity. Drops of various size will move at different velocities and if the concentration of drops is sufficiently high, many collisions will occur and the drops will tend to flocculate in masses.[83-85] The individual drops will either break away from the masses, coalesce with other drops in the groups, or remain as individual drops within large groups. This behavior will be governed by hydrodynamic factors and by the kinetics of coalescence. If the coalescence proceeds at the higher rate, large drops will be formed, but if it proceeds more slowly the agglomerations of drops will decompose. Any large drops thus formed will move with even higher velocity. At the ends of the vessel the large drops must coalesce into a continuous phase for complete separation. Slow kinetics of coalescence at this point will lead to incomplete separation in a settling process, for example. A quantitative description of a settling process, therefore, depends upon

very complex hydrodynamic and coalescence processes. Dispersion processes can be described in analogous manner.

D. Summary

In conclusion, a comparison will be made between the major theoretical arguments and their substantiation by experimental data.

The theory predicts that coalescence times should increase with drop radius. With the exception of runs complicated by disturbances caused by the falling drop and contamination, the size effect was most definitely observed. Because the prediction of rest-times requires a knowledge of disturbance patterns, it could not be determined whether the size effect shown was correct quantitatively.

The theory yielded a complicated dependence of drop rest times on physical properties. The theory stated that a low μ_2 should promote rapid coalescence, as was demonstrated experimentally. The theory showed a different effect of $\Delta\rho$ and σ on the two mechanisms making up the coalescence process. It indicated that a low $\Delta\rho$ and high σ would cause the phase 2 film to thin rapidly, but that a high $\Delta\rho$ and low σ would cause a Taylor instability to grow most rapidly. Only a low σ is needed to cause a metastable flat film to rupture easily. The available experimental data showed that film rupture was the rate-determining step in most of the systems examined, and the predicted effect of physical properties was confirmed. Both film thinning and film rupture had strong rate-determining effects in mercury 84%-glycerol systems.

It was predicted that sonic disturbances would effect coalescence times by causing metastable film rupture. This effect was shown experimentally in the TBP-water system with sufficiently intense disturbances. Less success was experienced with water-benzene because of the higher value of σ, the greater day-to-day scatter because of contamination, and the lower intensity of the disturbances. The decreasing effect of higher frequency disturbances shown was also in agreement with the theory.

Subsonic disturbances were predicted to promote a Taylor instability in the phase 2 film. Because of the difficulty in generating low-frequency distrubances using interference beats, the results were not too satisfactory. The predicted effect was shown weakly, however.

The proposed coalescence mechanism requires the presence in the system of various frequencies and intensities of disturbances. A special microphone was used to detect and analyze these disturbances. Their intensities were much greater than those of the artificially induced disturbances, thus explaining the weak effect of the latter. No experimental method was devised for determining the distribution of these disturbances in time.

Contaminants, theoretically, should strongly effect coalescence times. A low-molecular-weight material would tend to decrease coalescence times if it were present in nonequilibrium quantities in the two phases. This effect would be caused by interfacial distrubances due to a Marangoni instability. The theory was confirmed by ethanol contamination in the chloroform-water system. High-molecular-weight materials would prolong rest times through mechanical and electrical effects. The experiments with surfactants most definitely confirmed a prolongation of coalescence times in the presence of even a minute concentration of surfactant.

A summary of the effect on coalescence times of the various variables discussed in this work is presented in Table XVIII.

Because of the microscopic nature of the coalescence theory and the macroscopic nature of the experimental data, simple experiments cannot be expected to provide an unequivocal test of the theory. It can be concluded, however, that the experimental evidence obtained does definitely support the proposed theory.

TABLE XVIII. Summary of effects of variables on coalescence times[a]

Variable	Dependence of coalescence time if thinning-film model is assumed rate-determining.	Dependence of coalescence time if Taylor-instability film-rupture model is assumed rate-determining.	Dependence of coalescence time if metastable film-rupture model is assumed rate-determining.
Drop radius	Time approx proportional to fifth power of drop radius.	No dependence.	No dependence.
μ_1	No dependence.	Time increases with increasing μ_1.	No dependence.
μ_2	Time directly proportional to μ_2.	Time increases with increasing μ_2.	No dependence.
$\Delta \rho$	Time approx proportional to $\Delta\rho$.	Time decreases with increasing $\Delta\rho$.	Time increases with increasing $\Delta \rho$ at very low frequencies. No dependence at higher frequencies.
σ	Time approx inversely proportional to σ^2.	Time increases with increasing σ.	Time increases with increasing σ.
P_{rms}	No dependence.	Time decreases with increasing P_{rms}.	A high P_{rms} will rupture films that cannot be ruptured by a lower P_{rms}.

TABLE XVIII (continued)

Variable	Dependence of coalescence time if thinning-film model is assumed rate-determining.	Dependence of coalescence time if Taylor-instability film-rupture model is assumed rate-determining.	Dependence of coalescence time if metastable film-rupture model is assumed rate-determining.
Disturbance frequency	No dependence	Coalescence times pass through a minimum between 0 cps and the maximum frequency determined by the stability criteria.	Higher P_{rms} is required to rupture films at higher frequencies.
Low-molecular-weight solute (not present in equilibrium concentrations in both phases)	No dependence at very low concentrations.	Time decreases due to presence of solute if interfacial turbulence is created.	If presence of sol. causes interfacial turbulence, film may be ruptured.
High-molecular-weight solute (below critical micelle conc.)	Time increases with increasing concentration of solute.	Time increases with increasing concentration of solute.	Higher P_{rms} is required to rupture films at higher concentrations of solute.

[a]More precisely, time in the thinning-film model means the time required for the film to decrease in thickness to a specified constant value, at which time coalescence would occur; time in the Taylor-instability model refers to the time required for a specified thickness film to be ruptured; in the metastable film-rupture model, a given distribution of various intensity disturbances is assumed, and the coalescence time represents the time lapse until a sufficiently intense disturbance (high P_{rms}) occurs.

ACKNOWLEDGMENTS

I wish to express my thanks to Professor Charles R. Wilke for his encouragement, advice, and helpful suggestions throughout the course of this work. I am also grateful for the suggestions of Professor Theodore Vermeulen and Professor Peter W. M. John.

I especially appreciate the continual encouragement of my wife, Lili. Her editing and typing of the rough draft of this thesis was invaluable.

My sincerest thanks to Mr. H. S. Powell and Mr. G. G. Young and their co-workers whose skills were reflected in the experimental equipment used in this study. I also wish to thank the many other people at the Lawrence Radiation Laboratory who contributed their advice and abilities to this project.

The author is grateful for the financial support given by the University of California and the National Science Foundation.

This work was partially performed under the auspices of the U.S. Atomic Energy Commission.

APPENDICES

A. Statistical Analyses

Certain statistical designs were used in the analysis of the experimental data. A description of their use, and some calculations, is presented in the following sections. Detailed instructions for the use of the statistical designs were taken from Cochran and Cox.[57]

1. Experimental Run-Consistency Test

The experimental coalescence runs were normally subdivided into four groups of 12 or 13 coalescence measurements each. After completion of a group of measurements, the hypodermic syringe was refilled, the interface was made planar, and the constant-temperature-bath water pump was turned on. An experimental mishap was most likely to occur, therefore, between the groups of measurements. Accordingly, each group was considered to be a treatment in a completely randomized experimental design.[57] An analysis of variance was performed to determine if any difference existed between treatments (groups). The F-test[58] was used to check the statistical significance of the ratio of the treatments mean square to the residual mean square. The analysis-of-variance table for Run 82 is given in Table XIX. No effect of treatments (groups) was significant at the 5% level.

2. Statistical Analysis of the Effect of Material Purification Method

In the preliminary runs, it was desired to check the effect of different methods of preparation of the materials used. However, this effect was not considered sufficiently important to be studied alone. Accordingly, it was decided also to examine the effects of drop size and drop-fall height simultaneously in a balanced-incomplete-block design (BIBD). The smallest available BIBD plan (Plan 11.1, reference 57) could handle 4 treatments and 6 blocks (containing two treatments each). Four methods of purification were selected as treatments and six drop-size and drop-fall height combinations were selected for the blocks.

TABLE XIX. Analysis of variance for Run 82—data consistency test.

Source	Sum of squares	Degrees of freedom	Mean square	F Test[a]
Treatments	1108.395	3	369.46	1.47
Residual	11585.370	46	251.86	
Total	12693.765	49		

[a] $F_{5\%,3,46} = 2.81$; $F_{1\%,3,46} = 4.24$.

The mean rest-times of the runs were used in the analysis. Occasionally, several runs were made under the same treatment and block conditions. For those cases, the mean rest times of the runs were averaged, but no allowance was made for this averaging in the analysis. Table XX summarizes the information concerning treatments and blocks. The calculation method used in preparing the analysis of variance given in Table XXI did not make use of interblock information (see paragraph 11.55, reference 57) because the blocks were not random, but rather corresponded to fixed conditions of operation. The analysis shows that differences in treatments (methods of preparation)are statistically significant at the 2.5% level.

3. Statistical Analysis of the Effect of Drop Aging

Two effects were examined in Run 29. The drop-aging times were 0 sec, 15 sec, 1 min, or 3 min. The time period between groups of 12 measurements was either 15 min or 1 hour. In order to use a two-factor experimental design, the two types of effects were ordered by a table of random permutations. The four values of drop-aging time were selected as the first factor, and the two values of time period between groups were selected as the second factor. The experiment was replicated three times in the first factor. The experiment was then broken into eight blocks and the effect of the second factor was extracted as a single degree of freedom from the sums of squares of blocks. All the data, subdivided into treatments and blocks, is given in Table XXII. The analysis of variance[57] is given in Table XXIII. In the analysis of variance, the effect of the first factor was subdivided into the contrasts: 0 vs 15 sec, 1 min vs 3 min, and 0 and 15 sec vs 1 and 3 min. The drop-aging-time factor and the 0 and 15 sec vs 1 and 3 min contrast were both significant at the 1% level. Neither the block effect nor the time between groups were statistically significant at the 5% level. Accordingly, all drops were aged in succeeding experiments for 1 minute, and 15 minutes was allowed between groups.

Table XX. Treatments and blocks used in statistical analysis of the effect of material purification method.

Treatment No.	Treatment	Block No.	Block
1	Distilled benzene; deionized, filtered H_2O	1	Dropping tip 1, min. fall height
2	Distilled benzene; distilled, unfiltered H_2O	2	Dropping tip 7, min. fall height
3	Crystallized benzene; deionized, filtered H_2O	3	Dropping tip 3, min. fall height
4	Phillips Research Grade benzene; deionized, filtered H_2O	4	Dropping tip 2, min. fall height
		5	Dropping tip 1, 12 mm fall height
		6	Dropping tip 3, 12 mm fall height

Treatment No.	Block No.	Mean rest time (sec)
1	1	5.18
3	2	5.32
1	3	3.27
2	4	4.86
1	5	3.97
2	6	3.91
2	1	6.60
4	2	6.83
3	3	3.59
4	4	6.05
4	5	7.38
3	6	3.37

TABLE XXI. Analysis of variance--effect of material purification method.

Source	Sum of squares	Degrees of freedom	Mean square	F Test[a]
Treatments (adjusted)	8.4301	3	2.8100	19.29[b]
Blocks (unadjusted)	13.8407	5	2.7681	
Error	0.4372	3	0.1457	
Total	22.7080	11		

[a] $F_{5\%,3,3} = 9.28$; $F_{1\%,3,3} = 29.46$.

[b] Statistical significance at at least 5% level.

TABLE XXII. Run 29 data--drop aging effect.

Blocks (time between groups)	1 hr	1 hr	15 min	15 min	1 hr	15 min	15 min	1 hr	Treatment Total	Treatment Average
Treatments (drop-aging time)										
0 sec	4.3	4.3	3.4	2.9	2.9	4.5	2.9	4.5		
	4.6	2.5	2.1	3.7	2.5	3.3	4.2	4.1		
	4.3	4.6	3.9	4.7	2.3	3.1	2.3	2.5	84.4	3.52
15 sec	3.7	4.1	4.2	3.7	3.4	3.5	3.9	3.8		
	3.5	4.3	1.1	2.5	1.6	4.2	2.5	4.5		
	6.6	3.7	5.3	5.6	3.3	4.3	3.8	5.9	93.0	3.87
1 min	4.2	3.8	3.2	5.1	4.8	3.9	6.0	5.3		
	5.1	5.3	5.0	4.3	3.7	2.7	4.4	4.5		
	3.6	3.8	4.3	5.6	3.2	5.3	5.0	4.9	107.0	4.46
3 min	1.7	4.7	4.0	6.8	3.0	1.7	3.9	3.3		
	5.7	4.7	5.0	5.2	5.3	5.9	7.0	5.3		
	2.9	5.3	3.6	3.7	4.5	4.0	4.9	4.1	106.2	4.42
Block totals	50.2	51.1	45.1	53.8	40.5	46.4	50.8	52.7		

Block total (15 min groups) = 196.1, Block total (1 hr groups) = 194.5

TABLE XXIII. Analysis of variance for Run 29--drop-aging effect.

Source	Sum of squares	Degrees of freedom	Mean square	F test[a]
Treatments	14.9046	3	4.9682	4.23[b]
0 sec vs 15 sec	1.5409	1	1.5409	1.31
1 min vs 3 min	0.0133	1	0.0133	0.01
0, 15 sec vs 1, 3 min	13.3504	1	13.3504	11.35[b]
Blocks	11.6496	7	1.6642	1.42
15 min vs 1 hr between groups	0.0267	1	0.0267	0.02
Residual	99.9521	85	1.1759	
Total	126.5063	95		

[a] $F_{5\%,1,85} = 3.95$; $F_{1\%,1,85} = 6.95$; $F_{5\%,3,85} = 2.71$; $F_{1\%,3,85} = 4.03$; $F_{5\%,7,85} = 2.11$; $F_{1\%,7,85} = 2.86$.

[b] Statistical significance at at least the 1% level.

4. Statistical Analysis of Sonic Frequency Disturbance Runs

A chain design was used in the analysis of the sonic frequency disturbance runs. Each day was considered to be a block effect. Thus this design enabled the effect of day-to-day drift in system purity to be cancelled out by the establishment of a daily adjustment factor. The median drop rest times were used in the analysis. Table XXIV contains the treatment and block data used in the chain design for the tributyl phosphate-water runs. The adjusted treatment means, and the block effect adjustment factor, are also shown.

In a chain design analysis, the variances for comparing treatments depend upon whether the treatment being compared appear in the same or in different blocks. We also note that the "Level of statistical significance" column in Table XI should be examined, rather than the "Change in median rest time due to disturbance" column, in studying the effects of frequency on coalescence times.

TABLE XXIV. Chain design analysis for sonic frequency disturbances—tributyl phosphate-water runs

Block (day)	1	2	3	4	Adjusted treatment means[a]
Treatment (run numbers)					
54, 67	7.4			7.3	7.22
56, 57	5.7	5.3			5.85
62, 64		4.6	6.1		5.48
65, 68			7.9	8.0	7.60
55	7.9				7.89
59		5.3			6.01
66			6.0		5.54
69				6.7	6.46
Block effect adjustment factor[a]	0.01	-0.71	0.46	0.24	

[a]Adjusted treatment means for treatments 54, 57 = 1/2 [(7.4 - 0.01) + (7.3 - 0.24)] = 7.22, for example.

B. Coalescence-Run Experimental Data

All the experimental data on coalescence times are given in this appendix. Preceding the tabular coalescence data for each run is a short list of the more important details concerning the run. The date on which each run was performed is given so the reader may better appreciate the factors concerning day-to-day drift in operating conditions. Two or more runs are occasionally described in a single tabulation. This situation indicates that the runs were performed at different times during the day for randomization, but that they were obtained for a single set of operating conditions. The group divisions for the data-consistency test are indicated. All rest times are given in seconds.

The phase designated "water" in many of the runs means distilled, deionized, filtered water, unless the description is qualified further. The phase designated "benzene" means reagent grade benzene that has been purified by triple fractional crystallization and by filtration, unless the description is qualified further.

Run No. 1 (2-22-61)

Purpose: Preliminary studies.
Materials: Phase 1: Water.
Phase 2: Distilled benzene.
Dropping tip: 1.
r_e: 0.415 cm.
Induced sonic disturbances: None.
Rest-times: Mean: 5.73, Median: 5.2, 10 percentile: 2.3, 90 percentile: 7.9, Variance: 2.87.
Data-consistency test: Group effect significant at 1% level.
Comments: Data divided into 6 groups. Accidental contamination in Runs 1-5.
Rest-times (sec):

Group 1	Group 2	Group 3	Group 4	Group 5	Group 6
2.3	4.7	6.3	5.1	12.9	9.9
4.0	4.9	7.3	4.3	9.3	5.1
	1.1	7.9	3.7	7.8	4.7
	3.9	4.6	6.7	7.8	5.1
	2.3	5.9	6.4	6.6	7.5
	4.3	5.7	5.2	7.9	10.9
	3.9		5.9	4.1	6.3
			6.6	7.3	7.3
			4.3	8.0	6.3
			3.1	1.9	6.1
				4.9	7.5
				2.9	5.7
					2.3

Run No. 2 (2-24-61)

Purpose: Preliminary studies.
Materials: Phase 1: Water.
Phase 2: Distilled benzene.
Dropping tip: 1. r_e: 0.415 cm.

Induced sonic disturbances: None.
Rest-times: Mean: 14.33, Median: 12.0, 10 percentile: 7.9, 90 percentile: 22.3, Variance: 19.59.
Data-consistency test: Group effect not significant at 5% level.
Comments: Accidental contamination in Runs 1-5.
Rest-times (sec):

Group 1	Group 2	Group 3	Group 4
13.7	11.7	20.3	22.3
10.3	10.9	7.7	11.7
12.1	6.8	9.1	20.5
9.0	20.7	21.4	11.7
11.0	22.5	10.9	14.9
20.9	19.5	17.0	7.5
18.7	11.1	10.5	7.5
21.7	18.3	8.5	5.1
12.3	19.5	16.7	7.9
11.5	23.3	30.2	9.1
23.3	10.3	15.5	18.5
10.5		16.8	11.3
		12.0	10.5
			11.7

Run No. 3 (2-24-61)

Purpose: Preliminary studies.
Materials: Phase 1: Water.
Phase 2: Distilled benzene.
Dropping tip: 1. r_e: 0.415 cm.
Induced sonic disturbances: None.
Rest-times: Mean: 11.55, Median: 9.3, 10 percentile: 3.5,
90 percentile: 23.7, Variance: 32.46.
Data-consistency test: Group effect significant at 1%.
Comments: Data divided into 7 groups. Accidental contamination in Runs 1-5.
Rest-times (sec):

Group 1	Group 2	Group 3	Group 4	Group 5	Group 6	Group 7
30.3	22.9	3.3	5.1	9.7	11.5	7.2
13.7	24.7	4.5	11.2	6.5	3.5	8.3
11.1	31.8	5.5	3.1	6.7	17.5	
9.3	9.5	3.3	8.1	3.2	19.1	
12.2	45.6	11.9	7.1	4.3	7.0	
16.1	23.9	1.2	3.9	7.5	9.9	
13.9	10.9	6.5	8.9	5.6	12.9	
12.7	31.0	4.4	7.1	11.7	9.8	
15.1	27.5	5.7	8.8	5.4	19.9	
	21.1	4.7	7.1	15.5	10.9	
	8.3	4.7	10.1	10.3	16.0	
	26.7	2.3	5.1	7.3	10.7	

Run No. 4 (2-27-61)

Purpose: Preliminary studies.
Materials: Phase 1: Water. Phase 2: Distilled benzene.
Dropping tip: 1. r_e: 0.415 cm.
Induced sonic disturbances: None.
Rest-times: Mean: 25.24, Median: 16.6, 10 percentile: 5.9,
90 percentile: 50.0, Variance: 376.53.
Data-consistency test: Group effect not significant at 5% level.
Comments: Accidental contamination in Runs 1-5.
Rest-times (sec):

Group 1	Group 2	Group 3	Group 4
16.9	38.4	8.3	10.0
72.5	26.1	4.7	43.2
5.7	14.7	7.1	9.1
8.5	17.5	3.9	16.3
75.3	22.9	7.9	13.3
53.0	49.2	17.5	50.0
19.7	69.3	72.7	30.4
30.2	37.8	11.1	46.8
35.2	16.7	13.5	35.4
31.5	43.4	24.1	
35.6	19.7	3.1	
9.3	23.5	12.1	
7.5	14.1		
12.7	9.3		
	5.3		

Run No. 5 (2-27-61)

Purpose: Preliminary studies.
Materials: Phase 1: Water.
Phase 2: Distilled benzene.
Dropping tip: 1. r_e: 0.415 cm.
Induced sonic disturbances: None.
Rest-times: Mean: 15.95, Median: 13.9, 10 percentile: 5.5, 90 percentile: 33.3, Variance: 63.01.
Data-consistency test: Group effect significant at 1% level.
Comments: Accidental contamination in Runs 1-5.
Rest-times (sec):

Group 1	Group 2	Group 3	Group 4
15.7	34.9	4.9	8.7
4.5	24.7	19.7	16.5
13.9	25.3	3.9	11.5
12.5	21.9	25.9	20.5
5.5	14.1	15.1	22.9
8.5	18.9	18.5	6.4
6.9	48.6	13.3	7.3
11.5	33.3	18.1	6.0
8.7	4.1	15.0	12.7
7.9	46.2	7.4	7.8
14.3	36.0	7.5	18.6
9.5	30.8	13.2	
10.5	19.9	7.5	

Run No. 6 (3-1-61)

Purpose: Preliminary experiments.
Materials: Phase 1: Water.
Phase 2: Distilled benzene.
Dropping tip: 1. r_e: 0.415 cm.
Induced sonic disturbances: None.
Rest-times: Mean: 5.61, Median: 5.5, 10 percentile: 2.7, 90 percentile: 8.5, Variance: 4.30.
Data-consistency test: Group effect not significant at 5% level.
Comments: None.
Rest-times (sec):

Group 1	Group 2	Group 3	Group 4
4.3	4.1	2.7	6.1
4.3	7.7	4.1	2.5
3.3	3.5	6.5	6.5
3.2	4.7	3.7	6.5
5.6	4.9	9.9	7.7
7.3	5.5	5.7	2.7
3.7	8.5	5.7	2.3
3.7	5.5	6.7	2.7
6.3	6.5	8.7	8.7
7.1	6.9	4.3	11.0
2.3	6.9	5.1	9.1
4.9	5.6	5.3	7.3
4.7	8.1		

Run No. 7 (3-1-61)

Purpose: Preliminary studies.
Materials: Phase 1: Water.
Phase 2: Distilled benzene.
Dropping tip: 1. r_e: 0.415 cm.
Induced sonic disturbances: None.
Rest-times: Mean: 5.93, Median: 5.9, 10 percentile: 3.0, 90 percentile: 8.3, Variance: 3.70.
Data-consistency test: Group effect not significant at 5% level.
Comments: Pump circulating water to experimental tank was allowed to operate.
Rest-times (sec):

Group 1	Group 2	Group 3	Group 4
5.9	4.7	5.6	5.3
7.0	3.1	3.0	6.0
3.1	5.7	5.9	9.9
6.9	7.5	3.9	4.1
7.3	8.7	5.3	5.9
4.3	6.3	7.9	5.9
6.1	5.1	2.7	4.7
7.7	4.7	1.9	8.3
7.5	9.9	5.7	6.9
6.7	8.5	7.3	8.1
7.7	4.1	4.9	2.7
6.9	2.7	5.3	8.3
		7.7	5.3

Run No. 8 (3-1-61)

Purpose: Preliminary studies.
Materials: Phase 1: Water.
Phase 2: Distilled benzene.
Dropping tip: 1. r_e: 0.415 cm.
Induced sonic disturbances: None.
Rest-times: Mean: 6.27, Variance: 5.34.
Comments: Run discontinued after 9 measurements because of faulty equipment operation.
Rest-times (sec):

4.3
6.1
10.1
7.9
4.9
9.2
5.7
4.9
3.3

Run No. 9 (3-3-61)

Purpose: Preliminary studies.
Materials: Phase 1: Water.
Phase 2: Distilled benzene.
Dropping tip: 1. r_e: 0.415 cm.
Induced sonic disturbances: None.
Rest-times: Mean: 3.99, Median: 3.9, 10 percentile: 2.1, 90 percentile: 5.1, Variance: 1.02.
Data-consistency test: Group effect significant at 1% level.
Comments: None.
Rest-times (sec):

Group 1	Group 2	Group 3	Group 4
2.0	5.5	2.9	4.7
4.3	5.1	4.3	4.3
4.9	4.0	1.3	3.5
3.9	5.0	3.5	4.9
2.1	6.5	4.5	3.9
2.7	5.1	3.7	3.1
4.1	5.7	2.9	3.7
4.3	4.9	2.5	3.3
1.9	7.7	3.3	3.5
	5.1	3.7	4.7
	6.7	2.9	5.1
	2.7	1.7	4.7
	4.7	3.9	3.5
	4.5	2.3	

Run No. 10 (3-3-61)

Purpose: Preliminary studies.
Materials: Phase 1: Water.
Phase 2: Distilled benzene.
Dropping tip: 3. r_e: 0.267 cm.
Induced sonic disturbances: None.
Rest-times: Mean: 3.27, Median: 3.1, 10 percentile: 1.9, 90 percentile: 4.7, Variance: 0.98.
Data-consistency test: Group effect not significant at 5% level.
Comments: None.
Rest-times (sec):

Group 1	Group 2	Group 3	Group 4
4.5	3.1	2.3	3.3
3.1	4.7	2.9	1.6
4.0	3.3	3.1	4.9
1.9	3.1	3.1	2.7
4.5	4.7	3.3	3.5
4.7	5.5	1.3	1.9
2.3	4.5	2.7	3.1
4.1	3.0	3.7	2.1
2.7	4.9	3.3	2.9
2.7	3.1	3.5	3.3
2.3	1.9	3.3	5.1
1.5	3.1	2.1	3.5
3.3			
4.3			

Run No. 11 (3-3-61)

Purpose: Preliminary studies.
Materials: Phase 1: Water.
Phase 2: Distilled benzene.
Dropping tip: 1. r_e: 0.415 cm.
Induced sonic disturbances: None.
Rest-times: Mean: 3.97, Median: 3.8, 10 percentile: 1.7, 90 percentile: 5.9, Variance: 2.29.
Data-consistency test: Group effect not significant at 5% level.
Comments: Drops fell 10-15 mm to interface from dropping tip.
Rest-times (sec):

Group 1	Group 2	Group 3	Group 4
3.5	4.3	6.5	5.3
3.8	4.7	7.5	5.1
1.6	3.1	2.9	2.9
1.0	2.9	2.3	2.7
1.7	4.7	6.7	4.3
5.7	3.9	5.9	3.3
5.7	4.5	3.7	4.1
2.1	3.1	2.9	2.9
2.9	5.9	3.5	1.1
5.5	5.9	4.9	4.5
6.1	5.3	2.9	3.3
4.5		6.1	2.1
3.1		4.1	
1.7			

Run No. 12 (3-14-61)

Purpose: Preliminary studies.
Materials: Phase 1: Water.
Phase 2: Benzene.
Dropping tip: 3. r_e: 0.267 cm.
Induced sonic disturbances: None.
Rest-times: Mean: 3.51, Median: 3.5, 10 percentile: 2.3, 90 percentile: 4.5, Variance: 0.83.
Data-consistency test: Group effect significant at 5% level.
Comments: Run made at night to avoid building vibration.
Rest-times (sec):

Group 1	Group 2	Group 3	Group 4
3.5	3.3	2.5	4.3
3.1	3.4	4.5	2.8
1.9	3.7	4.3	3.9
2.9	3.8	3.1	3.5
3.6	5.2	3.7	3.1
2.1	2.3	3.3	5.1
2.7	5.3	2.5	4.4
2.5	3.9	5.0	4.0
3.9	5.3	4.9	2.3
3.5	3.5	3.7	2.5
3.5	4.1		
2.3	3.7		
2.1			
4.5			
2.3			
4.1			
1.5			
4.5			

Run No. 13 (3-15-61)

Purpose: Preliminary studies.
Materials: Phase 1: Water.
Phase 2: Benzene.
Dropping tip: 3. r_e: 0.267 cm.
Induced sonic disturbances: None.
Rest-times: Mean: 3.48, Median: 3.5, 10 percentile: 2.3, 90 percentile: 4.7, Variance: 0.79.
Data-consistency test: Group effect not significant at 5% level.
Comments: Interface was not renewed during run or during 10 hour period preceding run. Run divided into 5 groups.
Rest-times (sec):

Group 1	Group 2	Group 3	Group 4	Group 5
1.5	3.7	4.7	3.1	2.7
4.9	3.5	2.3	3.7	3.9
2.9	3.3	4.1	3.9	2.3
2.8	3.5	3.7	2.9	3.9
5.1	2.8	4.7	2.3	2.5
3.3	3.1	1.3	3.3	4.5
4.1	4.7	3.7	3.7	4.1
3.5	3.1	2.5	3.9	3.3
4.3	3.4	2.9	2.5	3.7
	2.8	4.7		
	3.9			
	4.9			
	4.1			

Run No. 14 (3-15-61)

Purpose: Preliminary studies.
Materials: Phase 1: Water.
Phase 2: Benzene.
Dropping tip: 3. r_e: 0.267 cm.
Induced sonic disturbances: None.
Rest-times: Mean: 3.79, Median: 3.7, 10 percentile: 2.3, 90 percentile: 5.3, Variance: 1.49.
Data-consistency test: Group effect not significant at 5% level.
Comments: None.
Rest-times (sec):

Group 1	Group 2	Group 3	Group 4
2.5	3.7	3.6	3.4
1.9	4.1	4.4	3.7
5.3	4.1	5.5	2.7
2.3	3.5	3.5	3.1
3.3	2.3	4.1	3.4
3.7	3.5	3.9	3.7
2.8	2.1	3.9	2.9
2.0	2.1	4.7	7.1
2.9	3.9	3.6	4.5
6.7	5.3	4.9	2.8
2.3	5.9	5.1	5.1
4.9	3.9	2.3	4.3
	2.9		5.6

Run No. 15 (3-15-61)

Purpose: Preliminary studies.
Materials: Phase 1: Water.
Phase 2: Benzene.
Dropping tip: 7. r_e: 0.349 cm.
Induced sonic disturbances: None.
Rest-times: Mean: 5.32, Median: 5.3, 10 percentile: 3.5, 90 percentile: 6.7, Variance: 1.75.
Data-consistency test: Group effect not significant at 5% level.
Comments: None.
Rest-times (sec):

Group 1	Group 2	Group 3	Group 4
4.3	5.5	5.3	4.7
4.9	5.5	5.5	5.7
4.1	3.7	8.9	5.7
3.3	3.1	6.3	4.9
6.3	8.7	5.5	5.3
6.7	5.9	5.3	7.7
3.9	4.7	4.1	6.5
3.9	5.7	4.9	5.7
4.1	4.3	3.5	7.1
5.4	5.3	6.5	5.5
6.4	6.1	6.3	6.7
7.1	4.5	4.1	4.1
3.5		3.5	

Run No. 16 (3-15-61)

Purpose: Preliminary studies.
Materials: Phase 1: Water.
Phase 2: Benzene.
Dropping tip: 3. r_e: 0.267 cm.
Induced sonic disturbances: None.
Rest-times: Mean: 3.37, Median: 3.3, 10 percentile: 1.9, 90 percentile: 4.9, Variance: 1.52.
Data-consistency test: Group effect not significant at 5% level.
Comments: Drops fell about 10 mm to interface from dropping tip.
Rest-times (sec):

Group 1	Group 2	Group 3	Group 4
4.7	1.9	1.9	3.3
5.1	2.9	4.5	3.1
3.1	4.3	5.9	2.3
3.3	3.5	3.7	3.9
2.7	4.7	5.9	4.9
1.1	3.5	3.9	2.3
2.9	4.1	3.5	2.3
1.9	6.1	2.9	2.9
2.1	3.3	2.9	3.9
1.5	3.5	3.1	4.5
1.5	2.3	4.5	5.5
3.9	2.0	3.5	3.5
	0.6	3.3	

Run No. 17 (3-17-61)

Purpose: Preliminary studies.
Materials: Phase 1: Distilled water.
Phase 2: Benzene.
Dropping tip: 3. r_e: 0.267 cm.
Induced sonic disturbances: None.
Rest-times: Mean: 3.91, Median: 3.7, 10 percentile: 2.9, 90 percentile: 5.1, Variance: 0.82.
Data-consistency test: Group effect not significant at 5% level.
Comments: Drops fell about 10 mm to interface from dropping tip.
Rest-time (sec):

Group 1	Group 2	Group 3	Group 4
3.9	3.3	3.9	3.5
3.9	2.9	5.3	3.7
5.1	3.3	4.7	3.1
4.9	3.5	4.1	3.3
3.0	4.5	6.3	2.7
1.4	3.7	3.3	4.4
3.7	5.5	5.1	3.5
3.5	4.7	3.9	3.9
4.5	4.5	4.1	5.3
4.7	4.1	4.1	3.5
3.1	2.7	2.5	5.1
3.3	2.9	4.9	3.5
3.7		3.5	

Run No. 18 (3-17-61)

Purpose: Preliminary studies.
Materials: Phase 1: Distilled water. Phase 2: Benzene.
Dropping tip: 2. r_e: 0.340 cm.
Induced sonic disturbances: None.
Rest-times: Mean: 4.86, Median: 5.1, 10 percentile: 2.7, 90 percentile: 6.3, Variance: 1.12.
Data-consistency test: Group effect significant at 1% level.
Comments: None.
Rest-time (sec):

Group 1	Group 2	Group 3	Group 4
2.7	3.7	4.5	6.3
4.1	4.7	5.7	5.1
1.3	4.5	3.5	6.1
3.9	6.3	5.3	6.3
3.1	4.3	5.5	6.3
3.4	6.1	4.5	5.5
4.5	4.7	5.9	6.3
4.3	2.3	5.9	5.3
5.1	6.3	5.5	6.5
4.3	4.3	5.9	6.1
6.9	2.7	5.3	5.3
1.9	4.5	4.9	5.5
4.7		5.3	

Run No. 19 (3-17-61)

Purpose: Preliminary studies.
Materials: Phase 1: Distilled water.
Phase 2: Benzene.
Dropping tip: 1. r_e: 0.415 cm.
Induced sonic disturbances: None.
Rest-times: Mean: 6.60, Median: 6.7, 10 percentile: 5.1,
90 percentile: 7.7, Variance: 1.23.
Data-consistency test: Group effect significant at 1% level.
Comments: 75 measurements rather than 50 taken.
Rest-times (sec):

Group 1	Group 2	Group 3	Group 4	Group 5	Group 6
6.7	5.7	7.3	7.3	6.7	7.5
5.3	5.9	10.7	6.5	7.1	6.3
2.9	3.3	7.5	7.1	6.9	7.1
2.9	6.8	8.5	5.1	8.7	5.7
5.6	6.4	8.1	6.7	7.3	8.8
6.0	6.2	4.8	6.7	7.7	7.5
5.1	5.5	7.3	7.1	5.9	7.1
5.1	7.1	7.3	6.7	7.9	5.7
5.8	6.3	8.3	10.0	8.3	6.3
6.0	4.7	6.9	6.3	7.7	7.5
6.2	7.1	6.7	7.1	7.3	5.5
4.9	5.5	6.7	5.5		7.1
6.3		6.3	6.5		
			7.3		

Run No. 20 (3-20-61)

Purpose: Preliminary studies.
Materials: Phase 1: Water.
Phase 2: Research grade benzene.
Dropping tip: 1. r_e: 0.415 cm.
Induced sonic disturbances: None.
Rest-times: Mean: 7.38, Median: 7.1, 10 percentile: 5.1,
90 percentile: 10.6, Variance: 5.23.
Data-consistency test: Group effect not significant at 5% level.
Comments: Drops fell 10-15 mm to interface from dropping tip.
Rest-times (sec):

Group 1	Group 2	Group 3	Group 4
7.7	7.1	12.1	7.9
8.5	7.1	5.9	10.7
7.7	11.7	8.7	10.3
6.7	5.3	7.3	3.7
9.9	3.3	8.5	4.3
8.7	8.7	7.3	5.1
6.9	6.3	7.7	8.4
8.9	1.3	10.3	6.5
8.5	7.1	6.3	5.4
5.2	5.9	5.1	12.3
10.6	5.5	6.9	7.1
5.5	5.1	9.7	5.3
10.8		6.0	

Run No. 21 (3-20-61)

Purpose: Preliminary studies.
Materials: Phase 1: Water.
Phase 2: Research grade benzene.
Dropping tip: 7. r_e: 0.349 cm.
Induced sonic disturbances: None.
Rest-times: Mean: 6.83, Median: 6.7, 10 percentile: 5.1, 90 percentile: 8.1, Variance 1.52.
Data-consistency test: Group effect not significant at 5% level.
Comments: None.
Rest-times (sec):

Group 1	Group 2	Group 3	Group 4
5.7	5.1	6.3	6.9
4.7	6.3	6.7	5.5
6.7	6.3	6.9	8.0
6.3	6.6	6.5	7.5
8.1	8.5	6.9	7.5
9.1	8.1	9.3	5.5
6.3	7.0	8.5	6.0
6.7	5.3	9.3	8.7
5.7	8.1	7.5	7.1
5.9	4.9	5.7	7.3
7.7	4.9	8.1	5.5
8.1	7.7	6.6	5.9
6.9		5.1	

Run No. 22 (3-20-61)

Purpose: Preliminary studies.
Materials: Phase 1: Water.
Phase 2: Research grade benzene.
Dropping tip: 2. r_e: 0.340 cm.
Induced sonic disturbances: None.
Rest-times: Mean: 6.05, Median: 5.7, 10 percentile: 4.3, 90 percentile: 8.1, Variance: 2.94.
Data-consistency test: Group effect not significant at 5% level.
Comments: None.
Rest-times (sec):

Group 1	Group 2	Group 3	Group 4
8.1	7.7	7.1	9.1
6.7	5.8	4.9	4.4
4.1	5.9	4.9	4.2
5.7	4.9	6.5	5.7
8.5	7.9	7.3	6.1
9.1	5.5	5.7	4.3
3.5	6.5	5.5	5.5
1.3	5.1	7.6	5.5
10.9	4.5	6.1	4.5
6.7	6.3	5.9	5.3
5.5	7.5	4.5	7.1
5.5	4.3	5.3	8.1
8.3		5.4	

Run No. 23 (6-1-61)

Purpose: Sonic disturbances (telephone speaker).
Materials: Phase 1: Water.
Phase 2: Benzene.
Dropping tip: 3. r_e: 0.267 cm.
Induced sonic disturbances: None.
Rest-times: Mean: 3.99, Median: 3.9, 10 percentile: 2.6,
90 percentile: 5.7, Variance: 1.64.
Data-consistency test: Group effect not significant at 5% level.
Comments: None.
Rest-times (sec):

Group 1	Group 2	Group 3	Group 4
5.1	3.8	4.5	4.9
3.3	4.4	3.3	3.7
4.3	3.7	5.6	3.7
3.7	3.5	5.3	3.7
2.7	2.5	4.1	5.5
5.7	5.7	6.1	1.5
2.9	2.6	4.5	2.5
2.5	2.9	4.5	4.3
4.1	5.5	6.1	4.7
2.5	1.1	4.0	5.9
2.7	5.7	3.7	3.9
0.9	6.1	2.7	3.7
3.8		5.5	

Run No. 24 (6-1-61)

Purpose: Sonic disturbances (telephone speaker).
Materials: Phase 1: Water.
Phase 2: Benzene.
Dropping tip: 3. r_e: 0.267 cm.
Induced sonic disturbances: 500 cps, 398 dynes/cm^2 rms sound pressure.
Rest-times: Mean: 3.62, Median: 3.7, 10 percentile: 2.3,
90 percentile: 4.9, Variance: 0.87.
Data-consistency test: Group effect not significant at 5% level.
Comments: None.
Rest-times (sec):

Group 1	Group 2	Group 3	Group 4
4.3	5.1	4.0	4.9
3.5	3.3	2.3	3.7
4.1	3.7	2.0	3.7
2.9	3.1	4.1	3.7
3.5	4.7	4.7	5.5
2.3	3.9	3.7	1.5
4.7	2.9	2.7	2.5
5.7	4.1	3.3	4.3
3.7	3.9	2.9	4.7
2.9	2.3	2.7	5.9
2.7	3.3	3.3	3.9
4.0	3.7	3.2	3.7
2.9		2.8	

Run No. 25 (6-2-61)

Purpose: Sonic disturbances (telephone speaker).
Materials: Phase 1: Water.
Phase 2: Benzene.
Dropping tip: 3. r_e: 0.267 cm.
Induced sonic disturbances: None.
Rest-times: Mean: 5.29, Median: 4.9, 10 percentile: 2.9, 90 percentile: 7.3, Variance: 1.96.
Data-consistency test: Group effect significant at 1% level.
Comments: None.
Rest-times (sec):

Group 1	Group 2	Group 3	Group 4
3.6	6.9	4.5	2.9
2.7	3.9	4.7	5.5
2.7	6.1	3.9	4.9
4.3	4.9	6.7	7.1
4.1	6.5	8.3	4.7
3.9	7.7	6.9	4.2
4.7	7.7	7.3	6.3
4.8	3.7	6.7	4.1
2.9	2.1	5.1	7.2
6.3	6.5	5.5	6.6
3.6	6.5	4.7	4.5
4.4	6.3	6.3	7.9
4.7		6.3	

Run No. 26 (6-2-61)

Purpose: Sonic disturbances (telephone speaker).
Materials: Phase 1: Water.
Phase 2: Benzene.
Dropping tip: 3. r_e: 0.267 cm.
Induced sonic disturbances: 100 cps, 4.6 dynes/cm^2 runs sound pressure.
Rest-times: Mean: 5.56, Median: 5.3, 10 percentile: 3.9, 90 percentile: 7.1, Variance: 1.61.
Data-consistency test: Group effect not significant at 5% level.
Comments: None.
Rest-times (sec):

Group 1	Group 2	Group 3	Group 4
6.7	6.3	4.3	6.1
7.9	6.3	5.1	6.1
4.5	3.7	7.0	5.3
3.9	6.9	4.2	4.9
3.7	6.7	6.7	6.3
5.1	5.1	4.7	3.3
2.7	7.1	7.3	6.6
7.2	4.3	4.3	4.5
7.7	6.7	5.7	4.7
5.1	5.1	6.7	5.9
4.3	5.1	5.1	5.3
6.3	5.3	7.3	4.1
	6.9	6.1	

Run No. 27 (6-2-61)

Purpose: Sonic disturbances (telephone speaker).
Materials: Phase 1: Water.
Phase 2: Benzene.
Dropping tip: 3. r_e: 0.267 cm.
Induced sonic disturbances: None.
Rest-times: Mean: 4.91, Median: 4.8, 10 percentile: 3.5, 90 percentile: 6.3, Variance: 0.73.
Data-consistency test: Group effect significant at 5% level.
Comments: Only 20 measurements in two groups made.
Rest-times (sec):

Group 1	Group 2
6.5	3.5
5.3	3.3
6.3	5.7
5.5	5.5
5.7	3.5
6.7	4.8
5.1	4.8
4.7	4.5
4.1	3.9
4.5	4.3

Run No. 28 (6-5-61)

Purpose: Drop aging.
Materials: Phase 1: Water.
Phase 2: Benzene.
Dropping tip: 3. r_e: 0.267 cm.
Induced sonic disturbances: None.
Comments: An attempt to analyze data as a completely randomized design was unsuccessful. Each drop was aged for period indicated below before release from dropping tip.
Rest-times (sec):

Aged 0 sec	Aged 15 sec		Aged 1 1/2 min	Aged 2 min
3.9	2.0	4.7	6.1	6.0
2.0	4.1	4.9	6.3	5.1
2.8	3.3	5.2	5.1	5.6
1.1	3.3	3.9	5.1	3.9
2.0	1.1	5.2	2.7	3.7
2.1	4.6	4.9	5.6	4.7
3.7	2.7	4.5	5.7	7.8
2.1	1.7	2.4	6.1	6.4
4.6	4.4	5.1	6.1	5.2
2.7	2.1	4.9	5.7	5.6
2.0	1.5	4.1	2.7	4.1
4.0	5.2	5.3	4.5	6.6
4.0	4.1	4.1		5.4
	4.9	3.9		1.5
				4.4

Run No. 29 (6-6-61)

Purpose: Drop aging.
Materials: Phase 1: Water.
Phase 2: Benzene.
Dropping tip: 3. r_e: 0.267 cm.
Induced sonic disturbances: None.
Comments: Data analyzed as randomized block design. Data and analysis are given in Appendix A-3.

Run Nos. 30 and 33 (6-13-61)

Purpose: Sonic disturbances (telephone speaker).
Materials: Phase 1: Water.
Phase 2: Benzene.
Dropping tip: 3. r_e: 0.267 cm.
Induced sonic disturbances: None.
Rest-times: Mean: 4.79, Median: 4.8, 10 percentile: 3.0, 90 percentile: 6.1, Variance 1.32.
Data-consistency test: Group effect not significant at 5% level.
Comments: None.
Rest-times (sec):

Run 30		Run 33	
Group 1	Group 2	Group 3	Group 4
3.0	7.1	3.3	2.3
4.8	4.7	5.5	6.4
1.5	4.1	5.3	5.5
4.2	4.9	5.9	4.7
3.3	4.0	5.5	5.7
4.5	4.4	4.9	3.7
4.4	6.1	5.1	6.3
5.7	4.5	5.7	4.9
1.5	4.9	4.7	5.3
5.7	4.7	4.1	4.3
2.7	6.3	4.6	5.8
6.2	4.7	5.5	5.9
4.7		6.1	

Run No. 31 (6-13-61)

Purpose: Sonic disturbances (telephone speaker).
Materials: Phase 1: Water.
Phase 2: Benzene.
Dropping tip: 3. r_e: 0.267 cm.
Induced sonic disturbances: 500 cps, 398 dynes/cm^2 rms sound pressure.
Rest-times: Mean: 5.87, Median: 5.9, 10 percentile: 3.4, 90 percentile: 8.3, Variance: 2.70.
Data-consistency test: Group effect significant at 5% level.
Comments: None.
Rest-times (sec):

Group 1	Group 2	Group 3	Group 4
3.7	3.1	7.5	6.3
3.4	7.0	5.5	7.3
2.9	6.1	4.5	6.5
3.8	8.5	6.9	4.5
5.9	8.3	6.5	9.3
5.1	6.3	4.8	9.1
6.4	5.0	5.6	3.3
6.3	5.9	7.7	3.4
5.1	3.5	5.3	7.2
5.1	5.3	7.2	8.7
6.1	4.8	7.7	8.9
5.1	4.3	8.9	5.9
3.1		4.7	

Run No. 32 (6-13-62)

Purpose: Sonic disturbances (telephone speaker).
Materials: Phase 1: Water.
Phase 2: Benzene.
Dropping tip: 3. r_e: 0.267 cm.
Induced sonic disturbances: 250 cps, 152 dynes/cm^2 rms sound pressure.
Rest-times: Mean: 7.05, Median: 6.9, 10 percentile: 4.1, 90 percentile: 9.3, Variance: 3.34.
Data-consistency test: Group effect significant at 5% level.
Comments: None.
Rest-times (sec):

Group 1	Group 2	Group 3	Group 4
6.5	8.8	6.9	11.3
2.5	7.3	6.1	10.0
7.5	7.9	7.2	8.9
5.3	7.7	10.3	9.0
3.5	5.5	7.8	5.1
9.0	6.7	7.8	7.0
6.9	6.1	8.7	8.5
6.5	7.5	6.6	8.8
7.7	9.3	6.6	8.0
4.1	6.5	7.3	10.8
4.7	9.3	5.5	3.0
6.8	6.8	4.1	5.3
6.3		5.3	

Run Nos. 34 and 37 (6-14-61)

Purpose: Sonic disturbances (telephone speaker).
Materials: Phase 1: Water.
Phase 2: Benzene.
Dropping tip: 3. r_e: 0.267 cm.
Induced sonic disturbances: 500 cps, 398 dynes/cm^2 rms sound pressure.
Rest-times: Mean: 6.15, Median: 6.1, 10 percentile: 3.5,
90 percentile: 8.1, Variance: 2.71.
Data-consistency test: Group effect not significant at 5% level.
Comments: None.
Rest-times (sec):

Run 34		Run 37	
Group 1	Group 2	Group 3	Group 4
4.9	5.2	7.9	5.6
5.2	6.0	5.1	5.7
6.8	6.3	6.7	4.7
6.1	3.5	4.6	6.9
5.4	9.2	6.0	7.7
3.3	6.5	4.2	3.4
4.6	7.1	7.4	8.5
7.6	7.6	6.7	5.8
5.7	2.9	6.0	8.3
6.3	2.7	7.3	10.9
3.9	4.8	6.4	7.8
5.0	6.7	8.6	7.5
6.2		8.1	

Run No. 35 (6-14-61)

Purpose: Sonic disturbances (telephone speaker).
Materials: Phase 1: Water.
Phase 2: Benzene.
Dropping tip: 3. r_e: 0.267 cm.
Induced sonic disturbances: 500 cps, 398 dynes/cm^2 rms sound pressure.
Rest-times: Mean: 5.08, Median: 5.2, 10 percentile: 3.3,
90 percentile: 6.5, Variance: 1.24.
Data-consistency test: Group effect not significant at 5% level.
Comments: None.
Rest-times (sec):

Group 1	Group 2	Group 3	Group 4
4.7	6.9	5.0	5.3
4.5	5.5	5.9	4.1
6.3	4.7	5.3	4.8
3.3	7.5	3.3	5.7
4.1	3.9	6.0	5.5
4.1	3.6	6.0	6.0
6.5	6.1	4.9	5.5
4.3	3.3	5.7	5.3
5.2	6.1	5.3	6.5
4.9	6.9	3.5	4.3
4.0	6.7	2.3	5.1
5.4	5.1	2.9	5.1
5.1		5.8	

Run No. 36 (6-14-61)

Purpose: Sonic disturbances (telephone speaker).
Materials: Phase 1: Water.
Phase 2: Benzene.
Dropping tip: 3. r_e: 0.267 cm.
Induced sonic disturbances: 2500 cps, 23.9 dynes/cm^2 rms sound pressure.
Rest-times: Mean: 5.31, Median: 5.5, 10 percentile: 4.0,
90 percentile: 6.5, Variance: 0.84.
Data-consistency test: Group effect not significant at 5% level.
Comments: None.

Rest-times (sec):

Group 1	Group 2	Group 3	Group 4
3.7	5.2	3.8	3.0
6.0	4.8	6.5	6.4
6.2	7.4	5.7	4.4
7.0	5.6	5.8	3.5
7.1	5.7	5.5	4.5
4.1	5.6	5.4	4.4
5.5	4.8	4.5	6.1
7.0	5.4	5.6	6.0
5.5	4.0	5.4	4.8
5.5	5.4	4.6	4.7
6.3	5.2	5.0	5.9
5.7	5.0	5.0	5.5
5.7		4.3	

Run. Nos. 38 & 41(7-13-61)

Purpose: Sonic disturbances.
Materials: Phase 1: Water.
Phase 2: Benzene.
Dropping tip: 3
r_e: 0.267 cm.
Induced sonic disturbances: None.
Rest-times: Mean: 5.12, Median: 5.1, 10 percentile: 3.8, 90 percentile: 6.4, Variance: 0.70.
Data-consistency test: Group effect not significant at 5% level.
Comments: None.
Rest-times(sec):

Run 38		Run 41	
Group 1	Group 2	Group 3	Group 4
4.1	6.1	5.3	5.8
4.4	5.7	5.6	5.3
5.4	6.4	5.1	4.9
4.6	4.0	4.9	6.5
4.6	4.5	3.8	5.3
4.3	5.2	5.7	3.5
4.7	4.8	3.8	5.1
2.9	5.0	4.5	5.4
6.5	5.7	5.7	6.5
5.2	5.7	5.9	5.8
5.1	7.4	3.7	4.8
5.5	5.3	5.1	4.9
5.2		5.0	

Run No. 39 (7-13-61)

Purpose: Sonic disturbances.
Materials: Phase 1: Water.
Phase 2: Benzene.
Dropping tip: 3.
r_e: 0.267 cm.
Induced sonic disturbances: 500 cps, 25.5 dynes/cm^2 rms sound pressure.
Rest-times: Mean: 4.79, Median: 5.2, 10 percentile: 2.3, 90 percentile: 6.5, Variance: 1.89.
Data-consistency test: Group effect significant at 1% level.
Comments: None.

Rest-times (sec):

Group 1	Group 2	Group 3	Group 4
2.3	6.7	6.0	4.2
2.0	3.5	5.3	3.6
1.3	4.8	5.3	5.7
3.3	5.5	7.0	5.2
2.6	4.3	6.5	3.2
2.0	5.1	6.0	4.5
2.3	2.7	5.5	5.7
3.5	6.8	4.5	6.2
4.7	4.0	3.9	5.7
4.9	7.0	4.7	5.7
6.1	6.5	6.4	3.7
6.1	5.3	6.2	2.7
6.9		6.1	

Run No. 40 (7-13-61)

Purpose: Sonic disturbances.
Materials: Phase 1: Water.
Phase 2: Benzene.
Dropping tip: 3.
r_e: 0.267 cm.
Induced sonic disturbances: 500 cps, 125 dynes/cm^2 rms sound pressure.
Rest-times: Mean 4.60, Median: 4.8, 10 percentile: 2.8,
90 percentile: 6.1, Variance: 1.74.
Data-consistency test: Group effect not significant at 5% level.
Comments: None.

Rest-times (sec):

Group 1	Group 2	Group 3	Group 4
2.8	5.1	2.9	5.5
4.9	6.3	6.3	4.5
4.6	3.5	2.1	4.2
0	5.7	5.7	3.5
1.7	6.3	6.4	4.1
3.5	5.5	4.7	4.6
6.0	6.7	2.5	4.3
3.6	5.3	3.1	5.6
5.7	4.9	4.1	5.9
5.9	4.9	3.8	5.0
4.9	4.1	4.2	4.7
4.8	6.1	3.2	4.9
5.6		6.0	

Run. Nos. 42 & 45 (7-14-61)

Purpose: Sonic disturbances.
Materials: Phase 1: Water.
Phase 2: Benzene.
Dropping tip: 3.
r_e: 0.267 cm.
Induced sonic disturbances: 500 cps, 25.5 dynes/cm^2 rms sound pressure
Rest-times: Mean: 5.84, Median: 5.8, 10 percentile: 3.9,
90 percentile: 7.2, Variance: 2.10.
Data-consistency test: Group effect not significant at 5% level.
Comments: None.
Rest-times (sec):

Run 42		Run 45	
Group 1	Group 2	Group 3	Group 4
5.7	5.7	6.3	5.7
6.1	3.9	5.6	3.5
6.6	7.2	4.1	5.1
6.9	7.4	2.9	4.3
8.7	7.5	5.4	5.3
4.9	11.3	5.8	6.1
4.3	6.9	5.9	6.5
6.7	6.7	5.5	6.0
6.9	8.4	4.0	6.6
4.1	3.6	4.5	5.5
6.4	4.5	6.0	6.1
3.8	6.9	4.6	5.7
6.9		7.2	

Run No. 43 (7-14-61)

Purpose: Sonic disturbances.
Materials: Phase 1: Water.
Phase 2: Benzene.
Dropping tip: 3.
r_e: 0.267 cm.
Induced sonic disturbances: 50 cps, 18.4 dynes/cm^2 rms sound pressure.
Rest-times: Mean: 6.22, Median: 6.4, 10 percentile: 4.7,
90 percentile: 7.7, Variance: 1.34.
Data-consistency test: Group effect significant at 5% level.
Comments: None.

Rest-times (sec):

Group 1	Group 2	Group 3	Group 4
5.4	7.1	7.5	5.6
7.3	6.4	7.1	7.7
5.2	7.9	5.4	5.8
5.5	6.5	3.1	4.9
6.1	6.0	8.0	7.8
6.1	6.0	6.4	6.9
3.5	6.6	4.9	5.0
6.2	6.4	5.6	6.4
4.1	6.5	6.7	5.9
4.7	8.7	7.3	7.2
6.7	9.3	5.8	5.3
6.9	6.7	4.1	6.6
5.9		6.5	

Run No. 44 (7-14-61)

Purpose: Sonic disturbances.
Materials: Phase 1: Water.
Phase 2: Benzene.
Dropping tip: 3.
r_e: 0.267 cm.
Induced sonic disturbances: 250 cps, 40 dynes/cm^2 rms sound pressure.
Rest-times: Mean: 5.45, Median: 5.5, 10 percentile: 3.2,
90 percentile: 7.1, Variance: 1.73.
Data-consistency test: Group effect significant at 5% level.
Comments: None.

Rest-times (sec):

Group 1	Group 2	Group 3	Group 4
6.3	4.9	6.8	5.5
3.1	2.9	6.0	5.9
2.3	5.5	6.9	5.3
6.4	5.5	6.0	5.2
4.1	5.2	6.7	5.7
5.5	7.3	6.3	3.2
3.2	8.8	6.3	5.1
6.1	3.6	7.1	5.1
5.3	8.0	7.1	5.7
4.2	6.7	4.6	4.2
4.5	8.5	5.8	4.7
5.1	5.1	4.1	5.5
5.4		4.0	

Run Nos. 46 & 49(7-17-61)

Purpose: Sonic disturbances.
Materials: Phase 1: Water.
Phase 2: Benzene.
Dropping tip: 3.
r_e: 0.267 cm.
Induced sonic disturbances: 50 cps, 18.4 dynes/cm^2 rms sound pressure.
Rest-times: Mean: 7.35, Median: 7.6, 10 percentile: 5.0,
90 percentile: 9.3, Variance: 2.76.
Data-consistency test: Group effect significant at 5% level.
Comments: None.

Rest-times (sec):

Run 46		Run 49	
Group 1	Group 2	Group 3	Group 4
4.1	7.4	9.9	4.3
8.7	9.9	3.8	7.0
9.9	5.1	8.4	7.1
8.1	6.3	6.7	5.0
7.7	8.8	5.2	8.6
10.1	6.0	7.0	4.0
8.9	7.9	6.9	6.9
8.7	9.3	7.7	6.5
7.9	8.8	6.0	6.7
11.6	5.5	6.1	7.8
9.0	7.9	7.5	3.4
7.6	8.3	8.1	9.0
8.2		6.1	

Run No. 47 (7-17-61)

Purpose: Sonic disturbances.
Materials: Phase 1: Water.
Phase 2: Benzene.
Dropping tip: 3.
r_e: 0.267 cm.
Induced sonic disturbances: 738 cps, 15.3 dynes/cm^2 rms sound pressure.
Rest-times: Mean: 5.21, Median: 5.2, 10 percentile: 4.1,
90 percentile: 6.1, Variance: 0.71.
Data-consistency test: Group effect not significant at 5% level.
Comments: None.

Rest-times (sec):

Group 1	Group 2	Group 3	Group 4
6.3	1.9	4.5	5.7
5.1	5.9	6.8	4.4
5.3	5.8	5.6	5.8
4.6	4.1	4.5	4.5
4.6	4.4	4.1	5.6
5.9	4.1	5.9	5.2
6.2	5.8	6.1	5.8
6.1	5.2	6.6	5.2
6.5	4.9	5.2	5.1
3.9	4.7	5.6	5.3
6.1	5.1	5.5	5.7
4.7	5.1	5.7	4.6
4.7		4.7	

Run No. 48 (7-17-61)

Purpose: Sonic disturbances.
Materials: Phase 1: Water.
Phase 2: Benzene.
Dropping tip: 3.
r_e: 0.267 cm.
Induced sonic disturbances: 2095 cps, 85 dynes/ cm^2 rms sound pressure.
Rest-times: Mean: 5.90, Median: 5.8, 10 percentile: 4.3,
90 percentile: 7.7, Variance: 1.46.
Data-consistency test: Group effect not significant at 5% level.
Comments: None.

Rest-times (sec):

Group 1	Group 2	Group 3	Group 4
7.8	6.3	4.1	7.5
5.8	5.7	7.7	5.3
6.9	5.3	4.5	7.3
4.3	4.3	5.9	6.4
6.5	5.5	4.9	6.1
5.7	5.2	6.5	3.9
6.1	4.3	5.5	5.9
5.7	5.0	6.3	6.2
7.3	5.3	7.7	4.7
4.1	6.1	8.3	5.7
5.7	7.5	4.5	6.6
6.2	8.1	6.0	5.5
7.7		3.7	

Run Nos. 50 & 53 (7-19-61)

Purpose: Sonic disturbances.
Materials: Phase 1: Water.
Phase 2: Benzene.
Dropping tip: 3.
r_e: 0.267 cm.
Induced sonic disturbances: 738 cps, 15.3 dynes/cm^2 rms sound pressure.
Rest-times: Mean: 5.67, Median: 5.6, 10 percentile: 4.1,
90 percentile: 7.0, Variance: 1.58.
Data-consistency test: Group effect not significant at 5% level.
Rest-times (sec):

Run 50		Run 53	
Group 1	Group 2	Group 3	Group 4
4.8	6.2	5.4	5.0
4.8	6.8	5.2	6.7
6.5	3.1	5.3	5.1
4.9	6.7	6.1	4.5
4.9	7.6	4.3	7.0
4.8	6.1	9.5	6.2
6.5	6.0	4.0	5.3
6.3	3.2	5.4	6.4
6.3	6.7	5.0	4.5
6.5	5.4	7.2	4.4
4.5	6.5	5.8	3.9
3.3	7.0	7.0	7.1
6.1		5.6	

Run No. 51 (7-19-61)

Purpose: Sonic disturbances.
Materials: Phase 1: Water.
Phase 2: Benzene.
Dropping tip: 3.
r_e: 0.267 cm.
Induced sonic disturbances: 50 cps, 3.4 dynes/cm^2 rms sound pressure.
Rest-times: Mean: 5.86, Median: 5.9, 10 percentile: 4.7, 90 percentile: 6.7, Variance: 1.08.

Data-consistency test: Group effect significant at 5% level.
Comments: None.
Rest-times (sec):

Group 1	Group 2	Group 3	Group 4
5.7	9.5	6.4	6.5
5.7	6.6	2.1	8.0
5.5	5.4	6.0	3.8
5.2	6.3	5.1	7.0
5.3	5.8	5.2	4.7
5.1	6.3	5.1	5.7
5.5	6.0	5.9	7.4
6.2	5.9	6.2	5.2
4.0	6.7	5.1	6.5
6.7	6.5	4.3	5.4
6.7	6.0	5.2	7.2
5.3	6.7	6.2	6.4
6.0		5.7	

Run No. 52 (7-19-61)

Purpose: Sonic disturbances.
Materials: Phase 1: Water.
Phase 2: Benzene.
Dropping tip: 3.
r_e: 0.267 cm.
Induced sonic disturbances: None.
Rest-times: Mean: 5.87, Median: 5.8, 10 percentile: 4.5, 90 percentile: 6.9, Variance: 0.91.

Data-consistency test: Group effect not significant at 5% level.
Comments: None.

Rest-times (sec):

Group 1	Group 2	Group 3	Group 4
6.6	5.9	4.9	5.7
4.7	6.9	4.9	6.7
8.5	6.2	7.3	5.6
4.1	6.0	5.8	6.7
6.7	5.5	6.3	6.3
5.3	5.5	5.5	5.3
6.4	6.3	5.3	3.9
6.2	5.6	6.1	6.1
6.8	6.1	7.3	7.0
5.6	4.7	6.8	4.5
4.3	4.4	5.6	6.9
5.2	5.6	6.0	5.5
7.0		5.3	

Run No. 54 (9-26-61)

Purpose: Sonic disturbances.
Materials: Phase 1: TBP.
Phase 2: Water.
Dropping tip: 3.
r_e: 0.325 cm.

Induced sonic disturbances: None.
Rest-times: Mean: 9.87, Median: 7.4, 10 percentile: 5.3, 90 percentile: 19.6, Variance: 32.55.
Data-consistency test: Group effect not significant at 5% level.
Comments: None.

Rest-times (sec):

Group 1	Group 2	Group 3	Group 4
10.8	9.5	22.5	10.5
15.2	4.7	6.3	28.0
7.5	8.2	7.5	6.9
7.0	4.5	7.4	11.7
6.0	19.6	23.2	5.5
13.5	19.0	6.7	10.4
10.5	7.3	6.5	22.9
7.7	7.2	10.3	6.6
8.7	6.2	7.2	10.1
4.9	4.6	5.5	8.7
6.7	7.1	7.3	9.7
7.7	7.1	21.8	6.3
7.3		5.3	

Run No. 55 (9-26-61)

Purpose: Sonic disturbances.
Materials: Phase 1: TBP.
Phase 2: Water.
Dropping tip: 3.
r_e: 0.325 cm.

Induced sonic disturbances: 110 cps, 260 dynes/cm^2 rms sound pressure.
Rest-times: Mean: 9.67, Median: 7.9, 10 percentile: 4.2, 90 percentile: 16.2, Variance: 41.92.
Data-consistency test: Group effect not significant at 5% level.
Comments: None.

Rest-times (sec):

Group 1	Group 2	Group 3	Group 4
4.7	15.6	11.9	9.9
9.3	4.9	7.9	5.9
3.8	9.7	5.3	8.9
11.7	10.3	9.5	9.1
6.2	15.8	4.9	12.2
11.1	7.8	4.6	9.5
23.8	4.5	4.1	11.5
3.9	10.4	5.1	7.9
11.3	8.5	4.4	7.5
16.2	4.2	14.0	6.3
5.4	17.1	24.6	16.9
6.3	3.1	5.7	38.7
5.8		5.7	

Run No. 56 (9-26-61)

Purpose: Sonic disturbances.
Materials: Phase 1: TBP.
Phase 2: Water.
Dropping tip: 3.
r_e: 0.325 cm.
Induced sonic disturbances: 500 cps, 135 dynes/cm^2 rms sound pressure.
Rest-times: Mean: 6.23, Median: 5.7, 10 percentile: 4.7, 90 percentile: 8.5, Variance: 2.34.
Data-consistency test: Group effect significant at 1% level.
Comments: None

Rest-times (sec):

Group 1	Group 2	Group 3	Group 4
8.9	13.3	5.1	5.1
8.5	6.1	5.8	4.7
6.3	5.4	5.2	6.3
6.1	7.9	5.5	6.4
4.4	7.4	8.1	4.9
5.6	7.7	5.1	2.6
5.3	9.1	7.8	5.1
6.3	8.6	5.0	5.5
4.2	7.5	5.7	5.7
5.8	6.1	7.4	5.1
4.1	5.1	7.3	5.4
6.2	9.7	5.1	5.5
4.7		5.7	

Run No. 57 (10-3-61)

Purpose: Sonic disturbances.
Materials: Phase 1: TBP.
Phase 2: Water.
Dropping tip: 3.
r_e: 0.325 cm.
Induced sonic disturbances: 500 cps, 135 dynes/ cm^2 rms sound pressure.
Rest-times: Mean: 4.63, Median: 3.7, 10 percentile: 3.1, 90 percentile: 6.5, Variance: 3.56.
Data-consistency test: Group effect significant at 1% level.
Comments: Contamination in Groups 3 and 4.

Rest-times (sec):

Group 1	Group 2	Group 3	Group 4
3.5	3.9	3.1	3.3
10.2	3.1	3.5	3.1
4.7	5.3	3.8	3.5
2.7	5.9	3.7	3.4
5.8	5.2	3.7	3.3
2.8	4.9	3.9	3.3
5.4	4.1	3.3	3.3
10.0	7.4	3.4	3.5
5.7	14.5	3.9	3.0
6.5	8.0	3.5	3.3
5.5	5.7	3.5	3.4
4.1	6.0	3.3	3.2
4.7		3.5	

Run No. 58 (10-3-61)

Purpose: Sonic disturbances.
Materials: Phase 1: TBP.
Phase 2: Water.
Dropping tip: 3.
r_e: 0.325 cm.
Induced sonic disturbances: White noise.
Rest-times: Mean: 3.63, Median: 3.5, 10 percentile: 3.2, 90 percentile: 4.5, Variance: 0.47.
Data-consistency test: Group effect not significant at 5% level.
Comments: Contamination in all 4 groups.

Rest-times (sec):

Group 1	Group 2	Group 3	Group 4
4.5	3.7	3.5	3.2
4.5	0.1	3.4	3.5
4.5	3.9	3.3	3.3
3.3	4.3	3.5	3.3
4.5	4.0	3.3	3.2
4.3	4.1	3.6	3.4
4.5	3.8	3.3	3.5
2.1	3.8	3.7	3.3
4.5	4.1	3.7	3.3
4.5	4.0	3.5	3.3
3.0	4.3	3.5	3.3
4.1	3.6	3.5	3.1
4.4		3.8	

Run No. 59 (10-3-61)

Purpose: Sonic disturbances.
Materials: Phase 1: TBP.
Phase 2: Water.
Dropping tip: 3.
r_e: 0.325 cm.
Induced sonic disturbances: 200 cps, 29 dynes/cm^2 rms sound pressure.
Rest-times: Mean: 4.23, Median: 3.6, 10 percentile: 2.8, 90 percentile: 6.5, Variance: 2.10.
Data-consistency test: Group effect significant at 1% level.
Comments: Contamination in Groups 3 and 4.

Rest-times (sec):

Group 1	Group 2	Group 3	Group 4
6.3	5.3	2.8	3.6
6.5	5.1	3.1	3.8
6.5	5.3	3.2	3.6
6.8	5.5	3.1	3.5
6.0	0	2.9	3.7
8.1	5.4	3.1	3.3
7.8	4.7	3.2	3.5
5.9	4.3	2.8	3.5
6.9	4.7	3.0	3.7
1.3	4.7	3.2	3.3
5.6	4.5	3.2	3.5
0	4.4	3.2	3.1
8.1		3.1	

Run No. 60 (10-5-61)

Purpose: Sonic disturbances.
Materials: Phase 1: TBP.
Phase 2: Water.
Dropping tip: 3.
r_e: 0.325 cm.
Induced sonic disturbances: 500 cps, 135 dynes/ cm^2 rms sound pressure.
Rest-times: Mean: 24.15, Median: 24.1, 10 percentile: 7.3, 90 percentile: 41.0, Variance: 79.96.
Data-consistency test: Group effect significant at 1 % level.
Comments: Contamination. Only 25 measurements in two groups were made.

Rest-times (sec):

Group 1	Group 2
48.2	5.5
28.3	8.6
23.4	7.3
26.7	9.5
24.1	9.5
35.1	10.0
32.8	12.3
43.7	41.0
30.1	38.0
22.0	32.7
26.7	11.5
34.6	12.7
37.1	

Run No. 61 (10-10-61)

Purpose: Sonic disturbances.
Materials: Phase 1: TBP.
Phase 2: Water.
Dropping tip: 3.
r_e: 0.325 cm.
Induced sonic disturbances: 500 cps, 135 dynes/cm^2 rms sound pressure.
Rest-times: Mean: 16.2, Median: 12.1, 10 percentile: 0.1, 90 percentile: 33.3, Variance: 167.74.
Data-consistency test: Group effect not significant at 5% level.
Comments: Meniscus concave upwards. Data erratic because many drops struck side of cell.

Rest-times (sec):

Group 1	Group 2	Group 3	Group 4
0	4.8	0.1	26.1
10.5	14.1	38.4	20.1
34.6	30.9	35.8	36.4
0	25.9	3.9	15.3
24.1	29.9	32.3	9.4
8.9	15.0	1.3	33.4
0.1	12.1	7.7	0.6
0	23.3	26.4	33.3
14.9	2.1	28.0	11.3
17.7	8.7	47.0	10.1
13.0	1.2	10.3	8.3
28.3	24.3	3.3	6.5
11.3		3.8	

Run No. 62(10-10-61)

Purpose: Sonic disturbances.
Materials: Phase 1: TBP.
Phase 2: Water.
Dropping tip: 3.
r_e: 0.325 cm.
Induced sonic disturbances: White noise.
Rest-times: Mean: 7.01, Median: 4.6, 10 percentile: 1.0,
90 percentile: 13.7, Variance: 36.74.
Data-consistency test: Group effect not significant at 5% level.
Comments: None.

Rest-times: (sec):

Group 1	Group 2	Group 3	Group 4
10.5	14.8	6.2	1.0
13.7	6.9	0.7	1.3
3.4	1.0	3.3	1.1
7.1	9.1	30.2	2.3
36.3	7.0	3.3	0.6
9.2	12.5	2.0	3.5
1.5	8.1	11.7	3.4
2.9	18.1	3.4	11.4
0.2	1.9	10.7	3.6
11.0	2.0	2.5	6.1
0.6	3.5	20.8	4.6
5.8	4.9	8.7	1.9
5.7		8.5	

Run No. 63 (10-10-61)

Purpose: Sonic disturbances.
Materials: Phase 1: TBP.
Phase 2: Water.
Dropping tip: 3.
r_e: 0.325 cm.
Induced sonic disturbances: 200 cps, 29 dynes/cm^2 rms sound pressure.
Rest-times: Mean: 12.72, Median: 8.8, 10 percentile: 1.3,
90 percentile: 30.1, Variance: 143.75.
Data-consistency test: Group effect significant at 1% level.
Comments: Meniscus concave upwards. Data erratic because many drops struck side of cell.

Rest-times (sec):

Group 1	Group 2	Group 3	Group 4
6.9	8.3	1.3	12.7
65.7	27.1	2.9	2.3
13.0	22.6	3.3	2.6
8.9	10.5	2.7	0
1.4	59.7	2.7	1.7
11.7	8.8	2.8	25.2
10.7	25.3	7.5	5.4
10.3	23.3	5.1	1.5
25.4	23.7	2.8	1.4
14.2	14.4	13.9	0.1
10.1	17.4	1.3	0.1
30.1	38.4	11.3	0.1
36.0		1.5	

Run No. 64 (10-12-61)

Purpose: Sonic disturbances.
Materials: Phase 1: TBP.
Phase 2: Water.
Dropping tip: 3.
r_e: 0.325 cm.

Induced sonic disturbances: White noise.
Rest-times: Mean: 6.30, Median: 6.1, 10 percentile: 1.6,
90 percentile: 10.2, Variance: 4.71.
Data-consistency test: Group effect significant at 1% level.
Comments: None.

Rest-times (sec):

Group 1	Group 2	Group 3	Group 4
0.7	7.7	7.6	1.6
10.2	6.5	6.5	4.1
6.1	9.0	5.1	3.9
9.4	0	7.1	1.6
9.9	5.4	5.5	5.4
8.1	5.3	7.6	3.7
8.8	5.8	4.1	5.3
11.1	4.7	6.2	5.5
9.8	4.5	6.9	0
10.3	5.3	6.7	5.1
11.3	6.7	7.9	2.7
11.5	5.5	5.2	6.5
10.7		8.9	

Run No. 65 (10-12-61)

Purpose: Sonic disturbances.
Materials: Phase 1: TBP.
Phase 2: Water.
Dropping tip: 3.
r_e: 0.325 cm.

Induced sonic disturbances: 1000 cps, 670 dynes/cm^2 rms sound pressure.
Rest-times: Mean: 8.06, Median: 7.9, 10 percentile: 6.1,
90 percentile: 10.1, Variance: 4.57.
Data-consistency test: Group effect not significant at 5% level.
Comments: None.

Rest-times(sec):

Group 1	Group 2	Group 3	Group 4
5.7	7.9	6.9	8.3
8.3	6.7	9.7	8.7
7.9	6.5	7.9	9.0
6.5	7.7	7.0	5.4
6.1	8.7	5.5	6.6
6.7	7.3	8.1	9.2
7.3	6.5	9.5	7.0
10.4	6.4	10.1	8.9
8.7	8.8	6.8	8.1
9.5	9.7	9.7	5.7
7.4	7.3	11.0	8.9
7.3	11.2	10.6	7.1
10.9		9.8	

Run No. 66 (10-12-61)

Purpose: Sonic disturbances.
Materials: Phase 1: TBP.
Phase 2: Water.
Dropping tip: 3.
r_e: 0.325 cm.
Induced sonic disturbances: 300 cps, 48 dynes/ cm^2 rms sound pressure.
Rest-times: Mean: 6.24, Median: 6.0, 10 percentile: 3.6,
90 percentile: 8.7, Variance: 3.65.
Data-consistency test: Group effect significant at 5% level.
Comments: None.

Rest-times (sec):

Group 1	Group 2	Group 3	Group 4
4.7	7.5	3.3	3.7
5.9	7.1	2.4	5.7
8.7	3.9	3.9	4.8
4.5	7.3	7.7	6.0
7.3	5.1	6.6	5.7
8.4	2.5	6.4	5.3
4.2	6.9	3.1	5.4
9.1	8.7	9.3	4.7
7.7	8.5	8.3	3.6
8.2	8.2	5.5	4.8
8.5	8.1	9.1	3.9
8.8	3.9	8.4	3.8
8.5		8.5	

Run No. 67 (10-19-61)

Purpose: Sonic disturbances.
Materials: Phase 1: TBP.
Phase 2: Water.
Dropping tip: 3.
r_e: 0.325 cm.
Induced sonic disturbances: None.
Rest-times: Mean: 7.48, Median: 7.3, 10 percentile 5.8,
90 percentile: 9.3, Variance: 1.45.
Data-consistency test: Group effect significant at 5% level.
Comments: None.

Rest-times (sec):

Group 1	Group 2	Group 3	Group 4
6.9	5.6	7.1	6.4
7.5	8.7	8.5	10.5
6.5	9.6	4.0	8.5
7.2	6.7	6.7	9.2
7.1	7.5	8.3	7.4
7.0	8.5	8.3	6.4
5.8	9.0	9.4	6.7
7.2	9.5	9.3	6.8
6.7	8.0	5.8	6.5
8.0	7.8	7.3	6.7
5.9	7.7	7.5	7.7
6.3	10.0	7.7	7.0
5.8		7.6	

Run No. 68 (10-19-61)

Purpose: Sonic disturbances.
Materials: Phase 1: TBP.
Phase 2: Water.
Dropping tip: 3.
r_e: 0.325 cm.
Induced sonic disturbances: 1000 cps, 670 dynes/cm^2 rms sound pressure.
Rest-times: Mean: 7.95, Median: 8.0 10 percentile: 6.3, 90 percentile: 9.6, Variance: 2.44.
Data-consistency test: Group effect not significant at 5% level.
Comments: None.
Rest-times (sec):

Group 1	Group 2	Group 3	Group 4
7.4	8.9	8.5	7.0
9.6	8.1	4.5	7.3
12.6	9.7	8.2	9.7
7.3	8.5	7.3	7.3
8.8	5.7	6.9	7.7
9.0	8.0	6.8	7.2
8.5	8.0	8.3	8.9
5.1	8.8	7.5	8.9
8.4	7.9	6.3	9.1
7.9	6.3	7.1	8.9
7.1	7.5	9.3	9.8
2.7	7.8	9.6	8.7
7.7		9.3	

Run No. 69 (10-19-61)

Purpose: Sonic disturbances.
Materials: Phase 1: TBP.
Phase 2: Water.
Dropping tip: 3.
r_e: 0.325 cm.
Induced sonic disturbances: 70 cps, 250 dynes/cm^2 rms, sound pressure.
Rest-times: Mean: 7.34, Median: 6.7, 10 percentile: 4.4, 90 percentile: 10.7, Variance: 4.94.
Data-consistency test: Group effect significant at 1% level.
Comments: None.
Rest-times (sec):

Group 1	Group 2	Group 3	Group 4
9.9	7.7	5.7	6.9
8.5	6.0	3.1	5.1
6.7	3.9	6.5	3.3
9.4	7.3	6.3	4.9
7.3	7.9	10.7	5.8
6.3	11.0	14.0	5.3
9.6	6.3	12.7	6.1
8.9	7.7	5.1	7.0
9.0	7.5	7.5	8.6
13.8	8.5	6.7	5.5
4.4	5.1	5.6	7.8
16.8	6.9	6.1	5.6
4.0		4.7	

Run No. 70 (19-24-61)

Purpose: Physical properties.
Materials: Phase 1: TBP.
Phase 2: Water.
Dropping tip: 3.
r_e: 0.325 cm.
Induced sonic disturbances: None.
Rest-times: Mean: 9.34, Median: 10.1, 10 percentile: 4.5, 90 percentile: 11.5, Variance: 4.59.
Data-consistency test: Group effect significant at 1% level.
Comments: None.

Rest-times (sec):

Group 1	Group 2	Group 3	Group 4
10.9	4.5	4.0	8.7
10.5	12.1	9.5	4.0
10.9	10.6	12.3	8.8
10.9	10.6	10.0	7.1
8.9	10.5	10.1	6.9
12.5	10.4	10.1	8.3
10.3	10.7	10.5	8.2
11.4	10.5	10.7	8.1
11.5	11.2	8.8	1.6
10.9	11.5	10.0	5.3
10.9	11.6	2.1	9.5
8.9	11.8	9.7	9.3
10.3		8.7	

Run No. 71 (10-24-61)

Purpose: Physical properties.
Materials: Phase 1: TBP.
Phase 2: Water.
Dropping tip: 2.
r_e: 0.415 cm.
Induced sonic disturbances: None.
Rest-times: Mean: 5.05, Median: 5.3, 10 percentile: 4.1, 90 percentile: 5.5, Variance: 0.42.
Data-consistency test: Group effect not significant at 5% level.
Comments: None.
Rest-times (sec):

Group 1	Group 2	Group 3	Group 4
4.1	5.3	6.1	5.8
5.5	4.8	5.4	5.1
4.3	5.1	4.5	5.3
5.1	3.1	5.3	5.2
3.5	3.1	5.3	4.7
5.5	5.0	5.4	5.0
5.6	5.4	5.5	5.3
5.5	5.4	5.7	4.6
5.3	5.5	3.5	5.1
5.5	4.6	5.1	5.1
5.4	4.8	5.5	4.9
5.3	5.6	5.3	4.9
5.3		5.5	

Run No. 72 (10-24-61)

Purpose: Physical properties.
Materials: Phase 1: TBP.
Phase 2: Water.
Dropping tip: 1.
r_e: 0.508 cm.
Induced sonic disturbances: None.
Rest-times: Mean: 5.85, Median: 6.1, 10 percentile: 2.7,
90 percentile: 7.3, Variance: 2.99.
Data-consistency test: Group effect not significant at 5% level.
Comments: None.

Rest-times (sec):

Group 1	Group 2	Group 3	Group 4
5.2	2.7	5.5	6.3
6.7	6.9	6.2	7.3
6.1	5.3	6.5	6.3
6.9	6.5	7.3	8.1
6.1	0.2	6.3	2.3
6.1	7.6	6.6	5.4
6.1	6.5	5.8	7.0
4.9	7.1	5.6	5.5
0.1	6.4	5.8	5.9
7.0	6.0	1.9	5.9
6.3	7.5	8.0	5.7
5.1	5.9	6.8	6.6
7.1		5.7	

Run No. 73 (10-26-61)

Purpose: Physical properties.
Materials: Phase 1: Water.
Phase 2: Benzene.
Dropping tip: 3.
r_e: 0.267 cm.
Induced sonic disturbances: None.
Rest-times: Mean: 4.59, Median: 4.7, 10 percentile: 2.1,
90 percentile: 6.6, Variance: 2.82.
Data-consistency test: Group effect not significant at 5% level.
Comments: None.

Rest-times (sec):

Group 1	Group 2	Group 3	Group 4
2.8	6.1	3.4	7.0
3.1	3.7	1.6	4.5
4.3	0.8	4.7	7.1
4.7	3.3	4.9	3.3
4.3	2.1	6.7	2.9
1.7	5.9	4.0	2.1
4.7	6.0	4.7	5.9
6.1	2.5	2.7	5.5
4.9	7.0	6.1	3.9
3.3	6.0	6.6	4.9
3.8	5.9	4.2	8.7
3.3	5.8	6.3	5.6
5.3		4.9	

Run No. 74 (10-26-61)

Purpose: Physical properties.
Materials: Phase 1: Water.
Phase 2: Benzene.
Dropping tip: 2.
r_e: 0.340 cm.
Induced sonic disturbances: None.
Rest-times: Mean: 4.86, Median: 4.8, 10 percentile: 2.6, 90 percentile: 7.3, Variance: 3.39.
Data-consistency test: Group effects not significant at 5% level.
Comments: None.

Rest-times (sec):

Group 1	Group 2	Group 3	Group 4
9.0	5.3	5.2	5.5
6.3	4.8	6.4	4.9
4.1	6.7	2.6	6.3
3.9	1.3	5.0	3.4
4.1	3.7	2.7	7.5
4.2	4.3	6.1	4.5
2.1	5.7	5.8	3.3
3.6	4.1	6.1	3.7
5.2	4.1	3.3	2.1
6.5	4.5	3.7	3.1
4.9	3.1	1.5	9.4
8.5	6.5	4.9	6.6
5.4		7.3	

Run No. 75 (10-27-61)

Purpose: Physical properties.
Materials: Phase 1: Water.
Phase 2: Benzene.
Dropping tip: 1.
r_e: 0.415 cm.
Induced sonic disturbances: None.
Rest-times: Mean: 4.85, Median: 4.7, 10 percentile: 2.1, 90 percentile: 6.9, Variance: 1.82.
Data-consistency test: Group effects significant at 1% level.
Comments: None.

Rest-times (sec):

Group 1	Group 2	Group 3	Group 4
4.3	6.3	4.3	7.3
4.9	2.1	6.7	6.1
3.0	4.1	5.1	6.7
2.0	5.3	3.3	6.9
3.3	6.4	4.4	5.7
1.7	6.1	2.9	7.5
2.9	6.5	4.5	5.8
4.7	6.7	4.0	8.5
3.5	5.0	5.3	6.1
1.8	8.3	2.8	8.1
2.1	5.4	5.6	3.7
4.4	6.0	3.5	3.2
3.1		4.4	

Run No. 76 (10-27-61)

Purpose: Physical properties.
Materials: Phase 1: Water.
Phase 2: Benzene.
Dropping tip: 1.
r_e: 0.415 cm.
Induced sonic disturbances: None.
Rest-times: Mean: 5.68, Median: 5.4, 10 percentile: 2.3, 90 percentile: 9.5, Variance: 5.88.
Data-consistency test: Group effect significant at 1% level.
Comments: Drops fell 10-15 mm to interface from dropping tip.

Rest-times: (sec):

Group 1	Group 2	Group 3	Group 4
9.5	2.3	9.5	4.8
5.6	5.0	7.9	5.4
1.3	3.0	6.9	7.3
7.0	4.2	7.1	4.3
5.1	1.8	5.2	2.2
10.3	4.8	5.8	7.8
2.3	3.7	10.1	6.4
7.5	3.3	7.9	6.6
6.5	3.9	14.2	5.9
3.4	4.9	1.2	8.4
3.3	3.1	5.8	10.7
3.2	5.5	6.8	5.1
2.6		7.8	

Run No. 77 (11-21-61)

Purpose: Physical properties.
Materials: Phase 1: Water.
Phase 2: Benzene.
Dropping tip: 6.
r_e: 0.209 cm.
Induced sonic disturbances: None.
Rest-times: Mean: 4.61, Median: 4.9, 10 percentile: 2.8, 90 percentile: 5.8, Variance: 1.45.
Data-consistency test: Group effect not significant at 5% level.
Comments: None.

Group 1	Group 2	Group 3	Group 4
3.4	5.2	3.8	4.6
5.4	5.2	1.6	5.5
4.4	4.9	2.8	4.8
6.1	5.9	5.8	5.1
1.7	4.9	5.5	4.3
5.1	2.8	3.9	5.2
4.5	5.1	4.6	5.7
3.6	5.7	6.0	6.4
1.9	5.9	2.7	3.0
5.1	5.3	5.7	3.5
5.3	4.8	5.7	4.9
4.8	3.5	5.8	3.5
4.6		5.2	

Run No. 78 (11-28-61)

Purpose: Physical properties.
Materials: Phase 1: Water.
Phase 2: Aroclor 1248.
Dropping tip: 5.
r_e: 0.180 cm.
Induced sonic disturbances: None.
Rest-times: Mean: 72.34, Median: 59.3 10 percentile: 8.3,
90 percentile: 137.4 Variance: 2303.55.
Data-consistency test: Group effect significant at 1% level.
Comments: None.

Rest-times (sec):

Group 1	Group 2	Group 3	Group 4
104.6	179.5	35.3	203.1
107.0	137.4	145.6	5.5
130.1	133.3	132.1	19.0
56.0	170.3	121.7	7.7
73.7	59.3	138.8	7.9
43.5	56.4	91.6	8.9
99.3	28.7	81.5	8.7
25.7	36.7	51.2	10.1
125.1	28.1	101.1	8.3
126.8	78.2	125.9	8.3
45.1	80.1	78.5	15.9
62.8	29.5	57.7	44.8
0.2		90.4	

Run No. 79 (11-28-61)

Purpose: Physical properties.
Materials: Phase 1: Water.
Phase 2: Aroclor 1248.
Dropping tip: 4.
r_e: 0.288 cm.
Induced sonic disturbances: None.
Rest-times: Mean:273.81 Median: 208.2, 10 percentile: 54,
90 percentile: 607.3 Variance: 51694.23.
Data-consistency test: Group effect not significant at 5% level.
Comments: Only 25 measurements, divided into 2 groups, were made because of extremely long rest-times.

Rest-times (sec):

Group 1	Group 2
94.7	71.5
117.9	339.9
66.7	194.9
110.7	253.1
8.5	604.0
120.1	339.2
149.1	208.2
240.9	261.5
528.8	607.3
575.6	485.4
167.0	919.0
281.2	53.5
	46.6

Run No. 80 (11-29-61)

Purpose: Physical properties.
Materials: Phase 1: Water.
Phase 2: Aroclor 1248.
Dropping tip: 6.
r_e: 0.141 cm.
Induced sonic disturbances: None.
Rest-times: Mean: 47.82, Median: 42,2,10 percentile: 14.7, 90 percentile: 84.6,Variance: 538.44.
Data-consistency test: Group effect significant at 1% level.
Comments: None.

Rest-times (sec):

Group 1	Group 2	Group 3	Group 4
41.8	57.0	22.4	78.2
42.2	76.8	35.4	45.2
16.5	75.7	28.5	37.4
8.6	72.3	64.9	26.6
21.9	94.7	78.7	66.3
17.3	45.6	39.2	54.9
16.0	89.0	84.6	14.7
16.5	30.1	61.1	49.4
23.7	50.5	41.5	27.9
14.5	64.5	43.0	24.7
13.9	119.0	5.8	79.7
52.7	123.1	61.5	81.3
20.0		94.0	

Run No. 81 (12-5-61)

Purpose: Surfactant.
Materials: Phase 1: 0.031 milli-molar Span 80 in water.
Phase 2: 1.14 milli-molar Span 80 in benzene.
Dropping tip: 6.
r_e: 0.143 cm.
Induced sonic disturbances: None.
Rest-times: Mean: 21.79, Median: 26.8, 10 percentile: 7.5, 90 percentile: 38.3, Variance: 112.39.
Data-consistency test: Group effect significant at 5% level.
Comments: None.

Rest-times (sec):

Group 1	Group 2	Group 3	Group 4
14.1	15.7	21.3	24.0
20.7	38.3	18.3	18.4
50.9	34.0	14.5	23.3
3.9	29.9	7.5	8.5
15.9	17.1	7.5	18.3
34.4	2.9	21.3	13.6
17.8	34.1	20.1	20.3
17.7	35.0	16.2	22.3
43.0	7.3	6.3	8.3
38.5	35.0	21.4	15.8
44.3	28.4	21.5	23.8
12.9	19.5	12.2	27.8
39.6		25.9	

Run No. 82 (12-5-61)

Purpose: Surfactant.
Materials: Phase 1: 0.031 milli-molar Span 80 in water.
Phase 2: 1.14 milli-molar Span 80 in benzene.
Dropping tip: 5.
r_e: 0.182 cm.
Induced sonic disturbances: None.
Rest-times: Mean: 27.15, Median: 28.6, 10 percentile: 5.4, 90 percentile: 47.2, Variance: 251.82.
Data-consistency test: Group effect not significant at 5% level.
Comments: None.

Rest-times (sec):

Group 1	Group 2	Group 3	Group 4
0.7	1.7	43.8	64.1
51.4	23.3	9.9	11.3
37.0	13.3	2.6	29.5
24.5	13.6	5.4	53.3
16.0	34.6	37.4	27.1
10.5	33.4	13.1	13.6
34.5	41.5	1.5	45.9
7.5	35.8	13.9	41.8
13.0	36.0	51.2	42.0
28.8	43.4	35.7	20.2
28.6	8.3	23.7	22.3
33.0	35.4	34.8	47.2
49.8		10.7	

Run No. 83 (12-6-61)

Purpose: Surfactant.
Materials: Phase 1: 0.031 milli-molar Span 80 in water.
Phase 2: 1.14 milli-molar Span 80 in benzene.
Dropping tip: 4.
r_e: 0.230 cm.
Induced sonic disturbances: None.
Rest-times: Mean: 89.23, Median: 93.4, 10 percentile: 25.3, 90 percentile: 139.3, Variance: 1784.72.
Data-consistency test: Group effect not significant at 5% level.
Comments: None.

Group 1	Group 2	Group 3	Group 4
5.0	96.2	93.4	104.0
25.3	184.7	137.1	93.1
49.0	29.6	124.2	139.3
92.1	72.5	121.1	168.6
121.7	27.5	113.0	42.5
30.6	4.2	92.9	101.8
147.6	155.1	71.4	88.9
80.6	10.2	124.3	55.4
101.4	115.1	104.4	120.5
40.5	112.3	96.0	138.5
83.7	2.8	88.1	149.1
78.7	49.2	63.8	105.4
97.2		111.8	

Run No. 84 (12-7-61)

Purpose: Surfactant.
Materials: Phase 1: 0.0031 milli-molar Span 80 in water.
Phase 2: 0.114 milli-molar Span 80 in benzene.
Dropping tip: 5.
r_e: 0.245 cm.
Induced sonic disturbances: None.
Rest-times: Mean: 8.08, Median: 8.1, 10 percentile: 3.5, 90 percentile: 12.1, Variance: 10.66.
Data-consistency test: Group effect not significant at 5% level.
Comments: None.

Rest-times (sec):

Group 1	Group 2	Group 3	Group 4
10.5	5.7	11.1	5.4
4.7	10.6	12.1	5.3
9.9	8.6	5.1	8.5
1.5	5.3	4.6	3.2
2.9	4.1	11.1	8.7
3.7	5.3	8.3	8.1
13.1	5.9	3.6	7.1
11.9	15.9	11.4	11.9
3.5	8.5	5.7	12.3
6.4	14.5	9.8	4.1
3.1	14.5	12.0	11.8
6.7	9.9	12.1	12.1
6.5		5.6	

Run No. 85 (12-7-61)

Purpose: Surfactant.
Materials: Phase 1: 0.0031 milli-molar Span 80 in water.
Phase 2: 0.114 milli-molar Span 80 in benzene.
Dropping tip: 6.
r_e: 0.191 cm.
Induced sonic disturbances: None.
Rest-times: Mean: 8.10, Median: 7.5, 10 percentile: 2.8, 90 percentile: 13.9, Variance: 18.87.
Data-consistency test: Group effect not significant at 5% level.
Comments: None.

Rest-times (sec):

Group 1	Group 2	Group 3	Group 4
11.6	3.1	2.1	6.9
2.8	7.2	3.2	7.5
2.7	8.1	6.1	7.9
5.7	14.4	13.7	13.5
8.5	9.2	2.7	9.0
13.7	14.5	16.7	11.6
3.5	10.3	7.3	7.3
3.0	3.1	14.0	18.0
12.2	8.9	7.3	13.9
8.6	5.1	12.1	9.6
3.3	3.3	3.0	4.0
7.2	1.8	11.5	4.7
10.9		8.5	

Run No. 86 (12-7-61)

Purpose: Surfactant.
Materials: Phase 1: 0.0031 milli-molar Span 80 in water.
Phase 2: 0.114 milli-molar Span 80 in benzene.
Dropping tip: 4.
r_e: 0.310 cm.
Induced sonic disturbances: None.
Rest-times: Mean: 7.55, Median: 6.7, 10 percentile: 2.9, 90 percentile: 12.7, Variance: 13.31.
Data-consistency test: Group effect not significant at 5% level.
Comments: None.

Rest-times(sec):

Group 1	Group 2	Group 3	Group 4
2.9	2.9	2.2	4.5
3.7	8.3	5.5	12.7
10.5	5.7	2.9	3.1
11.7	6.1	9.8	12.1
3.9	7.9	5.3	2.5
4.2	3.5	9.8	6.5
8.2	10.3	9.1	8.1
8.3	2.5	6.3	9.3
5.2	6.7	7.5	4.6
6.5	13.1	9.8	17.1
6.4	7.5	10.3	13.1
6.5	7.3	16.8	13.0
4.8		10.9	

Run No. 87 (1-16-62)

Purpose: Surfactant.
Materials: Phase 1: 0.00244 milli-molar Tween 81 in water.
Phase 2: Benzene.
Dropping tip: 5.
r_e: 0.236 cm.
Induced sonic disturbances: None.
Rest-times: Mean: 5.60, Median: 5.1, 10 percentile: 2.9, 90 percentile: 8.6, Variance: 5.05.
Data- consistency test: Group effect not significant at 5% level.
Comments: None.

Rest-times (sec):

Group 1	Group 2	Group 3	Group 4
4.5	8.9	10.7	7.5
2.3	4.5	2.9	6.7
3.3	7.3	7.7	7.6
7.3	3.8	5.9	4.7
3.3	4.4	8.6	1.9
3.7	5.9	3.3	5.8
6.5	3.3	4.8	5.2
8.1	6.5	5.1	7.7
3.7	6.1	4.5	4.7
3.7	4.4	7.2	4.0
6.5	9.2	9.8	8.1
1.9	3.9	4.0	2.1
9.3		7.2	

Run No. 88 (1-16-62)

Purpose: Surfactant.
Materials: Phase 1: 0.00244 milli-molar Tween 81 in water.
Phase 2: Benzene.
Dropping tip: 6.
r_e: 0.184 cm.
Induced sonic disturbances: None.
Rest-times: Mean: 3.94, Median: 3.9, 10 percentile: 1.3, 90 percentile: 5.7, Variance: 2.51.
Data-consistency test: Group effect significant at 1% level.
Comments: None.

Rest-times: (sec):

Group 1	Group 2	Group 3	Group 4
4.9	5.7	3.2	1.6
7.9	4.3	2.7	1.8
4.4	5.1	2.0	1.5
7.7	3.5	4.1	5.7
8.0	5.2	2.2	5.1
3.9	4.8	1.7	6.5
4.1	3.8	1.8	4.4
2.4	1.0	2.8	3.2
5.4	1.4	4.0	4.7
4.0	3.0	1.0	3.6
4.0	5.3	4.3	3.4
8.9	3.9	3.3	3.4
4.5		2.1	

Run No. 89 (1-16-62)

Purpose: Surfactant.
Materials: Phase 1: 0.00244 milli-molar Tween 81 in water.
Phase 2: Benzene.
Dropping tip: 4.
r_e: 0.299 cm.
Induced sonic disturbances: None.
Rest-times: Mean: 5.38, Median: 4.5, 10 percentile: 1.6, 90 percentile: 9.3, Variance: 6.53.
Data-consistency test: Group effect significant at 1% level.
Comments: None.

Rest-times (sec):

Group 1	Group 2	Group 3	Group 4
5.0	8.1	2.3	8.7
4.3	3.7	1.4	8.1
1.6	8.5	4.1	7.1
6.3	7.3	2.7	4.9
4.1	10.7	1.6	13.5
2.7	2.7	1.1	2.3
2.9	2.9	1.3	9.3
3.7	9.3	2.1	9.2
2.3	10.5	1.9	3.8
6.5	8.6	2.1	4.5
8.3	11.7	2.7	3.5
6.9	6.5	7.1	7.3
5.8		5.4	

Run No. 90 (1-17-62)

Purpose: Surfactant.
Materials: Phase 1: 0.0244 milli-molar Tween 81 in water.
Phase 2: Benzene.
Dropping tip: 4. r_e: 0.266 cm.
Induced sonic disturbances: None.
Rest-times: Mean: 11.58, Median: 11.3, 10 percentile: 5.5, 90 percentile: 17.4, Variance: 15.59.
Data-consistency test: Group effect significant at 5% level.
Comments: None.
Rest-times (sec):

Group 1	Group 2	Group 3	Group 4
21.0	21.5	8.9	18.8
14.9	10.7	11.3	12.3
8.9	7.6	9.1	16.9
5.5	4.8	9.7	14.3
5.5	10.1	6.7	11.3
8.5	8.7	5.7	14.5
7.1	4.6	14.1	13.4
12.9	5.9	11.5	12.1
15.2	10.5	14.5	17.7
5.4	11.1	10.1	17.4
13.9	15.1	14.4	12.1
9.5	11.5	12.1	14.2
8.1		17.5	

Run No. 91 (1-17-62)

Purpose: Surfactant.
Materials: Phase 1: 0.0244 milli-molar Tween 81 in water.
Phase 2: Benzene.
Dropping tip: 6. r_e: 0.164 cm.
Induced sonic disturbances: None.
Rest-times: Mean: 6.50, Median: 5.7, 10 percentile: 3.2, 90 percentile: 11.4, Variance: 10.93.
Data-consistency test: Group effect significant at 5% level.
Comments: None.
Rest-times (sec):

Group 1	Group 2	Group 3	Group 4
3.1	7.1	3.5	3.3
3.7	5.5	19.5	2.5
6.1	6.3	6.5	14.3
5.7	4.1	13.7	3.5
5.7	11.1	8.9	6.3
3.9	10.2	4.9	5.3
5.9	4.7	12.1	5.7
3.6	8.1	7.1	7.3
2.6	3.5	5.4	4.0
2.7	12.4	4.8	6.4
7.8	10.6	7.3	6.2
3.2	11.4	5.2	3.9
4.9		3.7	

Run No. 92 (1-17-62)

Purpose: Surfactant.
Materials: Phase 1: 0.0244 milli-molar Tween 81 in water.
Phase 2: Benzene.
Dropping tip: 5. r_e: 0.210 cm.
Induced sonic disturbances: None.
Rest-times: Mean: 9.91, Median: 9.5, 10 percentile: 4.3, 90 percentile: 15.9, Variance: 19.37.
Data-consistency test: Group effect not significant at 5% level.
Comments: None.
Rest-times (sec):

Group 1	Group 2	Group 3	Group 4
5.1	7.1	5.9	9.3
6.7	7.3	15.9	10.4
5.3	9.5	14.1	4.3
13.7	12.5	10.1	4.7
19.1	14.1	19.7	10.4
7.4	13.3	12.0	19.5
4.4	15.1	7.3	7.7
9.2	11.5	7.9	4.3
9.5	11.0	4.1	12.0
2.7	5.8	9.8	16.6
10.3	9.9	15.5	4.5
4.2	10.5	18.9	10.2
6.7		8.5	

Run No. 93 (1-18-62)

Purpose: Surfactant.
Materials: Phase 1: 0.244 milli-molar Tween 81 in water.
Phase 2: Benzene.
Dropping tip: 5. r_e: 0.168 cm.
Induced sonic disturbances: None.
Rest-times: Mean: 84.80, Median: 70.1, 10 percentile: 16.5, 90 percentile: 160.0, Variance: 3238.07.
Data-consistency test: Group effect not significant at 5% level.
Comments: None.
Rest-times (sec):

Group 1	Group 2	Group 3	Group 4
145.5	43.2	61.9	94.4
16.7	183.5	146.3	54.0
181.7	39.8	114.7	142.6
15.7	29.0	131.1	143.7
84.1	111.5	36.5	12.9
86.1	16.9	4.7	63.9
16.5	36.2	122.5	33.9
138.1	118.8	70.1	86.0
22.1	22.5	110.7	185.9
8.1	31.3	138.3	157.2
47.2	120.9	174.1	160.0
52.2	173.8	22.5	65.1
106.8		58.7	

Run No. 94 (1-18-62)

Purpose: Surfactant.
Materials: Phase 1: 0.244 milli-molar Tween 81 in water.
Phase 2: Benzene.
Dropping tip: 6. r_e: 0.132 cm.
Induced sonic disturbances: None.
Rest-times: Mean: 62.19, Median: 58.5, 10 percentile: 9.7,
90 percentile: 111.6, Variance: 1623.80.
Data-consistency test: Group effect not significant at 5% level.
Comments: None.
Rest-times (sec):

Group 1	Group 2	Group 3	Group 4
63.7	21.9	53.6	9.2
98.7	22.9	17.1	4.9
6.7	100.2	96.0	117.6
111.4	66.1	53.6	133.0
57.3	93.9	78.2	107.0
56.4	43.6	23.9	60.5
111.6	34.4	88.5	85.2
80.6	75.1	58.5	165.6
66.3	40.6	11.7	163.0
39.3	18.9	22.3	60.4
141.1	65.1	10.7	27.0
91.1	72.5	38.1	29.3
		5.5	

Run No. 95 (1-18-62)

Purpose: Surfactant.
Materials: Phase 1: 0.244 milli-molar Tween 81 in water.
Phase 2: Benzene.
Dropping tip: 4. r_e: 0.213 cm.
Induced sonic disturbances: None.
Rest-times: Mean: 150.60, Median: 133.7, 10 percentile: 10.9,
90 percentile: 298.1, Variance: 9509.43.
Data-consistency test: Group effect not significant at 5% level.
Comments: Only 25 measurements divided into two groups were taken because of long rest-times.
Rest-times (sec):

Group 1	Group 2
1.7	210.9
139.9	120.7
137.1	35.1
81.5	78.7
155.7	227.0
247.4	188.1
361.2	42.0
116.3	30.3
298.1	119.4
330.8	133.7
103.8	243.8
10.9	156.7
194.1	

Run Nos. 96-98 (1-23-62)

Purpose: Sub-sonic disturbances.
Materials: Phase 1: Water.
Phase 2: Benzene.
Dropping tip: 5. r_e: 0.267 cm.
Comments: Runs 96-98 were analyzed as a single run. Sub-sonic disturbances used are described with data.
Rest-times (sec):

	No vibration	Pure 70 cps (94 dynes/cm^2)	1 beat/sec (133 dynes/cm^2)	5 beats/sec (133 dynes/cm^2)	10 beats/sec (133 dynes/cm^2)
Run 96	5.9	8.2	46.8	9.8	9.1
	2.5	5.3	220.2	5.1	6.4
	4.3	2.1	26.4	9.7	4.5
	1.3	11.3	25.1	6.3	6.3
	7.5	11.0	27.4	0	2.7
	3.5	23.8	11.4	7.3	4.1
	3.2	41.1	29.4	8.1	7.5
	6.3	6.7	9.5	17.7	5.9
	6.1	16.6	12.1	10.5	3.3
	5.1	9.1	9.5	6.9	7.5
Run 97	3.2	9.3	8.1	10.1	7.5
	5.5	8.3	9.5	9.3	8.7
	7.3	9.5	9.3	14.9	3.3
	5.1	8.1	9.5	13.3	6.1
	6.5	13.4	6.5	9.0	7.9
	3.1	14.9	7.7	10.1	2.5
	5.3	13.5	8.1	9.3	8.1
	4.7	13.7	3.1	9.9	9.8
	6.9	10.3	8.7	9.5	9.3
	3.0	6.3	8.5	9.0	8.3
Run 98	6.5	16.7	8.3	13.5	7.4
	4.7	20.3	9.1	8.3	9.7
	5.3	42.0	7.7	9.3	8.8
	4.3	99.4	7.3	9.2	4.7
	6.1	61.7	4.8	10.5	7.9
	7.7	25.1	17.5	13.9	6.7
	6.5	20.3	8.2	11.4	7.6
	4.3	20.5	9.7	15.2	8.2
	5.5	23.5	32.8	11.0	6.1
	4.3	16.3	31.9	9.3	8.1

Run No. 99 (1-24-62)

Purpose: Surfactant.
Materials: Phase 1: 0.0556 milli-molar sodium oleate in water.
Phase 2: Benzene.
Dropping tip: 5. r_e: 0.253 cm.
Induced sonic disturbances: None.
Rest-times: Mean: 9.93, Median: 10.3, 10 percentile: 5.7, 90 percentile: 14.8, Variance: 13.88.
Data-consistency test: Group effect not significant at 5% level.
Comments: None.
Rest-times (sec):

Group 1	Group 2	Group 3	Group 4
10.9	9.5	8.5	15.1
6.7	11.3	5.9	4.1
10.3	13.5	8.8	6.1
3.7	10.4	16.5	6.7
12.4	6.5	14.1	14.8
5.7	12.6	10.4	11.6
5.7	11.6	10.1	5.9
17.4	11.0	14.3	11.8
10.1	6.9	13.5	11.3
11.1	6.3	14.8	6.2
11.3	10.3	8.9	5.5
16.7	11.1	6.8	12.3
7.4		2.1	

Run No. 100 (1-24-62)

Purpose: Surfactant.
Materials: Phase 1: 0.0556 milli-molar sodium oleate in water.
Phase 2: Benzene.
Dropping tip: 6. r_e: 0.200 cm.
Induced sonic disturbances: None.
Rest-times: Mean: 7.82, Median: 7.7, 10 percentile: 3.1, 90 percentile: 11.7, Variance: 13.84.
Data-consistency test: Group effect not significant at 5% level.
Comments: None.
Rest-times (sec):

Group 1	Group 2	Group 3	Group 4
5.7	1.9	4.6	4.9
7.9	4.7	7.7	6.1
13.0	6.9	6.4	5.4
7.9	19.4	5.3	4.9
9.2	9.1	4.9	11.1
17.2	3.1	10.3	4.8
9.5	8.5	8.9	5.5
8.3	10.5	7.7	10.3
1.4	8.4	7.7	5.1
11.1	6.3	15.2	5.3
10.7	6.8	7.8	9.8
11.7	2.9	2.7	14.0
6.5		6.1	

Run No. 101 (1-24-62)

Purpose: Surfactant.
Materials: Phase 1: 0.0556 milli-molar sodium oleate in water.
Phase 2: Benzene.
Dropping tip: 4. r_e: 0.321 cm.
Induced sonic disturbances: None.
Rest-times: Mean: 8.71, Median: 7.3, 10 percentile: 2.5, 90 percentile: 16.0, Variance: 32.86.
Data-consistency test: Group effect not significant at 5% level.
Comments: None.
Rest-times (sec):

Group 1	Group 2	Group 3	Group 4
12.5	5.9	5.1	3.9
11.8	2.5	7.9	8.3
5.7	9.3	3.6	9.3
11.2	6.5	14.8	9.9
7.5	4.9	11.1	7.1
20.1	6.1	9.2	7.3
1.7	7.5	1.7	18.3
2.5	5.5	3.1	20.2
15.3	3.9	4.6	9.3
15.3	2.7	7.3	5.4
25.2	10.5	16.0	9.4
1.1	2.7	8.1	27.7
3.9		4.9	

Run No. 102 (1-25-62)

Purpose: Surfactant.
Materials: Phase 1: 0.556 milli-molar sodium oleate in water.
Phase 2: Benzene.
Dropping tip: 4. r_e: 0.277 cm.
Induced sonic disturbances: None.
Rest-times: Mean: 33.56, Median: 25.6, 10 percentile: 5.9, 90 percentile: 62.5, Variance: 351.60.
Data-consistency test: Group effect significant at 1% level.
Comments: None.
Rest-times (sec):

Group 1	Group 2	Group 3	Group 4
26.8	10.3	25.6	11.5
36.7	56.0	63.1	24.0
6.8	55.4	44.4	55.1
9.5	25.8	35.4	120.9
12.0	54.3	17.7	158.1
5.5	12.8	16.1	3.1
24.0	62.5	19.1	31.3
15.5	31.1	28.0	29.8
5.9	28.1	45.8	25.3
13.7	23.8	73.0	115.7
16.3	9.5	10.3	56.3
5.5	35.0	14.6	39.4
2.9		28.7	

Run No. 103 (1-25-62)

Purpose: Surfactant.
Materials: Phase 1: 0.556 milli-molar sodium oleate in water.
Phase 2: Benzene.
Dropping tip: 6. r_e: 0.171 cm.
Induced sonic disturbances: None.
Rest-times: Mean: 28.25, Median: 23.1, 10 percentile: 4.9, 90 percentile: 52.4, Variance: 400.99.
Data-consistency test: Group effect not significant at 5% level.
Comments: None.
Rest-times (sec):

Group 1	Group 2	Group 3	Group 4
49.6	30.4	38.4	34.0
42.2	17.2	10.1	12.7
75.3	19.3	8.9	9.9
26.3	67.3	12.9	8.2
3.3	39.8	0.2	49.4
17.9	25.0	4.9	21.6
18.9	52.4	9.6	30.8
3.5	33.0	43.6	9.3
22.2	37.8	20.3	12.0
26.2	15.3	68.9	37.0
23.1	68.1	82.3	32.2
1.9	40.6	20.3	26.4
12.3		39.8	

Run No. 104 (1-25-62)

Purpose: Surfactant.
Materials: Phase 1: 0.556 milli-molar sodium oleate in water.
Phase 2: Benzene.
Dropping tip: 5. r_e: 0.218 cm.
Induced sonic disturbances: None.
Rest-times: Mean: 39.23, Median: 35.1, 10 percentile: 7.3, 90 percentile: 67.3, Variance: 457.80.
Data-consistency test: Group effect significant at 1% level.
Comments: None.
Rest-times (sec):

Group 1	Group 2	Group 3	Group 4
2.5	82.5	72.7	12.2
17.7	26.7	64.7	38.0
30.2	66.1	60.6	41.0
8.9	36.4	5.5	60.3
7.3	24.8	21.4	53.2
33.7	9.1	34.6	82.3
49.0	20.1	50.1	88.6
16.4	35.1	64.8	50.4
56.3	16.6	53.8	41.0
54.3	26.8	26.8	94.6
4.9	8.7	34.6	47.2
9.6	47.6	45.0	67.3
5.1		54.6	

Run No. 105 (1-26-62)

Purpose: Surfactant.
Materials: Phase 1: 5.56 milli-molar sodium oleate in water.
Phase 2: Benzene.
Dropping tip: 5. r_e: 0.152 cm.
Induced sonic disturbances: None.
Rest-times: Mean: 12.56, Median: 12.1, 10 percentile: 9.1, 90 percentile: 14.9, Variance: 12.22.
Data-consistency test: Group effect not significant at 5% level.
Comments: Run subdivided into 2 groups of 25 measurements each.
Rest-times (sec):

Group 1	Group 2
5.9	31.7
11.9	18.0
10.9	8.8
9.1	10.8
7.9	9.8
9.3	10.5
8.7	13.9
10.4	12.8
11.2	13.5
11.1	11.1
13.5	11.6
12.1	11.7
11.5	11.7
14.9	14.1
11.7	14.1
11.3	13.5
12.1	13.1
13.9	14.3
14.0	12.6
13.0	11.1
9.9	15.3
16.3	12.2
14.7	13.7
10.9	12.5
14.2	15.3

Run No. 106 (1-26-62)

Purpose: Surfactant.
Materials: Phase 1: 5.56 milli-molar sodium oleate in water.
Phase 2: Benzene.
Dropping tip: 4. r_e: 0.193 cm.
Induced sonic disturbances: None.
Rest-times: Mean: 9.16, Median: 9.0, 10 percentile: 7.5, 90 percentile: 10.5, Variance: 1.87.
Data-consistency test: Group effect not significant at 5% level.
Comments: Run subdivided into 2 groups of 25 measurements each.
Rest-times (sec):

Group 1	Group 2
13.3	7.0
13.6	8.7
8.4	8.9
9.5	10.5
9.2	8.9
7.4	9.5
7.8	9.2
9.9	11.2
10.5	10.5
11.5	9.2
9.4	8.7
9.8	10.0
7.5	7.5
8.9	8.2
9.9	10.3
6.5	8.7
8.6	7.7
9.1	7.5
8.1	8.1
8.9	8.3
10.1	10.2
8.6	8.3
9.3	9.0
8.9	9.1
9.0	9.2

Run No. 107 (1-26-62)

Purpose: Surfactant.
Materials: Phase 1: 5.56 milli-molar sodium oleate in water.
Phase 2: Benzene.
Dropping tip: 6. r_e: 0.120 cm.
Induced sonic disturbances: None.
Rest-times: Mean: 6.40, Median: 6.3, 10 percentile: 5.4, 90 percentile: 7.8, Variance: 0.99.
Data-consistency test: Not applicable.
Comments: Run not subdivided into groups.
Rest-times (sec):

4.8	5.8
4.5	6.2
6.3	6.2
6.2	6.2
3.4	6.2
6.5	6.5
6.3	5.4
4.8	8.2
6.1	5.9
5.5	5.6
5.6	7.0
7.1	6.3
8.2	8.0
7.8	6.6
7.8	5.9
7.8	6.4
8.5	6.1
7.6	6.1
6.7	6.5
7.2	6.3
5.9	8.0
6.2	6.3
7.0	6.6
5.9	5.7
6.2	6.3

Run No. 108 (1-30-62)

Purpose: Physical properties.
Materials: Phase 1: Water.
Phase 2: Anisole.
Dropping tip: 4. r_e: 0.772 cm.
Induced sonic disturbances: None.
Rest-times: Mean: 50.45, Median: 35.6, 10 percentile: 7.1, 90 percentile: 90.2, Variance: 3921.12.
Data-consistency test: Group effect not significant at 5% level.
Comments: None.
Rest-times (sec):

Group 1	Group 2	Group 3	Group 4
82.6	2.1	6.3	214.8
44.3	16.3	7.1	63.1
16.9	8.0	83.3	6.5
74.5	43.4	21.5	39.1
77.5	17.5	14.5	36.2
7.1	104.9	18.6	90.2
54.9	86.9	11.6	80.1
135.1	35.8	16.2	78.4
12.2	48.2	35.6	75.9
148.2	31.3	70.7	113.1
89.2	78.9	29.4	2.5
88.1	16.0	24.8	28.2
8.5		26.2	

Run No. 109 (1-30-62)

Purpose: Physical properties.
Materials: Phase 1: Water.
Phase 2: Anisole.
Dropping tip: 5. r_e: 0.598 cm.
Induced sonic disturbances: None.
Rest-times: Mean: 20.47, Median: 12.3, 10 percentile: 4.7, 90 percentile: 45.3, Variance: 226.71.
Data-consistency test: Group effect significant at 5% level.
Comments: None.
Rest-times (sec):

Group 1	Group 2	Group 3	Group 4
61.3	57.0	6.3	11.7
4.6	50.8	21.9	2.5
28.5	55.9	5.1	32.4
10.8	28.1	10.9	8.3
23.9	24.6	8.3	16.6
5.4	45.3	10.7	5.5
4.7	5.4	21.1	33.2
11.8	54.0	39.7	20.9
32.1	7.7	24.3	8.0
18.0	6.1	38.8	23.3
6.1	38.7	12.3	9.9
3.7	25.4	20.9	10.6
4.5		6.1	

Run No. 110 (2-2-62)

Purpose: Physical properties.
Materials: Phase 1: Ethylene glycol.
Phase 2: Benzene.
Dropping tip: 5. r_e: 0.125 cm.
Induced sonic disturbances: None.
Rest-times: Mean: 19.76, Median: 20.5, 10 percentile: 6.9,
90 percentile: 30.8, Variance: 39.26.
Data-consistency test: Group effect significant at 1% level.
Comments: None.
Rest-times (sec):

Group 1	Group 2	Group 3	Group 4
5.4	11.1	22.3	19.5
4.5	6.2	31.0	31.2
13.9	7.8	20.5	21.5
6.2	7.8	27.8	26.5
12.0	13.5	32.0	27.1
13.2	13.3	24.3	35.8
10.4	26.7	29.4	40.4
15.0	30.8	19.7	27.8
7.9	22.1	25.8	27.7
12.2	6.9	12.1	25.9
24.0	19.0	21.9	27.1
13.7	22.3	24.8	24.5
15.2		20.3	

Run No. 111 (2-2-62)

Purpose: Physical properties.
Materials: Phase 1: Ethylene glycol.
Phase 2: Benzene.
Dropping tip: 4. r_e: 0.159 cm.
Induced sonic disturbances: None.
Rest-times: Mean: 16.70, Median: 14.0, 10 percentile: 10.5,
90 percentile: 22.3, Variance: 47.86.
Data-consistency test: Group effect significant at 1% level.
Comments: None.
Rest-times (sec):

Group 1	Group 2	Group 3	Group 4
41.2	4.7	11.5	18.1
50.9	11.9	12.7	12.3
43.0	16.2	14.9	7.5
34.8	13.3	22.3	12.1
16.3	12.4	20.6	12.3
26.3	11.0	19.1	12.1
19.2	10.9	19.4	13.3
19.0	10.8	19.2	11.9
15.7	10.8	20.1	10.3
15.9	10.5	17.5	14.0
15.8	10.2	18.0	10.5
16.9	14.4	11.3	12.3
17.4		12.2	

Run No. 112 (2-2-62)

Purpose: Physical properties.
Materials: Phase 1: Ethylene glycol.
Phase 2: Benzene.
Dropping tip: 1. r_e: 0.195 cm.
Induced sonic disturbances: None.
Rest-times: Mean: 24.82, Median: 23.5, 10 percentile 9.0,
90 percentile: 40.0, Variance: 60.81.
Data-consistency test: Group effect significant at 1% level.
Comments: None.
Rest-times (sec):

Group 1	Group 2	Group 3	Group 4
10.1	20.8	24.5	12.1
4.3	24.1	47.1	33.0
14.1	18.4	49.2	35.6
12.7	15.5	54.8	35.4
5.8	18.3	34.9	32.6
5.5	19.8	48.1	34.3
9.0	13.1	25.1	36.2
13.8	23.5	38.1	23.6
6.4	18.5	28.5	25.5
16.1	15.9	26.9	27.5
11.6	23.4	23.7	36.9
20.3	16.0	59.1	35.8
15.3		40.0	

NOMENCLATURE

Latin Letters

a--radius of sphere in film-thinning and spherical shell models (cm).

a--radius of cylinder after perturbation (cm).

a--half of time duration of periodic disturbance (sec).

a--capillary constant (cm).

a_0--radius of cylinder before perturbation (cm).

A--area covered by wave system set up by falling drop (cm^2).

A, A_n--constants.

A--horizontal coordinate of fluid particle in trochoidal wave theory, when wave length becomes zero (cm).

b--parameter describing amplitude of trochoidal wave; also vertical coordinate of fluid particle when wave length becomes zero (cm).

B, B_n--constants.

c--radius of disc (cm).

c--velocity of propagation of a trochoidal wave (cm/sec).

c--velocity of propagation of sound in a medium (cm/sec).

c_1, c_2, c_3--constants.

C--concentration of solute (g mols/l).

C--constant.

C_0--concentration of solute in oil phase (g mols/l).

C_p--phase velocity of waves (cm/sec).

C_w--concentration of solute in water phase (g mols/l).

d--separation distance in microphone calibration (cm).

ds--differential surface element (cm^2).

dv--differential volume element (cm^3).

D--constant.

e'_{oc}--open-circuit voltage response of test microphone to sound source (V).

e^x_{oc}--open-circuit voltage response of reversible microphone to sound source (V).

E--trochoidal wave total energy per unit wave length by unit width ($ergs/cm^2$).

E--voltage (V).

E_g--trochoidal wave gravitational potential energy per unit wavelength by unit width (ergs/cm^2).

E_K--trochoidal wave kinetic energy per unit wavelength by unit width (ergs/cm^2).

E_σ--trochoidal wave surface potential energy per unit wave length by unit width (ergs/cm^2).

$\bar{E}_D$--average rate of energy dissipation due to viscosity per unit wave length by unit width (ergs/cm^2 sec).

$\bar{E}_W$--average energy content of surface waves per unit wavelength by unit width (ergs/cm^2).

E'_{oc}--open circuit voltage response of test microphone to reversible transducer (V).

E_T^x--voltage driving reversible transducer (V).

f(t)--random disturbance as a function of time.

f(r/a), $f(r/v^{1/3})$--function used in drop-volume method for determining interfacial tension.

F--force in film-thinning model (dynes).

F--tensiometer ring correction factor.

F_U, F_D--upward and downward forces, respectively, in quasi-equilibrium force balance (dynes).

g--acceleration due to gravity (cm/sec^2).

$g(\omega)$--true frequency spectrum of random disturbance.

$\hat{g}(\omega_0)$--frequency spectrum of random disturbance given by wave analyzer at angular frequency setting, ω_0.

h--half-thickness of flat film (cm).

h'--thickness of spherical shell (cm).

H--dimensionless film thickness, equals h'/a.

H.L.B.--hydrophilic-lipophilic balance.

$\mathcal{H}$ (H)-- $\mathcal{H}$ (H) $\equiv a^4(H^4/6 + H^3/3)$.

i--$i = \sqrt{-1}$.

I--current (amps).

I_T^x--current driving reversible transducer (amps).

$J(p)$--function of p defined by Eq. (19).

k, k_n--wave number, equals $2\pi/\lambda$ or $2\pi/\lambda_n$, respectively (cm^{-1}).

k--constant.

$k(\phi)$--function of ϕ used in finding solution to differential equation.

K_1--term in trochoidal wave theory, equals $1 + e^{2bk}$.

K_2--term in trochoidal wave theory, equals $2\ e^{bk}$.

$K(\epsilon, \omega-\omega_0)$--band width accepted by wave analyzer.

L--defined by Eq. (84).

L--inductance (henries).

L--distance between centers of gravity of drop before and after it falls to interface (cm).

M--defined by Eq. (84).

M--tensiometer reading.

M_0', M_0^x--voltage sensitivities of test microphone and reversible transducer, respectively (volts/dyne/cm^2).

n--index.

n--outward normal to a surface.

N--defined by Eq. (84).

N_ϕ, $N_{\phi+\Delta\phi}$--rate of flow in spherical shell channel at ϕ and $\phi + \Delta\phi$, respectively (cm^3/sec).

p--angle defined in Fig. 3 (degrees or radians).

P--power (watts).

P, P_0--pressure in spherical shell film at angle p and at vertical axis, respectively (dynes/cm^2).

P, P_{rms}--sound pressure amplitude and rms sound pressure, respectively (dynes/cm^2).

$P_{I,1}$, $P_{I,2}$, $P_{II,2}$, $P_{II,3}$--pressures at interfaces I or II, in phases 1, 2, or 3 (dynes/cm^2).

$P(p)$--trigonometric function of p defined by Eq. (15).

$P_n(\mu)$--Legendre polynomial of order n.

q, q_n--growth constant in stability analysis when q is real; $q = C_p k$ when q is imaginary (sec^{-1}).

q_v--growth constant considering viscous damping (sec^{-1}).

$Q(p)$--trigonometric function of p defined by Eq. (3).

r--radius coordinate in spherical coordinate system.

r--dropping tip radius (cm).

r_e--equivalent spherical radius of drop, defined by $v=4/3\ \pi\ r_e^3$ (cm).

R--dimensionless radius, equals r/a.

R--resistance (ohms).

R--radius of tensiometer ring (cm).

R--gas constant (dyne cm^{-2} 1 g mol^{-1} $^oK^{-1}$).

R_1, R_2--defined by Eqs. (52) and (54), respectively.

$R(r)$--radius-dependent variable in spherical shell stability model.

s--dimension defined in Fig. 3 (cm).

S--surface area of cylinder (cm^2).

t--time (sec).

t_0--time displacement of random disturbance from the origin of time scale (sec).

$\bar{t}$, t_m, $t_{0.10}$, $t_{0.90}$--mean, median, 10 percentile, and 90 percentile drop rest-times, respectively (sec).

T--absolute temperature (^oK) .

u, $u_\phi(r, \phi)$--velocity and tangential velocity as a function of radius and angle ϕ , respectively (cm/sec).

$$T\text{--}T = \frac{(t_2 - t_1) \text{ from spherical shell model}}{(t_2 - t_1) \text{ from flattened-sphere model}} .$$

v--volume of liquid drop (cm^3).

V--volume of cylinder or shell (cm^3).

w--dimension defined in Fig. 3 (cm).

w--defined by $r = e^w$.

x--Cartesian coordinate.

x--defined by $X = kx$.

X_L--inductive reactance, (ohms).

$X(\phi)$--angular dependent variable in spherical shell model.

y--Cartesian coordinate.

z--Cartesian coordinate.

Z--impedance (ohms).

Z^x--impedance of reversible transducer (ohms).

Greek Letters

α--amplitude of a wave on a Rayleigh cylinder, at the upper interface of a flat film, or at interface I of a spherical shell film (cm).

$\alpha_{h,\,n}$, $\alpha_{-h,\,n}$--amplitude of waves of wave number k_n at upper and lower interfaces of flat film, respectively (cm).

β--amplitude of a wave at the lower interface of a flat film or at interface II of a spherical shell film (cm).

γ--amplitude ratio, equals α/β.

Γ--height of crest of trochoidal wave above trough (cm).

$\Gamma_3^{1,2}$--surface excess of component 3 relative to a dividing surface where components 1 and 2 are present in their bulk concentrations (g mols/cm^2).

$\delta(\omega-\omega_0)$--Dirac delta function.

Δ--finite change in a quantity.

ϵ--measure of narrowness of band width of wave analyzer.

ζ--defined by $\zeta \equiv z + h$.

η_h, η_{-h}, η_I, η_{II} --elevation of upper and lower surfaces of a flat film, surfaces I and II of a spherical shell film, respectively (cm).

θ--azimuthal angle in spherical coordinate system, defined by $x = r \cos\theta \sin\phi$, $y = r \sin\theta \sin\phi$.

θ--defined by $\theta = g(\rho_1-\rho_2) - \sigma k^2$.

θ--parameter used in describing surface of trochoidal wave, defined by $\theta = kA + qt$.

λ--wave length (cm).

Λ--number of particles contributed to a system by a molecule of solute, used in computing surface-excess quantities.

μ--defined by $\mu = \cos\phi$.

μ_1, μ_2--absolute viscosity of phases 1 and 2, respectively (poises or cp).

ν--frequency (cps).

ν_0--set point of wave analyzer (cps).

ξ--defined by $\xi \equiv z - h$.

ξ--defined by Eq. (60).

ρ_1, ρ_2, ρ_3, $\Delta\rho$--densities of phases 1, 2, and 3, and density difference, respectively (g/cm^3).

σ--surface or interfacial tension (dynes/cm).

σ^2--statistical variance.

Σ--summation operator.

Σ--surface area over which integration is to be performed (cm^2).

τ--viscous damping constant (sec^{-1}).

ϕ--polar angle in spherical coordinate system, defined by $x = r \cos \theta \sin \phi$, $y = r \sin \theta \sin \phi$.

Φ--velocity potential (cm^2/sec).

Φ--viscous dissipation function ($ergs/sec\ cm^3$).

χ--defined by Eq. (14).

ψ--defined by $\psi = - g (\rho_1 - \rho_2) - \sigma k^2$.

$\psi(\phi)$--angular dependent term of velocity distribution in spherical shell, defined by Eq. (4).

ω--angular frequency, equals $2\pi \nu$ (rad/sec).

ω_0--angular frequency of a discrete disturbance (rad/sec).

ω_0--angular frequency set point of wave analyzer (rad/sec).

Ω--potential term in equations of motion (cm^2/sec^2).

Other Symbols

∇--nabla or del, vector operator.

∇^2--Laplacian operator.

REFERENCES

1. Osborne Reynolds, Chem. News 44, 211 (1881).
2. L. D. Mahajan, Kolloid-Z. 69, 16 (1934).
3. E. G. Cockbain and T. S. McRoberts, J. Colloid Sci. 8, 440 (1953).
4. T. Gillespie and E. K. Rideal, Trans. Faraday Soc. 52, 173 (1956).
5. Robert G. Picknett, Ph.D. Thesis, University of London (1957).
6. L. E. Nielsen, R. Wall, and G. Adams, J. Colloid Sci. 13, 441 (1958).
7. G. A. H. Elton and R. G. Picknett, The Coalescence of Aqueous Droplets with an Oil/Water Interface, in Second International Congress of Surface Activity, (Butterworth & Company, London, 1957), Vol. I, p. 288.
8. Takehiko Watanabe and Makoto Kusui, Bull. Chem. Soc. Japan, 31, 236 (1958).
9. George E. Charles, Ph.D. Thesis, McGill University (1959).
10. G. E. Charles and S. G. Mason, J. Colloid Sci. 15, 105 (1960).
11. G. E. Charles and S. G. Mason, J. Colloid Sci. 15, 236 (1960).
12. R. S. Allan, G. E. Charles, and S. G. Mason, J. Colloid Sci. 16, 150 (1961).
13. R. S. Allan and S. G. Mason, Trans. Faraday Soc. 57, 2027 (1961).
14. B. V. Deriagin and P. S. Prokhorov, The Study of Causes for Non-Coalescence of Liquid Drops under Static Conditions (Under Lengthy Contact), Novye Idei v Oblasti Izucheniya Aerozolei, Akad. Nauk S.S.S.R., Inst. Fiz. Khim., Sbornik Statei (1949), p. 84; [translated, Lawrence Radiation Laboratory Report UCRL Trans. 601, Berkeley, California, 1960) (unpublished)].
15. P. S. Prokhorov, Explanation of the Mechanism of Non-Coalescence of Water Drops During Collision, Novye Idei v Oblasti Izucheniya Aerozolei, Akad. Nauk S.S.S.R., Inst. Fiz. Khim., Sbornik Statei, (1949), p. 102 [translated, Lawrence Radiation Laboratory UCRL Trans. 601, Berkeley, California, 1960 (unpublished)].
16. P. S. Prokhorov, Discussions Faraday Soc, No. 18, p. 41 (1954).
17. J. W. Telford, N. S. Thorndike, and E. G. Bowen, Quart. J. Roy. Meteorol. Soc. 81, 241 (1955).
18. G. D. Kinzer and W. E. Cobb, J. Meterol. 15, 138 (1958).

19. Lord Rayleigh, Proc. Lond. Math. Soc. 10, 4 (1878).
20. Lord Rayleigh, Proc. Roy. Soc. (London), A29, 71 (1879).
21. Sir Geoffrey Taylor, Proc. Roy. Soc. (London), A201, 192 (1950).
22. R. Bellman and R. H. Pennington, Quart. Appl. Math. 12, 151 (1954).
23. J. B. Keller and I. Kolodner, J. Appl. Phy. 25, 918 (1954).
24. S. G. Bankoff, A.I.Ch.E. Journal, 7, 485 (1961).
25. B. Derjaguin and M. Kussakov, Acta Physicochim. U.R.S.S. 10, 25 (1939).
26. B. Derjaguin and M. Kussakov, Acta Physicochim. U.R.S.S. 10, 153 (1939).
27. Richard S. Burington, Handbook of Mathematical Tables and Formulas, 3rd ed. (Handbook Publishers, Inc., Sandusky, Ohio, 1949), p. 14.
28. Shih-i Pai, Viscous Flow Theory: Volume I, Laminar Flow, (D. Van Nostrand Company, Inc., Princeton, New Jersey, 1956), p. 31.
29. Osborne Reynolds, Phil. Trans. Roy. Soc. London A 177, 157 (1886).
30. W. E. Ewers and K. L. Sutherland, Australian J. Sci. Research, Ser. A, 5, 697 (1952).
31. D. C. Chappelear, J. Colloid Sci. 16, 186 (1961).
32. R. B. Bird, W. E. Stewart, and E. N. Lightfoot, Transport Phenomena, (John Wiley & Sons, Inc., New York, 1960), p. 87.
33. G. A. H. Elton, Proc. Roy. Soc. (London), A194, 259 (1948).
34. G. A. H. Elton, Proc. Roy. Soc. (London), A 194, 275 (1948).
35. J. Frenkel, Kinetic Theory of Liquids, (Dover Publications, Inc., New York, 1955), pp. 332-342.
36. Lloyd L. Smail, Calculus, (Appleton-Century-Crofts, Inc., New York, 1949), pp. 323-325.
37. P. F. Byrd and M. D. Friedman, Handbook of Elliptic Integrals For Engineers and Physicists, (Springer-Verlag, Berlin, 1954).
38. Constantin Weber, Z. angew. Math. Mech. 11, 136 (1931).
39. A. Haenlein, Forsch. Gebiete Ingenieurw. 2, 139 (1931).
40. S. Tomotika, Proc. Roy. Soc. (London), A150, 322 (1935).
41. S. Tomotika, Proc. Roy. Soc. (London), A153, 302 (1936).
42. C. V. Boys, Soap-Bubbles, Their Colours and The Forces Which Mould Them, (Dover Publications, Inc., New York, 1959), pp. 62-88.

43. R. A. Castleman, Jr., J. Research Nat. Bur. Standards 6, 369 (1931).
44. D. J. Lewis, Proc. Roy. Soc. (London), A202, 81 (1950).
45. R. H. Aranow and L. Witten, J. Colloid Sci. 16, 127 (1961).
46. L. M. Milne-Thomson, Theoretical Hydrodynamics, 3rd ed. (The MacMillan Company, New York, 1955).
47. Sir Horace Lamb, Hydrodynamics, 6th ed. (Dover Publications, Inc., New York, 1945).
48. Arthur W. Adamson, Physical Chemistry of Surfaces, (Interscience Publishers, Inc., New York, 1960), pp. 4-6, 22-27, 52-54, 388-402, 415.
49. S. G. Bankoff, Phys. Fluids 2, 576 (1959).
50. M. Koussakov, Acta Physicochim. U.R.S.S. 19, 286 (1944).
51. J. L. Powell and B. Crasemann, Quantum Mechanics (Addison-Wesley Publishing Company, Inc., Reading, Mass. 1961), p. 190.
52. A. N. Tychonoff and A. A. Samarski, Differentialgleichungen der mathematischen Physik, (Veb deutscher Verlag der Wissenschaften, Berlin, 1959), pp. 592-595.
53. L. D. Landau and E. M. Lifshitz, Fluid Mechanics, (Pergamon Press, London, 1959), pp. 233, 253-256.
54. J. J. Bikerman, J. Phys. Chem. 56, 164 (1952).
55. Ian N. Sneddon, Fourier Transforms, (McGraw-Hill Book Company, Inc., New York, 1951), pp. 32-34.
56. W. D. Harkins, The Physical Chemistry of Surface Films, (Reinhold Publishing Corporation, New York, 1952), pp. 71-79, 303.
57. W. G. Cochran and G. M. Cox, Experimental Designs, 2nd ed. (John Wiley & Sons, Inc., New York, 1957).
58. E. S. Pearson and H. O. Hartley, Biometrika Tables for Statisticians, Vol. I, (Cambridge University Press, Cambridge, 1954), Table 18.
59. Theodor Lohnstein, Ann. Physik 20, Ser. 4, 237 (1906).
60. Theodor Lohnstein, Ann. Physik 20, Ser. 4, 606 (1906).
61. H. Dunken, Ann. Physik 41, Ser. 5, 567 (1942).
62. C. L. Strong, Sci. American 203, 185 (Oct. 1960).
63. Leo L. Beranek, Acoustic Measurements, (John Wiley & Sons, Inc., New York, 1949), pp. 113-122.

64. F. W. Schwab and E. Wichers, J. Research Nat. Bur. Standards 32, 253 (1944).

65. Herman E. Ries, Jr., Sci. American 204, 152 (March, 1961).

66. B. J. Mair, A. R. Glasgow, Jr., and F. D. Rossini, J. Research Nat. Bur. Standards 26, 591 (1941).

67. A. R. Glasgow, Jr., A. J. Streiff, and F. D. Rossini, J. Research Nat. Bur. Standards 35, 355 (1945).

68. J. T. Davies and E. K. Rideal, Interfacial Phenomena, (Academic Press, New York, 1961), pp. 17-31, 196-213, 322-327, 359-386.

69. E. Jahnke and F. Emde, Tables of Functions with Formulae and Curves, 4th ed. (Dover Publications, Inc., New York, 1945), Addenda, pp. 32-35.

70. Arnold Weissberger, Physical Methods of Organic Chemistry, 3rd ed. (Interscience Publishers, Inc., New York, 1959), Vol. I, Part 1, pp. 786-797.

71. H. H. Zuidema and G. W. Waters, Ind. Eng. Chem. Anal. Ed. 13, 312 (1941).

72. International Critical Tables, edited by Edward W. Washburn, (McGraw-Hill Book Company, Inc., New York, 1926).

73. Handbook of Chemistry, edited by Norbert A. Lange, 8th ed. (Handbook Publishers, Inc., Sandusky, Ohio, 1952), p. 1689.

74. American Society for Test Materials, Test for Kinematic Viscosity, ASTM Method D445-53T, 1953.

75. H.-G. Könnecke, Z. physik. Chem. (Leipzig) 211, 208 (1959).

76. Handbook of Chemistry and Physics, edited by Charles D. Hodgman, 34th ed. (Chemical Rubber Publishing Company, Cleveland, Ohio, 1952).

77. H. Groothuis and F. J. Zuiderweg, Chem. Eng. Sci. 12, 288 (1960).

78. C. V. Sternling and L. E. Scriven, A. I. Ch. E. Journal 5, 514 (1959).

79. L. E. Scriven and C. V. Sternling, Nature 187, 186 (1960).

80. J. Gibbs, Scientific Papers, (Dover Publications, Inc., New York, 1961), Vol. I, pp. 300-314.

81. Lawrence Radiation Laboratory Counting Handbook, UCRL-3307-Rev, Jan. 1959.

82. Robert J. Graham, Separation of Immiscible Liquids by Gravity Settling and Induced Coalescence. Part I: Horizontal Gravity Settlers. Part II: Gravity Settling with Induced Coalescence, Lawrence Radiation Laboratory Report UCRL-10048, Feb. 5, 1962 (unpublished).

83. M. Van Den Tempel, Rec. trav. chim. 72, 433 (1953).

84. W. Bartok and S. G. Mason, J. Colloid Sci. 12, 243 (1957).

85. W. Bartok and S. G. Mason, J. Colloid Sci. 14, 13 (1959).

86. A. Weissberger, E. S. Proskauer, J. A. Riddick, and E. E. Toops, Jr., Technique of Organic Chemistry, Volume VII, Organic Solvents, Physical Properties and Methods of Purification, 2nd ed. (Interscience Publishers, Inc., New York, 1955), p. 251.

This report was prepared as an account of Government sponsored work. Neither the United States, nor the Commission, nor any person acting on behalf of the Commission:

A. Makes any warranty or representation, expressed or implied, with respect to the accuracy, completeness, or usefulness of the information contained in this report, or that the use of any information, apparatus, method, or process disclosed in this report may not infringe privately owned rights; or

B. Assumes any liabilities with respect to the use of, or for damages resulting from the use of any information, apparatus, method, or process disclosed in this report.

As used in the above, "person acting on behalf of the Commission" includes any employee or contractor of the Commission, or employee of such contractor, to the extent that such employee or contractor of the Commission, or employee of such contractor prepares, disseminates, or provides access to, any information pursuant to his employment or contract with the Commission, or his employment with such contractor.